Model Selection in a Multi-Hypothesis Test Setting: Applications in Financial Econometrics

DCU Business School

December, 2017

Author:

Francesco P. Esposito

Supervisor:

Dr. Mark Cummins

Thesis submitted to Dublin City University Business School in partial fulfilment of the requirements for the Degree of Doctor of Philosophy

I hereby certify that this material, which I now submit for assessment on the programme of study leading to the award of Ph.D. is entirely my own work, and that I have exercised reasonable care to ensure that the work is original, and does not to the best of my knowledge breach any law of copyright, and has not been taken from the work of others save and to the extent that such work has been cited and acknowledged within the text of my work.

Signed  ID No.: 12211600 Date: 19/12/17

Acknowledgments

I would like to express my sincere gratitude to my advisor Dr. Mark Cummins for his wise suggestions and guidance and, furthermore, for having allowed the realisation of this project under unconventional circumstances.

Besides Mark, I would like to thank Ludovica, for her precious friendship through the years and her encouraging words.

Foremost, I wish to thank my wife Tina for her love, trust and patience.

Model Selection in a Multi-Hypothesis Test Setting: Applications in Financial Econometrics

F. P. Esposito

Abstract

In this thesis, we investigate model selection in a general setting and perform several exercises in financial econometrics. We present the multi-hypothesis testing (MHT) framework, with which we design different type of model comparisons. We distinguish between test of model performance significance, of relative and absolute model performance and apply our framework to market risk forecasting model, to latent factor jump-diffusion models employed for the estimation of the statistical measure of an equity index, as well as to equity option pricing models. We develop original tests and, with regard to the proper exercise of model selection from an initial battery of models without any reference to a benchmark model, we combine the MHT approach with the model confidence set (MCS) to deliver a novel test of model comparison that is performed along with the established version of the MCS, as well as with an alternative simplified new MCS test that are detailed in the course of this work. We collect empirical evidence concerning model comparison in several subjects. With respect to market risk forecasting models, we have found that models capturing volatility clustering or targeting directly an auto-correlated conditional distribution percentile, perform better than the target model set and in particular, better than the historical simulation, widely employed by practitioners, and better than the so called RiskMetrics model. With respect to the equity index data dynamics, we have found that the popular affine jump-diffusion model requires a CEV augmentation to perform appropriately and that those models are slightly overperformed by an alternative stochastic volatility model, characterised by stochastic hazard with high frequency small jumps. The test performed over a large model set employed in the option pricing exercise points to a wide similarity of the results obtained by the many model specifications of the superior exponential volatility model, therefore suggesting a more careful adjustment of the model complexity. The model selection framework has proven very flexible in dealing with the varied collection of statistical problems. In particular, our main contribution represented by the generalised MHT based MCS test provides a method for model selection that is robust to finite sample distribution and that has the advantage of an adjustable tolerance for false rejections, allowing conservative to aggressive testing profiles.

Keywords: Multi-hypothesis test, generalised family-wise error rate, tail probability of false discovery proportion, stationary bootstrap, step-down algorithm, model confidence set, value-at-risk, expected shortfall, likelihood function, second order non-linear filter, jump-diffusion, stochastic volatility, stochastic hazard, option pricing model, partial integral-differential equation, finite difference method.

Contents

1 Model Selection Framework **1**

1.1 The Model Selection Strategy 4

1.2 Multiple Hypothesis Testing 5

1.2.1 The Implementation of the MHT Procedure 8

1.2.2 The Step-Down Algorithm 10

1.2.3 The Stationary Bootstrap 12

1.3 The Model Confidence Set 14

1.3.1 The *max*-MCS 15

1.3.2 The t-MCS 17

1.3.3 The γ-MCS 19

1.4 Thesis Summary 21

1.5 Concluding Remarks 26

2 Model Selection of Market Risk Models **27**

2.1 The Conditional Distribution Model Set 29

2.2 Model Comparison Testing 32

2.3 Experimental Section 34

2.3.1 Preliminary Considerations 34

2.3.2 Market Data Experiment . . . 37
2.4 Concluding Remarks . . . 40
Tables . . . 42

3 Model Selection of Jump-Diffusion Models **55**
3.0.1 Some clarifications . . . 58
3.1 The Jump-Diffusion Model Set . . . 61
3.1.1 Parameter Estimation . . . 64
3.1.2 The Second Order Non-Linear Filter . . . 65
3.2 Model Comparison Testing . . . 66
3.2.1 Likelihood Ratio . . . 67
3.2.2 Distance from the Latent Component . . . 68
3.2.3 LR with Latent Component . . . 69
3.3 Experimental Section . . . 70
3.3.1 Preliminary Considerations . . . 70
3.3.1.1 Benchmarking the NLF^2 with Particle Filtering . . . 74
3.3.2 Monte Carlo Experiment . . . 76
3.3.3 Market Data Experiment . . . 79
3.4 Concluding Remarks . . . 82
Tables . . . 84
Figures . . . 101

4 Model Selection of Derivative Pricing JD Models **107**
4.1 The Derivative Pricing Model Set . . . 109
4.2 Model Comparison Testing . . . 112
4.2.1 Mispricing MSE . . . 113
4.3 Experimental Section . . . 115
4.3.1 Preliminary Considerations . . . 115
4.3.2 Market Data Experiment . . . 119
4.4 Concluding Remarks . . . 121
Tables . . . 123
Figures . . . 131

5 Conclusions **137**

Bibliography **143**

A Algorithms **153**
A.1 The Approximate Likelihood Function . . . 153
A.1.1 The Marginalisation Procedure . . . 154
A.1.2 The Approximation of the Transition Density . . . 155
A.2 The PIDE solution . . . 156
A.3 The Nonlinear Filter . . . 158

A.3.1 The Time-Propagation Equation 160
A.3.2 The Update Equation 163
A.3.3 The Expectation Proxy 164
A.3.4 The NLF^2 of the SD and SH Classes 166
A.4 Model Transformations 167

B Pseudo-Codes **171**
B.1 The AML algorithm 172
B.2 The SIR−PF algorithm 174
B.3 The MSE algorithm 175

List of Tables

1 VaR and ExS Forecasting Models 42
2 VaR MHT 43
3 ExS MHT 44
4 L/V VaR MHT 45
5 H/V VaR MHT 46
6 MCS VaR 1% 1d 47
7 MCS VaR 5% 1d 48
8 MCS ExS 1% 1d 49
9 MCS ExS 5% 1d 50
10 MCS VaR 1% 2w 51
11 MCS VaR 5% 2w 52
12 MCS ExS 1% 2w 53
13 MCS ExS 5% 2w 54

14 Model Set Acronyms 84
15 Standard Models and the Model Set 85
16 Simulation MHT Model Parameters and Standardised Moments 86
17 Financial Market Data Model Parameters Estimates 87

18 Simulated LRMHT . . . 88
19 Simulated LCMHT. . . . 89
20 Simulated LRMCS-max. . . . 90
21 Simulated LRMCS-γ. . . . 91
22 Simulated LRMCS-t. . . . 92
23 Simulated LCMCS-max. . . . 93
24 Simulated LCMCS-γ. . . . 94
25 Simulated LCMCS-t. . . . 95
26 Market Data LRMHT. . . . 96
27 Market Data TGMHT. . . . 97
28 Market Data LRLCMHT. . . . 98
29 Market Data MCS. . . . 99
30 The NLF^2 and the SIR Particle Filter. . . . 100

31 The Call Option Average Implied Volatility. . . . 123
32 The Put Option Average Implied Volatility. . . . 124
33 The Call Option Data Distribution. . . . 125
34 The Put Option Data Distribution. . . . 126
35 The OTM Call/Put Option Average Implied Volatility. . . . 127
36 The OTM Call/Put Option Data Distribution. . . . 128
37 Bootstrap MCS-γ fix at 20% and 40% OTM and ALL sample. . . . 129
38 Bootstrap MCS-*max* at 10% ALL sample. . . . 130

List of Figures

1 The Likelihood Function Algorithm. 101
2 An example of Information Loss. 102
3 The Distributional Shape of the Model Set. 103
4 Several Implementation Issues. 104
5 Market Data Applications. 105

6 S&P500 Index Level. 131
7 Put/Call Parity Distribution. 132
8 The Selection of the Option Price Sample. 133
9 Time Series Features of the Option Price Sample. 134
10 The RMSE Time Series. 135
11 The Volatility Surface Quantile Regression. 136

Model Selection Framework

The question that is debated in this thesis is central to a wide range of statistical applications. The research objective can be summarised as follows: given a set of models returning output that is data explanatory or data forecasting, which model or which model subset produces the best performance? Further characterisation is required by demanding: what degree of uncertainty can be associated with, and how robust is the decision concerning the best model set? This task is referred to as *model selection*. In statistics, this term is usually associated with the comparison of models as partial representations of the data generating process (DGP). In this work, on the contrary, we use this label in a wider sense. In general terms, we deal with a given set of objects, namely *models*, which characterise the execution of a certain *action* on the experimental observations or indirect measurements of the phenomenon under analysis, that is the *data*. The concept of a "model" has to be interpreted in abstract terms as a set of rules prescribing the data processing function, although it will ultimately be associated with a probability distribution hypothesis[1]. The action of the model is intended as a transformation of the experimental

[1] The term *model* that is adopted throughout this thesis is in line with the practiotioners' use of this word. In Office of the Comptroller of the Currency (2011) "the term model refers to a quantitative method, system, or approach that applies statistical, economic, financial or mathematical theories, techniques, and assumptions to process input data into quantitative estimates. A model consists of three components: an information component, which delivers assumptions and data to the model; a processing component, which transforms inputs into estimates; a reporting component, which translates those estimates into useful business information." Nonetheless, with very few exceptions in this manuscript, a model might still

data that provides explanatory information about or forecasts the behaviour of the underlying system of variables. The result of this action feeds a *model performance* indicator, which enables the comparison of the model set, as prescribed by the model selection criterion. The focus is tilted towards the statistical distribution of this loss function rather than to the approximation of the DGP, two aspects of the decision problem that might not directly coincide as such, for instance, in the linear constrained regression problem of Toro-Vizcarrondo and Wallace (1968), whereby the minimum squared error criterion is regarded as the discerning factor for the evaluation of the model performance, whereas testing the likelihood of the model restrictions does not necessarily provide a matching result. In the lecture note Rao and Wu (2001), the authors propose a classification of the model selection process, which is mostly methodological. According to the authors, model selection can be characterised into several problem types. In fact, it is either conducted as a sequence of hypotheses testing, as a forecasting error minimisation problem, through information theoretic criteria, based on bootstrap methods or approached in a Bayesian set-up. Other categories that are mentioned in the lecture note pertain to specific statistical problem classes, such as cross-validation, order selection in time series, categorical data analysis, non-parametric regression and data-oriented penalty. The literature on the subject is overwhelming, therefore this introduction does not serve as a complete review of such a vast and varied subject matter. In this section, we demarcate this research and identify the areas from which we draw the methodology and the instruments to devise the econometric applications presented in this thesis.

Model selection is deeply rooted in the origins of statistics. The major problem is that of model specification, which can be traced back to discipline establishing works such as Fisher (1922, 1924) and Pearson (1936), which advocated, respectively, the method of maximum likelihood and the method of moments as procedures for model identification. Tests for model specification were devised later involving a single specification hypothesis on the model significance, such as the Lagrange multiplier test (Silvey, 1959; Breusch and Pagan, 1980), the Hausman (1978) test, the information matrix test and the score test of White (1982), the Newey (1985) test, the approach of Wooldridge (1990). Tests involving direct pairwise model comparisons can be referenced, for instance, to the Wald (1943) test for model parameters restrictions, the likelihood ratio statistic of Wilks (1938) and more generally the testing framework of Vuong (1989). Eventually, it was the work of Akaike (1974, 1981) that provided the model specification task with a criterion allowing for a more extensive model comparison. Furthermore in the context of model specification, a direct pairwise comparison exploiting the AIC was pursued with the test of Linhart (1988), which was later employed in conjunction with the model subset selection procedure of Gupta and Huang (1976) to construct the *confidence set of models* of Shimodaira (1998), probably the first procedure providing a multiple comparison model selection test with a general application in the realm of maximum likelihood. In this perspective, this aspect of model selection as a multiple comparison statistical test is central to this thesis work. We adopt the multiple hypothesis testing (MHT) framework of Beran (1988a,b, 1990, 2003) and Romano and Wolf (2005a, 2007, 2010) in constructing balanced confidence set based multiple comparison tests for the sake of model selection. For our purposes, we seek a general procedure that is not only applicable to likelihood tests but that is capable of handling virtually any kind of model comparison problem, requiring a minimum set of assumptions. The general setup is related to several works

be associated with an hypothesis regarding the DGP, although we employ the former definition.

in model forecasting performance, such as Diebold and Mariano (1995), West (1996) in a pairwise model comparison setting, and the works of White (2000) and Hansen (2005), in a multiple comparison context. Although not only confined to forecasting model comparison, the latter multiple comparison tests suffer from the lack of ability to identify the best performing models, yielding an inference as to whether the model set contains items that perform better than a given reference model. This fact has been noted in Romano and Wolf (2005b), who deliver a step-wise procedure version of the reality check approach of White (2000) and Hansen (2005) that isolates the subset of models that perform better than the reference model, see also Romano et al. (2008). We indicate this type of test as *relative model comparison*. Finally, we remark that, whenever the problem is configured such that the specification of a reference model is not required, the collection of multiple model comparison tests just referenced are limited. We indicate the problem of model selection without a pre-specified term of comparison as *absolute model comparison*. In this regard, we build upon the Hansen et al. (2011) version of the model confidence set (MCS) to design a generalised multiple hypothesis test for model comparison that does not require the choice of a reference model, with several applications in financial econometrics showcased. This multiple comparison model selection procedure, which we coin the γ-MCS, is a characterisation of the MHT controlling for the number k of tolerated false discoveries and, in an extended version, the γ tail probability of the false discovery proportion can also be triggered; both cases allow for a complete analysis of the set of model comparisons. The hypotheses testing is structured to embed the complete multi-dimensional nature of the model selection exercise and draw inference with respect to individual model comparisons, at the same time controlling for test dependencies. The model selection procedures are powered by a simulation engine represented by a type of block bootstrap device such as the stationary bootstrap of Politis and Romano (1994a,b), rendering the test robust to finite sample statistic distribution. The bootstrap approach enables the method to handle virtually any model selection problem, without resorting to pivotal results, in this case meaning without resorting to the asymptotic normality of the statistics. Thus, the exercise is reduced to a matter of experimental design, an attractive characteristic for financial practitioners. In fact, with the empirical applications in this thesis, we are able to construct model selection procedures whereby the models are misspecified in nature and the model battery may contain parametric and non parametric models, whereby we could could compare continuous and discrete time models, we could include nested and non-nested model specifications, or further we could operate in a context of partial information. In several applications, the exercise is worsened by the finite precision of the several numerical procedures involved in the calculation of the crucial measures of model performance, a feature that can be improved at the cost of overall computational demand.

With this Chapter 1, we provide the fundamental link between all parts of this thesis by means of formally introducing the model selection approach pursued throughout. We introduce the general problem of test dependencies, articulated and solved within the framework of Beran (1988a,b, 1990, 2003) and Romano and Wolf (2005a, 2007, 2010), whereby the balanced confidence set for the MHT are constructed and combined with generalised error controlling algorithms. Building on the model comparison test design based on the loss function of Diebold and Mariano (1995), West (1996) White (2000) and Hansen (2005), we outline performance significance and relative model comparison MHT. Finally, invoking the MCS concept drawn by Hansen et al. (2011), we provide an original contribution to the literature by merging

the generalised MHT and the MCS to develop the γ-MCS test. In our interpretation, the MCS is a set restriction hinging on a preference relationship amongst the model set, which is ultimately defined through a statistical test. The inference process delivers the equivalence set of best performing models that, although preserves some coherence across different types of test, is not necessarily unique. We provide this important insight through the construction of a simplified MCS test of model selection, which utilises the same comparison strategy as the γ-MCS, but which does not retain its superior MHT properties. We indicate this test as the t-MCS. In general, when the main model clusters are very distinct, the tests tend to deliver the same results, whereas when the models are tightly competing, the test dependencies play a major role, whereby the γ-MCS reveals greater flexibility in its model discrimination capability, represented by the generalised controlling mechanism.

In the following Section 1.1 we develop the model selection strategy, whereas in Section 1.2 we present the technical details for the construction of the multiple hypothesis test with balanced confidence intervals, which represent the main instrument for the pursuing of the several model comparison exercises. In Section 1.3 we characterise the procedure for discarding the benchmark model in the model selection test and constructing the model confidence set. In this section, the main MCS test of Hansen et al. (2011) is detailed, while the additional t-MCS and γ-MCS tests are presented. Section 1.4 provides an overview of the thesis by introducing the motivation for and the layout of the chapter experiments, emphasising the contributions and main findings in each case. Section 1.5 concludes this methodological chapter.

1.1 The Model Selection Strategy

In our set-up, a model is ultimately conceived as a conjecture on a probability distribution $\mathbf{P}$, by which we identify the model itself. We define the initial model set as $\mathcal{M}_0 \equiv \{\mathbf{P}_0, \mathbf{P}_1, \ldots, \mathbf{P}_{m_0}\}$. The performance of model $\mathbf{P}_i \in \mathcal{M}_0$ is measured by the data transform $L_{i,t} := L(\mathbf{X}_t, \mathbf{P}_i)$, that is a numerical function of the data set $\mathbf{X}_t$ observed at time t, evaluated according to the model prescriptions defined by $\mathbf{P}_i$. A classic exercise of hypotheses testing that will be accomplished within the experimental part of Chapter 2 concerns the construction of tests of *significance of the model performance*, where the model performance metric is compared with a target value, whenever this one can be defined. However, tests of this type are not suited for the purpose of model comparison, as they do not involve pitting the models against one another. In fact, models producing significant performances do not necessarily produce superior output when contrasted with competitors. This brings us to the following discussion of methods for model comparison.

A model comparison is defined as the contrasting of models $\mathbf{P}_i$ and $\mathbf{P}_j$, whose outcome is a preference ordering that decides which model is best, or that both models are equivalent. Whenever model i is preferred to model j, we write $\mathbf{P}_i \succ \mathbf{P}_j$ or $\mathbf{P}_j \prec \mathbf{P}_i$ and we say, respectively, that model i is superior to model j or that model j is inferior to model i. The equivalence between the two models is written as $\mathbf{P}_i \sim \mathbf{P}_j$. The objective of this thesis is the characterisation of the decision rule establishing the preference structure upon the model set $\mathcal{M}_0$. This task in general corresponds to a statistical testing procedure that might involve a sequence of tests or a joint multivariate test, delivering in addition a

model ranking system. In the model comparison framework we are devising, the model performance measure L is a model loss function, that the lower this figure, the better. The reference metric is the relative performance measure $d_{ij,t} := L_{i,t} - L_{j,t}$, where the ordering is important. The testing procedures presented in the rest of this chapter target either the quantity $\mu_{ij} := \mathbb{E}[d_{ij,t}]$, such that $\mathbf{P}_i \succ \mathbf{P}_j$, if $\mu_{ij} < 0$ or $\mathbf{P}_i \sim \mathbf{P}_j$, if $\mu_{ij} = 0$. Whenever a model $\mathbf{P}_0 \in \mathcal{M}_0$ is attributed with the special role of being a benchmark, we refer to this as a *relative model performance* test, where the objective is to determine whether $\mathcal{M}_0$ contains a model preferable to the benchmark. In the literature there are several examples of relative performance tests such as the reality check (RC) of White (2000) or the superior predictive ability (SPA) test of Hansen (2005). These types of tests are known to be very conservative[2]. In Chapter 3 we present two applications of our alternative form of relative model performance test, whereby the benchmark is either clearly identified, or the test is run by recursively selecting the benchmark model, revealing model clusters and the full collection of model preferences. This feature might be useful in suboptimal decision making, that is whenever the usage of the best model is prevented, the mapping of the full set of model comparison results allows the choice of second best models. However, synthesising the information provided by this form of test is subjective to some extent as it lacks a procedure for the automatic selection of superior models. There, to address this, a contribution of this study is the construction of a general model selection procedure in an MHT setting, designed to automatically select the superior models from a given model set. We indicate this type of statistical test as an *absolute model performance* test.

In the next section we introduce the generalised MHT procedure by which we construct the test of significance of model performance, the relative performance test, as well as the main step of the MHT based absolute model performance tests. In Section 1.3 we introduce the fundamental concept of MCS as in Hansen et al. (2011), by which we complete the design of the novel γ-MCS along with the introduction of more MCS tests.

1.2 Multiple Hypothesis Testing

A multiple hypothesis test is a statistical test on the set of hypotheses $H_1, \ldots, H_m$. The distinctive feature of the test is that the H_j's are considered jointly and hence the test statistic is, in general, an m dimensional vector. The construction of a procedure for MHT requires some subtleties. When dealing with multiple hypothesis testing the notions of a rejection region and confidence level acquire higher complexity, and it is not immediate the translation of a single testing procedure into an MHT which takes into account the multiple dimension of the decision under analysis. In the case of a single null H_0 versus an alternative H_A, the criterion in hypothesis testing prescribes the construction of a rejection

[2] The formal null hypothesis is $H_0 \colon \max_{i=1,\ldots,m} \mu_{0i} \leq 0$ which corresponds to the hypothesis that "no model in the model set $\mathcal{M}_0$ is superior to the benchmark $\mathbf{P}_0$". As noted in Corradi and Distaso (2011), the introduction of a poorly performing model, although it does not have any impact on the asymptotic value of the statistic because $\max_{1,\ldots,m+1} \mu_{0i} = \max_{1,\ldots,m} \mu_{0i}$, it will certainly affect the percentiles and then the p-value of the statistic distribution. Indeed, the poorly performing model $\mathbf{P}_{m+1}$ will have a consistent impact on the distribution of the max statistic. The introduction of a poorly performance model will therefore have the effect of inflating the p-value, which can actually be made large at will, by including bad performing objects in the target model set. This is a substantial limitation of the reality check, which still persists in the standardised version of the test, see Hansen (2005). To attenuate the dependence on the outlier bad model, the author proposes to discard the bootstrap generated performance measures that exceed an asymptotic threshold. It is not clear, however, if the superior predictive ability test is more powerful than the reality check, cfr. Corradi and Distaso (2011).

region Γ, whereby the inclusion of the sample determined statistic $T \in \Gamma$ leads to the rejection of the null hypothesis, whereas $T \notin \Gamma$ leads to its acceptance. The probability measure of the rejection region $\mathbb{P}(\Gamma) = \alpha$ represents the *confidence level*, which is the probability of committing a **type I** error that is the rejection of H_0 when it is true. A **type II** error occurs when $T \notin \Gamma$ implies the acceptance of the null, while H_A is actually true. The *power of the test* is given by $1 - \mathbb{P}\{T \notin \Gamma, s.t. |H_A| = 1\}$, where in general terms $|A|$ is the Boolean value of the event A. On the other hand, when considering the problem of testing m null hypotheses simultaneously, the situation is more intricate. Now there are many intersections of type I and type II errors and it is not clear how to define a rejection region Γ and what measure to be targeted in defining multiple hypotheses tests. To understand intuitively the importance of appropriately identifying this set, it is useful to refer to the following simple example borrowed from Romano et al. (2010). Consider 100 independent statistical tests, each of them with a confidence level of $\alpha = 0.05$; the probability of rejecting at least one of these tests assuming all are in fact true is extremely high, that is $1 - 0.95^{100} = 0.994$. Hence, the probability of committing a joint type I error is close to certainty, implying the need for a procedure capable of controlling the probability of false rejections in the presence of a multiple test structure. The classical approach to solving the multiplicity problem consists of introducing control of the *family-wise error rate* (FWER), that is the probability of rejecting at least one true hypothesis; or otherwise stated, the probability of making at least one false discovery. A generalisation of the FWER concept is the

$$k\text{-FWER}=\mathbb{P}\{\text{reject at least } k \text{ hypotheses } H_s \colon |H_s| = 1\}$$

whereby the FWER is the same as the 1-FWER special case. The k family-wise error rate has been conceived and implemented within the confidence set approach in Romano and Wolf (2005a, 2007, 2010).

However, when the number of hypotheses grows large, it is more convenient to consider a further generalisation of the concept of k-FWER, which is referred to as the *false discovery proportion* (FDP), that is the ratio of the false rejections to the total number of rejections. The FDP is useful as it provides a method for the automatic selection of the k, the number of tolerated false rejections, by simply setting the ratio of the number of accepted false rejections to that of the number of the actual rejections, a coefficient that is independent of the size of the hypothesis set. Given the user specified ratio $\gamma \in [0, 1)$, the target quantity for the construction of a rejection region is the tail probability of the FDP, or formally

$$\gamma\text{-TPFDP}=\mathbb{P}\{\text{FDP}>\gamma\}, \text{ for all } H_s$$

Controlling the generalised family-wise error rate or the false discovery proportion involves fixing a confidence level α such that $k\text{-FWER} \leq \alpha$ or $\gamma\text{-TPFDP} \leq \alpha$. Another approach that has also been used in literature is represented by the *false discovery rate*, which defines the MHT control of the $\mathbb{E}(FDP) \leq \gamma$, for all H_s. For this criterion compare, e.g. Benjamini and Hochberg (1995, 2000) and Storey (2002). A strong limitation of the latter error rate is that it does not allow for the probabilistic control of the false discoveries, as the probability of the false discovery rate being larger than a given threshold might occur to be quite large, cfr. Romano and Wolf (2010).

In the course of this research we deal with several model selection exercises. We construct test of model

performance significance and relative model performance MHT, which control for the k-FWER, and further introduce a novel MHT of absolute model performance, controlling for the γ-TPFDP. In the financial econometric application of Section 2.3, we construct an MHT for the significance of the model performance, investigating the outcome of a forecasting model in relation to target values. With the various other applications, we look at the research objective from the same angle, when we observe that a model selection test is by construction a multiple hypothesis problem corresponding to the combined paired comparisons. In a relative model selection test one model is fixed, such as for instance the experiment in Section 3.3. In contrast, all combinations are explored in an absolute model selection exercise, like those delivered in Section 2.3, Section 3.3 and Section 4.3. With respect to the latter task though, an auxiliary concept will be needed in order to deliver the final MHT absolute model performance test, an instrument developed in Section 1.3.

Specifically and with reference to the methodological approach of model selection we implement in this thesis, in Chapter 2 we construct several multiple hypothesis tests of *statistical significance* for the market risk forecasting models considered, see Section 2.3. The MHT is structured as follows:

$$H_i : \nu_i = 0, \ \forall \mathbf{P}_i \in \mathcal{M}. \tag{1.1}$$

whereby ν_i is the expected forecasting error of model $\mathbf{P}_i$. It is implicit that, in order to derive such a measure for the test (1.1), a reference forecasting target should be identifiable.

In contrast, when structured as an MHT, a model selection test is a multiple hypothesis problem formulated on the full range of paired comparisons. We distinguish between relative and absolute model comparison test in this context. In a *relative model selection*, one reference model, say $\mathbf{P}_k$, is kept fixed and designated as the benchmark, thus the MHT corresponds to the joint hypotheses that exist equivalent models in $\mathcal{M} \backslash \mathbf{P}_k$. The relative performance model selection MHT we adopt is the equivalence joint hypotheses test

$$H_{ik} : \mu_{ik} = 0, \ \forall \mathbf{P}_i \in \mathcal{M}, \ i \neq k. \tag{1.2}$$

The test is bidirectional, whereby breaches of the right or left thresholds indicate, respectively, superior or inferior models, in practice partitioning the non equivalent models into two further subgroups. In one exercise employing this type of test, we iterate the benchmarking $\mathbf{P}_k$ across the model set $\mathcal{M}$ to investigate the model clustering. The test defined in (1.2) is applied experimentally in Section 3.3.

Finally, as the major contribution of this research, we construct *absolute model selection* tests under the MHT framework. The approach pursued in this thesis for constructing tests of model selection consists in the explicit analysis of the following pairwise model performance comparisons:

$$H_{ij} : \mu_{ij} \geq 0, \ \forall \mathbf{P}_i, \mathbf{P}_j \in \mathcal{M}, i \neq j \tag{1.3}$$

The multiple hypothesis (1.3) is structured such that the null hypothesis H_{ij}, for each scalar test, consists of a conjecture on *at least* equivalence of model $\mathbf{P}_j$ with respect to $\mathbf{P}_i$. The procedure for the absolute

model selection is completed with the extraction of the MCS defined by the γ-MCS algorithm and detailed in Section 1.3.3. In Section 2.3, Section 3.3 and Section 4.3 we investigate, respectively, the MCS in (i) market risk forecasting models, (ii) maximum likelihood estimation and filtering of stochastic volatility models and (iii) option pricing models.

1.2.1 The Implementation of the MHT Procedure

In order to construct tests of multiple hypotheses, we adopt the method of the balanced confidence set, see Beran (1988a, 1990) and Romano and Wolf (2010). Assume the DGP of the data $\mathbf{X}$ is determined by the unknown probability distribution $\mathbf{P}$ and consider the problem of simultaneously testing s hypotheses

$$H_j \colon r_j \in \mathbf{C}_j, \quad j = 1, \ldots, s \tag{1.4}$$

where the H_j represents the j-th hypothesis defined by the event r_j and the subset $\mathbf{C}_j \subset \mathbf{T}$ is the restriction of the domain of events $\mathbf{T}$ which characterises the j-th hypothesis. In practice, the multiple hypothesis test defined upon the region (1.4) is determined by the data function $R_{n,j}(\mathbf{X}; \mathbf{P})$, where the dependency on the sample size n has also been made explicit. In this section we present the method for constructing multiple dimension confidence set that are right semi-intervals. Nevertheless, the implementation of the tests (1.1) and (1.2) requires the construction of bi-directional intervals that can be achieved by repeating the procedure at the left side of the sample domain. We wish to determine the right-hand confidence set

$$\mathbf{C}_j = \{r_j \in \mathbf{T} \colon R_{n,j}(\mathbf{X}; \mathbf{P}) \leq c_{n,j}(\alpha; \mathbf{P})\}. \tag{1.5}$$

Further, the joint confidence set $\mathbf{C} := \mathbf{C}_1 \cap \cdots \cap \mathbf{C}_s$ is required to have coverage probability $1 - \alpha$ and be *balanced*, in the sense that all tests contribute equally to error control. The first constraint forces the MHT to put in place a mechanism for controlling the FWER, while the second constraint, that is balancing, is a very important property of the test: if lacking balance then the joint test would determine tighter (wider) confidence bands for more (less) variable r_j. In terms of model comparison, the lack of balance would translate into tighter equivalence conditions for worse models and wider equivalence conditions for better ones. The aforementioned procedure is achieved through *pre-pivoting*, see Beran (1988a,b). In fact, indicating with $\mathbf{J}_{n,j}(\cdot)$ the cumulative distribution function of $R_{n,j}$ and with $\mathbf{J}_n(\cdot)$ the left continuous distribution of $\max\{\mathbf{J}_{n,j}, \forall j\}$, the right boundary of the confidence set $\mathbf{C}_j$ is then

$$c_{n,j} = \mathbf{J}_{n,j}^{-1}\left[\mathbf{J}_n^{-1}(1-\alpha)\right]. \tag{1.6}$$

In case of the construction of a double sided confidence set with joint probability $1 - \bar{\alpha}$, define $\alpha = \bar{\alpha}/2$ and compute (1.6) as the right boundaries whereas to determine the left edge, consider the left sided version of $c_{n,j}$, this time defining $\mathbf{J}_n := \min\{\mathbf{J}_{n,j}, \forall j\}$. The solution to (1.6) is the "plug-in" estimate

$$\hat{c}_{n,j}(\alpha, \widehat{\mathbf{P}}) = \widehat{\mathbf{J}}_{n,j}^{-1}\left[\widehat{\mathbf{J}}_n^{-1}(1-\alpha)\right], \tag{1.7}$$

calculated with bootstrapping, cfr. the following Section 1.2.3 and see also Beran (1988a, 1990, 2003). In the series of papers Romano and Wolf (2005a, 2007, 2010), the authors introduce procedures for

the MHT extending the concept of family-wise error rate to that of the k-FWER presented in the previous section, eventually generalising the balanced FWER controlling procedure of Beran (1988a). The generalised FWER expands the capability of targeting multiple false discoveries. Setting k-FWER=α means controlling for the joint probability of *at least* k false discoveries, thereby introducing a target probability of committing joint errors of Type I. The presented procedure allows the construction of the multiple rejection region, complementary to (1.5), which controls the generalised confidence level and which is balanced. In order to obtain balanced right sided confidence sets with k-FWER=α set

$$\mathbf{J}_n := k\text{-}\max\left\{\mathbf{J}_{n,j}, \forall j\right\},$$

in (1.6), with $k\text{-}\max\{y_1 < y_2 < \cdots < y_s\} := y_{s-k+1}$, $k \leq s$.

The procedure just introduced provides a double benefit to multiple testing: first, the extension to controlling the k-FWER of balanced multiple hypothesis tests raises the tolerance to false rejections, therefore it makes the acceptance threshold tighter, eventually increasing the significance of the null hypothesis that are accepted; second, the parameter k draws attention on individual test statistics that are not excessively far away from the acceptance region, whereby adjusting the k-FWER, it is possible to detect weak departures from the null hypothesis.

The definition of the k, the number of tolerated false rejections, might be arbitrary and in general it is good practice to make this number proportional to the total number of hypotheses. To extend the tools available for the MHT, Romano and Wolf (2007, 2010) provide a new algorithm for the automatic selection of the k, with the further benefit of controlling for the tail probability of the *false discovery proportion*. The γ-TPFDP controlling MHT procedure builds directly upon the latter, as the following algorithm shows.

Algorithm FDP: Control of the γ-TPFDP via k-FWER

- Let $j = 0$ and $k_j = 0$;
- **do**
  $j = j + 1$ and $k_j = k_{j-1} + 1$;
  call the k_j-FWER procedure and let N_j be the number of hypotheses it rejects;
  while $N_j \geq k_j/\gamma - 1$;
- reject all the hypotheses rejected by k_j-FWER and **stop**;

The FDP algorithm consists of a sequence of k-FWER procedures, starting with $k = 1$. The routine terminates when the γ fraction of the actual rejections plus one is greater than or equal to the current number of tolerated rejections k_j. Romano and Wolf (2007, 2010) proved that the FDP algorithm delivers balanced asymptotic control of the proportion of false discoveries building upon any k-FWER controlling procedure. The procedure for constructing balanced k-FWER controlling multiple hypothesis tests and the FDP algorithm constitute the engines for the application of MHT to the model selection approach in this thesis.

To further summarise the general MHT approach pursued in this study, we remark that the tests defined in (1.1), in (1.2) and in (1.3) are performed via the construction of the multi-rectangle $\mathbf{C}$ in $\mathbf{T}$ retaining the properties of a balanced confidence set controlling for the joint measure of type I error k-FWER and for its extension γ-TPFDP. Whenever the latter is implemented, the procedure is capable of selecting the k-FWER automatically by targeting the tail probability of the false discovery proportion, a more appropriate control measure for the tolerance level of false rejections that are best selected when scaled to the total number of hypotheses. In order to realise the operating principles of the MHT algorithms presented in this thesis, it is important to notice here the peculiarity of the confidence set method we adopt to implement the hypothesis testing. We do not alter the confidence set[3] and thus target the theoretical critical value, rather than the bootstrap sample means. In the MHT (1.1) and (1.2), the null hypotheses of, respectively, significant performance and benchmark equivalence, are tested by controlling that the target forecast and the zero point fall within each confidence interval. With the MHT (1.3), the distinctiveness of the method is more evident. For each scalar test, we reject the null hypothesis if the zero point falls in the right tail of the statistic distribution, thus we control that the upper bound of the interval is greater than zero to accept the null.

1.2.2 The Step-Down Algorithm

The result achieved by the balanced MHT controlling for the k-FWER can be further improved by means of a *step-down method*, see Romano and Wolf (2005a, 2007) and Romano and Shaikh (2006). This procedure represents an augmentation of the step-wise method conceived to achieve increased power of the MHT, as it has been employed in several experiments of this thesis. The step-down method is designed to increase the probability of to not commit a type **II** error, but it does come at the cost of being computationally intensive when the multiplicity of hypotheses is excessively large. With a step-down procedure, a sequence of MHT is performed by progressively rejecting the least significant hypothesis and hence testing the subset of surviving H_j until no further hypotheses are rejected. These methods aim at strengthening the test result by increasingly pressuring the decision of acceptance of the previous MHT steps. Step-down methods implicitly estimate the dependency structure of the individual tests achieving an improvement in the power of the MHT. The algorithm of Romano and Wolf (2005a) can be described as follows. Let the MHT be the set of m (right hand sided) simultaneous hypotheses

$$H_j \colon R_{n,j} \leq c_{n,K,j}(\alpha, k) \tag{1.8}$$

where now we directly refer to the operational version of the confidence set and further make explicit the association with a set of hypothesis indexes $K = \{1, \ldots, s\}$ and the dependency of c on k. The sets A_m and B_m are, respectively, the sets of accepted and rejected hypotheses at the step m. At the start of the procedure, set $A_0 \equiv K$, i.e. the full set of hypotheses, and the counter $m := 0$. The pseudo-code in algorithm **A** below presents the mechanics of the generic step-down method with control of the k-FWER.

[3] Alternatively, the test might be structured by re-centring the bootstrap distribution around the critical point and hence testing for the bootstrap average. The approach we adopt is a mere programming choice and both procedures are equivalent. In fact, the pre-pivoting of the sample data implies that the confidence set is independent of the location parameter.

Algorithm A: Generic step-down method for control of the k-FWER

– If $R_{n,j} \leq \hat{c}_{n,A_0,j}(\alpha, k)$, $\forall j \in A_0$, then accept all the hypothesis and stop; otherwise, reject any H_j for which $R_{n,j} > \hat{c}_{n,A_0,j}(\alpha, k)$ and include j in B_1; set $A_1 := A_0 \backslash B_1$ and increase the step m by 1;

– **while** $|B_m| \geq k$
reject any H_j for which $R_{n,j} > \hat{d}_{n,A_m,j}(\alpha, k)$ and include j in B_{m+1}, where

$$\hat{d}_{n,A_m,j}(\alpha, k) := \max_{\substack{I \subseteq B_m \\ |I|=k-1}} \{\hat{c}_{n,D,j}(\alpha, k) \colon D = A_m \cup I\};$$

set $A_{m+1} := A_m \backslash B_{m+1}$ and increase the step m by 1;
end

The algorithm **A** is capable of increasing the statistical power, that is the probability of rejecting a false null hypothesis, because at each iteration the subset of the lowest p-value statistics is excluded, tightening confidence bands in the subsequent iteration and hence strengthening the ability to pick true discoveries. However, accounting for *at least* $k > 1$ false discoveries involves the possibility that at the previous stage we have rejected true hypothesis, but hopefully *at most* $k - 1$. As a consequence, at step m we have to consider within the current MHT the event of having previously dismissed $k - 1$ true nulls, a fact that would affect the current critical values. In practice, at each iteration the step-down algorithm searches among all the possible sets of surviving hypotheses augmented with at most $k - 1$ potentially false rejections, to determine tighter new confidence set to run a more stringent test on the accepted H_j's. However, it is not known which of the rejected hypotheses may represent false discoveries. Hence, it is necessary to circulate through all combinations of B_m, of size $(k - 1)$, in order to obtain the appropriate critical values. The algorithm determines a maximum critical value $\hat{d}_{n,A_m,j}(\alpha, k)$ for each hypothesis test j. Iterating through the set B_m to include the event "rejection of $k - 1$ true nulls" might turn out to be a formidable task due to a rapidly growing number of possible combinations of size $k - 1$ from the previously rejected hypotheses. For this reason, the authors propose a streamlined algorithm, which simplifies the computational burden of algorithm **A**.

The rationale of algorithm **B** is to reduce the computational burden due to the number of combinations generated by calculating critical values $\hat{d}_{n,A_s,j}$ by limiting the pool of rejected hypotheses to those that are least significant. The streamlined step-down method tries to reduce the computational effort, limiting the set to be explored to the hypotheses that are most likely to be rejected. As a consequence, the algorithm is as close as possible to the generic algorithm **A** in the sense that it maintains much of the attractive properties of the generic algorithm.[4]. The step-down algorithm defines a search path to strengthen the power of the MHT, driven by the implicit dependency structure of the individual tests. At each iteration the algorithms **A** and **B** minimise the Type **II** error probability, hence improving the statistical power. Notice that in the case of two sided confidence sets the previous algorithms have to

[4] The generic algorithm offers a number of attractive features. Firstly, the generic algorithm is conservative in its rejection of hypotheses. Secondly, the generic algorithm also allows for finite sample control of the k-FWER under P_θ. And thirdly, the bootstrap construction is such that the generic algorithm provides asymptotic control in the case of contiguous alternatives. Romano and Wolf (2007) provide a more detailed discussion.

be modified accounting for left critical values computed as minima across the search set and furthermore including left p-values in the operational method. In this research, MHT applications exploiting the step-down algorithm are presented in Section 2.3 and Section 3.3, whereby both statistical significance and relative performance tests implement the k-FWER procedure with the step-down algorithm.

Algorithm B: Streamlined step-down method for control of the k-FWER

– If $R_{n,j} \leq \hat{c}_{n,A_0,j}(\alpha, k)$, $\forall j \in A_0$, then accept all the hypothesis and stop; otherwise, reject any H_j for which $R_{n,j} > \hat{c}_{n,A_0,j}(\alpha, k)$ and include j in B_1; set $A_1 := A_0 \backslash B_1$ and increase the step m by 1;

– **while** $|B_m| \geq k$
for each $j \in B_m$ calculate the p-value $\hat{p}_{n,j} = 1 - \mathbf{J}_{n,j}$ and sort them in descending order $\hat{p}_{n,r_1} \geq \cdots \geq \hat{p}_{n,r_{|B_m|}}$, where $\{r_1, r_2, \ldots, r_{|B_m|}\}$ is the appropriate permutation of the p-value indices that gives this ordering; then pick a user specified integer $N_{\max} \leq \binom{|B_m|}{k-1}$ and let M be the largest integer such that $\binom{M}{k-1} \leq N_{\max}$;
reject any H_j for which $R_{n,j} > \tilde{d}_{n,A_m,j}(\alpha, k)$ and include j in B_{m+1}, where

$$\tilde{d}_{n,A_m,j}(\alpha, k) := \max_{\substack{|I|=k-1 \\ I \subseteq \{r_1, r_2, \ldots, r_M\}}} \{\hat{c}_{n,D,j}(\alpha, k) \colon D = A_m \cup I\}$$

set $A_{m+1} := A_m \backslash B_{m+1}$ and increase the step m by 1;
end

1.2.3 The Stationary Bootstrap

In order to pursue the ultimate goal of isolating the best performing models the criteria for model selection are required to operate in a particularly problematic statistical context. In the experimental part of this work, we tackle the general problem of model selection in the presence of misspecification, complicated by the inclusion in the model set of non-nested models. We encounter conditions of insufficient information set in defining the complete system dynamics, whereby the system state is partially observable. The derivation of exact or asymptotic statistical tests applied to this class of problems should take into account the further restraint represented by the finite precision of the several numerical procedures involved in the calculation of the crucial measures of model performance. These strong restrictions suggest that limiting distributions encompassing the statistical test are extremely difficult to obtain for reasonably general problems. Therefore, we approach the construction of the tests for model selection by exploiting a sample-based simulation engine that is capable of producing robust estimates of multiple hypothesis statistic distributions. This device is the *bootstrap*.

The bootstrap (Efron, 1979) is a versatile method for investigating a general form of functions depending on the full sample history. In the original form of this procedure, we search for an estimate of the statistic[5]

[5] In the model selection framework, the data function R relies also on a modelling hypothesis $\mathbf{P}_j$ which characterise it. In this paragraph and successively, the probability distribution $\mathbf{P}$ represents the "true" distribution of the observations, that is the DGP, whereby we suppress the model dependency, indicating it if necessary with a subscript j, that is $R_j(\mathbf{X}; \mathbf{P})$,

$R(\mathbf{X};\mathbf{P})$ with $\mathbf{X} = \{X_i\}_{i=1,\dots n}$ and $X_i \overset{\text{iid}}{\sim} \mathbf{P}$. The bootstrap method allows one to construct an estimate of the statistic distribution using the sample distribution $\widehat{\mathbf{P}}$

$$R^\star = R(\mathbf{X}^\star;\widehat{\mathbf{P}}),$$

which consists of repeatedly drawing with replacement observations $X \in \mathbf{X}$, each weighted with probability $1/n$. The distribution estimate of R is generated through the re-sampling $\mathbf{X}^\star$, (m resamplings of $\mathbf{X}$). This procedure is valid under the i.i.d. hypothesis for X. A further generalisation is achieved, for example, with the methods in Künsch (1989), Liu and Singh (1992) or in Politis and Romano (1994b), whereby the bootstrap delivers robust estimates of the distribution of the sample function, R, for stationary and weakly dependent time series. In this work, we employ the *stationary bootstrap* of Politis and Romano (1994a,b). The theoretical justification for the use of this versatile and general procedure can be retrieved from the early works of these two authors. We reproduce here the major result. Let $\mathcal{H}$ be an Hilbert space,

Theorem 1.2.1 (Theorem 3.1 Politis and Romano, 1994a)**.** *Let $X_1,\dots,X_n$ be a stationary sequence of $\mathcal{H}$-valued random variables with mean m and mixing sequence $\alpha_X(\cdot)$. Assume the X_i are essentially bounded and $\Sigma_j \alpha_X(j) < \infty$. Let $\bar{X}_n = n^{-1}\Sigma_{i=1}^n X_i$ and $Z_n = \sqrt{n}(\bar{X}_n - m)$; also, let $L(Z_n)$ denote the law of Z_n. Conditional on $X_1,\dots,X_n$, let $X_1^*,\dots,X_n^*$ be generated according to the stationary bootstrap resampling scheme, with $p = p_n$ satisfying $p_n \to 0$ and $np_n^2 \to \infty$. The bootstrap approximation to $L(Z_n)$ is the distribution, conditional on $X_1,\dots,X_n$ of Z_n^* where $Z_n^* = \sqrt{n}(\bar{X}_n^* - m)$ and $\bar{X}_n^* = n^{-1}\Sigma_{i=1}^n X_i^*$; denote this distribution by $L(Z_n^*|X_1,\dots,X_n)$. Then $\rho\left(L(Z_n), L(Z_n^*|X_1,\dots,X_n)\right) \to 0$ in probability, where ρ is any metric metrising weak convergence in H.*

Proof. See the cited reference. □

In practice, this result establish week convergence for bootstrap estimates that are smooth functionals of the data. We rely on this result to construct non parametric estimates of the target MHT statistics, conceived as function of the sample data $R(\mathbf{X};\mathbf{P})$. Recently, the assumptions for asymptotic and consistency results for the stationary bootstrap have been weakened to more general results, cfr. Gonçalves and White (2002), Hwang and Shin (2012).

Operationally, the stationary bootstrap algorithm starts by "wrapping" the data in circle, such that $Y_t = X_{\tilde{t}}, \forall t \in \mathbb{N}$, with $\tilde{t} := (t \bmod n)$ and the convention that $X_0 := X_n$. A pseudo-time series $\mathbf{X}^\star$ is produced retaining the stationary properties of the original data sample $\mathbf{X}$. The re-sampling scheme requires the construction of blocks $B_{i,l} = \{Y_i, Y_{i+1},\dots,Y_{i+l-1}\}$, generated through the withdrawal of i.i.d. discrete uniform random numbers $I_1,\dots,I_s \in \{1,..,n\}$ and geometric random block lengths $L_1,\dots,L_s$, with distribution function $\mathbf{D}\{L_i = k\} = p(1-p)^{(1-k)}$, $k \in \mathbb{N}$. The generic re-sampled time series is $\mathbf{X}^\star := \{B_{I_1,L_1},\dots,B_{I_s,L_s}\}$. Although optimally choosing the expected block length $1/p$ does not affect the consistency properties of the bootstrap, the optimal p grants the fastest convergence rate of the estimates and therefore their minimum variability, cfr. Politis and White (2004). In the several applications assembled in this work, the artificial samples employed with the purpose of generating

however entailing $R(\mathbf{X},\mathbf{P}_j;\mathbf{P})$.

bespoke statistics distributions are simulated with preconditioning on the optimal p according to the procedure of Politis and White (2004), Patton et al. (2009). In terms of bias and variability of the variance of the pseudo-time series, the stationary bootstrap of Politis and Romano (1994b) is equivalent to other techniques for bootstrapping stationary and weakly dependent sample data. This characteristics was not originally noticed in the work of Lahiri (1999) when comparing several bootstrapping techniques, but successively corrected by Nordman (2009). The most attractive characteristic of the bootstrap approach is its high degree of flexibility. In particular, it can be used with parametric and non-parametric models, non-pivotal statistics, i.e. statistics lacking asymptotic distribution results, and mostly it can capture features of finite sample statistics whose distributions might be sensibly different from asymptotic pivotal results, see Horowitz (2001) for a review on the topic. These features are very appealing in the present context where the goal is to design experiments for model selection based on the performance of models with different statistical properties and targeting measures that might have unknown finite sample or asymptotic properties. Finally, we remark that the analysis that has been conducted in this thesis strongly relies on bootstrap results, the performance of which we do not analyse. However, we notice the result of Beran (1988b), concerning the efficiency of parametric bootstrap estimators with respect to pivotal tests results. In that work, while discussing prepivoting, i.e. the trasformation of the bootstrap test data by its bootstrap null cdf, the author proved that the prepivoted bootstrap quantile, when compared to asymptotic statistics quantile, has a smaller or equivalent order of error in the confidence level if, respectively, the statistic is a pure pivot[6] or it is parameter dependent. Moreover, in the latter case, the order of error of the bootstrap statistic can be made smaller by reiterating pivoting.

1.3 The Model Confidence Set

The central problem of this research has been formalised in Section 1.1, whereby model comparison is achieved by means of a loss function determined by the contrasting of the target model performance measures. In Section 1.2 we have introduced a statistical framework to handle virtually any statistical problem presenting a multiplicity of hypotheses. In the MHT setup, the implementation of simple tests of significance or tests of relative model performance can be derived by simply arranging the appropriate hypotheses, reducing the model selection problem to a matter of experimental design, as for the tests (1.1) and (1.2). Likewise, a general MHT test for the absolute model performance taking into account the complete collection of pairwise model comparisons is outlined in (1.3). Nevertheless, at this stage it has not yet been clarified how to identify the subset of best performing models and draw final conclusions. We might, in the first instance, reject models that do not produce significant performances, if a target value can be identified, and successively iterate across all the relative model comparisons to map out all the pairwise precedence. But how does one synthesise this information into the final partition of the set into superior and inferior models? Is it possible to produce a further model ranking across the set of superior models? For this purpose, it is necessary to consider a framework designed to extract the superior group from the battery of models. The framework we utilise is the model confidence set (MCS). In this section we introduce the MCS along with several procedures to obtain it from the initial model set. It will turn out that the MCS is not unique and it is strictly dependent on the statistical decision rule that controls

[6] In statistics, a pure pivot is a theoretical sample statistic that does not depend on unknown parameters.

the rejection of inferior models. In the following, we present one version of the algorithms introduced by the seminal article Hansen et al. (2011), followed by a novel test inspired by the procedure in Corradi and Distaso (2011) and finally, as a further contribution to the literature, we construct a new algorithm bringing the MCS within the generalised MHT framework and complete the definition of the test (1.3).

The MCS is the key concept that we exploit in this research for the construction of an absolute performance model selection procedure that is the subset $\mathcal{M}^\star$ of the initial model set $\mathcal{M}_0$ that with a certain degree of confidence represents the best sub-group of equivalent models. The MCS (Hansen et al., 2011) is the subset of best models that have equivalent performance, formally defined as

Definition 1.3.1. *The set of superior models is*

$$\mathcal{M}^\star \equiv \{\mathbf{P}_i \in \mathcal{M}_0 \colon \mu_{ij} \leq 0,\ \forall \mathbf{P}_j \in \mathcal{M}_0\}\,.$$

From 1.3.1, the set of best models is the subset $\{\mathbf{P}_i\}$ of equivalent models such that any other model in $\mathcal{M}_0 \backslash \mathcal{M}^\star$ has an inferior expected performance. The characterisation of the property $\mu_{ij} \leq 0,\ \forall \mathbf{P}_j \in \mathcal{M}_0$ will thus determine the final MCS. Actually, it turns out that methods to construct MCS can be various. In fact, with the procedure of Hansen et al. (2011), the MCS final property is deduced from an iterative procedure exploiting the $T_{R,\mathcal{M}}$ statistic, instead of the direct analysis of the null hypotheses $t_{ij} = 0$. On the contrary, in this study we aim at constructing the MCS by actually testing the complete set of model comparisons and hence extracting the final MCS by the analysis of the testing outcome. In the following we introduce a plain version of this novel test that isolates the MCS by testing individually the pairwise comparisons for model superiority. Furthermore, when combining the MCS property with the generalised MHT in the original contribution provided in this thesis, the MCS is constructed by testing the full set of pairwise comparisons taking into account the test dependencies and controlling for the k-FWER. The immediate consequence of the various configurations that the test might display is that the MCS will not be unique as a result of the statistical rule discriminating the hypotheses about multiple comparisons. However, we would expect that algorithms selecting the MCS return outputs that entail at least set inclusion. This is an important property that is explored only empirically, in this research.

In the following we introduce several procedures to obtain $\mathcal{M}^\star$, as well as the confidence levels entrusted to the MCS.

1.3.1 The *max*-MCS

The original idea of the MCS was introduced in Hansen et al. (2011). The implementation of the test involves an augmentation of the RC / SPA test, combined with a sequential approach that relies on the Holm (1979) sequence of scalar *equivalence tests* $H_{0,\mathcal{M}_k} \colon T_k = 0,\ k = 0, 1, \ldots,$ producing the model sequence $\mathcal{M}_0 \supset \mathcal{M}_1 \supset \cdots \supset \mathcal{M}_k$. With reference to the test version we adopt in the empirical application of this work, the statistic T_k is defined as

$$T_{R,\mathcal{M}_k} = \max_{\mathbf{P}_i, \mathbf{P}_j \in \mathcal{M}_k} t_{ij} \tag{1.9}$$

and involves the calculation of the sample statistics $\bar{d}_{ij} = \frac{1}{T}\sum_t d_{ij,t}$ and their standardised values $t_{ij} = \bar{d}_{ij} \Big/ \sqrt{\frac{1}{T}\sum_t d_{ij,t}^2 - \bar{d}_{ij}^2}$. The target statistic (1.9) is the scalar analogue of the multiple hypothesis of equivalence among the models and, in its maximisation, grants control of the probability of committing at least one false rejection (the family-wise error rate, cfr. Section 1.2). The test sequence terminates the first time that the null hypothesis is accepted, that is at $\min k\colon |H_{0,\mathcal{M}_k}| = 1$. Each time $|H_{0,\mathcal{M}_k}| = 0$, the model with the worst target statistic is expelled from the model set $\mathcal{M}_k$. This is the *elimination rule*. Concerning the definition of $T_{R,\mathcal{M}_k}$, it has to be noticed that the version adopted in this work of the test $H_{0,\mathcal{M}}$ based on the statistic (1.9) is not constructed from the absolute value of t_{ij} as in the reference article. In the case of adopting the absolute value of the statistic, the worst and the best relative model comparisons, say t_{uv} and t_{vu} would produce the same p-value, leaving ambiguity as to which model to reject at the current step. We represent the general algorithm with the following pseudo-code:

Algorithm max-**MCS**: Hansen et al.'s MCS (2011)

Let $\mathcal{M}_0 \equiv \{\mathbf{P}_i\}_{i=1,\dots,m}$, $k = -1$
do
  $k = k + 1$
  compute the $c(1-\alpha)$ quantile of the $T_{R,\mathcal{M}_k}$ distribution under $H_{0,\mathcal{M}_k}$
  if any $t_{ij} > c$ **then**
    Let $\mathbf{P}_r$ be the model producing the highest t_{rs}
    $\mathcal{M}_{k+1} \equiv \mathcal{M}_k \setminus \{\mathbf{P}_r\}$
  endif
while $|H_{0,\mathcal{M}_k}| = 0$
set $\mathcal{M}^\star \equiv \mathcal{M}_k$ and **stop**

The construction of the test is based on the CLT result $\sqrt{T}(\bar{Z} - \mathbb{E}\bar{Z}) \xrightarrow{d} N(0, \Omega)$, as $T \to \infty$, with $\bar{Z}_s^{(k)} = \bar{d}_{ij}$, $\mathbf{P}_i, \mathbf{P}_j \in \mathcal{M}_k$ and $i \neq j$, with $s = 1, \dots, m_k(m_k - 1)$. For the implementation of the MCS, we need to structure the equivalence hypothesis among the test comparisons as jointly distributed as a multivariate normal $\xi^{(k)}$ and then derive the asymptotic distribution for $T_{R,\mathcal{M}_k}$ that corresponds to the distribution of the $\max_s \xi_s^{(k)}$. The matrix Ω_ξ is estimated with a bootstrap technique. A full bootstrap version of the test can be obtained by centring around the zero the bootstrap distributions of the d_{ij}. The standardisation of the relative performance measures introduces a balancing factor by the homogenisation of the domain of variation of the target variables, in the sense that if the individual statistics were all distributed as the standard normal, the same critical value would produce matching confidence at the individual test level and with respect to the FWER. To define a p-value for this MCS, we indicate with $\hat{p}_{\mathcal{M}_i}$ the sought value for the max test at step i and eventually the sequence $\hat{p}_j \equiv \max_{i \leq j} \hat{p}_{\mathcal{M}_i}$ up to the last model set $\mathcal{M}_k$ before the MCS, whereas $\hat{p}_s$, for $k < s \leq m$ are the p-values of the best models computed from the max distribution associated with $\mathcal{M}^\star$, see Hansen et al. (2011) for further discussion and illustration of the MCS p-value. The MCS test is a powerful tool, which allows one to automatically select the subset of best performing models, at the same time producing a model ranking as a result of the elimination sequence.

1.3.2 The t-MCS

With the second method we present in this study, we introduce the core argument by which novel MCS tests are constructed. The intuition consists in assembling statistical tests that target the full collection of pairwise model comparisons, whose outcome is exploited for the identification of the models that are characterised by the MCS property 1.3.1. The main feature of our alternative tests is that of direct model performance comparison, whereas in contrast the *max*-MCS hinges on the equivalence between the model confrontation and the max statistics. The first contribution we provide is indicated as the t-MCS, whereby we are inspired by the procedure presented in Corradi and Distaso (2011) and design two variations of a new plain test of model multiple comparison. An application of the *max*-MCS and the t-MCS to market risk model selection is presented in Cummins et al. (2017). From an operational perspective, the MCS performs a random sequence of model benchmarking, whereby at each iteration inferior models are rejected until all the surviving models are deemed equivalent. The rejected model set may include the current benchmark, if inferior to any competitors. The following pseudo-code describes the algorithm:

Algorithm t-MCS: Corradi et al.'s MCS (2011)

Let $k = 0$, $\mathcal{M}_0 \equiv \{\mathbf{P}_i\}_{i=1,\dots,m}$, $\mathcal{B}_0 \equiv \emptyset$
do
  pick any $\mathbf{P}_j \in \mathcal{M}_k \backslash \mathcal{B}_k$
  compute the t_{ij}, $\forall i \neq j$
  call the *relative performance test* and let $\mathcal{E} \equiv \{\mathbf{P}_u \in \mathcal{M}_k : \mathbf{P}_u \prec \mathbf{P}_j\}$
  if there is a $\mathbf{P}_s \in \mathcal{M}_k : \mathbf{P}_s \succ \mathbf{P}_j$ **then**
    $\mathcal{E} \equiv \mathcal{E} \cup \mathbf{P}_j$
  endif
  $k = k + 1$, $\mathcal{M}_k \equiv \mathcal{M}_{k-1} \backslash \mathcal{E}$, $\mathcal{B}_k \equiv \mathcal{B}_{k-1} \cup \mathbf{P}_j$
while $\mathcal{M}_k \backslash \mathcal{B}_k \not\equiv \emptyset$
set $\mathcal{M}^\star \equiv \mathcal{M}_k$ and **stop**

The random benchmarking will generate a unique outcome if the decision rule is independent from the sequencing. This can be achieved by considering a test statistic and hence critical values that remain unchanged irrespective of the benchmark picking process. Nonetheless, the randomised sequence is not strictly necessary for the construction of the test. In fact, if we consider all possible benchmark sequencing we see that a model belongs to the MCS only if the collection of its expected relative performances are significantly equivalent or superior to each and every competitor when it is either taken as the benchmark or it is compared to a benchmark. By the symmetry of the t_{ij}'s, the statistical preference rule that defines the t-MCS leads to the same result whether the benchmark is $\mathbf{P}_i$ or $\mathbf{P}_j$. Therefore, a model will enter the MCS if and only if no dominant model can be identified. The t-MCS can therefore be simplified by circulating the benchmark through $\mathcal{M}_0$ and rejecting the benchmarks that have at least one dominant model, allowing the identification of the MCS in one single step. The pseudo-code for this modified algorithm can be written as:

ALGORITHM MODIFIED t-MCS

Let $\mathcal{M}_0 \equiv \{\mathbf{P}_i\}_{i=0,\dots,m}$, $\mathcal{B}_{-1} \equiv \emptyset$
for $k = 0$ **to** m
  compute t_{ik} $\forall i \neq k$
  call *relative performance test*
  if there is a $\mathbf{P}_i \in \mathcal{M}_0$: $\mathbf{P}_i \succ \mathbf{P}_k$ **then**
    $\mathcal{B}_k \equiv \mathcal{B}_{k-1} \cup \mathbf{P}_k$
  else
    $\mathcal{B}_k \equiv \mathcal{B}_{k-1}$
  endif
endfor
set $\mathcal{M}^\star \equiv \mathcal{M}_0 \backslash \mathcal{B}_m$ and **stop**

In contrast to Corradi and Distaso (2011)[7], we define the model preference rule by appealing to the CLT for dependent sequences to construct asymptotic scalar tests for each relative model comparison. The single fixed critical value $\Phi^{-1}(1-\alpha)$, that is the α-right tail inverse cumulative normal distribution, is exploited for the individual scalar relative model comparison test. This strategy allows control of the confidence level for each scalar model comparison, but does not take into account test dependencies, which are considered with joint model multiple comparison. This MCS test achieves model comparison by either a random sequence or by a thorough cycle, which are equivalent procedures. As noticed at the opening of this section, the approach we take with the analysis of the complete collection of model confrontations is the building block of our alternative test, that in the forthcoming Section 1.3.3 is combined with the generalised MHT framework to derive the novel γ-MCS. The t-MCS designed here, can be considered as a streamlined version of that one, hinging on independent asymptotic statistics. In this light, it will be interesting to compare the results of this test with those of the γ-MCS, which, as presented below, employs the full arsenal of the MHT framework. Refining the t-MCS, we introduce a ranking system for the MCS, a feature that cannot be produced by the original version of the t-MCS. For this ranking system, we define the t-MCS p-value by taking the worst expected relative performance for each model as determined by the bootstrap method and computing the complement of its quantile on a standard normal distribution. This number represents the probability of committing a false rejection under the hypothesis of equivalence with its best competitor. Akin to the case of the *max*-MCS p-value, the higher our t-MCS p-value the more confidence we have that a model is a member of the MCS.

We finally remark that for the *max*-MCS and t-MCS experiments pursued in this study, we compute the sample statistics as bootstrap expectations, in order to render the testing results more robust to small sample bias.

[7] In Corradi and Distaso (2011) the authors chose $\sqrt{2 \log \log T / T}$, a value that grants what they call a doubly consistent MCS, that is a model confidence set estimate which contains the "true" MCS with probability one and includes inferior models with probability zero.

1.3.3 The γ-MCS

With the t-MCS introduced in the previous subsection, we have provided a test whereby the multitude of hypotheses of the problem is central. The MCS is achieved with an algorithm employing scalar relative performance tests. However, as anticipated, a limitation of this new elaboration is the disregard of the dependency of the hypotheses. In this subsection, this alternative test construction is combined with the general MHT approach to reconcile the multiple comparison nature of the model selection problem with the MCS concept obtaining a new statistical test for the selection of the set of the best equivalent models from a given model set of competitors. The proposed test can be seen as an extension to the plain t-MCS device, which explores the model selection problem in a complete direct model contrasting, taking into account the multi-hypothesis nature of the problem. The motivation for constructing an alternative MCS test that takes into account test dependencies, can be found in the conjecture that the MCS is not unique. This hypothesis is indirectly explored with the experimental exercises that have been conducted in this thesis. Concerning the *max*-MCS, the solution provided exploits the correspondence between the hypotheses set represented by the sequence $H_{0,\mathcal{M}_k}$ and the multiple hypothesis $\{H_{ij}\}$, providing also control for the FWER. This correspondence, however, holds asymptotically whereas small sample distributions might not grant that an MCS constructed through the *max* statistic corresponds to an MCS constructed with a statistical test exploring the whole combinations of pairwise comparisons and furthermore controlling for the generalised k-FWER. In this thesis, we will learn through empirical evidence that the latter conjecture is verified, providing further confirmation that the MCS is not unique and, indeed, depends on the statistical procedure structuring the model preference ordering.

As an original contribution to the model comparison testing problem, we propose a new version of the MCS test developed within the MHT approach, which achieves a further level of flexibility by allowing balancing and strong control of k-FWER. Indeed, the intuition lies in noting that the construction of the MCS corresponds to the identification of the models that are inferior to no other model. The setup of the test has been anticipated in Section 1.2 when defining the test in (1.3), which is reproduced here for the reader's convenience. The MHT for the identification of the set of equivalent superior models is structured as follows:

$$H_{ij}: \mu_{ij} \geq 0, \ \forall \mathbf{P}_i, \mathbf{P}_j \in \mathcal{M}_0, i \neq j$$

which represents the complete set of the hypotheses[8] of *at least* model equivalence to be submitted to the testing framework. The rejection of the inferior models in $\mathcal{M}_0$ would leave the set of equivalent superior models $\mathcal{M}^\star$. A γ-TPFDP version of the MCS, which is coined γ-MCS, corresponds to the following steps, as outlined in pseudo-code:

[8] It is interesting to notice that the number of hypotheses that the construction of the MCS actually involves is way larger than the number of models m. Therefore, allowing for flexibility in controlling for the k-FWER provides an additional instrument that permits to raise the tolerance above the model level rather than controlling for the false rejection of individual model comparisons.

Algorithm γ**-MCS**: MCS with MHT controlling for the γ-TPFDP

Let $\mathcal{M}_0 \equiv \{\mathbf{P}_i\}_{i=0,\dots,m}$, $\mathcal{B} \equiv \emptyset$

call the γ-TPFDP(α) procedure and

store the joint confidence set $\mathbf{C}$

set $\mathcal{B} \equiv \{\mathbf{P}_j \in \mathcal{M} \colon \exists$ at least a $\mathbf{P}_i$ such that $|H_{ij}| = 0$ with $c_{ij}(1-\alpha) < 0\}$

set $\mathcal{M}^\star \equiv \mathcal{M}_0 \backslash \mathcal{B}$ and **stop**

In practice, the test is essentially made up of two steps: a first step where a γ-TPFDP(α) is run and inference is jointly drawn about the model $\mathbf{P}_j$'s equivalence or superiority hypotheses $\{H_{ij}\}$, that is the generalised MHT on the full set of pairwise comparisons are progressively constructed until the loop breaking condition of the FDP algorithm in Section 1.2.1 is reached[9]; a second step where the collection of the outcomes is explored to search for rejection events, whereby the inferior models are identified and dropped from $\mathcal{M}_0$. The latter step is necessary because the MHT returns hypotheses on the individual comparisons that must be searched in order to identify those elements that contradict the Definition 1.3.1. As noticed in Section 1.2 each individual hypothesis is formulated as a right-tailed test, whereby the conjecture for the generic statistic t_{ij} is "model $\mathbf{P}_j$ is at least equivalent to model $\mathbf{P}_i$". Operationally, we search for confirmation that the zero is at the left of the right hand boundary of the balance confidence interval $c_{ij}(1-\alpha)$. Were we to test equivalence[10], we should control for the left hand boundary $c_{ij}(\alpha)$. However, our effective target is the identification of the MCS, therefore after the MHT, we only need to select the rejected hypotheses, which correspond to models that are inferior to at least another element of $\mathcal{M}_0$. The correspondence is one-to-one as we are considering the full set of right-tailed hypotheses, therefore targeting the model $\mathbf{P}_j$, with the test statistic t_{ij}. Finally and to conclude the test, the procedure moves from the test results to the model set $\mathcal{B}$, by collapsing the hypotheses collection to the set of models that have been rejected at least once. After the latter set has been removed from the initial model set $\mathcal{M}_0$, we are left with the MCS, because the set $\mathcal{M}^*$ does not contain any inferior models, therefore the survivors must be all equivalent. The model set $\mathcal{M}^*$, obtained as described, thus satisfies the definition (1.3.1). With the γ-MCS, we are investigating the MCS as the remainder class, once the inferior models have been eliminated. In fact, $\mathcal{M}_0 \backslash \mathcal{B}$ contains equivalent models that are at least equivalent to any other model in $\mathcal{M}_0$. If that was not the case and the final set contained an inferior model, than the procedure would yield a contradiction. On the other hand, if two models in the remainder were not equivalent then either of the two would be an inferior model, yielding another contradiction.

Notwithstanding the superior statistical properties of the γ-MCS inherited from the MHT framework

[9] If the implemented version requires a k-FWER that is set in advance, the γ-TPFDP loop is discarded and the algorithm runs directly the MHT with the target number of least amount of tolerated false rejections, with a given probability.

[10] The choice of constructing the algorithm by targeting the right hand tails is a programming strategy, whereas an algorithm considering the (numerically more restricted) set of bidirectional hypotheses and therefore employing hypotheses such as "models $\mathbf{P}_i$ and $\mathbf{P}_j$ are equivalent" could be employed, as well. The substantial difference would be that in our algorithm the distribution of the $\mathbf{J}_n$ in (1.6) involves the right tail of t_{ij} and its left tail through t_{ji} by merging them, whereas a two-sided test would keep left and right tails of t_{ij} distinct and there would not be the need of a t_{ji} statistic. In the latter case though, including the first or the second statistic would affect the distribution of k-min$\{\mathbf{J}_{n,j}, \forall j\}$ and k-max$\{\mathbf{J}_{n,j}, \forall j\}$ and therefore change the outcome of the test, inducing non-uniqueness of the result. Avoiding the latter issue would entail the inclusion of both hypotheses of equivalence for t_{ij} and t_{ji}, therefore eliminating the problem of which sequence of the orientation of the axis of the L's characterises the set of equivalence. Nonetheless, another problem arises because under this configuration we would be duplicating the actual test hypotheses and therefore overstructuring the rejection region. The solution employed for the construction of the γ-MCS entails no ambiguity for the region of rejection and produces a unique bootstrap distribution of the multivariate statistic.

which this construction relies upon, this procedure cannot produce either a ranking across the initial and the rejected model sets, as it lacks an Holm-like sequence as in *max*-MCS. Exploiting the bootstrap machinery, we resort to a wider definition of the MCS p-value, which, as opposed to the more conventional MCS test, is independent from the algorithm that isolates the set of best models. We define the p-value attached to model i by the γ-MCS as the probability of observing a relative model performance less than zero, with respect to the probability distribution of the union of the events t_{ij}, $\forall \mathbf{P}_j \in \mathcal{M}^\star$ and represents the probability of observing a superior performance of model i with respect to the model confidence set $\mathcal{M}^\star$. We notice that the target value represents the probability of model i to be included within the MCS, as of the multivariate distribution of the model performance measures, estimated via the bootstrap. The γ-MCS p-value contrasts with the *max*-MCS p-value taken out of $\mathcal{M}_k$ for model i, which represents the probability of observing worst performances off the worst performance statistic $T_{R,\mathcal{M}_k}$, were the models equivalent and compared at step k. The γ-MCS p-value is also different from the t-MCS p-value attached to model i, as the latter represents the probability of observing worst performances of the benchmark i, were it equivalent to its best performer, as identified by the bootstrap expectations. We notice further that the latter two MCS procedures rely on asymptotic normal results, whereas the γ-MCS hinges on the balanced bootstrap confidence sets and therefore it is expected to be more robust to non pivotal sample distribution.

1.4 Thesis Summary

The last few decades have witnessed an increased complexity in the average model employed in the financial industry. This complexity is continuing to rise and permeating all aspects of financial decision making. Complex models are used not only in derivative pricing but are as well employed to measure and control market risk, investment credit risk, counterparty risk, liquidity risk, and more. The potential for operational risks resulting from the misuse, or worse from the misunderstanding of the functioning of, a model is remarkable. In April 2011, the US Board of Governors of the Federal Reserve System published the Supervisory Guidance on Model Risk Management (SR 11-7), which defines model risk as the "potential for adverse consequences from decisions based on incorrect or misused model outputs and reports", Office of the Comptroller of the Currency (2011, p. 3). SR 11-7 typifies incorrect model outputs, taking account of all errors at any point from design through to implementation. The European Banking Authority's Supervisory Review and Evaluation Process (SREP) requires that model risk be identified, mapped, tested and reviewed. For this purpose, financial institutions have been structuring internal model validation units in charge of the whole process of model risk evaluation. Among the many aspects of model validation, one important step consists of the benchmarking of the chosen model, with the ultimate objective of ranking the model set according to meaningful model performance measures. In defining the tasks of model validation in Basel Committee on Banking Supervision (2009, p. 6), the regulator remarks that the valuation results should be confronted with an "independent benchmark model". Within this industry and regulatory context, the studies presented in this thesis would be of particular interest to financial practitioners. We provide a statistically robust framework whereby model comparison and hence selection can be performed within a systematised approach, which only requires the definition

of the target model performance measure. With this thesis, we organise methods for model selection that reduce the complex task of the comparison and ranking of models to a question of experimental design.

The experimental model selection exercises assembled and performed in this thesis provide new evidence in applied statistics for finance. Drawing on the suite of methods set out in Section 1.3.1, Section 1.3.2 and Section 1.3.3, we tackle several model selection problems, applying relative model performance MHT, the MCS and, through our methodological contribution, an MHT version of the MCS. The novel MCS test allows to control the generalised k-FWER and further the γ-TPFDP. As we concentrate on largely flexible model selection procedures, the subjects can be varied. We have decided to look at three typical prototype problems in investment portfolios exposed to market risk, that is the estimation of several portfolio risk metrics such as the VaR and the ExS, as well as the estimation of the historical and the risk-neutral measures of widely employed stochastic processes in finance, such as jump-diffusion models. The choice of these subjects of investigation is mainly related to the background of the author of this manuscript, who has spent more than a decade working with applied econometrics in the wealth management industry. We argue that these problems have an immediate appeal for practitioners. Nonetheless, this choice is merely discretional as several other applications can be envisaged in the field of applied econometrics. The following describes the layout of the thesis and sets out the main contributions of each chapter, while highlighting a range of interesting findings that emerge. The concluding paragraphs of this section summarise the evidence in relation to the comparison of the testing procedures that have been implemented in this thesis.

In Chapter 2, we deal with the forecasting of some key measures in market risk management. These are the value-at-risk and the expected-shortfall. We employ several econometric techniques to construct market risk forecasting models that are confronted in an exercise similar to that of Bao et al. (2006). The original contribution of our work lies in the application of generalised MHT and MCS techniques to market risk forecasting model performance comparison. By means of the MHT framework, we provide new evidence departing from the results of Bao et al. (2006), while at the same time delivering robust inference for the identification of the best market risk models. While the MHT based tests from this chapter have already been published in Esposito and Cummins (2015), post this publication, the analysis for this chapter has been extended to include the construction of the *max*-MCS, t-MCS and γ-MCS. The empirical results that we obtain diverge significantly from the evidence collected in Bao et al. (2006). The target risk measures are the VaR and ExS forecast on 1-day and 10-day time horizons. We apply model performance significance tests that are balanced and control for the k-FWER, with the auxiliary benefit of the statistical power augmentation delivered by the step-down method. The absolute model performance tests introduced with the MCS concept, have the ability to identify the subset of the best performing models and produce a model ranking via the p-value measure, providing results that are more informative than the RC p-value, which in Bao et al. (2006) fails to detect any model superiority over the benchmark RiskMetrics model. In general, we find that models which account for volatility mean reversion and fat-tailedness result in the best performance. This result is in contrast with previous findings and shows that GARCH rolling window parameter estimates introduce high model uncertainty, inevitably compromising their forecasting performance. The quantile regressions approach is shown to

perform quite well. Model performance is generally found to be more widespread on longer horizons. The expected-shortfall at 5% on a 1d horizon seems to be the most difficult to forecast, exhibiting the smallest MCS. Historical Simulation, which is a common practice approach in industry, performs reasonably, resulting in mid-ranking performance. Risk Metrics, another popular model among practitioners, does not exhibit a noticeable performance and on the short term horizon enters the MCS only in the value-at-risk at the 5% level.

In Chapter 3 we approach the problem of time-series estimation of jump-diffusion (JD) models, producing experiments involving models of stochastic volatility and state dependent jumps with a latent single-factor. In an important contribution, we investigate the model aliasing of structurally different models, whereby model aliasing in our context is the observed behaviour that models, which have distinct dynamic features, nonetheless produce densities and estimates of the latent factor that are similar and statistically exchangeable. In the same context, we develop a market data exercise that contributes with experimental information to works such as Andersen et al. (2002), Chernov et al. (2003), Eraker et al. (2003), showing, with the support of multiple comparison model selection procedures, that alternative models are able to produce superior model performances with parsimonious parametrisation. We present a novel exercise of model selection applied to likelihood estimation and the latent factor filtering with a JD model set acting on simulated and financial market data. We uniquely employ MHT and MCS techniques to produce relative and absolute model performance comparison. Moreover, for estimation purposes in our JD setting, we extend the second order filtering procedure in Maybeck (1982) to allow jump components in the system state. The model set we consider contains the popular affine single factor stochastic volatility model, augmented with a CEV parameter. The affine model is extended with rare jumps in return under several specifications. The model set is extended with a stochastic intensity high frequency jump class coupled with a constant volatility diffusion component, representing a non standard alternative model family. The latter model class is taken into account as an alternative specification, whereby the volatility clustering is generated by means of mean-reverting stochastic intensity. Both model families can include a jump in the latent affine factor, generating either stochastic diffusion or stochastic intensity. Under simulated tests, the respective nesting models prove to be able to produce similar features to one another, with respect to the performance measures. The latter result reinforces the findings of the empirical exercise, whereby the stochastic intensity family exhibits superior models in the majority of the tests. The strong conclusions that we are able to make from the analysis is that there is a redundancy to jumps in volatility when measuring marginalised likelihoods, as well as a non-significant prevalence of this component with respect to the latent component filtering measures. The contribution of jumps in volatility appears to be dubious, contrary to the findings of Eraker et al. (2003) and more in line with the model selection results of Chernov et al. (2003), though our findings are more explicit than the latter. Secondly, high empirical kurtosis and moderate asymmetry are found to be prevalent features, that can be captured with both conventional and non conventional models, that is CEV with jumps as well as stochastic hazard models with high average frequency of jumps, with the latter class performing slightly better under the filtering measures. Third, our findings point to the redundancy of mixing both stochastic diffusion and stochastic intensity to model historical equity financial time series.

Finally, with Chapter 4, we make a unique contribution through channelling, for the first time, the flexibility and robustness of MHT and MCS methods to the problem of derivative pricing, whereby we test different families of stochastic volatility models augmented with several types of jumps. The battery of tests allow the comparison of option pricing models with respect to the mean squared pricing errors. We employ a large sample of S&P 500 index options in our empirical analysis. We contribute to literature in several directions. We construct model comparison tests with novel MCS techniques targeting a vast array of option pricing models, the majority of which result from original combinations of jump and volatility specifications relative to the existing literature. This study provides empirical evidence of strong aliasing amongst many option pricing models, ranging from high to lower levels of complexity. This suggests scope for model simplification, which counters the trend in the academic literature towards ever more complex derivatives pricing models. The model selection procedures we apply provide robust evidence indicating that the popular single factor affine specification, extended in several directions, is strongly rejected. Moreover, model augmentation such as jump in volatility, stochastic hazard and the parametrisation of the elasticity of the diffusion factor are probably excessive complications. A simple model, such as the correlated exponential volatility diffusion, perform very well in the OTM option sample, whereas the inclusion of a compensated single directional exponential jump in returns produces one of the top performances for the ALL option sample.

In the Appendix A we provide technical details regarding the main algorithms developed throughout the experimental parts and some proofs, whereas the Appendix B presents several algorithms in pseudo-code that have been used for the experiments.

With respect to a thorough comparison of the flagship tests of this thesis, i.e. our version of the established MCS test and our novel MHT based MCS, we remark that this task is beyond the scope of this work. However, here we elaborate further as to why the MHT approach should be preferred. A first important theoretical reason for our inclination towards the γ-MCS is certainly the lack of control for the generalised FWER of the method of Hansen et al. As noticed in Romano and Wolf (2007), when the number of tests in an MHT becomes large, control of the mere FWER becomes too stringent. In fact in the latter scenario, the possibility of committing at least one false rejection grows to certainty, whereas controlling at a high confidence level might force the test to accept a larger number of nulls. This reasoning led the authors to a relaxation of the family-wise error concept, namely, the k-FWER. Another important theoretical reason for preferring the MHT approach is represented by the concept of *strong* control of the FWER as opposed to the *weak* control, the latter defined as the control of the FWER conditional on the joint full set of hypotheses being true, whereas the former is referred to the conditioning on any subset of hypotheses picked from the complete set. It is acknowledged that allowing for strong control might be revealed as a formidable task. In the seminal paper Romano and Wolf (2005a), the authors point out that the closure method of Marcus et al. (1976) can be used to construct methods that control the FWER of the MHT H_i, $i \in \{1, \ldots, k\}$, if we know how to test each intersection hypothesis H_K, which denotes the hypothesis that all H_j are true, with $j \in K$ and for any $K \subset \{1, \ldots, k\}$. This method can be used together with the idealised method of Romano and Wolf (2005a) to construct a stepdown algorithm that grants strong control of the FWER. From the perspective of this latter work, the MCS algorithm

of Hansen et al. (2011) can be viewed as an idealised stepdown method, whereby the $T_{n,i}$ statistics are the max over all j models loss functions $L_{i,j}$, for each benchmark model i, and the critical value c_{n,K_s} is the *max* statistic at iteration s for the set of surviving models K_s. In their seminal paper Romano and Wolf point out that, with the purpose of avoiding the construction of $2^k - 1$ tests and allowing for strong control, it is possible to construct k-order methods, provided that the theoretical statistic satisfies at least the subset pivotality condition[11] of Westfall and Troendle (2008) or the *monotonicity condition*[12], which is at the base of their bootstrap and subsampling construction of stepdown methods allowing for strong control of the simple and generalised FWER. To the best of our knowledge, it is not clear if the MCS of Hansen et al. (2011) grants for strong control of the FWER[13]. The latter should be the topic of more focused future research.

In more practical terms, what we have achieved in this thesis, with regard to the confrontation of the two MCS methods, is the collection of qualitative evidence. We have encountered diverse circumstances. In the market risk forecasting exercise of Chapter 2, the model set elements achieve moderately homogeneous performances, at least on the one day horizon, allowing the *max*-MCS and the γ-MCS to isolate the cluster of best models. The MHT based test can furthermore modulate the sensitivity to false rejections and incrementally reduce the model confidence set, which exhibits sensitivity to this parameter. Higher tolerance to false discovery shrinks the MCS toward the t-MCS outcome, which in general manifests a more aggressive outcome, providing a more restricted MCS in the majority of the experiments. When the model comparison is more ambiguous as in the ten day market risk forecast horizon or in the artificially generated model aliasing of the jump-diffusion model estimation experiments of Chapter 3, all of the MCS tests struggle to identify the best model set, although the γ-MCS provides a more informative model ranking measure, while the t-MCS results in a tighter selection. The latter test might be useful as a quick diagnostic tool to identify the region containing the candidate best models or in conditions where it is difficult to distinguish models, the t-MCS might provide a term of comparison for various γ values in the γ-MCS. The behaviour of the tests in the market data experiment of the jump-diffusion model estimation exercise presents a condition where all the statistics agree upon the size of the MCS. In this case, the MCS is pretty much insensitive to the γ-TPFDP controlling parameter. Finally, in the last chapter, Chapter 4, of this thesis we are confronted with a very large option pricing model set experiment, whereby the model components are shown to perform very closely to one another. In this exercise, the ability of the γ-MCS to modulate the result by targeting different k-FWER allows one to focus upon the set of best performing models, whereas the benchmark test *max*-MCS is incapable of providing any screening of the large option pricing model set, failing to reduce the initial set at a 10% confidence level. This is an interesting outcome that shows the limitations of the *max*-MCS in the presence of a large model set and should be connected to the control of the simple FWER, which is revealed to be too stringent is such a context. A further indication of this relation can be found in the ability of the γ-MCS to restrict

[11] The subset pivotality condition states that, heuristically, the statistic joint distribution that is used to test the subset of true hypothesis is not dependent on the truth or falsehood of the remaining hypotheses.

[12] The monotonicity condition is satisfied if the algorithm is such that, given the set J contained in set K, $J \subset K$, then the critical values produced by the algorithm $c_{n,J}$ and $c_{n,K}$ associated, repectively, with the set J and K, are such that $c_{n,J} \leq c_{n,K}$.

[13] It has to be noticed that in Romano and Wolf (2005a), the authors remark that the *reality check* of White (2000), which might be seen as a subcomponent of the MCS test, allows for the weak only control of the FWER.

the final set by relaxing the number of allowed false rejections at the target confidence level. Moreover, as the MHT based MCS permits the direct testing of the complete set of model comparisons by constructing specific confidence intervals, a more granular check of the order of precedence is possible, whereby in a tightly competing model set, several model contrasting measures might be close to the rejection tail and the triggering of the k-FWER would allow the user to expose these borderline behaviours. A further point of comparison can be identified in the behaviour of the p-value, that in the case of the max-MCS exhibits the tendency for a lack of discriminating capacity between the top section of the MCS components. This feature might be related to a finite sample distribution bias, a characteristic that has not been explored. Ultimately, the p-value model ranking measure that we construct for our novel test, provides a highly significant ranking factor that does not produce the counterintuitive result of the max-MCS's p-value.

1.5 Concluding Remarks

In this chapter we have defined the model selection framework to be used in the applied econometrics exercises of the following chapters, whereby we have specified the notion of significance of the model performance, relative and absolute model comparison. In the following chapters we produce statistical experiments of the latter type. Furthermore, we have introduced the multiple hypothesis testing framework and defined the model confidence set. With respect to the latter concept, we design a MCS test with the Hansen et al. (2011) approach, the max-MCS and introduce two alternative novel tests, the t-MCS and the γ-MCS. Both tests hinge on the full collection of the pairwise comparisons of the model set components. In the first procedure, the test dependencies are disregarded and each model comparison is dealt with as an individual scalar test hinging on CLT results. With the second procedure, the major contribution of this chapter, we combine the MCS concept with the arsenal of the MHT approach, producing a novel MCS test relying on non pivotal results, which exploit balanced confidence sets and allows strong control for the k-FWER. In the course of this thesis, the latter innovation provides an important means of refinement of the initial model set.

Model Selection of Market Risk Models

Value-at-Risk, or more simply VaR, has gained popularity among practitioners in the past years because of the increasing exposure to market risk of large financial companies and financial divisions of non-financial firms, and mostly because of the ability of this metric to deliver a readable quantity concerning overall risk borne. This popularity has increased as a result of the many "crises" and large corporate defaults due to market exposure, which have become more frequent since the early 90's and largely publicised by the media. VaR[1] is used by risk managers in banks and wealth management companies to monitor the market risk of large and varied portfolios of financial securities and over-the-counter products in order to trigger action by the management on the back of the information packed into this number. This metric summarises the optimistic loss in a worst case scenario, with a given probability on a certain time horizon. This calculation has also become part of regulatory requirements, e.g., in banking regulations such as in Europe, whereby it is used to determine the amount of regulatory and economic

[1] We keep referring to VaR in this work although we always mean the target quantile of the empirical returns. Nevertheless, originally, the VaR is defined as a monetary measure that better refers to a consolidated portfolio of asset values rather than returns. However, it is theoretically easy to switch from one measure to another.

capital. From an operational point of view, however, VaR in general lacks the important property of subadditivity, Artzner et al. (1999). Practically, this means that the VaR of a weighted sum of individual quantities is not equal to the weighted sum of each VaR, hence requiring multiple layers of calculation when aggregating from subsets to the consolidated portfolio level. This feature led to a shift of focus towards the alternative risk measure of expected-shortfall (ExS), see Artzner et al. (1999), which holds the subadditivity property and provides further information: namely, the expected loss in a worst case scenario, with a given probability on a certain time horizon. This measure represents also a complementary indicator that accounts for the magnitude of losses exceeding the VaR threshold and draws attention to the full shape of the tail event distribution.

The statistical testing of risk models is an important step towards assessing the ability of these tools to provide reliable output and to contribute to the decision-making process hinged on market risk exposure. From a practitioner perspective, there are serious implications for a financial institution from its choice of risk model in terms of its overall risk management performance and more importantly its capital adequacy requirements. So for industry, the question of which risk model performs bests in capturing and forecasting risk exposure is crucial. Historically the first contributions in backtesting the performance of risk-models are those of Kupiec (1995) and Christoffersen (1998), who construct unconditional and conditional tests based on the mere sequence of VaR breaches. Thereafter, research focused on specific issues affecting the VaR prediction ability, such as the time-horizon of the forecast, the inclusion of time-varying volatility and accounting for fat-tailed distributions generated by volatility clustering and jumps in returns, see BIS (2011) for a review. On the other hand, backtesting ExS is more problematic due to the peculiarity of its functional form which in principle requires the estimation of the entire tail distribution. The literature on model prediction of ExS is not as extensive as that on VaR, possibly due to the latter reason. The main contributions in this field are Berkowitz (2001) and Kerkhof and Melenberg (2003), who use the probability transform Rosenblatt (1952) to process the data and construct tests of ExS prediction based, respectively on the likelihood ratio and the δ-functional method Van der Vaart (1998). Both these works focus on the development of a test for ExS.

In this chapter, we build on the work of Bao et al. (2006) in that we use a similar model set but investigate model predictive ability not only for the VaR but also for the ExS models with respect to different time horizons and volatility conditions. The main contribution of this work consists of the application of the MHT framework to the backtesting of market risk measures. We test the statistical significance of the forecasting performance of a varied set of market risk models, targeting the VaR and the ExS risk metrics. We design MHT exploiting the empirical coverage probability as the sample statistic for the VaR, whereas we use the sample shortfall as we develop a new test of significance and model comparison for the ExS. Moreover, in this thesis, we extend the already published work (Esposito and Cummins, 2015), aiming our sights at the absolute model comparison of market risk forecasting models. Employing the methodological approach developed in Section 1.1 and Section 1.3, we designed MCS tests of the market risk absolute model performance hinging on the *max*-MCS of Hansen et al. (2011), as constructed in Section 1.3.1, our new *t*-MCS inspired by Corradi and Distaso (2011), as constructed in Section 1.3.2,

and the novel γ-MCS, as constructed in Section 1.3.3, settling the MCS in an MHT framework[2].

We construct bootstrap MHT of risk model predictive ability, analysing the out-of-sample performance over 1-day and 10-day time horizons. We extend the investigation to forecasts that target a time horizon wider than a single day, an exercise that might either confirm the predictive power of a model or highlight situations whereby the forecast deteriorates fast. We also observe the model performance under stressed market scenarios. The inference procedure is accomplished via a direct measure of the VaR predictive ability or rather exploiting the idea first popularised by Diebold et al. (1998) and used by Berkowitz (2001), Kerkhof and Melenberg (2003), Bao et al. (2007), in that we use the probability transform Rosenblatt (1952) to construct statistics which are functionals of the model probability distribution and thereby indirectly test the data via the probability transformed sample. The battery of tests draws inference about two aspects of the model forecasting ability. In a first exercise, we construct tests of statistical significance of the forecasting ability of each model, with reference to the target quantities to be predicted. The latter can be easily recognised in the VaR forecasting test, whereas in the ExS test we resort to pre-pivoting to obtain a data domain standardisation and construct a new simple test for the backtesting of the model predictive ability of the expected-shortfall. With this backtesting exercise, we estimate confidence sets for the target statistic and derive joint balanced tests which control for the k-FWER. This experiment also presents an application of the streamlined step-down algorithm, as presented in Section 1.2.2, a procedure of recursive testing that potentially allows for further rejections, in an attempt to increase the statistical power of the test. In a second application, we explore model superiority in market risk forecasting with an absolute model performance test. We derive the *max*-MCS, the t-MCS and the γ-MCS.

The chapter is organised as follows. In Section 2.1 we briefly introduce the conditional distribution models that form the suite of competing market risk forecasting instruments, whereas in Section 2.2 we define the target risk measures and the sample statistics, further describing the structure of the testing exercise. The experimental Section 2.3 describes the data set, the modelling approach and discusses the empirical evidence exhibited. This section also introduces the first application of the MCS tests providing some examples of the operational characteristics of the model confidence set tests. Section 2.4 concludes.

2.1 The Conditional Distribution Model Set

In this chapter we introduce the components of the market risk forecasting model set $\mathcal{M}$. The output of the models we are interested in is the conditional probability density forecast delivered by the different techniques. Although it is sufficient to model just the tail of $\mathbf{P}$ to produce the inference that is sought, in certain cases we will need the full distribution to project the system forward. The model set includes:

[2] In a previous version of this analysis, we approach the absolute model comparison by exploring the bootstrap generated multidimensional distribution of the model performances, measuring the probability that each $L_i \leq L_j$ of pairwise superiority, for each d_{ij}. This information is then collated into a synthetic table presenting a model ranking index that represents, for each model, the number of time this probability is greater than 0.5, providing an instrument for measuring the model superiority across the model set. In this work we do not present this information as it resemble the results of the absolute comparison test we are introducing, whereas the statistical properties of the latter approach have been extensively studied in the literature.

heuristic models such as the historical simulation (HS), which is a rolling window histogram, a rolling window Normal model (G) and RiskMetrics (RM)[3]; a non-parametric model based on a kernel regression (KR); parametric models such as the autoregressive conditional heteroskedastic model (CH), the quantile auto-regression model (QR) and several parametric distribution assumptions such as normality, student-t, generalized error distribution (GED) and the generalised Pareto distribution (GPD).

Historical Simulation

The historical simulation (HS) model consists of a rolling window histogram of the return distribution. The implicit assumption is that a t-left neighbourhood data sample histogram is a good local estimate of the conditional distribution $\mathbf{P}_t$. Although this might be acceptable as an estimate of $\mathbf{P}_t\left(X_{t+\varepsilon}\right), \varepsilon > 0$, a model-free approach seems inadequate when $\varepsilon \gg 0$. Under the i.i.d. assumption, we can compute the distribution Δ lags forward with numerical convolution or Monte Carlo integration. This model is the most widespread in the financial community, because of the ease of implementation and mainly because it allows one to aggregate easily the many varieties of financial exposures which would otherwise require the design of an all-inclusive market risk model.

Normal Hypothesis

The classical assumption of the Black-Scholes model is that log-returns are normal. A practical approach to the estimation of a conditional mean-variance model is the plugging in of a rolling window sample mean and variance into the normal function to construct a model of $\mathbf{P}_t\left(X_{t+\varepsilon}\right)$. This model should be able to capture some momentum and volatility clustering.

RiskMetrics

The RM model, J.P.Morgan (1996), consists of an exponential smoothing of the squared returns, which is used for a $t+1$ variance proxy. Formally,

$$h_t = \theta \cdot h_{t-1} + (1-\theta) \cdot x_{t-1}^2. \tag{2.1}$$

It was originally designed as a simple alternative to the GARCH model on the observation that the lag polynomial is often close to the stability condition and the GARCH parameters for financial time series are not widely different across a large collection of data. It presents the disadvantage that it cannot be projected forward. As a working template, we use the normal hypothesis to compute projections of the conditional probability distribution, assuming innovation of the variance proxy at current h.

Kernel Regression

A robust and efficient (but biased) technique to estimate a conditional distribution is to exploit the kernel regression of Nadaraya-Watson, cfr. Nadaraya (1964), Watson (1964) and Bierens (1987) for

[3] The RiskMetrics model is presented as a heuristic model because the model parameter θ is fixed a-priori and we assume conditional normality to project the system forward.

several statistical results. Formally,

$$\widehat{\mathbf{E}}\{y|x\} = \frac{\sum_j y_j K_h(x - x_j)}{\sum_j K_h(x - x_j)} \tag{2.2}$$

A drawback of this estimator is that it shows high variability when conditioning on values of $x_{t-\Delta}$ that are far away from the centre of gravity of the sample distribution, therefore producing unstable estimates of the tails. On the other hand, an attractive feature of the KR estimator is that it can generate directly an estimate of the distribution conditional on any lag; in this case the projection exercise is a direct output of the estimation function.

Quantile Regression, CAViaR

The quantile regression model, Koenker and Bassett (1978), is a statistical model of empirical percentile. Basically, it is a parametric model of relations between the explanatory variables and the percentile of the target variable. In this work, we employ the specification in Engle and Manganelli (2004), which accounts for autoregressive features of the model quantile. The model has been designed pretty much for the estimation of an auto-regressive VaR, therefore the epithet of conditional autoregressive VaR, designated as CAViaR. Formally, letting $X_{t-1} = \{y_{t-1}, \ldots, y_{t-i}, \ldots\}$, a quantile auto-regression model is defined as

$$\begin{aligned} y_t &= f\left(X_{t-1}; \beta\right) + \varepsilon_t^\theta \\ &= f_t\left(\beta\right) + \varepsilon_t^\theta, \end{aligned}$$

with the auxiliary assumption that the θ^{th}-quantile of the ε_t^θ distribution is equal to 0. The model estimation is carried out with the minimisation of the loss function

$$\min_\beta \frac{1}{T} \sum_t \left(\theta - \mathbf{1}_{\{y_t < f_t(\beta)\}}\right)\left(y_t - f_t(\beta)\right) \tag{2.3}$$

which is minimal whenever $f_t \equiv \theta$.

In this work we employ four different CAViaR specifications: the adaptive; the symmetric; the asymmetric; and the indirect GARCH. The latter three models are specified as in Engle and Manganelli (2004), whereas the adaptive CAViaR is defined as

$$f_t = f_{t-1} + \left[\mathbf{1}_{\{y_{t-1} < f_{t-1}\}} \cdot b_1 + \mathbf{1}_{\{y_{t-1} \geq f_{t-1}\}} \cdot b_2\right] \cdot (y_{t-1} - f_{t-1}). \tag{2.4}$$

For each model, we estimate a quantile regression for the 1^{st}-5^{th} percentiles, in addition to the 7.5% and 10% levels, in order to smooth out the borders of the distribution. Hence, we use those percentiles as a point-wise tail estimate. The extreme value distribution is assumed to have a linear to higher order polynomial decay, matching the all-time minimum, with polynomial degree ranging from 1 to 20. In this exercise we are modelling the tail of the conditional distribution function only. We project the distribution forward, simply multiplying the knot points, that is the estimated percentiles, by the square root of time.

GARCH-EVD Models

Financial time series exhibit volatility clustering features and fat tailed distributions. The generalised autoregressive conditional heteroskedastic models, Engle (1982), Bollerslev (1986), represent the most successful statistical device in mimicking the evolution of financial time series in the past thirty years. The GARCH models come in a variety of fashions. However, a GARCH(1,1) does not seem an unreasonable assumption for financial time series, cfr. Hansen and Lunde (2005). In the MHT experiment we account for modelling time series volatility clustering with conditional heteroskedastic models, and incorporate asymmetry with exponential or threshold GARCH, cfr. Nelson (1991) and Glosten et al. (1993). Specifically, we estimate symmetric GARCH models, Engle (1982), Bollerslev (1986)

$$h_t = \alpha_0 + \alpha_1 \varepsilon_{t-1}^2 + \beta_1 h_{t-1} \tag{2.5}$$

and models capable of producing asymmetric distributions such as the TARCH(1,1) of Glosten et al. (1993)

$$h_t = \alpha_0 + \left(\alpha_1 + \gamma \mathbf{1}_{\{\varepsilon_{t-1}<0\}}\right) \varepsilon_{t-1}^2 + \beta_1 h_{t-1} \tag{2.6}$$

and the EGARCH(1,1) of Nelson (1991)

$$\log h_t = \alpha_0 + \alpha_1 \left(|v_{t-1}| - \mathbf{E}\,|v_{t-1}|\right) + \beta_1 \log h_{t-1}, \tag{2.7}$$

with $\varepsilon_t = v_t \sqrt{h_t}$.

The stochastic driver v_t is such that $\mathbf{E}v_t = 0$, $\mathbf{E}v_t^2 = 1$ and $v_t \sim G(\theta)$, where $G(\theta)$ is a parametric distribution of type normal or student-t. However, it is common knowledge that financial time series exihibit fat tailed[4] distributions, Longin (1996). Further improvement is achieved by augmenting the model with a piecewise distribution for $G(\theta)$. Thereby, we adapt extreme-value distributions to each tail of the residuals with a quasi-maximum likelihood estimation (QMLE) of the model classes introduced above, while a conditional normal or GED is estimated for the mid percentiles. In order to parametrise a GPD for each tail, we exploit the idea in Gonzalo and Olmo (2004) and maximise the Kolmogorov-Smirnov statistic of the empirical distribution of the exceedances. This approach is different from that taken by Bao et al. (2006), whereas the threshold is picked at a conventional level. A robust alternative semi-parametric estimation technique has been proposed in Mancini and Trojani (2011). The described econometric setup is able to capture the time dependency described by volatility clustering, the asymmetric effect and the thick tails phenomenon.

2.2 Model Comparison Testing

The design of tests of market risk model forecasting performance requires the determination of the target risk measures employed with the loss functions L. The target risk measures are the VaR and

[4] When we refer to fat-tailedness in this thesis, we refer to model distribution tails that are not exponentially boundend. High kurtosis, on the other hand, is a measure of the distribution shape that can be referred to as the "peakedness" of the distribution. The kurtosis might be affected by fat-tailedness.

the ExS[5]. In this regard, it is important to notice that in this chapter we refer to the VaR measure as obtained under the log-transform of the price, which is therefore the corresponding quantile of the return distribution forecast. Under a monotonic transformation, quantiles are preserved. However, this is not true for the ExS, which is thus the expected shortfall of the portfolio return, not the value. Formally, let $F_{t,\Delta}(x) := \mathbf{P}_t\left(X_{t+\Delta} \leq x\right)$ and define the value-at-risk

$$\mathrm{VaR}_t(\Delta, \alpha) = F^{-1}_{t,\Delta}(\alpha) \tag{2.8}$$

that is the α percentile of the return conditional distribution over the target time horizon Δ, and the expected-shortfall

$$\mathrm{ExS}_t(\Delta, \alpha) = \tfrac{1}{\alpha}\mathbb{E}_{\mathbf{P}_t}\left[X_{t+\Delta}\mathbf{1}_{\{X_{t+\Delta}<\mathrm{VaR}_t(\Delta,\alpha)\}}\right]. \tag{2.9}$$

that is the return expectation, conditional upon observing values below the $\mathrm{VaR}_t(\Delta, \alpha)$. The corresponding sample measures of the quantities defined in (2.8) and (2.9) are either employed in the construction of simultaneous confidence set for the statistical significance test or enter the loss function defined as the absolute difference between the realised values and their ex-ante expectations. The type of tests we set up concern the model forecasting ability of VaR and ExS over 1-day and 10-day time horizons, under low, high and average volatility conditions. We test the VaR model predictive performance, cfr. Bao et al. (2006), Kerkhof et al. (2009), using the sample measures of the *empirical coverage probability* (ECP). Assuming a sample of T observations, starting from the first datum after the minimum amount of data needed for the estimation, we define the ECP as

$$\rho := \tfrac{1}{T-\Delta+1}\sum_{t=\Delta}^{T}\mathbf{1}_{\{X_t<\mathrm{VaR}_{t-\Delta}\}} \tag{2.10}$$

To obtain tests targeting the expected shortfall, we transform the data with the Δ-step ahead conditional distribution $\mathbf{P}_t\left(x_{t+\Delta}\right)$ to construct the probability transform $y_{t+\Delta} = \int_{-\infty}^{x_{t+\Delta}}\mathrm{d}\mathbf{P}_t(s;\Delta)$, obtaining the random variable Y that is independent uniformly distributed, cfr. Rosenblatt (1952), Diebold et al. (1998). Exploiting the sequentially independence property of Y, the latter work derives tests for probability density forecasting performance whereby the loss function measures the divergence of the transformed data from the uniform distribution. Building on this approach, several formal methods of testing density forecasts and applications to financial risk measurement have been designed, based on the likelihood-ratio test, cfr. Berkowitz (2001), the Kullback-Leiblier information criterion, cfr. Bao et al. (2007) and the δ-functional method, cfr. Van der Vaart (1998) and Kerkhof and Melenberg (2003). In this study instead, we apply the probability transform and then derive the sample measure

$$\rho := \frac{\sum_{t=\Delta}^{T} Y_t\mathbf{1}_{\{Y_t<\nu\}}}{\sum_{t=\Delta}^{T}\mathbf{1}_{\{Y_t<\nu\}}} \tag{2.11}$$

where ν indicates the reference percentile of Y, with respect to the sought shortfall. It is appropriate for a forecasting model selection exercise defining the loss function L_i of model i for the various measures as

[5] To be rigorous, see e.g. Kerkhof and Melenberg (2003), the $\mathrm{VaR}_t(\Delta, \alpha)$ might have a finite probability ($\mathbf{P}$ not surjective) or an interval on X might have 0 probability ($\mathbf{P}$ not injective). In the most general definition, $\mathrm{VaR}_t(\Delta, \alpha) := \inf\{x \in \mathbb{R}\colon \mathbf{P}_t\left(X_{t+\Delta} \leq x\right) \geq \alpha\}$ and $\mathrm{ExS}_t(\Delta, \alpha) := \frac{\mathbb{E}_{\mathbf{P}_t}\left[X_{t+\Delta}|E\right]+\left[\mathbf{P}_t(\bar{E})-\mathbf{P}_t(E)\right]\cdot\mathrm{VaR}_{\Delta,\alpha}}{\mathbf{P}_t(\bar{E})}$ with $E = \{X_{t+\Delta} < \mathrm{VaR}_t(\Delta, \alpha)\}$. However, this extended definition is redundant for operational purposes.

the distance from the theoretical forecast, that is

$$L_i := |\rho_i - \rho_*| \tag{2.12}$$

For reference, the target critical values ρ_* for the statistics undergoing the testing procedures are summarised in the following scheme:

	$\alpha = 1\%$	$\alpha = 5\%$
$\mathrm{VaR}_t(\Delta,\alpha)$	0.010	0.050
$\mathrm{ExS}_t(\Delta,\alpha)$	0.005	0.025

In practice, the VaR model forecasting ability test of significance can be obtained referencing to the ECP as the critical value, whereas the loss function employed in the absolute model performance tests corresponds to the sample distance of the empirical coverage probability (2.10) from the reference quantile value, either from the transformed or directly from the unprocessed data. On the other hand, testing the model performance for the ExS forecasting ability, necessarily requires the data transformation in order to avoid assumptions about the true shortfall value. After the domain standardising probability transform, expected shortfall forecasting model performance measures can be constructed by comparing the sample ExS to that of a uniform distribution at the sought confidence level. To our knowledge, this is the first time that such a test for the expected-shortfall has been devised.

Relative forecasting ability has been first investigated by the seminal work of White (2000), who designs the Reality Check (RC), a joint statistical inference procedure that extends the methods of Diebold and Mariano (1995) and West (1996), and which has been in turn extended in several directions, cfr. Hansen (2005) and Corradi and Swanson (2006). In recent years, several works on risk model backtesting, see for instance Gonzales-Rivera et al. (2003), Bao et al. (2006), Kerkhof et al. (2009), and density forecast, cfr. Bao et al. (2007) have used the RC framework to cope with joint testing of model forecasting ability. This work is different in that we produce an experiment of forecasting performance statistical significance as defined in (1.1), hinging on the MHT and controls for the k-FWER, which is further refined by a step-down algorithm B, as the one presented in Section 1.2.2. In the empirical section, we discuss the test results under several forecast scenarios. To complete the model selection exercise targeting market risk forecasting measures and employing the algorithms presented, respectively, in Section 1.3.1, Section 1.3.2 and Section 1.3.3, we produce the max-MCS, the t-MCS and the γ-MCS for the ECP and the realised ExS of the probability transformed data, as described above.

2.3 Experimental Section

2.3.1 Preliminary Considerations

The data set consists of a large sample of a well diversified equity stock index, that is the Dow Jones Industrial Average index, ranging from December 31$^{\mathrm{st}}$ 1970 to April 22$^{\mathrm{nd}}$ 2013. We work with log-returns of the index daily close level series. This large sample allows us to consider at least two comparable volatility peaks, around October 1987 and October 2008 as well as a high number of volatility waves. To

perform the backtesting experiment, we split the data sample into in-sample and out-of-sample segments, assuming size $T = R + P$, where R indicates the size of the in-sample data used for model estimation and P indicates the size of the sample used for prediction in the out-of-sample segment. The full sample size is $T = 10,674$. The working assumption here is that there exists stable transition probability distributions, albeit unknown. We subtract the sample average from the return sub-sample ending on December, 31^{st} 1998, assuming thereon a zero off-set constant. We draw on a large sub-sample for first estimation and set $R = 6,572$, that is we start the out-of-sample exercise on January, 1^{st} 1997 and use the same parameters for the parametric models throughout 260 observations, after which the model is estimated again. As a consequence we split the out-of-sample exercise into 16 blocks which are re-sampled 2,000 times with the stationary bootstrap of Politis and Romano (1994b). We choose the sample size such that we observe sensible smoothing of the statistic distributions. The optimal bootstrap block-length is estimated on the growing sample base with the Patton et al. (2009) algorithm. We deliberately discard the rolling-window approach for parametric models like GARCH-EVD and CAViaR because this practice increases rather than shrinks the forecast variability. For instance, the autoregressive coefficient of the symmetric GARCH equation exhibits wide variations if resulting from a two-year rolling sample monthly estimate as opposed to the procedure employed in the experiments consisting of a yearly estimate on a growing sample basis. For reference, the mentioned rolling-window approach for a symmetric GARCH model would produce an average autoregressive coefficient of 0.869 with a standard deviation of 0.073 and a spike at 0.346, whereas the growing sample approach delivered an average coefficient of 0.920 with a standard deviation of 0.002. We believe that is the main reason for the poor performance of the GARCH models in, e.g., Kerkhof et al. (2009) and Bao et al. (2006). Hence, in this study we do not include rolling window versions of the GARCH or CAViaR models, relying on the results of similar models employed by other authors for reference. The rolling window approach applied to models that are designed to produce conditional and stationary distributions of the data generating process, is more likely to hurt their performances by the increased model uncertainty introduced with the parameter variability, rather than improving their local forecasts. Concerning the estimation risk, we adopt the working hypothesis that the parameters or the non-parametric estimates are set to their p-limits, due mainly to restrictions to the currently available computational power. We plan to expand this feature in future experiments and include estimation risk in the full simulation.

In this empirical study, we generate the sample statistics with resampling from subsamples of 260 days. There are two reasons for this: firstly to avoid the phenomenon of *location bias*, Corradi and Swanson (2007), that is the bias in resampling for recursive problems, whereby earlier observations are used more frequently than temporally subsequent observations when forming test statistics; and secondly to construct artificial samples with classified volatility, in order to investigate the model performance in different volatility environments. The average block size for the resampling procedure is computed according to the Patton et al. (2009) procedure, resulting in a 195 day block size. We construct model predictive ability measures on 1-day and 10-day projections of the target risk measures, the latter time-horizon corresponding to 2-weeks of calendar days. The risk measures presented in this report are the empirical coverage probability, for VaR models, and the realised ExS of the probability transformed sample distributions. However, the analysis has been performed on a slightly larger set of measures, containing the

empirical loss function and the VaR of the pivoted sample, essentially producing the same results. As described earlier, the out-of-sample data is divided into 16 blocks of 1 calendar year.[6] We investigate the full out-of-sample performance of the models. Furthermore, we back-test the performance in low / high volatility scenarios each corresponding to four blocks labelled as L/V and H/V, representing extreme sample years. The blocks are not necessarily time-contiguous.

Where necessary, the model 1-step and 10-step distributions are constructed via Monte Carlo integration. In order to consistently reduce the computational time, the GARCH-EVD distributions are constructed on a grid for the conditioning variable entailing an array of forecast distributions, which is used at run time by truncating over the prescribed grid the dependency on the current value. The historical simulation is projected forward via Monte Carlo integration. The RiskMetrics distributional assumption is Gaussian with h_t variance. The Kernel regression estimate is constructed in a similar manner as the GARCH-EVD distributions, that is on a grid for the conditioning variable that is determined on the historical sample as well. In order to reduce the computational time, the Kernel regression is also kept fixed until the subsequent estimation. The rolling window models are recalculated daily at time $t-1$. The CAViaR equation requires some inventiveness to be employed. As they stand, the quantile regressions cannot be projected forward or input in the probability transform, because they have naturally been designed to be free of any distributional assumption. This model is appealing both for the short term memory quantile feature as well as for the absence of an explicit probability assumption. Nevertheless, we need a conditional distribution to feed the Rosenblatt functional and construct the ExS backtesting procedure. Therefore, we proceed by estimating several quantile auto-regressions to construct a linear approximation of the tail of interest. We need to expand on the inner side in order to avoid polarisation on the quantile of interest, that is the 5^{th} in this exercise. Meanwhile, on the outer side, we need a tail assumption to work with. We start joining the all time minimum with the first percentile with a straight line and then with a (translated and scaled) polynomial of degree 5, 10 and 20. To be sure that the operation model we are designing produces reasonable results, we ought to prove that the percentile order is what is expected to be. In this case, we rely on the careful choice of the pivot points, on the constraint preventing the autoregressive quantiles to cross each other, were that to happen and, of course, on the empirical evidence. The quantiles are carried forward in time simply multiplying by the square root of time.

Furthermore, we are also interested in the significance of conditioning in the presence of model misspecification. We include in the model a fully unconditional distribution assumption, based on a dual tail GPD distribution with constrained normal or GED distribution for the mid quantiles, estimated through MLE on the base sample. We also consider for the 10-step ahead forecast the unconditional distribution of the GARCH-EVD models. This distribution is constructed taking the expectation with respect to the conditioning variable, formally $\mathbb{P}(X) = \mathbb{E}^Y [\mathbb{P}(X|Y)]$, which corresponds to the k-step unconditional distribution under the modelling specification. The rationale in testing these models relies on the possibility that the forecast 10 steps ahead is possibly distorted by the conditioning, firstly because of the speed of the mean reversion of the volatility, which should be ruled out by the preliminary tests on the model

[6] The last block is less than 1 year but the resampled data is let run for a full year.

parameters significance, but mostly because of possibly a misspecification of the model that might include unexpected innovations that impact rapidly and significantly the model projections. Tab. 1 provides a summary of the models and the acronyms that are used in the next section.

2.3.2 Market Data Experiment

In this section, we summarise the empirical evidence obtained from our testing.

With respect to the full sample of the target market risk measures and then the VaR numbers for the L/V and H/V blocks, Tab. 2 to 5 present the balanced k-FWER confidence sets investigating the statistical significance of each model market risk forecasts under the MHT paradigm, augmented with the step-down algorithm. Finally, from 6 to 13 we presents model confidence sets identified by the several algorithms introduced in Section 1.3, that is the max-MCS, the t-MCS and the γ-MCS. The statistical significance test tables show the balanced confidence set estimates before the application of the step-down procedure, while the shaded cells correspond to those models rejected at the termination of the aforementioned algorithm. Therefore, the greyed cells represents models that exhibit not significant performance for the corresponding risk metrics. The empty cells are associated to models that have not been employed for the corresponding risk metrics exercise. These tables also show the bootstrap mean of the target statistic for each model, which represents the expected model performance. The critical values are applied according to the following scheme[7],

Measure	Horizon	Confidence	k
ECP	1d	99%	3
ECP	10d	95%	4
ExS	1d	99%	4
ExS	10d	95%	5

In Tab. 2 we exhibit the full sample results for the VaR forecasting experiment. Although the MHT for the empirical coverage probability (ECP) of the VaR(1d, 5%) shows that the HS and the Gaussian models are significant good predictors, in forecasting VaR(1d, 1%) the class of heteroskedastic models augmented with EVD deliver superior results, as well as in the former experiment. The KR can surprisingly capture the 1d first percentile, while being rejected in estimating the fifth percentile: this model generally shows quite erratic performance. The Nadaraya-Watson kernel is quite sensitive to tail data and so is especially erratic in the tails; this model could possibly improve its performance slightly if iterating the estimation daily or using a weighted version of the kernel.[8] The CAViaR exhibits the same underestimation effect (higher empirical coverage) that is visible in the designers' work Engle and Manganelli (2004), probably due to finite sample effect. Increasing the sample size reduces the bias effect allowing improved performance. The Student-t type models seem to suffer on the 5^{th} percentile exercise. The unconditional models DT_n and DT_ged are systematically rejected in the 1d horizon. In the 10d forecasting exercise the higher variability produces more widespread acceptable model performance, despite having relaxed the Type I error and the the generalised FWER. The EVD models seem to slightly overestimate the

[7] We allow for lower confidence on longer time horizons, because of the increased variability of the statistics, while we keep the number of false rejections across the tests in the range of $10 - 13\%$.

[8] We have run some experiments with the weighted version of this model which did not seem to stabilise the tails.

quantile over the 10d projection; this might be connected to the necessity for improving the likelihood optimisation. The good performance of the CH*t_avg model in the VaR(5%,10d) case, whereby this model is usually affected by critical performance of the higher percentile yet nevertheless performs well in the longer horizon exercise, seems to suggest that the joint estimation of the GARCH filter and the tail model may add to predictive power. In fact, this is the only fat-tailed GARCH model which has been estimated with full MLE. The unconditional GARCH-EVD models are accepted in both experiments and also the DT_* models are significant in the 5^{th} quantile experiment. This performance raises the question concerning "how far" the conditional distribution is from the stationary one over the projection horizon. The RM model produces significant forecasts, except in the short time short tail experiment.

Turning to the ExS experiment in Tab. 3, we notice the large number of rejections over the 1d horizon. Contrary to the common sense intuition, the number of models that pass the test is greater in the smaller tail. The non-Gaussian heteroskedastic models with fat tail innovations provide statistically significant predictors for the ExS(1d, 1%), whereas only the symmetric EVD and CH3t are significant at the fifth percentile. In general, the GARCH-EVD are good predictors on the shorter horizon, whereas they tend to show slightly biased forecast on the 10d horizon, though still significant. The tail adjustment in the QR model delivers significant results in several cases for the first percentile exercise. The historical simulation proves to be an acceptable choice on the short term horizon and for ExS(10d, 5%), while it fails on the far tail at the long horizon. The 10d horizon exercise shows again more wide spread significant results in the longer tail forecast, whereas in the small tail experiment only a few models outside the CH class can deliver significant results. We exclude unconditional models from the ExS forecasting model suite, which basically produce the same conclusions as the VaR experiment.

In a stress test experiment, we evaluate the significance of the VaR predictive ability of the model battery in a controlled volatility environment characterised by low (L/V) and high (H/V) volatility, respectively shown in Tab. 4 and Tab. 5. The general result is that Gaussian models tend to outperform with low volatility, while the GARCH-EVD class, mimicking more probability distribution characteristics, outperform almost systematically. In the low volatility scenario the RM can also deliver significant results.

To conclude this empirical section as well as this chapter about market risk forecasting model selection, we introduce a first application of the main instrument for assessing model comparison that is among the objectives of this work. In the Tab. 6 to 13 we present the model confidence sets for the market risk forecasting models that are estimated with the *max*-MCS test exploiting the approach of Hansen et al. (2011), the *t*-MCS inspired to the remark in Corradi and Distaso (2011) and the novel γ-MCS algorithm, developed in Section 1.3.3 and exploiting the MHT approach presented in Section 1.2. The latter results involving the *max*-MCS and the *t*-MCS are presented in Cummins et al. (2017). The MCS test exhibits the appealing characteristic of the automatic partitioning of the model set between superior and inferior models, at the same time providing a ranking across the model set. With other approaches involving the analysis of the model performance significance or the recursive relative performance benchmarking, this exercise involves partially subjective judgement. Although showing set inclusion, the exercise of this chapter and the several other MCS tests of this thesis, differ in the structure of the test, in the way they

consider test dependencies and in targeting finite sample distributions. Despite the fact that a comparison of the MCS algorithms is beyond the scope of this thesis at the moment, we present the outcome of these techniques concurrently as they quite resemble gradations of the same concept. As the data analysis proceeds however, some form of qualitative comparison of the several MCS procedures will emerge. In this respect, it seems evident that the t-MCS is quite aggressive, as a result of the lack of consideration for the test dependencies. The max-MCS and the γ-MCS produce similar results although the TPFDP control mechanism embedded in the latter provides a trigger to modulate the tolerance for false rejections and hence produce a further skimming across the subset of best performing models. In our study, the focus of the empirical application of MCS techniques remains on the cut-off they produce on $\mathcal{M}$, dividing the model set into inferior and equivalently superior models as well as the generated model ranking.

Concerning the application of MCS tests to the market risk forecasting models discussed so far, we produce VaR and ExS model confidence sets for the full sample with the max-MCS, the t-MCS and the γ-MCS algorithm with $\gamma = 10\%$ and $\gamma = 50\%$. In general, the results look similar for the MCS that have been applied, whereby the t-MCS tend to reject slightly more models most of the times, whereas the γ-MCS sometimes allows to modulate the result between the max-MCS and the t-MCS. The MCS allows model selection and model ranking. Concerning the latter concept, the experiment reveals the intricacies we face when coping with a multiplicity of dependent tests. The models at the border between the γ-MCS and the subset of the rejected models are not necessarily ordered if taken together as the probability of observing superior performances of the first rejected model, for instance, might be quite high. The definition of MCS only demands that if a model is rejected there exist at least one other model which is superior to it, whereas if the statistical preference rule ascertain that it is superior or at most equivalent to any other model, the model enters the MCS, despite its probability of observing superior performance upon the union of the counted events might be lower than a rejected model. The definition of MCS requires that only models that are never rejected are considered superior, whereas it might happen that a rejected model might exhibit the probability of being superior to any of the models of the MCS that is actually larger than the worst component of the MCS. This phenomenon though, seems to happen only in a neighbourhood of the MCS border. Turning to the experimental results, we notice that, in general, models producing non-significant performances do not enter the model confidence set, which is an expected outcome, which is an expected outcome. As for the most distinctive results, we notice the performance of the CH1 models with EVD extensions, which are persistently among the top models and produce significant forecasts for all the measures and across all the scenarios, with the only exception being the L/V environment, whereby all the models perform poorly with the exception of the RM. On the short term horizon, the heteroskedastic models with fat tails are among the best performers. In the case of the VaR(1d,5%) the CH*g enters the MCS as well, indicating that volatility clustering matters more than fat-tailedness around this percentile. The HS model performs well on short horizons, whereby it is included within the MCS with a central or a borderline ranking most of the time. The RM model performs well only in the case of the five percentile VaR, whereas the best model for the ExS(1d,1%) is the augmented CAViaR with 10-th degree polynomial tail. Over the longer horizon, the model confidence set is more ample, confirming a larger variability of the model performances. It is interesting to notice under this configuration that the max-MCS can hardly produce a ranking among the best model set, a

fact which is reflected by the low variability of the p-values of the top performers in the γ-MCS. The QR and the unconditional heteroskedastic models perform well in forecasting the expected-shortfall on a bi-weekly horizon, whereas a VaR(2w,5%) can easily be captured by a Gaussian rolling window or by a RM model. The latter is the only scenario whereby unconditional DT models perform decently. The first percentile requires slightly more sophisticated models, although virtually all the models can produce statistically equivalent performances.

2.4 Concluding Remarks

In this chapter, we apply the model selection paradigm proposed in this thesis to market risk forecasting models and extend the exercise carried out in Bao et al. (2006) by means of testing the statistical significance of the performance of a suite of models in forecasting 1-day and 10-day VaR and ExS with an MHT methodology. With the latter set of experiments we present a new simple test for the expected-shortfall, building on the probability transform. We further complement previous work (Esposito and Cummins, 2015) by introducing a first application of the model confidence set test under several specifications. The exercise prompts the discussion to focus on several operational aspects of the various MCS algorithms exploited here and in the rest of this work. We believe the model selection approach assembled in this research to be particularly appealing to practitioners, due to the fact that it allows one to design robust model comparison tests, which can easily accommodate decision-making problems in financial econometrics.

The empirical results that we obtain diverge significantly from previous evidence. We have used more stable parameters for the GARCH models and optimised the estimates of the thresholds for the GPD. Furthermore, we apply model performance significance tests that are balanced and control for the k-FWER, with the auxiliary benefit of the statistical power augmentation delivered by the step-down method. The absolute model performance tests introduced with the MCS concept, have the ability to identify the subset of the best performing models and produce a model ranking via the p-value measure, providing results that are more informative than the RC p-value, which in Bao et al. (2006) fails to detect any model superiority over the benchmark RiskMetrics. The experimental results of the latter article are extended and improved as we provide a test of significance of the target model performances within the MHT framework, we improve the performance of the filtered models with a more efficient estimation procedure that yields superior models as detected by the MCS procedures, which confirm and strengthen the experimental outcomes in Esposito and Cummins (2015). These tests exploited for the market risk model selection exercise, are capable of the automatic selection and the ranking of the model competitors, some features that cannot be achieved with a simple RC benchmarking test. We have compared the forecasting ability of several models with respect to different performance measures. In general, models which account for volatility mean reversion and fat-tailedness result in the best performance. This result is in contrast with previous findings and shows that GARCH rolling window parameter estimates introduce high model uncertainty, inevitably compromising their forecasting performance. On the contrary, we have found that several specifications of the GARCH model are among the top performers. The quantile regressions also perform quite well, in forecasting the 1% ExS on the 1d and 2w horizons, as well as the

5% ExS on the 2w horizons, which are all surprising results as the QR model has been extended for use in the ExS forecasting and forward projection in a practitioner manner. In this regard, the underlying hypothesis, which is adopted as a rule of thumb, is such that the distributional quantiles, which are referred to for the estimation of the ExS in the QR model, preserve their relative position with respect to the distributional domain, which is supposed to grow by the square root of time, as time elapses. The model performance is more widespread on longer horizons. The expected-shortfall at 5% on a 1d horizon seems to be the most difficult to forecast, exhibiting the smallest MCS. The Historical Simulation method also performs reasonably, resulting in mid-ranking performance. Risk Metrics, another popular model among practitioners, does not exhibit a noticeable performance and on the short term horizon enters the MCS only in the VaR at the 5% level.

Name	Model
CH1g	Gaussian GARCH(1,1)
CH1t	Student-t GARCH(1,1)
CH1x_n	GARCH(1,1) with $\varepsilon \sim$ dual GPD tailed and normal mid-quantile
CH1x_ged	GARCH(1,1) with $\varepsilon \sim$ dual GPD tailed and GED mid-quantile
CH2g	Gaussian TARCH(1,1)
CH2t	Student-t TARCH(1,1)
CH2x_n	TARCH(1,1) with $\varepsilon \sim$ dual GPD tailed and normal mid-quantile
CH2x_ged	TARCH(1,1) with $\varepsilon \sim$ dual GPD tailed and GED mid-quantile
CH3g	Gaussian EGARCH(1,1)
CH3t	Student-t EGARCH(1,1)
CH3x_n	EGARCH(1,1) with $\varepsilon \sim$ dual GPD tailed and normal mid-quantile
CH3x_ged	EGARCH(1,1) with $\varepsilon \sim$ dual GPD tailed and GED mid-quantile
CH1g_avg	Unconditional Gaussian GARCH(1,1)
CH1t_avg	Unconditional Student-t GARCH(1,1)
CH1x_n_avg	Unconditional GARCH(1,1) with $\varepsilon \sim$ dual GPD tailed and normal mid-quantile
CH1x_ged_avg	Unconditional GARCH(1,1) with $\varepsilon \sim$ dual GPD tailed and GED mid-quantile
CH2g_avg	Unconditional Gaussian TARCH(1,1)
CH2t_avg	Unconditional Student-t TARCH(1,1)
CH2x_n_avg	Unconditional TARCH(1,1) with $\varepsilon \sim$ dual GPD tailed and normal mid-quantile
CH2x_ged_avg	Unconditional TARCH(1,1) with $\varepsilon \sim$ dual GPD tailed and GED mid-quantile
CH3g_avg	Unconditional Gaussian EGARCH(1,1)
CH3t_avg	Unconditional Student-t EGARCH(1,1)
CH3x_n_avg	Unconditional EGARCH(1,1) with $\varepsilon \sim$ dual GPD tailed and normal mid-quantile
CH3x_ged_avg	Unconditional EGARCH(1,1) with $\varepsilon \sim$ dual GPD tailed and GED mid-quantile
DT_n	Unconditional dual GPD tailed and normal mid-quantile
DT_ged	Unconditional dual GPD tailed and GED mid-quantile
G0	2 years rolling window Gaussian with 0 mean
Gm	2 years rolling window Gaussian
HS	2 years rolling window Histogram
KR	Kernel Regression
RM	RiskMetrics
QR1	Adaptive CAViaR
QR1_005	Adaptive CAViaR with 5 degree rational tail
QR1_010	Adaptive CAViaR with 10 degree rational tail
QR1_020	Adaptive CAViaR with 20 degree rational tail
QR2	Symmetric CAViaR
QR2_005	Symmetric CAViaR with 5 degree rational tail
QR2_010	Symmetric CAViaR with 10 degree rational tail
QR2_020	Symmetric CAViaR with 20 degree rational tail
QR3	Asymmetric CAViaR
QR3_005	Asymmetric CAViaR with 5 degree rational tail
QR3_010	Asymmetric CAViaR with 10 degree rational tail
QR3_020	Asymmetric CAViaR with 20 degree rational tail
QR4	GARCH Indirect CAViaR
QR4_005	GARCH Indirect CAViaR with 5 degree rational tail
QR4_010	GARCH Indirect CAViaR with 10 degree rational tail
QR4_020	GARCH Indirect CAViaR with 20 degree rational tail

Table 1: **VaR and ExS Forecasting Models.**

	VaR 1% 1d			VaR 5% 1d			VaR 1% 10d			VaR 5% 10d		
	Conf.	Set	mean	Conf.	Set	mean	Conf.	Set	mean	Conf.	Set	mean
CH1g	0.0146	0.0247	0.0194	0.0434	0.0595	0.0514	0.0052	0.0221	0.0125	0.0298	0.0617	0.0452
CH1t	0.0046	0.0114	0.0076	0.0292	0.0441	0.0367	0.0009	0.0115	0.0053	0.0152	0.0386	0.0263
CH1x_n	0.0075	0.0148	0.0108	0.0448	0.0605	0.0528	0.0026	0.0164	0.0086	0.0238	0.0528	0.0378
CH1x_ged	0.0075	0.0148	0.0108	0.0448	0.0605	0.0528	0.0026	0.0164	0.0086	0.0238	0.0528	0.0378
CH2g	0.0160	0.0254	0.0204	0.0458	0.0603	0.0532	0.0044	0.0194	0.0110	0.0297	0.0587	0.0439
CH2t	0.0053	0.0119	0.0083	0.0318	0.0454	0.0382	0.0006	0.0104	0.0047	0.0153	0.0373	0.0259
CH2x_n	0.0084	0.0154	0.0118	0.0497	0.0643	0.0569	0.0024	0.0149	0.0078	0.0251	0.0522	0.0384
CH2x_ged	0.0084	0.0154	0.0118	0.0497	0.0643	0.0569	0.0024	0.0149	0.0078	0.0251	0.0522	0.0384
CH3g	0.0173	0.0281	0.0224	0.0491	0.0640	0.0565	0.0047	0.0197	0.0114	0.0306	0.0615	0.0456
CH3t	0.0076	0.0148	0.0111	0.0380	0.0519	0.0449	0.0016	0.0131	0.0065	0.0200	0.0452	0.0321
CH3x_n	0.0097	0.0178	0.0136	0.0530	0.0688	0.0609	0.0031	0.0162	0.0089	0.0275	0.0567	0.0415
CH3x_ged	0.0097	0.0178	0.0136	0.0530	0.0688	0.0609	0.0031	0.0162	0.0089	0.0276	0.0566	0.0415
CH1g_avg	-	-	-	-	-	-	0.0103	0.0356	0.0219	0.0489	0.0911	0.0694
CH1t_avg	-	-	-	-	-	-	0.0041	0.0237	0.0126	0.0311	0.0666	0.0481
CH1x_n_avg	-	-	-	-	-	-	0.0070	0.0294	0.0169	0.0405	0.0803	0.0599
CH1x_ged_avg	-	-	-	-	-	-	0.0068	0.0293	0.0169	0.0407	0.0803	0.0598
CH2g_avg	-	-	-	-	-	-	0.0089	0.0327	0.0196	0.0469	0.0882	0.0669
CH2t_avg	-	-	-	-	-	-	0.0031	0.0219	0.0110	0.0303	0.0651	0.0470
CH2x_n_avg	-	-	-	-	-	-	0.0060	0.0282	0.0157	0.0405	0.0800	0.0596
CH2x_ged_avg	-	-	-	-	-	-	0.0060	0.0282	0.0157	0.0406	0.0803	0.0597
CH3g_avg	-	-	-	-	-	-	0.0085	0.0323	0.0194	0.0447	0.0854	0.0640
CH3t_avg	-	-	-	-	-	-	0.0042	0.0239	0.0126	0.0309	0.0663	0.0479
CH3x_n_avg	-	-	-	-	-	-	0.0063	0.0287	0.0162	0.0400	0.0794	0.0589
CH3x_ged_avg	-	-	-	-	-	-	0.0063	0.0287	0.0162	0.0400	0.0794	0.0590
DT_n	0.0112	0.0245	0.0176	0.0572	0.0826	0.0702	0.0101	0.0351	0.0215	0.0333	0.0697	0.0506
DT_ged	0.0112	0.0245	0.0176	0.0572	0.0826	0.0702	0.0100	0.0351	0.0215	0.0333	0.0697	0.0506
G0	0.0168	0.0297	0.0234	0.0440	0.0643	0.0542	0.0101	0.0330	0.0204	0.0334	0.0697	0.0511
Gm	0.0181	0.0305	0.0243	0.0460	0.0655	0.0560	0.0127	0.0353	0.0234	0.0418	0.0752	0.0587
HS	0.0102	0.0184	0.0141	0.0472	0.0644	0.0564	0.0107	0.0307	0.0201	0.0388	0.0712	0.0548
KR	0.0097	0.0198	0.0146	0.0171	0.0316	0.0245	0.0117	0.0332	0.0218	0.0482	0.0859	0.0666
RM	0.0143	0.0240	0.0192	0.0460	0.0628	0.0547	0.0068	0.0255	0.0153	0.0320	0.0636	0.0470
QR1	0.0135	0.0233	0.0181	0.0551	0.0722	0.0634	0.0074	0.0237	0.0150	0.0396	0.0700	0.0541
QR2	0.0133	0.0242	0.0183	0.0512	0.0689	0.0605	0.0069	0.0256	0.0152	0.0370	0.0719	0.0540
QR3	0.0145	0.0247	0.0196	0.0585	0.0739	0.0658	0.0089	0.0269	0.0172	0.0431	0.0769	0.0603
QR4	0.0163	0.0286	0.0225	0.0559	0.0755	0.0665	0.0096	0.0333	0.0209	0.0429	0.0813	0.0611

Table 2: **VaR MHT.** MHT with 1% 3-FWER for ECP and MHT with 5% 4-FWER for ECP. The table contains balanced confidence sets, with control of the generalised family-wise error rate. The grey shaded cells indicate model performance significance which have been rejected during the step-down algorithm. The performance of the CH1x_* models is remarkable, as it is consistent throughout the experiment, a result that is persistent for the ExS metric and in the majority of the stressed scenarios. The remaining heteroskedastic models produce relevant performances with some rejections. The unconditional heteroskedastic models CH**_avg all produce significant 2w forecast performance, a result that indicates that "on average" we could disregard conditioning, although it is evident from the stressed scenarios' results of this type of models that this strategy might incur into frequent errors. The performance of the remaining models is in general not significant.

	ExS 1% 1d			ExS 5% 1d			ExS 1% 10d			ExS 5% 10d		
	Conf.	Set	mean	Conf.	Set	mean	Conf.	Set	mean	Conf.	Set	mean
CH1g	0.0004	0.0027	0.0013	0.0144	0.0253	0.0196	0.0007	0.0093	0.0034	0.0152	0.0401	0.0262
CH1t	0.0038	0.0099	0.0066	0.0281	0.0399	0.0339	0.0031	0.0225	0.0106	0.0308	0.0659	0.0471
CH1x_n	0.0029	0.0069	0.0048	0.0193	0.0267	0.0228	0.0017	0.0142	0.0062	0.0207	0.0489	0.0333
CH1x_ged	0.0029	0.0069	0.0048	0.0193	0.0267	0.0228	0.0017	0.0142	0.0062	0.0207	0.0489	0.0333
CH2g	0.0003	0.0024	0.0011	0.0142	0.0230	0.0185	0.001	0.0103	0.0043	0.0173	0.0404	0.0277
CH2t	0.0034	0.009	0.0059	0.0277	0.0380	0.0326	0.0039	0.0235	0.0118	0.0324	0.0649	0.0476
CH2x_n	0.0028	0.0065	0.0044	0.0180	0.0245	0.0211	0.0023	0.0144	0.007	0.0219	0.0468	0.0333
CH2x_ged	0.0028	0.0065	0.0044	0.0180	0.0245	0.0211	0.0023	0.0144	0.007	0.0219	0.0468	0.0333
CH3g	0.0002	0.0019	0.0008	0.0120	0.0210	0.0163	0.0009	0.0101	0.0041	0.0165	0.0398	0.0267
CH3t	0.0023	0.0066	0.0043	0.0226	0.0311	0.0267	0.0025	0.0179	0.0083	0.0259	0.0557	0.0394
CH3x_n	0.0023	0.0057	0.0038	0.0159	0.0225	0.0191	0.0018	0.0132	0.006	0.0197	0.0443	0.0306
CH3x_ged	0.0023	0.0057	0.0038	0.0159	0.0225	0.0191	0.0018	0.0132	0.006	0.0197	0.0443	0.0305
DT_n	0.0007	0.0046	0.0020	0.0112	0.0202	0.0151	0.0001	0.0045	0.0009	0.0074	0.0349	0.0187
DT_ged	0.0007	0.0046	0.0020	0.0112	0.0202	0.0151	0.0001	0.0045	0.0009	0.0074	0.0349	0.0187
G0	0.0000	0.0009	0.0003	0.0105	0.0226	0.0154	0.0000	0.0039	0.0008	0.0083	0.0345	0.0188
Gm	0.0000	0.0008	0.0002	0.0099	0.0205	0.0143	0.0000	0.0027	0.0006	0.0068	0.0261	0.0147
HS	0.0032	0.006	0.0045	0.0183	0.0252	0.0215	0.0007	0.0045	0.0018	0.0101	0.0309	0.0184
KR	0.0000	0.0025	0.0003	0.0354	0.0626	0.0480	0.0002	0.0033	0.0011	0.0073	0.0231	0.0139
RM	0.0003	0.0021	0.0009	0.0132	0.0225	0.0176	0.0002	0.0067	0.002	0.0126	0.0377	0.0236
QR1	0.0091	0.0096	0.0093	0.0156	0.0221	0.0185	0.0090	0.0105	0.0096	0.0153	0.0334	0.0229
QR1_005	0.0065	0.0081	0.0073	0.0151	0.0216	0.0180	0.0063	0.0098	0.0080	0.0147	0.0332	0.0225
QR1_010	0.0046	0.0067	0.0057	0.0147	0.0212	0.0176	0.0043	0.0092	0.0066	0.0142	0.033	0.0222
QR1_020	0.0027	0.005	0.0038	0.0141	0.0207	0.0171	0.0021	0.0084	0.0049	0.0135	0.0329	0.0218
QR2	0.0090	0.0096	0.0094	0.0165	0.0245	0.0203	0.0090	0.0110	0.0096	0.0159	0.0363	0.0244
QR2_005	0.0063	0.0084	0.0074	0.0160	0.0242	0.0198	0.0061	0.0105	0.0080	0.0152	0.0362	0.0241
QR2_010	0.0044	0.0072	0.0058	0.0156	0.0239	0.0195	0.004	0.0099	0.0065	0.0146	0.036	0.0237
QR2_020	0.0024	0.0057	0.0039	0.0150	0.0236	0.0190	0.0019	0.0091	0.0048	0.0138	0.0358	0.0233
QR3	0.0091	0.0096	0.0094	0.0157	0.0221	0.0187	0.0090	0.0100	0.0095	0.0148	0.0309	0.0216
QR3_005	0.0064	0.0083	0.0074	0.0152	0.0217	0.0182	0.0061	0.0093	0.0078	0.0141	0.0307	0.0212
QR3_010	0.0045	0.007	0.0058	0.0147	0.0214	0.0178	0.004	0.0085	0.0062	0.0135	0.0306	0.0208
QR3_020	0.0025	0.0054	0.0038	0.0140	0.0210	0.0173	0.0019	0.0075	0.0044	0.0126	0.0304	0.0203
QR4	0.0088	0.0095	0.0091	0.0130	0.0205	0.0160	0.0087	0.0098	0.0093	0.0118	0.0298	0.0188
QR4_005	0.0055	0.0077	0.0066	0.0122	0.0200	0.0154	0.0052	0.0089	0.0071	0.0109	0.0295	0.0182
QR4_010	0.0033	0.0061	0.0046	0.0115	0.0196	0.0148	0.003	0.008	0.0053	0.01	0.0292	0.0177
QR4_020	0.0014	0.0045	0.0025	0.0107	0.0192	0.0142	0.0011	0.0067	0.0033	0.0089	0.029	0.0171

Table 3: **ExS MHT.** MHT with 1% 4-FWER for ExS and MHT with 5% 5-FWER for ExS. The table contains balanced confidence sets, with control of the generalised family-wise error rate. The grey shaded cells indicate model performance significance which have been rejected during the step-down algorithm. With respect to the ExS forecasting experiment, the only result that stands out is the performance of the CH1x_* models, whereas the remaining models produce non persistent results.

	VaR 1% 1d			VaR 5% 1d			VaR 1% 10d			VaR 5% 10d		
	Conf.	Set	mean	Conf.	Set	mean	Conf.	Set	mean	Conf.	Set	mean
CH1g	0.0041	0.0215	0.0120	0.0180	0.0479	0.0317	0.0000	0.0119	0.0030	0.0053	0.0481	0.0227
CH1t	0.0000	0.0101	0.0039	0.0094	0.0345	0.0210	0.0000	0.0081	0.0008	0.0005	0.0303	0.0118
CH1x_n	0.0004	0.0132	0.0060	0.0197	0.0490	0.0335	0.0000	0.0105	0.0016	0.0029	0.0400	0.0178
CH1x_ged	0.0004	0.0132	0.0060	0.0197	0.0490	0.0335	0.0000	0.0105	0.0016	0.0029	0.0400	0.0178
CH2g	0.0042	0.0202	0.0117	0.0177	0.0446	0.0308	0.0000	0.0114	0.0021	0.0046	0.0420	0.0201
CH2t	0.0000	0.0107	0.0044	0.0114	0.0346	0.0223	0.0000	0.0071	0.0006	0.0003	0.0280	0.0111
CH2x_n	0.0007	0.0130	0.0060	0.0199	0.0471	0.0334	0.0000	0.0084	0.0011	0.0025	0.0359	0.0161
CH2x_ged	0.0007	0.0130	0.0060	0.0199	0.0471	0.0334	0.0000	0.0084	0.0011	0.0025	0.0359	0.0161
CH3g	0.0054	0.0225	0.0132	0.0202	0.0498	0.0334	0.0000	0.0112	0.0029	0.0053	0.0449	0.0219
CH3t	0.0011	0.0148	0.0067	0.0154	0.0410	0.0270	0.0000	0.0101	0.0015	0.0025	0.0359	0.0159
CH3x_n	0.0017	0.0156	0.0076	0.0250	0.0510	0.0375	0.0000	0.0113	0.0020	0.0039	0.0413	0.0192
CH3x_ged	0.0017	0.0156	0.0076	0.0250	0.0510	0.0375	0.0000	0.0113	0.0020	0.0039	0.0413	0.0192
CH1g_avg	-	-	-	-	-	-	0.0000	0.0032	0.0001	0.0000	0.0190	0.0053
CH1t_avg	-	-	-	-	-	-	0.0000	0.0000	0.0000	0.0000	0.0088	0.0014
CH1x_n_avg	-	-	-	-	-	-	0.0000	0.0011	0.0000	0.0000	0.0135	0.0030
CH1x_ged_avg	-	-	-	-	-	-	0.0000	0.0011	0.0000	0.0000	0.0135	0.0030
CH2g_avg	-	-	-	-	-	-	0.0000	0.0017	0.0000	0.0000	0.0170	0.0046
CH2t_avg	-	-	-	-	-	-	0.0000	0.0000	0.0000	0.0000	0.0084	0.0012
CH2x_n_avg	-	-	-	-	-	-	0.0000	0.0004	0.0000	0.0000	0.0125	0.0026
CH2x_ged_avg	-	-	-	-	-	-	0.0000	0.0004	0.0000	0.0000	0.0125	0.0026
CH3g_avg	-	-	-	-	-	-	0.0000	0.0016	0.0000	0.0000	0.0149	0.0036
CH3t_avg	-	-	-	-	-	-	0.0000	0.0000	0.0000	0.0000	0.0088	0.0014
CH3x_n_avg	-	-	-	-	-	-	0.0000	0.0008	0.0000	0.0000	0.0127	0.0027
CH3x_ged_avg	-	-	-	-	-	-	0.0000	0.0008	0.0000	0.0000	0.0127	0.0027
DT_n	0.0000	0.0047	0.0010	0.0019	0.0215	0.0104	0.0000	0.0032	0.0001	0.0000	0.0095	0.0016
DT_ged	0.0000	0.0047	0.0010	0.0019	0.0215	0.0104	0.0000	0.0032	0.0001	0.0000	0.0095	0.0016
G0	0.0014	0.0181	0.0081	0.0115	0.0403	0.0256	0.0000	0.0163	0.0044	0.0022	0.0442	0.0191
Gm	0.0015	0.0181	0.0084	0.0126	0.0426	0.0274	0.0004	0.0196	0.0064	0.0066	0.0531	0.0261
HS	0.0012	0.0127	0.0065	0.0128	0.0409	0.0267	0.0000	0.0173	0.0056	0.0056	0.0496	0.0242
KR	0.0000	0.0047	0.0010	0.0000	0.0044	0.0010	0.0000	0.0044	0.0002	0.0000	0.0223	0.0079
RM	0.0066	0.0263	0.0158	0.0348	0.0649	0.0491	0.0026	0.0259	0.0103	0.0162	0.0656	0.0386
QR1	0.0039	0.0185	0.0103	0.0506	0.0825	0.0654	0.0008	0.0199	0.0066	0.0275	0.0779	0.0508
QR2	0.0012	0.0163	0.0079	0.0183	0.0496	0.0335	0.0000	0.0125	0.0032	0.0073	0.0560	0.0273
QR3	0.0010	0.0141	0.0066	0.0218	0.0518	0.0356	0.0000	0.0122	0.0025	0.0127	0.0517	0.0306
QR4	0.0000	0.0056	0.0013	0.0096	0.0363	0.0224	0.0000	0.0057	0.0003	0.0022	0.0393	0.0169

Table 4: **L/V VaR MHT.** L/V MHT with 1% 3-FWER for ECP and L/V MHT with 5% 4-FWER for ECP. The table contains balanced confidence sets, with control of the generalised family-wise error rate. The grey shaded cells indicate model performance significance which have been rejected during the step-down algorithm. The low volatility scenario is the only environment where the CH1x_* models do not produce significant performances, whereas the only model that performs well under this volatility condition is the RM.

	VaR 1% 1d			VaR 5% 1d			VaR 1% 10d			VaR 5% 10d		
	Conf.	Set	mean	Conf.	Set	mean	Conf.	Set	mean	Conf.	Set	mean
CH1g	0.0135	0.0367	0.0246	0.0460	0.0821	0.0640	0.0067	0.0541	0.0270	0.0377	0.1154	0.0756
CH1t	0.0039	0.0207	0.0115	0.0308	0.0628	0.0457	0.0004	0.0320	0.0133	0.0191	0.0799	0.0475
CH1x_n	0.0068	0.0255	0.0156	0.0471	0.0832	0.0650	0.0029	0.0424	0.0199	0.0302	0.1042	0.0653
CH1x_ged	0.0068	0.0255	0.0156	0.0471	0.0832	0.0650	0.0029	0.0424	0.0199	0.0302	0.1040	0.0653
CH2g	0.0147	0.0356	0.0254	0.0522	0.0851	0.0675	0.0060	0.0470	0.0239	0.0396	0.1114	0.0742
CH2t	0.0050	0.0202	0.0122	0.0335	0.0606	0.0474	0.0001	0.0283	0.0116	0.0192	0.0763	0.0464
CH2x_n	0.0080	0.0245	0.0162	0.0559	0.0902	0.0723	0.0028	0.0390	0.0183	0.0341	0.1029	0.0666
CH2x_ged	0.0080	0.0245	0.0162	0.0559	0.0902	0.0723	0.0028	0.0389	0.0183	0.0341	0.1029	0.0666
CH3g	0.0175	0.0414	0.0293	0.0553	0.0911	0.0732	0.0063	0.0489	0.0250	0.0431	0.1173	0.0785
CH3t	0.0072	0.0239	0.0159	0.0408	0.0714	0.0565	0.0016	0.0342	0.0152	0.0261	0.0888	0.0560
CH3x_n	0.0096	0.0279	0.0189	0.0589	0.0969	0.0778	0.0038	0.0423	0.0204	0.0380	0.1093	0.0722
CH3x_ged	0.0096	0.0279	0.0189	0.0589	0.0969	0.0778	0.0038	0.0423	0.0204	0.0381	0.1093	0.0722
CH1g_avg	-	-	-	-	-	-	0.0263	0.1172	0.0691	0.1001	0.2363	0.1655
CH1t_avg	-	-	-	-	-	-	0.0122	0.0820	0.0425	0.0704	0.1861	0.1261
CH1x_n_avg	-	-	-	-	-	-	0.0192	0.1012	0.0552	0.0860	0.2123	0.1472
CH1x_ged_avg	-	-	-	-	-	-	0.0192	0.1012	0.0552	0.0860	0.2123	0.1472
CH2g_avg	-	-	-	-	-	-	0.0233	0.1099	0.0627	0.0972	0.2311	0.1608
CH2t_avg	-	-	-	-	-	-	0.0095	0.0755	0.0373	0.0678	0.1823	0.1238
CH2x_n_avg	-	-	-	-	-	-	0.0172	0.0975	0.0518	0.0864	0.2129	0.1474
CH2x_ged_avg	-	-	-	-	-	-	0.0172	0.0975	0.0519	0.0867	0.2129	0.1476
CH3g_avg	-	-	-	-	-	-	0.0226	0.1092	0.0620	0.0931	0.2242	0.1561
CH3t_avg	-	-	-	-	-	-	0.0118	0.0816	0.0423	0.0693	0.1849	0.1257
CH3x_n_avg	-	-	-	-	-	-	0.0176	0.0988	0.0529	0.0848	0.2111	0.1457
CH3x_ged_avg	-	-	-	-	-	-	0.0176	0.0988	0.0529	0.0849	0.2112	0.1458
DT_n	0.0266	0.0729	0.0492	0.1063	0.1772	0.1434	0.0259	0.1162	0.0680	0.0755	0.1929	0.1312
DT_ged	0.0266	0.0729	0.0492	0.1063	0.1772	0.1434	0.0259	0.1162	0.0680	0.0755	0.1929	0.1312
G0	0.0233	0.0608	0.0416	0.0611	0.1129	0.0882	0.0147	0.0840	0.0459	0.0517	0.1540	0.1006
Gm	0.0239	0.0598	0.0421	0.0625	0.1131	0.0884	0.0159	0.0824	0.0459	0.0574	0.1463	0.1009
HS	0.0140	0.0363	0.0251	0.0684	0.1124	0.0915	0.0134	0.0756	0.0414	0.0544	0.1406	0.0958
KR	0.0218	0.0563	0.0393	0.0370	0.0808	0.0585	0.0302	0.1009	0.0640	0.0956	0.2108	0.1511
RM	0.0108	0.0318	0.0214	0.0423	0.0757	0.0590	0.0065	0.0526	0.0267	0.0315	0.1058	0.0670
QR1	0.0176	0.0412	0.0291	0.0514	0.0941	0.0727	0.0091	0.0599	0.0317	0.0455	0.1161	0.0794
QR2	0.0146	0.0412	0.0285	0.0591	0.1012	0.0800	0.0084	0.0669	0.0342	0.0490	0.1353	0.0902
QR3	0.0175	0.0421	0.0297	0.0678	0.1056	0.0867	0.0129	0.0669	0.0377	0.0569	0.1412	0.0960
QR4	0.0281	0.0684	0.0475	0.0793	0.1291	0.1050	0.0214	0.0996	0.0578	0.0657	0.1722	0.1160

Table 5: **H/V VaR MHT.** H/V MHT with 1% 4-FWER for ECP and H/V MHT with 5% 5-FWER for ECP. The table contains balanced confidence sets, with control of the generalised family-wise error rate. The grey shaded cells indicate model performance significance which have been rejected during the step-down algorithm. In a high volatility scenario, the sole models producing significant and persistent performance are the heteroskedastic symmetric models with fat tails, that is the CH*t and the CH1x_*.

max-MCS		MCS-10%		MCS-50%		t-MCS	
CH1x_ged	1	CH3t	0.7289	CH3t	0.5794	CH1x_n	0.57019
CH1x_n	1	CH1x_n	0.7216	CH1x_n	0.5658	CH1x_ged	0.57019
CH3t	1	CH1x_ged	0.7216	CH1x_ged	0.5658	CH3t	0.42981
CH2t	1	CH2t	0.6185	CH2t	0.4843	CH2t	0.38552
CH2x_ged	0.9997	CH2x_n	0.5490	CH1t	0.2884	CH2x_n	0.23733
CH2x_n	0.9997	CH2x_ged	0.5490	CH2x_n	0.2875	CH2x_ged	0.23733
CH1t	0.9973	CH1t	0.4655	CH2x_ged	0.2875	CH1t	0.18018
KR	0.7080	CH3x_n	0.2026	*****	*****	*****	*****
HS	0.5681	CH3x_ged	0.2026	CH3x_n	0.1099	KR	0.03719
CH3x_ged	0.5259	HS	0.1867	CH3x_ged	0.1099	HS	0.02463
CH3x_n	0.5259	KR	0.1498	KR	0.0804	CH3x_n	0.02177
DT_ged	0.0897	*****	*****	HS	0.0804	CH3x_ged	0.02177
DT_n	0.0897	DT_n	0.0138	DT_n	0.0111	DT_n	0.00225
*****	*****	DT_ged	0.0138	DT_ged	0.0111	DT_ged	0.00225
QR1	0.0058	QR1	0.0072	QR2	0.0021	QR1	0
QR2	0.0002	QR2	0.0039	RM	0.0005	QR2	0
RM	0.0001	RM	0.0016	QR1	0.0004	RM	0
QR4	0.0001	CH1g	0.0011	CH1g	0.0003	QR4	0
CH1g	0.0001	QR3	0.0008	QR3	0.0003	CH1g	0
QR3	0.0001	CH2g	0.0001	CH2g	0	QR3	0
G0	0	CH3g	0	CH3g	0	G0	0
CH2g	0	G0	0	G0	0	CH2g	0
Gm	0	Gm	0	Gm	0	Gm	0
CH3g	0	QR4	0	QR4	0	CH3g	0

Table 6: **VaR** 1% **1d.** This table contains the output of the MCS produced by the Hansen et al.'s, the modified Corradi et al's and this thesis MCS algorithms, applied to a market risk forecasting model set. Each column contains the output of the corresponding MCS test, indicating the model label, the model confidence set cut-off, represented by an asterisk line and the model ranking achieved within each set by means of the p-values. We produce the MCS-max the MCS-γ at 10% and 50% γ and the MCS-t. The confidence level is at 5%. Considering the k, the selected FWER levels for the MCS10% and the MCS50% are, respectively, $k = 13$ and $k = 93$. The MCS test can expose the best performing models and isolate them from the initial model set, at the same time producing a ranking measure through the p-value provided. In the 1d forecasting experiments, the CH1_* models are included in the MCS and rank as the top performers. It is worth mentioning the tendency of the max-MCS to assimilate the performance of the highest cluster with indiscriminate p-values, whereas the γ-MCS and the t-MCS can produce more diversified ranking measures. Another notice is for the HS model performance as ranked by the max-MCS and by the γ and the t test, whereby the former assigns a probability of 0.57 to the superiority of this model, whereas the latter two tests either rank the model very low or expel it from the MCS. The comments to this table are in Section 2.3.

max-MCS		MCS-10%		MCS-50%		t-MCS	
CH1g	1	CH1g	0.8453	CH1g	0.7924	CH1g	0.68824
CH2g	0.9999	CH2g	0.7276	CH2g	0.6023	CH2g	0.31176
CH1x_ged	0.9998	CH1x_n	0.7013	CH1x_n	0.5716	CH1x_n	0.26866
CH1x_n	0.9998	CH1x_ged	0.7013	CH1x_ged	0.5716	CH1x_ged	0.26866
CH3t	0.9996	G0	0.6085	G0	0.4991	CH3t	0.23502
G0	0.9995	RM	0.5240	CH3t	0.4019	G0	0.23264
RM	0.9877	CH3t	0.4920	RM	0.3598	RM	0.14665
Gm	0.9623	Gm	0.3941	Gm	0.2503	Gm	0.10926
HS	0.9385	HS	0.3478	HS	0.2009	HS	0.09201
CH3g	0.5527	CH3g	0.3260	*****	*****	*****	*****
CH2x_ged	0.1291	CH2x_n	0.2448	CH3g	0.2047	CH3g	0.02346
CH2x_n	0.1291	CH2x_ged	0.2448	CH2x_n	0.1749	CH2x_n	0.00322
*****	*****	QR2	0.033	CH2x_ged	0.1749	CH2x_ged	0.00322
QR2	0.0306	*****	*****	CH2t	0.0482	QR2	0.00050
QR1	0.0306	CH2t	0.0911	QR2	0.0375	QR1	0.00042
CH3x_ged	0.0008	CH1t	0.0607	CH1t	0.0324	CH3x_n	0
CH3x_n	0.0008	CH3x_n	0.0460	CH3x_n	0.0253	CH3x_ged	0
CH2t	0.0002	CH3x_ged	0.0460	CH3x_ged	0.0253	CH2t	0
QR4	0.0001	QR1	0.0232	QR1	0.0071	QR4	0
DT_ged	0.0001	QR4	0.0013	QR4	0.0018	DT_n	0
DT_n	0.0001	QR3	0.0012	QR3	0.0012	DT_ged	0
CH1t	0.0001	DT_n	0.0003	DT_n	0.0004	CH1t	0
QR3	0	DT_ged	0.0003	DT_ged	0.0004	QR3	0
KR	0	KR	0	KR	0	KR	0

Table 7: **VaR** 5% **1d.** This table contains the output of the MCS produced by the Hansen et al.'s, the modified Corradi et al's and this thesis MCS algorithms, applied to a market risk forecasting model set. Each column contains the output of the corresponding MCS test, indicating the model label, the model confidence set cut-off, represented by an asterisk line and the model ranking achieved within each set by means of the p-values. We produce the MCS-max the MCS-γ at 10% and 50% γ and the MCS-t. The confidence level is at 5%. Considering the k, the selected FWER levels for the MCS10% and the MCS50% are, respectively, $k = 10$ and $k = 67$. In this experiment, the heteroskedastic models perform best again, with EVD extension as well as the Gaussian type. Some practitioner models such as G0 and RM also enter the MCS. Although both tests produce the same MCS, the contrast between the *max*-MCS and the MHT based MCS can be seen from the p-value measure, whereby, for instance, the HS model is ranked at 0.94 in the former and 0.35 in the latter. The comments to this table are in Section 2.3.

max-MCS		MCS-10%		MCS-50%		t-MCS	
QR4_010	1	QR4_010	0.7407	QR4_010	0.7407	QR4_010	0.5717
CH1x_ged	1	CH1x_n	0.7044	CH1x_n	0.7044	CH1x_ged	0.4283
CH1x_n	1	CH1x_ged	0.7009	CH1x_ged	0.7009	CH1x_n	0.4280
HS	1	HS	0.6694	HS	0.6694	HS	0.4226
QR1_010	1	CH2x_n	0.5917	CH2x_n	0.5917	QR1_010	0.3814
QR3_010	1	CH2x_ged	0.5917	CH2x_ged	0.5917	QR3_010	0.3541
QR2_010	1	QR1_010	0.5790	QR1_010	0.5790	QR2_010	0.3514
CH2x_n	1	QR3_010	0.5424	QR3_010	0.5423	CH2x_n	0.3271
CH2x_ged	1	QR2_010	0.5302	QR2_010	0.5301	CH2x_ged	0.3265
CH2t	1	CH3t	0.5188	CH3t	0.5188	CH2t	0.2867
CH3t	0.9999	CH2t	0.4697	CH2t	0.4697	CH3t	0.2329
CH1t	0.9775	QR2_020	0.3569	QR2_020	0.3570	CH1t	0.1006
QR2_020	0.9351	QR3_020	0.3203	QR3_020	0.3203	QR2_020	0.0718
CH3x_n	0.9249	QR1_020	0.2983	QR1_020	0.2983	CH3x_n	0.0677
CH3x_ged	0.9248	CH3x_n	0.2826	CH1t	0.2677	CH3x_ged	0.0676
QR3_020	0.8951	CH3x_ged	0.2718	CH3x_n	0.2464	QR3_020	0.0579
QR1_020	0.6587	CH1t	0.2677	CH3x_ged	0.2464	*****	*****
*****	*****	*****	*****	*****	*****	QR1_020	0.0255
QR4_005	0.0017	QR4_005	0.1949	QR4_005	0.1949	QR4_005	0
DT_ged	0.0002	QR2_005	0.0441	QR2_005	0.0441	DT_ged	0
DT_n	0.0002	QR3_005	0.0416	QR3_005	0.0416	DT_n	0
QR4_020	0.0000	QR1_005	0.0393	QR1_005	0.0393	QR4_020	0
CH1g	0	QR4_020	0.0334	QR4_020	0.0334	CH1g	0
CH2g	0	DT_ged	0.0202	DT_ged	0.0202	CH2g	0
RM	0	DT_n	0.0200	DT_n	0.0200	CH3g	0
CH3g	0	CH1g	0.0065	CH1g	0.0065	G0	0
QR2_005	0	CH2g	0.0041	CH2g	0.0041	Gm	0
KR	0	RM	0.0034	RM	0.0034	KR	0
QR3_005	0	CH3g	0.0025	CH3g	0.0025	RM	0
QR1	0	KR	0.0008	KR	0.0008	QR1	0
QR3	0	QR4	0.0008	QR4	0.0008	QR1_005	0
QR4	0	G0	0.0006	G0	0.0006	QR2	0
Gm	0	QR1	0.0005	QR1	0.0005	QR2_005	0
G0	0	Gm	0.0005	Gm	0.0005	QR3	0
QR2	0	QR2	0.0005	QR2	0.0005	QR3_005	0
QR1_005	0	QR3	0.0005	QR3	0.0005	QR4	0

Table 8: **ExS** 1% **1d.** This table contains the output of the MCS produced by the Hansen et al.'s, the modified Corradi et al's and this thesis MCS algorithms, applied to a market risk forecasting model set. Each column contains the output of the corresponding MCS test, indicating the model label, the model confidence set cut-off, represented by an asterisk line and the model ranking achieved within each set by means of the p-values. We produce the MCS-max the MCS-γ at 10% and 50% γ and the MCS-t. The confidence level is at 5%. Considering the k, the selected FWER levels for the MCS10% and the MCS50% are, respectively, $k = 29$ and $k = 179$. In this exercise, the CH1x_* persistently perform at the top of the collective, whereas the QR4_010 model now achieves top performance. It is interesting to notice that the QR model has been structured in a creative way to allow the estimation of the ExS measure, indeed capturing the tail dynamics, by the joint modelling of multiple quantile autoregressions, as well as providing a consistent guess of the tail behaviour, by including a polynomially decaying curve to accommodate the transition density shape at the border. The comments to this table are in Section 2.3.

max-MCS		MCS-10%		MCS-50%		t-MCS	
CH3t	1	CH1x_ged	0.8688	CH1x_ged	0.7110	CH3t	0.5510
CH1x_ged	1	CH1x_n	0.7593	CH3t	0.6385	CH1x_ged	0.4490
CH1x_n	0.9654	CH3t	0.7357	CH1x_n	0.4555	CH1x_n	0.2382
HS	0.8836	HS	0.5009	HS	0.1918	HS	0.1668
CH2x_ged	0.0678	CH2x_ged	0.4956	*****	*****	*****	*****
CH2x_n	0.0677	CH2x_n	0.3593	CH2x_n	0.1606	CH2x_ged	0.0057
*****	*****	QR2	0.1934	CH2x_ged	0.1606	CH2x_n	0.0057
QR1	0.0274	CH1g	0.0844	QR2	0.0886	QR1	0.0016
QR2	0.0046	*****	*****	CH1g	0.0745	QR2	0.0002
CH1g	0.0026	QR2_005	0.1162	QR2_005	0.0626	CH1g	0
QR3	0.0000	CH2t	0.0992	QR2_010	0.0430	QR3	0
CH2g	0	QR2_010	0.0783	CH2t	0.0360	CH2g	0
KR	0	CH1t	0.0579	QR2_020	0.0285	KR	0
CH1t	0	CH3x_n	0.0541	CH3x_n	0.0225	CH1t	0
CH3x_n	0	CH3x_ged	0.0541	CH3x_ged	0.0225	CH3x_n	0
CH3x_ged	0	QR1	0.0526	CH2g	0.0211	CH3x_ged	0
CH2t	0	QR2_020	0.0426	CH1t	0.0206	CH2t	0
G0	0	QR3	0.0368	QR3	0.0141	CH3g	0
DT_ged	0	QR1_005	0.0321	RM	0.0116	DT_n	0
DT_n	0	QR3_005	0.0211	QR3_005	0.0110	DT_ged	0
QR2_005	0	CH2g	0.0199	QR3_010	0.0079	G0	0
QR4	0	QR1_010	0.0195	QR1	0.0076	Gm	0
QR4_005	0	QR1_020	0.0106	QR3_020	0.0058	RM	0
QR3_005	0	QR3_010	0.0105	QR1_005	0.0046	QR1_005	0
RM	0	RM	0.0059	CH3g	0.0044	QR1_010	0
CH3g	0	QR3_020	0.0049	G0	0.0041	QR1_020	0
QR2_010	0	G0	0.0036	QR1_010	0.0026	QR2_005	0
QR4_010	0	CH3g	0.0022	QR4	0.0013	QR2_010	0
QR2_020	0	DT_n	0.0010	QR1_020	0.0011	QR2_020	0
QR3_010	0	DT_ged	0.0010	DT_n	0.0010	QR3_005	0
QR4_020	0	QR4	0.0008	DT_ged	0.0010	QR3_010	0
QR3_020	0	Gm	0.0006	Gm	0.0010	QR3_020	0
Gm	0	QR4_005	0.0004	QR4_005	0.0006	QR4	0
QR1_005	0	QR4_010	0.0003	QR4_010	0.0006	QR4_005	0
QR1_010	0	QR4_020	0.0003	QR4_020	0.0005	QR4_010	0
QR1_020	0	KR	0	KR	0	QR4_020	0

Table 9: **ExS** 5% **1d.** This table contains the output of the MCS produced by the Hansen et al.'s, the modified Corradi et al's and this thesis MCS algorithms, applied to a market risk forecasting model set. Each column contains the output of the corresponding MCS test, indicating the model label, the model confidence set cut-off, represented by an asterisk line and the model ranking achieved within each set by means of the p-values. We produce the MCS-max the MCS-γ at 10% and 50% γ and the MCS-t. The confidence level is at 5%. Considering the k, the selected FWER levels for the MCS10% and the MCS50% are, respectively, $k = 25$ and $k = 187$. In this exercise, again the fat-tailed conditionally heteroskedastic models perform best. Divergence between the *max*-MCS and the tests performing a direct model comparison can be inferred from the HS model p-value, very high in the first case, whereas it exhibits borderline behaviour in the latter cases. The comments to this table are in Section 2.3.

max-MCS		MCS-10%		MCS-50%		t-MCS	
CH3x_ged	1	CH2g	0.7743	CH2g	0.7743	CH3x_ged	0.5065
CH3x_n	1	CH3g	0.7648	CH3g	0.7648	CH3x_n	0.4935
CH2g	1	CH3x_ged	0.7344	CH3x_ged	0.7344	CH2g	0.4789
CH3g	1	CH3x_n	0.7339	CH3x_n	0.7339	CH3g	0.4367
CH1x_n	1	CH2t_avg	0.7288	CH2t_avg	0.7288	CH1x_n	0.4340
CH1x_ged	1	CH1g	0.7215	CH1g	0.7215	CH1x_ged	0.4337
CH2t_avg	1	CH1x_n	0.7094	CH1x_n	0.7094	CH2t_avg	0.4142
CH2x_n	1	CH1x_ged	0.7094	CH1x_ged	0.7094	CH2x_n	0.3747
CH2x_ged	1	CH1t_avg	0.6987	CH1t_avg	0.6987	CH2x_ged	0.3738
CH1t_avg	1	CH3t_avg	0.6952	CH3t_avg	0.6952	CH1t_avg	0.3280
CH3t_avg	1	CH2x_n	0.6684	CH2x_n	0.6684	CH3t_avg	0.3253
CH1g	1	CH2x_ged	0.6680	CH2x_ged	0.6680	CH1g	0.3060
CH3t	1	CH3t	0.5921	CH3t	0.5921	CH3t	0.2438
QR1	1	QR1	0.5820	QR1	0.5820	QR1	0.1959
QR2	1	QR2	0.5748	QR2	0.5748	QR2	0.1442
CH2x_n_avg	1	CH2x_n_avg	0.5610	CH2x_n_avg	0.5610	CH2x_n_avg	0.1422
CH2x_ged_avg	1	CH2x_ged_avg	0.5585	CH2x_ged_avg	0.5585	CH2x_ged_avg	0.1416
RM	1	RM	0.5510	RM	0.5510	RM	0.1394
CH3x_n_avg	1	CH1t	0.5061	CH1t	0.5061	CH3x_n_avg	0.1237
CH3x_ged_avg	1	CH3x_n_avg	0.4999	CH3x_n_avg	0.4999	CH3x_ged_avg	0.1230
CH1t	1	CH3x_ged_avg	0.4969	CH3x_ged_avg	0.4969	CH1t	0.1146
CH1x_ged_avg	0.9994	CH2t	0.4539	CH2t	0.4539	CH1x_ged_avg	0.0863
CH1x_n_avg	0.9994	CH1x_ged_avg	0.4256	CH1x_ged_avg	0.4256	CH1x_n_avg	0.0862
QR3	0.9975	CH1x_n_avg	0.4247	CH1x_n_avg	0.4247	QR3	0.0699
CH2t	0.9966	QR3	0.4243	QR3	0.4243	CH2t	0.0668
G0	0.9553	CH3g_avg	0.3025	CH3g_avg	0.3025	*****	*****
QR4	0.9032	CH2g_avg	0.2760	CH2g_avg	0.2760	G0	0.0346
HS	0.8923	HS	0.2409	HS	0.2409	QR4	0.0248
CH3g_avg	0.8873	G0	0.2259	G0	0.2259	HS	0.0235
CH2g_avg	0.8480	QR4	0.1881	QR4	0.1881	CH3g_avg	0.0229
KR	0.7021	DT_ged	0.1494	DT_ged	0.1494	CH2g_avg	0.0194
DT_ged	0.5064	DT_n	0.1485	DT_n	0.1485	KR	0.0118
DT_n	0.5051	KR	0.1277	KR	0.1277	DT_ged	0.0063
CH1g_avg	0.4029	CH1g_avg	0.1092	CH1g_avg	0.1092	DT_n	0.0062
Gm	0.3389	Gm	0.0739	Gm	0.0739	CH1g_avg	0.0044
*****	*****	*****	*****	*****	*****	Gm	0.0034

Table 10: **VaR** 1% **2w.** This table contains the output of the MCS produced by the Hansen et al.'s, the modified Corradi et al's and this thesis MCS algorithms, applied to a market risk forecasting model set. Each column contains the output of the corresponding MCS test, indicating the model label, the model confidence set cut-off, represented by an asterisk line and the model ranking achieved within each set by means of the p-values. We produce the MCS-max the MCS-γ at 10% and 50% γ and the MCS-t. The confidence level is at 5%. Considering the k, the selected FWER levels for the MCS10% and the MCS50% are, respectively, $k = 1$ and $k = 1$. In the 2w forecasting experiments, the model performances are more widespread. The top models CH1x_* either rank at the top of the MCS or are there included. The comments to this table are in Section 2.3.

max-MCS		MCS-10%		MCS-50%		t-MCS	
RM	1	G0	0.6894	G0	0.6894	RM	0.5025
G0	1	QR1	0.6783	QR1	0.6783	G0	0.4975
QR1	1	RM	0.6753	RM	0.6753	QR1	0.4962
DT_n	1	CH3g	0.6619	CH3g	0.6619	DT_n	0.4746
DT_ged	1	DT_n	0.6596	DT_n	0.6596	DT_ged	0.4743
CH3g	1	DT_ged	0.6591	DT_ged	0.6591	CH3g	0.4736
CH1t_avg	1	QR2	0.6573	QR2	0.6573	CH1t_avg	0.4702
CH3t_avg	1	HS	0.6565	HS	0.6565	CH3t_avg	0.4675
HS	1	CH1t_avg	0.6530	CH1t_avg	0.6530	HS	0.4330
QR2	1	CH3t_avg	0.6487	CH3t_avg	0.6487	QR2	0.4288
CH2t_avg	1	CH1g	0.6332	CH1g	0.6332	CH2t_avg	0.4284
CH1g	1	CH2t_avg	0.6281	CH2t_avg	0.6281	CH1g	0.3863
CH2g	1	CH2g	0.6039	CH2g	0.6039	CH2g	0.3278
CH3x_n_avg	1	CH3x_n_avg	0.5311	CH3x_n_avg	0.5311	CH3x_n_avg	0.2573
CH3x_ged_avg	1	CH3x_ged_avg	0.5252	CH3x_ged_avg	0.5252	CH3x_ged_avg	0.2557
CH2x_n_avg	1	Gm	0.5126	Gm	0.5126	CH2x_n_avg	0.2320
CH2x_ged_avg	1	CH3x_ged	0.4990	CH3x_ged	0.4990	CH2x_ged_avg	0.2188
CH1x_ged_avg	1	CH3x_n	0.4939	CH3x_n	0.4939	CH1x_ged_avg	0.1938
CH1x_n_avg	1	CH2x_n_avg	0.4667	CH2x_n_avg	0.4667	CH1x_n_avg	0.1906
CH3x_ged	1	QR3	0.4567	QR3	0.4567	CH3x_ged	0.1865
CH3x_n	1	CH2x_ged_avg	0.4544	CH2x_ged_avg	0.4544	CH3x_n	0.1857
QR3	1	CH1x_ged_avg	0.4412	CH1x_ged_avg	0.4412	QR3	0.1831
QR4	1	CH1x_n_avg	0.4352	CH1x_n_avg	0.4352	QR4	0.1750
Gm	1	QR4	0.4242	QR4	0.4242	Gm	0.1676
CH3g_avg	0.9940	CH2x_n	0.3532	CH2x_n	0.3532	CH3g_avg	0.0696
CH2x_n	0.9932	CH2x_ged	0.3513	CH2x_ged	0.3513	CH2x_n	0.0677
CH2x_ged	0.9929	CH1x_n	0.3239	CH1x_n	0.3239	CH2x_ged	0.0672
KR	0.9901	CH1x_ged	0.3203	CH1x_ged	0.3203	KR	0.0620
CH1x_n	0.9875	CH3g_avg	0.3065	CH3g_avg	0.3065	CH1x_n	0.0587
CH1x_ged	0.9870	CH2g_avg	0.2165	CH2g_avg	0.2165	CH1x_ged	0.0581
CH2g_avg	0.8204	KR	0.2145	KR	0.2145	*****	*****
CH1g_avg	0.4149	CH3t	0.1634	CH3t	0.1634	CH2g_avg	0.0210
*****	*****	CH1g_avg	0.1424	CH1g_avg	0.1424	CH1g_avg	0.0054
CH3t	0.0298	*****	*****	*****	*****	CH3t	0.0002
CH1t	0.0000	CH1t	0.0860	CH1t	0.0860	CH1t	0
CH2t	0	CH2t	0.0777	CH2t	0.0777	CH2t	0

Table 11: **VaR** 5% **2w.** This table contains the output of the MCS produced by the Hansen et al.'s, the modified Corradi et al's and this thesis MCS algorithms, applied to a market risk forecasting model set. Each column contains the output of the corresponding MCS test, indicating the model label, the model confidence set cut-off, represented by an asterisk line and the model ranking achieved within each set by means of the p-values. We produce the MCS-max the MCS-γ at 10% and 50% γ and the MCS-t. The confidence level is at 5%. Considering the k, the selected FWER levels for the MCS10% and the MCS50% are, respectively, $k = 1$ and $k = 2$. In this experiment, some practitioner models, such as the G0 and the RM exhibit best performance. The QR1 also performs very well. This is the only experiment where the dual tail model ranks high in the model list. The comments to this table are in Section 2.3.

max-MCS		MCS-10%		MCS-50%		t-MCS	
QR4_010	1	QR4_010	0.8253	QR4_010	0.8180	QR4_010	0.6010
QR1_020	1	QR1_020	0.7883	QR1_020	0.7817	QR1_020	0.3990
QR3_020	1	QR3_020	0.7665	QR3_020	0.7603	QR3_020	0.3786
QR2_020	1	QR2_020	0.7629	QR2_020	0.7561	QR2_020	0.3244
QR3_010	1	QR3_010	0.7194	QR3_010	0.7054	QR3_010	0.2665
CH2x_ged_avg	1	CH1t_avg	0.6866	CH1t_avg	0.6793	CH2x_ged_avg	0.2400
CH2x_n_avg	1	CH2t_avg	0.6777	CH2t_avg	0.6696	CH2x_n_avg	0.2383
CH2g	1	CH2x_ged_avg	0.6525	CH2x_ged_avg	0.6457	CH2g	0.2264
CH3x_ged	1	QR2_010	0.6525	QR2_010	0.6357	CH3x_ged	0.2218
CH3x_n	1	QR1_010	0.6418	CH3x_ged	0.6278	CH3x_n	0.2217
CH1t_avg	1	CH3x_ged	0.6347	CH2x_n_avg	0.6267	CH1t_avg	0.2204
CH1x_ged	1	CH2x_n_avg	0.6343	QR1_010	0.6241	CH1x_ged	0.2188
CH1x_n	1	CH3t_avg	0.6305	CH3t_avg	0.6237	CH1x_n	0.2188
CH2t_avg	1	CH3x_n	0.6287	CH3x_n	0.6214	CH2t_avg	0.2080
QR1_010	1	CH2g	0.6154	CH2g	0.6071	QR1_010	0.1980
QR2_010	1	CH3g	0.6061	CH3g	0.5979	QR2_010	0.1979
CH2x_n	1	CH1x_n	0.5952	CH1x_n	0.5883	CH2x_n	0.1960
CH3t_avg	1	QR4_020	0.5932	QR4_020	0.5858	CH3t_avg	0.1959
CH2x_ged	1	CH1x_ged	0.5908	CH1x_ged	0.5837	CH2x_ged	0.1959
QR4_020	1	CH1x_ged_avg	0.5374	CH1x_ged_avg	0.5306	QR4_020	0.1851
CH3g	1	CH2x_n	0.5357	CH2x_n	0.5286	CH3g	0.1638
CH3t	1	QR4_005	0.5356	CH2x_ged	0.5184	CH3t	0.1534
CH1g	1	CH2x_ged	0.5258	CH1g	0.5169	CH1g	0.1393
CH1x_ged_avg	1	CH1g	0.5245	QR4_005	0.5120	CH1x_ged_avg	0.1380
CH1x_n_avg	1	CH1x_n_avg	0.5157	CH1x_n_avg	0.5078	CH1x_n_avg	0.1372
CH3x_ged_avg	0.9996	CH3x_n_avg	0.4903	CH3x_n_avg	0.4824	CH3x_ged_avg	0.1122
CH3x_n_avg	0.9996	CH3x_ged_avg	0.4800	CH3x_ged_avg	0.4717	CH3x_n_avg	0.1119
CH1t	0.9961	CH2g_avg	0.4176	CH2g_avg	0.4088	CH1t	0.0832
CH2g_avg	0.9956	QR3_005	0.4014	CH3t	0.3965	CH2g_avg	0.0812
RM	0.9658	CH3t	0.4008	QR3_005	0.3818	*****	*****
QR4_005	0.9568	QR2_005	0.3532	CH3g_avg	0.3211	RM	0.0493
CH2t	0.8985	QR1_005	0.3410	RM	0.3177	QR4_005	0.0458
CH1g_avg	0.8717	CH3g_avg	0.3283	CH1g_avg	0.3102	CH2t	0.0318
HS	0.8040	RM	0.3232	HS	0.2852	CH1g_avg	0.0278
G0	0.2473	CH1g_avg	0.3176	CH1t	0.2409	HS	0.0211
KR	0.2171	HS	0.2898	KR	0.1732	G0	0.0024
CH3g_avg	0.0585	CH1t	0.2413	CH2t	0.1496	KR	0.0020
*****	*****	KR	0.1750	DT_n	0.1423	CH3g_avg	0.0004
Gm	0.0269	CH2t	0.1491	DT_ged	0.1396	Gm	0.0001
QR1_005	0.0128	DT_n	0.1440	G0	0.1268	QR1_005	0
DT_n	0.0124	DT_ged	0.1415	*****	*****	DT_n	0
DT_ged	0.0124	G0	0.1288	QR2_005	0.3481	DT_ged	0
QR3_005	0.0118	*****	*****	QR1_005	0.3386	QR3_005	0
QR2_005	0.0063	QR4	0.1253	QR4	0.1305	QR2_005	0
QR4	0.0000	QR3	0.1043	QR3	0.1088	QR4	0
QR1	0.0000	QR2	0.0986	QR2	0.1034	QR1	0
QR3	0	QR1	0.0974	QR1	0.1019	QR2	0
QR2	0	Gm	0.0949	Gm	0.0941	QR3	0

Table 12: **ExS** 1% **2w.** This table contains the output of the MCS produced by the Hansen et al.'s, the modified Corradi et al's and this thesis MCS algorithms, applied to a market risk forecasting model set. Each column contains the output of the corresponding MCS test, indicating the model label, the model confidence set cut-off, represented by an asterisk line and the model ranking achieved within each set by means of the p-values. We produce the MCS-max the MCS-γ at 10% and 50% γ and the MCS-t. The confidence level is at 5%. Considering the k, the selected FWER levels for the MCS10% and the MCS50% are, respectively, $k = 3$ and $k = 19$. The MCS test for the ExS 1% and 5% 2w forecasting experiment shows the superior performance of the QR model, which is quite surprising if considering that the projection has been achieved through a rule of thumb multiplication by the square root of time. The CH1_* model still ranking high. The comments to this table are in Section 2.3.

max-MCS		MCS-10%		MCS-50%		t-MCS	
QR2	1	QR2	0.7444	QR2	0.7392	QR2	0.5083
QR1	1	QR1	0.7411	QR1	0.7358	QR1	0.4917
CH3g	1	QR2_005	0.7325	QR2_005	0.7271	CH3g	0.4169
QR3	1	QR2_010	0.7182	QR2_010	0.7125	QR3	0.4112
CH2t_avg	1	QR1_005	0.7144	QR1_005	0.7086	CH2t_avg	0.3836
CH2g	1	QR2_020	0.6970	QR2_020	0.6909	CH2g	0.3801
CH3t_avg	1	QR3	0.6949	QR3	0.6888	CH3t_avg	0.3648
CH1t_avg	1	CH3g	0.6944	CH3g	0.6879	CH1t_avg	0.3646
CH1g	1	QR1_010	0.6868	QR1_010	0.6804	CH1g	0.3485
QR2_005	1	CH1g	0.6829	CH1g	0.6763	QR2_005	0.3339
QR2_010	1	CH3t_avg	0.6635	CH3t_avg	0.6565	QR2_010	0.3120
QR2_020	1	CH1t_avg	0.6629	CH1t_avg	0.6559	QR2_020	0.2909
RM	1	CH2t_avg	0.6613	CH2t_avg	0.6541	RM	0.2829
CH3x_ged	1	CH2g	0.6591	CH2g	0.6518	CH3x_ged	0.2348
QR1_005	1	QR3_005	0.6579	QR3_005	0.6510	QR1_005	0.2288
QR1_010	1	QR1_020	0.6520	QR1_020	0.6449	QR1_010	0.2154
CH2x_ged_avg	1	RM	0.6504	RM	0.6435	CH2x_ged_avg	0.1951
QR1_020	1	QR3_010	0.6213	QR3_010	0.6137	QR1_020	0.1913
CH2x_n_avg	1	QR3_020	0.5767	QR3_020	0.5683	CH2x_n_avg	0.1863
G0	0.9998	CH3x_ged	0.5600	CH3x_ged	0.5502	G0	0.1450
DT_ged	0.9998	CH2x_ged_avg	0.5478	CH2x_ged_avg	0.5390	DT_ged	0.1439
DT_n	0.9998	CH3x_n	0.5428	CH3x_n	0.5326	DT_n	0.1439
HS	0.9998	CH2x_n_avg	0.5299	CH2x_n_avg	0.5208	HS	0.1432
CH3x_n	0.9996	CH3x_n_avg	0.4953	CH3x_n_avg	0.4854	CH3x_n	0.1298
QR3_005	0.9993	QR4	0.4853	QR4	0.4751	QR3_005	0.1190
CH1x_n	0.9991	CH3x_ged_avg	0.4771	CH3x_ged_avg	0.4668	CH1x_n	0.1130
CH1x_ged	0.9990	HS	0.4369	HS	0.4258	CH1x_ged	0.1122
QR4	0.9986	G0	0.4325	G0	0.4217	QR4	0.1051
QR3_010	0.9978	QR4_005	0.4269	QR4_005	0.4156	QR3_010	0.0985
CH2x_n	0.9930	CH1x_ged_avg	0.4220	CH1x_ged_avg	0.4107	CH2x_n	0.0787
QR3_020	0.9909	CH1x_n	0.4193	CH1x_n	0.4062	QR3_020	0.0747
CH1x_n_avg	0.9811	CH2x_n	0.4153	CH2x_n	0.4021	CH1x_n_avg	0.0632
CH1x_ged_avg	0.9800	DT_n	0.4066	DT_n	0.3954	CH1x_ged_avg	0.0623
CH3x_ged_avg	0.9498	CH1x_n_avg	0.4029	CH1x_n_avg	0.3910	*****	*****
CH3x_n_avg	0.9497	DT_ged	0.4009	DT_ged	0.3896	CH3x_ged_avg	0.0466
CH2x_ged	0.9394	CH1x_ged	0.3996	CH1x_ged	0.3861	CH3x_n_avg	0.0465
QR4_005	0.9063	CH2x_ged	0.3946	CH2x_ged	0.3810	CH2x_ged	0.0433
CH3g_avg	0.9026	QR4_010	0.3741	QR4_010	0.3618	QR4_005	0.0358
CH2g_avg	0.8626	QR4_020	0.3149	QR4_020	0.3016	CH3g_avg	0.0351
QR4_010	0.8253	CH3g_avg	0.2639	CH3g_avg	0.2497	CH2g_avg	0.0289
Gm	0.7842	CH2g_avg	0.2184	CH2g_avg	0.2034	QR4_010	0.0251
QR4_020	0.7079	Gm	0.1961	Gm	0.1812	Gm	0.0215
KR	0.5263	CH3t	0.1862	CH3t	0.1677	QR4_020	0.0165
CH3t	0.1366	CH1g_avg	0.1434	CH1g_avg	0.1273	KR	0.0090
*****	*****	KR	0.1414	KR	0.1252	CH3t	0.0012
CH1g_avg	0.0205	CH1t	0.0543	*****	*****	CH1g_avg	0.0001
CH1t	0.0001	*****	*****	CH1t	0.0543	CH1t	0
CH2t	0	CH2t	0.0465	CH2t	0.0402	CH2t	0

Table 13: **ExS** 5% **2w.** This table contains the output of the MCS produced by the Hansen et al.'s, the modified Corradi et al's and this thesis MCS algorithms, applied to a market risk forecasting model set. Each column contains the output of the corresponding MCS test, indicating the model label, the model confidence set cut-off, represented by an asterisk line and the model ranking achieved within each set by means of the p-values. We produce the MCS-max the MCS-γ at 10% and 50% γ and the MCS-t. The confidence level is at 5%. Considering the k, the selected FWER levels for the MCS10% and the MCS50% are, respectively, $k = 1$ and $k = 2$. The comments to this table are in Section 2.3.

Model Selection of Jump-Diffusion Models

With the model selection experiment of this chapter, we are interested in the econometric analysis of a large class of stochastic models, capable of matching observed financial market data characteristics. This chapter is focused on parametric model families that are designed to capture the historical equity stock price return dynamics. The model set is large enough to mimic the stylised features of the time series as evidenced in the literature. We focus on single factor stochastic volatility models and restrict the exercise to a suite of model types that are tested on several nested layers. A core challenge with any such model specification analysis is the performance of the estimation procedures in the presence of insufficient information, as the equity volatility is unobservable. As presented in Section 3.1, the observable variable, that is the equity stock return is assumed to be given as a linear function of a set of stochastic inputs that are either partially or completely unobserved. Specifically, we consider a jump-diffusion system which is characterised by a latent component that enters either the stochastic diffusion or the stochastic intensity driving the jump process. The benchmark model is represented by the stochastic volatility model of Heston (1993), which is extended in several directions and compared with a non conventional model

family. The Heston model and, in general, the affine model class have gained popularity and widespread use since their formalisation in Duffie and Kan (1996), Duffie et al. (2000) and Dai and Singleton (2000). This model class provides a convenient tool for capturing stochastic volatility, an important statistical characteristic of financial time series, at the same time allowing a certain ease of use due to the analytic form of their moment generating function. However, the single factor stochastic volatility SDE usually applied to model equity stocks can produce distributions with strong kurtosis only under extreme parameter configurations and in general can generate a very moderate skew. Incremental kurtosis can be achieved with the extension by an incremental parameter to trigger the elasticity of variance in the constant elasticity of variance (CEV) model specification, used in Beckers (1980), Macbeth and Merville (1980) and in a stochastic volatility context in Jones (2003) and Aït-Sahalia and Kimmel (2007). The introduction of jump components also increases the flexibility of the model in adapting to observed return distributions. In this regard, it is customary in finance to use jumps to explain rare events and usually the estimations provided concerning the jump frequency and size vary from one to nine jumps per year, with a negative average size of -3%, see Andersen et al. (2002), Eraker et al. (2003), Chernov et al. (2003) and Pan (2002). In Section 3.1 and Appendix A.4, we provide more information concerning the model details and their use in the literature. In this study, we counterbalance this application of the jump component by extending the model set with a class of stochastic hazard models that employs high frequency jumps in modelling financial time series. In this perspective, rare large jumps should be viewed as tail events of frequent small jumps, as opposed to the standard paradigm that jumps are rare events overall. The further major feature of this alternative model class, however, is that it is capable of generating stochastic volatility by combining frequent jumps and stochastic intensity, whereby the volatility clustering is produced by peaks of the frequency of jumps.

The model selection exercise is conducted in two different environments. In the first test environment, we arrange a simulation exercise to analyse the model ability in reproducing the sample characteristics of a known DGP by testing the model performance with respect to the target estimation functions. The purpose of this experiment involves testing the capacity of the models in reproducing each other's characteristics and hence provide alternative formulations for the econometric problem of interest. Specifically, we compare CEV stochastic diffusive models equipped with rare large jumps that occur in the returns process with constant intensity, a model class we indicate as the stochastic diffusion (SD) family, whereas the alternative class of models contains constant diffusion models with high intensity of small jumps characterised by stochastic hazard[1] (SH). Both classes allow for constant intensity asynchronous jumps in the latent factor. The complexity of the exercise is increased by the fact that the larger models within each class are themselves affected by aliasing among their components. The use of simulation allows the control of the sample features, whereby we have chosen to balance between the contribution to the data variability of the diffusion and the jump component, whenever the latter is present. This simulation parameters setting means that the unconditional variances of the diffusion and the jump component, which sum up to the total model unconditional variance, are programmed to be equal. In particular

[1] Two parametric models are nested if one can be derived from the other one by simply varying the parameters. Although there is a possibility for nesting the two model classes, this modelling choice is prevented and the nesting class (i.e. the model that is characterised simultaneously by CEV stochastic diffusion and CEV stochastic intensity, both driven by the same latent component) is excluded.

though, the variance produced by a jump component in the SD class is determined by rare large jumps, whereas the variance produces by a jump component in the SH class is determined by very frequent small jump. With the SH family we investigate a model whereby the volatility clustering can be generated by the jump component solely. The motivation as to why we choose to include the SH family in the model selection exercise and expand the overarching CEV class, is mainly scientific. This class has received no attention in the applied finance literature. However, discrete time models that are at the foundation of the econometrics discipline, can be viewed as high intensity jump models with non stochastic jump times. Furthermore, the full record of the daily transactions on a typical trading day for a liquid financial asset is intrinsically an high frequency stochastic intensity jump price sample. In the second test environment, we produce a market data experiment whereby we test the model set performance and draw inferences on real financial time series. The model set and estimation procedures applied to real market data, complemented with tests of model comparison, reveal information useful for empirical researchers. Concerning the test statistics, within the simulation test environment, they are produced with Monte Carlo, whereas within the market data test environment, the market sample data are resampled with the stationary bootstrap. The simulated experiment is suited for the application of a relative model comparison test, whereby the suite of models is tested against the benchmark generating the sample data. A relative model comparison is also arranged for the market data experiment, where the MHT is structured to circulate the benchmark across the model set. The relative model comparisons expose the detail of the preferences among individual models induced by the statistical test and reveal the full collection of equivalence hypotheses. Finally, we explore the absolute model performance, whereby MCS tests are applied to the data set to draw general conclusions regarding model superiority. Exploiting the flexibility of the approach of Section 1.1 and Section 1.3, we deliver MCS tests of the performance of jump-diffusion (JD) models targeting the historical measure of an equity index log-levels. The model comparisons are based on the *max*-MCS of Hansen et al. (2011), as constructed in Section 1.3.1, our new t-MCS inspired by Corradi and Distaso (2011), as constructed in Section 1.3.2, and the novel γ-MCS, of Section 1.3.3, combining the MCS and the MHT framework.

The econometric analysis of the historical measure of equity stock indices by means of stochastic volatility JD models is pursued in articles such as Andersen et al. (2002), Chernov et al. (2003) and Eraker et al. (2003). These articles, however, lack of a direct model comparison statistical procedure, whereby the model pairwise confrontation is at most achieved by comparing the EMM χ^2 statistics, or pursued with the approach of the Bayesian factors, which is not strictly based on hypothesis testing, but is rather a relative measure of the likelihood of a model. The contribution of this study is original as the model selection analysis is achieved explicitly via joint statistical testing targeting several measures of model performance. This chapter provides several contributions. First, we test the model aliasing hypothesis among two alternative classes of jump-diffusion models, namely the conventional affine stochastic volatility model class popular in the literature and the non-conventional stochastic hazard model class, that exhibit the ability to generate similar empirical time series features and that heretofore have not been pitted against each other in the literature. Second, we provide new insights into the stochastic hazard class, with the market data experiment showing such models to be highly ranked in performance. Third, we uniquely design and implement model comparison tests under recent and novel testing approaches, ex-

ploiting multiple hypothesis testing and the model confidence set techniques. Such techniques are ideally structured to allow us to explore the model aliasing hypothesis. Finally, as a methodological extension specific to this chapter, we extend the second order filtering procedure in Maybeck (1982) to allow jump components in the system state. The general information that we gather from the experiments of this study shows that the main model families exhibit strong aliasing and can produce similar features, with respect to the model performance measures. The fact that the models can in principles be each other substitutes, makes the market data experiment outcome more significant, whereby a particular alternative model reveals superior performance than the more conventional ones. This behaviour indicates that some SH models exhibit larger flexibility as they can structurally resemble the behaviour of SD models, at the same time producing distinctively top range performance in mimicking market data. On the other hand, the CEV model class delivers interesting performances and, specifically with respect to the likelihood performance measure, points to a simplified model structure in preference over more complex structures.

The chapter is organised as follows. In Section 3.1 we introduce the model set and define the general stochastic differential equation (SDE) describing the model components in Eqs. (3.1), (3.2), discussing also the general behaviour of the system. In Appendices A.1 to A.3 we detail the algorithms necessary for the parameter and latent state estimation, as well as the calculation of the performance measures by which the model selection exercise is addressed. Section 3.2 discusses the testing framework and presents the relative loss function defined upon the output of the likelihood function and the filtering procedure. Section 3.3 elucidates on several operational aspects of the exercises of this chapter and proposes a light comparison exercise between the filter technique employed in this work and a particle filter. The remainder of the latter section presents the results of the various experiments with simulated and financial market data. Section 3.4 gathers conclusions. The Appendix A collects several technical aspects concerning the analytics used throughout the article, whereas Appendix B provides more details about the implementation of the algorithms by which the experiments have been assembled.

Some clarifications

In econometrics, the aliasing effect is usually referred to the loss of information arising when discretely sampling continuous time processes. Specifically, the term originates from the theory of signals and refers to the lack of identifiability of the $\omega + 2\pi k$, $k \in \mathbb{Z}$ frequencies, as they will all appear to have frequency ω, cfr. for instance Priestley (1981). As a consequence, it might occur that two processes with the same sample spectra could differ in frequencies that cannot be observed because of the discrete data and thus be indistinguishable, from a statistical perspective. Another phenomenon that has been referred to as aliasing in econometrics, for instance, is the problem of estimating the parameters of the diffusion and the jump component in a jump-diffusion process, cfr. Aït-Sahalia (2004). The author of that study provides interesting intuition as to why the aliasing arises. In fact, for the reference Merton model, it is shown that suitably changing the diffusion and jump components' parameters, it is possible to obtain a fixed measure of the shape distribution, such as, for example, the variance or the kurtosis. Another interesting point is the rapidly decreasing probability of detecting a jump, when the sampling interval increases. Analytic results are obtained with respect to the simple prototype model, which show that the likelihood

can asymptotically detect the diffusion coefficient without the interference due to the presence of jumps, as long as the process is sampled at very short time intervals. Notwithstanding those results carried over an analytically tractable model, the asymptotic moments remain entangled with both diffusion and jump coefficients and therefore anticipating uncertainty when using the GMM.

In this thesis chapter we employ the term aliasing in a wide context, referring to model performances that are confusing in the sense that models that are structurally different produce similar outcomes. The sources of aliasing might be multiple. The models are expected to be misspecified or are rather misspecified by construction and the system is assumed to be partially observed. The point of testing for aliasing with simulation is as follows. Assume, for instance, we have two nested models. The question is to which extent the nested one is statistically equivalent to the overarching model when the former is adapted to a sample which is generated by the latter. We would expect that, foremost, the answer depends on the model performance measure. In particular, we are targeting a marginalised likelihood and the projection of the latent system state with an approximated non-linear filter, two measures that are constructed on a partial information set. We notice, for instance, that jump-less models hardly match discontinuous paths, whereas jumps in volatility have a more elusive sample feature. The exercise is limited in the sense that we only consider an affine SD family and a disjoint SH family hinging on the prior that the volatility clustering is produced by frequent small jumps hitting the system with stochastic intensity. A CEV extension is also considered, as well as several jump specifications. Another interesting result of the simulation is the very flexible performance of the SH models, that are among the top performers in the real market data exercise, as long as a good performing CEV specification is in place.

For the purpose of model selection, we distinguish the problem of parametrising the statistical distribution of the model set from that of filtering the latent state component, as we employ two procedures that target respectively and distinctively the likelihood of the observable and the projection of the unobserved component. The estimates are then used to perform computations and to evaluate model performance. We exploit an approximation of the likelihood function to estimate the model parameters that involves the marginalisation of the unobservable variable, whereas the path of the latent component is estimated through a filtering procedure which receives the model parameters as an input. The focal point of the analysis is the comparison of possibly misspecified models acting in a context of partial information, whereby their performance is measured in terms of the information they are capable of extracting from sample data, both from a distributional as well as from a dynamic behaviour perspective. The loss functions defining the model comparison statistics therefore measure the ability of the model in matching the sample information and therefore reproducing the distributional characteristics of the observed system and the ability of the model in inferring the dynamic behaviour of the latent components. The measures for model comparison are derived directly from the likelihood function and from the filtering algorithm. Despite the different objectives of the estimation approaches[2], they share a common origination in the forward equation, that is the partial integral-differential equation (PIDE) describing the transition density of the system. The inner component of the likelihood function is constructed as the

[2] The procedure of marginalisation of the latent component has been developed primarily to target the likelihood of the observed data, insulating the further complication of estimating the unobservable variable into a distinct computation. Incidentally, the algorithm improves the computational charge.

numerical solution of the forward equation and, combined with the marginalisation procedure, is used for the parameter estimation and to derive information theoretic loss measures. The filtering technique of Maybeck (1982), Nielsen et al. (2000), Baadsgaard et al. (2000), also used in Hurn et al. (2013), is constructed as a projection onto the observable set of information. The filtered latent path feeds either measures of path-wise distance or a joint likelihood loss indicator. Exploiting the procedure by which the (diffusion only) propagation equation is derived, we extend the filter by including a jump element that allows one to deal with more general JD models, as we pursue here. This jump-augmented filtering approach is another of the main contributions of this chapter. The form of the jump that the filter can handle is quite general, including synchronous or asynchronous jumps, state-dependent jump size distributions along with affine as well as non-affine state-dependent jump-intensities.

The specific statistical entanglement and the effects of truncation errors related to the algorithms employed are not subjects of research, as we focus on the application of the bootstrap methodology and the MHT-MCS framework to explore model similarities and superior performances in simulated and real data experiments. However, we pinpoint here several issues left for further examination. The analysis is executed with approximate maximum likelihood estimation methods, that is the likelihood of the chosen model is not known in closed form and therefore numerical methods have been employed to generate the estimation function. From a theoretical statistics point of view, the analysis can be set in the framework of Poulsen (1999) whereby, assuming consistent and asymptotically normal estimates (CAN) of the 'true' likelihood, only second order precision of the AML is required to obtain CAN as well. On the other hand, the AML can in general fall into the theory of misspecified models when the more practical misspecification hypothesis is assumed, see White (1982, 1994). The study of the empirical behaviour of the discretisation is beyond the scope of this thesis. Another complication of the analysis of this chapter, which deserves a separate analysis, is represented by the partial observation of the system state, entailing the exploitation of filtering techniques to measure the expected path of the latent component. We resort to an approximated non linear filter, which we trace back to Maybeck (1982). The peculiar feature of the filter is that it can disregard the estimation of the prior distributions, as it only requires the evolutionary equations of the latent state projections and provides a direct expression for the evolutionary equation of the system projection. To obtain an ordinary differential equation that can be employed for computation, the ODE can be expanded in some terms that involve the expectation operator, effectively rendering a second order approximated filter[3]. As a consequence of the higher order expansion, the estimate of the system state transition expectation is adjusted by a bias correction term. However, some crude estimation is then used when the observation density is required, in practice resorting to a (first order approximated) non linear least square of the expected posterior value. The consequences of these practical remedies in terms of precision of the estimates and possible improvements, deserve further research. A point we make is that we do not use the likelihood of a possible observation error in order to estimate the system parameters. In many simulation we do not report, the peculiar form of the system state which hosts already the observed variable, determines some odd behaviour of the latent state projection, as indeterminacy is already captured by the diffusion and possibly the jump component. Furthermore, this approach has been proved to be distorted, as the observation error exhibits high correlation with observable, as well as

[3] It has to be noticed that for affine and quadratic models the time-propagation equation is exact.

autocorrelation, see for instance Dempster and Tang (2011).

3.1 The Jump-Diffusion Model Set

In this chapter, we restrict the attention to a jump-diffusion system, which is designed to capture many of the stylised features of equity stock financial time series. The overarching model we consider is specified by the following parametric SDE

$$\begin{aligned} \mathrm{d}x &= \theta v^{\gamma_0}\mathrm{d}W_0 + J_0\,\mathrm{d}N_0 - m_0\mathrm{d}t \\ \mathrm{d}v &= \kappa(1-v)\,\mathrm{d}t + \sigma\sqrt{v}\,\mathrm{d}W_1 + J_1\,\mathrm{d}N_1 - m_1\mathrm{d}t, \end{aligned} \tag{3.1}$$

which represents a jump-diffusion family of models which is characterised by log-return process x and a volatility process v, both driven by defined diffusive and jump factors. The volatility process v is defined to evolve according to a square root process that can be affected by jumps, which may or may not be synchronous with the jumps in the returns process. The jump process are defined by the following two jump-related differentials describing jump arrival intensity:

$$\begin{aligned} \mathrm{d}\Lambda_0 &= \lambda_0 v^{2\gamma_1}\mathrm{d}t \\ \mathrm{d}\Lambda_1 &= \lambda_1\mathrm{d}t \end{aligned} \tag{3.2}$$

These are the hazard functions of the compounded Poisson jumps N_0 and N_1. The stochastic factor can enter either the constant elasticity[4] of variance (CEV) diffusion in x or the CEV stochastic hazard function of N_0, where we fix $0 \leq \gamma_0, \gamma_1 < 1$. The overarching model in Eq. (3.1) and (3.2) is intended to mimic the behaviour of the log-price of and equity stock. The x process is not characterised by any particular drift, which is expected to be null[5]. The model produces stochastic volatility, that is the clustering of price variations into high and low volatility regimes and further instantaneous acceleration of the price achieved through jump in level and possibly sudden spikes in volatility generated by jumps in the latent factor. As we allow for high frequency small jumps, the stochastic volatility can be generated by either a higher diffusion factor or by a peak in the number of jumps. The clustering of the returns is determined by the mean reversion feature of the latent factor, which exhibits some viscosity in pulling back to the long run level from a spike. We do not mix stochastic diffusion and stochastic intensity models, thus if $\gamma_0 \neq 0 \Rightarrow \gamma_1 = 0$ and viceversa. We make this choice as in the present study we exploit jump models with random jump frequency in an alternative fashion, allowing for an high intensity self-exciting system that uses the latent stochastic hazard function to generate stochastic volatility. The suggested hypothesis that is complementary is that combining stochastic diffusion and stochastic intensity determines an overidentifying restriction. Hence, the intensity of the jumps in x are either constant or random, whereas the intensity of the jump in the v factor is constant. The latter is the one that is considered latent in the simulation or is unobservable or partially observable in the

[4] In economics, the elasticity of the function $U(c)$ is defined as $-cU''/U'$. This corresponds to an elasticity of the function v^{γ} of $1-\gamma$.

[5] Contrary to market practice in defining log-transform models of affine stochastic volatility, we drop here the Jensen term that would result from the transformation of the price martingale, as the perspective that we take is mainly that of the historical data. As explained in the Appendix A.4, employing a log-return model with a stochastic volatility drift term should be justified by autocorrelation in the first difference of the data, which is not the case, see also Bollerslev and Zhou (2002).

market-data experiment. In term of parameters, we observe that we apply some simple transformations to popular versions of the model subcomponents, see Appendix A.4, to obtain a latent factor v that oscillates around a unitary mean, with mean reversion factor κ. The diffusion of the square root factor is determined by the parameter σ, whereas the jump component $J_1 \mathrm{d}N_1$ is compensated by the drift adjustment $m_1 \mathrm{d}t$; the constant intensity is λ_1. The latent factor enters either the diffusion of x, whereby it is scaled by θ and exponentiated by γ_0, which in the non CEV version is fixed to one half, or it enters the intensity function of the jump in return process $J_0 \mathrm{d}N_0$, whereby it is scaled by the parameter λ_0 and exponentiated by γ_1, which in the non CEV version is fixed to one half and in the SD model class is fixed to zero. The jumps compensation drifts m_0 and m_1 are constant. The mean reversion speed is requested to be higher than the jump drift and their difference greater than half the squared diffusion coefficient, that is $\beta - m_1 > \frac{\sigma^2}{2} > 0$, in order to obtain stationary variance, at the same time preventing the crossing of the zero level[6]. We allow for the presence of correlated diffusive random drivers[7] between the factor x and the stochastic volatility factor v, that is $\mathrm{d}[W_0, W_1] = \rho \, \mathrm{d}t$, the so called leverage effect, a phenomenon witnessed at least since Schmalensee and Trippi (1978) and modelled, for instance, in Glosten et al. (1993). If jumps in v are included, their expectation is required to be greater than one, cfr. (A.2) in Appendix A. The jump size distribution J_1 of the Poisson point process component in v is specified as a positive exponential, whereas in the case of N_0 a negative exponential jump is specified in the stochastic diffusion case, with constant jump intensity. A double-exponential distribution or a skewed normal jump is employed with the stochastic hazard model version of x, whereby in this case the jump size is constrained to a zero expected value. Moreover, we notice that the stochastic hazard family is not affine, as the covariance matrix of the diffusion component cannot be written in a linear form.

The models of the exercise in this chapter are organised into two major families, exhibiting stochastic volatility that is generated either by the diffusion factor, the SD class, or by the jump intensity of the Poisson component of the cumulative return process, the SH class. In fact, both the stochastic diffusion and the stochastic jump intensity version of the overarching model in Eqs. (3.1), (3.2) are stochastic volatility models, as it can be seen by taking their quadratic variation given by the v-dependent stochastic integral $\int \mathrm{d}t \, \left[\theta^2 v^{2\gamma_0} + \lambda_0 v^{2\gamma_1} \mathbb{E} J_0^2\right]$. The volatility clustering which characterises diffusive stochastic volatility models can be also produced by intensively jumping stochastic hazard models, which entails a concentration of larger variations of x during volatility peaks. In the case of the CEV version of the SH family, the γ_0 parameter will exacerbate this feature, for higher parametric values. The stochastic hazard models are characterised by high frequency jump intensity on average, whereas models of the stochastic diffusion class that manifest jumps in the level of the observable variable are expected to jump less frequently. A minor distinction between the stochastic diffusion and the stochastic hazard

[6] We will sometimes refer to the ratio $\frac{\sigma^2}{2(\beta - m_1)}$, as the volatility excursion factor. It should be between zero and one, whereby values close to the unity determine very spiked volatility paths, that is large excursion, whereas values close to zero entails that v rarely leaves a neighbourhood of the long-run level.

[7] This feature produces a bidimensional diffusion which tends to associate negative variations in x with increasing v and viceversa, but not necessarily couples large negative variations in x with peaks in volatility and the other way around, therefore producing only slight asymmetry in the marginal density of the observable x. That is to say, the correlated diffusion W_0 and W_1 do not produce higher volatility in the presence of negative trends in the price level, but they tend to associate negative returns with growing volatility, a feature that might happen at low levels of volatility as well. Therefore, affine models are not expected to produce strong asymmetry via the ρ coefficient. In practice, if were, for instance, to set a simulation of a correlated affine stochastic volatility model, we would observe that the first difference of x be correlated with the first difference of v but not with its level. From the simulation, we observe that in the presence of negative or bidirectional jumps, the likelihood manifest a strong aliasing between the correlation coefficient and the latter component.

classes lies in the direction of the jumps of x, if any, which is negative in the former case, whereas it it can be positive or negative in the latter case. From a distributional perspective this feature entails that the SD class can only produce negative symmetry that is the case of interest for market data applications.

The system in (3.1) contains or can be connected with several popular models used in financial econometrics applications, although not all of them are employed in the analysis here and in general some subcomponents are disconnected in order to obtain models exhibiting similar features but that are structurally different. Indeed, as the scope of this analysis covers discriminating among stochastic models in terms of explanatory power, the inclusion of an overall nesting model would not add any insight to the final result, because the overall nesting model would be capable of matching any behaviour of its components. One of the hypotheses we are investigating in the market data experiment consists in whether one of the model class is superior. The connection with popular models is only illustrative. Correspondence of the overarching model to model specifications prominent in the financial literature is shown in Tab. 15. However, a full illustration of the transformations needed to obtain more conventional models used in literature are presented in Appendix A.4. Parameters constraint associated to the latter models are as follows. If we exclude both jumps in return and volatility and set $\gamma_0 = \gamma_1 = 1/2$ we get the seminal stochastic volatility model of Heston (1993). Considering the jump in volatility and if the jump in x is skewed normal with null parameter of asymmetry, we obtain the SVS(C)J model of Eraker (2004), with uncorrelated jumps. If in the last model we set $\gamma_1 = 0$, we obtain Eraker et al. (2003), also included in Duffie et al. (2000), Bates (2000) and Pan (2002); if further zeroing $\lambda_1 = 0$, we get Bates (1996), also included in Duffie et al. (2000). If we leave γ_0 free, set $\lambda_0 = \lambda_1 = 0$ we can obtain the CEV models in either Beckers (1980) and Macbeth and Merville (1980) or Jones (2003) and Aït-Sahalia and Kimmel (2007). If we then set $\gamma_0 = \gamma_1 = 0$ and consider the Gaussian determination of the skewed Normal jump distribution, we get the Merton (1976) model, whereas with double-exponential jumps, we obtain the (Kou, 2002; Kou and Wang, 2004) model. Notwithstanding this established relation between the system in Eqs. (3.1), (3.2), and these prominent models in the financial literature, in this work we compare reduced and extended forms of these models to perform model comparison of conventional and unconventional models of stochastic volatility. The model set is first tested in a simulated environment to check for fungible characteristics. Successively, the model set is tested onto real market data to search for model superior performance. This research has to date provided evidence to support the adequacy of these increasing complicated model specifications, however, the work in this chapter is the first study to examine a wide range of jump-diffusion models where it is conjectured that there is a strong aliasing among these models, and further among individual components of these models, which offers the possibility of simplifying model structure, at least from an historical measure perspective. The trend in the literature has been towards increasingly complicated model specifications in an effort to better capture market dynamics, yet this comes at a cost in terms of increasing levels of estimation error and bias and, from a practitioner perspective, increasing disconnect with the regulatory requirements of industry. The analysis presented in this chapter offers new insights into the trade off between alternative model specifications using for the first time a rigorous MCS approach, which is further complemented with a direct multiple comparison test in the MHT testing, under the most general γ-MCS. The MCS approach taken here is ideally suited for the investigation of model aliasing among the suite of models considered.

3.1.1 Parameter Estimation

The parameter estimation of jump-diffusion models in quantitative finance has received extensive treatment, in the latter two decades. Methods to pursue this task are varied. Without any claim of compiling an exhaustive literary review on the topic, we recall the efficient method of moments of Gallant and Tauchen (1996), the empirical characteristic function approach of Singleton (2001), the spectral GMM of Chako and Viceira (2003). In the realm of the likelihood estimation, the methods to approximate the likelihood relies on simulation, as in the simulated maximum likelihood of Pedersen (1995b) and its extensions in Durham and Gallant (2002), or exploit the expansion of the transition density as in Aït-Sahalia (1996, 1999, 2002, 2008) or alternatively use PIDE methods to solve the transition equation. Example of the latter approach are Lo (1988), Poulsen (1999), Lindström (2007). In this study, we embrace an approximate maximum likelihood (AML) method of this type as it has proved to be very general and relatively easy to implement, with moderate computational costs. We favourite FDM to solve the main PIDE as polynomial expansion methods deliver oscillatory solutions. Moreover, the likelihood approach is theoretically the most efficient estimator and is characterised by a distinctive theory of model comparison when the models are misspecified, see for instance Akaike (1974), White (1982). We use likelihood methods for the parameter estimation of multivariate JDs with latent components, constructed as the numerical solution of the forward equation (A.6) combined with the marginalisation of the latent factor by weighting for its stationary density. Exploiting an approximate maximum likelihood approach, the procedure acquires the inherent optimal properties of the exact likelihood that can be achieved asymptotically by the approximation, cfr. Pedersen (1995a), Poulsen (1999). The same result extends to the PIDE version, provided uniform convergence of the solution, see Lindström (2007).

The likelihood function hinges on the marginal densities of the first difference of the x process, constructed around the transition density of the state vector. Symbolically, the log-likelihood is represented by index

$$\mathscr{L}_N(\Theta) = -\tfrac{1}{N}\sum_{i=1}^{N} \log \mathbb{P}_{\delta_{t_i}}\{\Delta x = \Delta x_i | 0_x; \Theta\} \tag{3.3}$$

which provides the measure for the construction of multiple hypothesis model selection tests, as detailed in Section 3.2. In the likelihood equation, Δx_i is the return over the time horizon δ_{t_i} and each likelihood solution $\mathbb{P}_{\delta_{t_i}}$ is centred at $x = 0$. For each model and sample data, the parameter vector Θ^* that optimises the data function (3.3), enters both the likelihood and the latent component loss functions. The main steps toward the practical implementation of the likelihood estimation algorithm adopted in the model comparison exercise are depicted in the Appendix A.1, which describes the logical step to achieve the marginalisation of the latent variable and therefore obtain the likelihood of the observable variable, as well as the setup for the approximation of the transition density. More information related to the numerical solution of the PIDE equation of this problem are given in Appendix A.2, which presents the construction of the solver by the FDM. The pseudo-code description of this algorithm is presented in Appendix B.1.

3.1.2 The Second Order Non-Linear Filter

In order to analysis the performance of the model set with respect to the latent component problem, we adopt the filtering technique of Maybeck (1982), employed in finance in applications such as Nielsen et al. (2000), Baadsgaard et al. (2000) and Hurn et al. (2013). As an auxiliary contribution of this work, we extend the second order non-linear filter (NLF^2) augmenting the time-propagation equation to include a jump component in the system. This approach is convenient and, in particular, it does not require the solution of the PIDE associated with (3.1), relying instead on the transition equation of the expectation function derived from the forward equation. In Appendix A.3 we present the particular approach undertaken in the construction of the time-propagation equation of the filter, as well as the jump extension introduced in this study. In the appendix we also illustrate the standard approach in determining the update equation and explain the second order expansion by which non linear expectation are dealt with in the application section. Appendix A.3 also exhibits some examples. As this solution does not involve time expensive calculations, we can afford an increased system state dimension and hence split the x variable into its main stochastic drivers, namely the diffusion and the jump component, further introducing a new observable, that is the *integrated variance*. The integrated variance is an elaboration of x which makes observable the cumulative second order moment of the return process. Specifically, rearranging the system of Eq. (3.1) and introducing the auxiliary observable w, we concentrate the analysis on the system

$$\begin{aligned} \mathrm{d}\xi &= \theta v^{\gamma_0}\,\mathrm{d}W_0 - m_0\mathrm{d}t \\ \mathrm{d}v &= \kappa(1-v)\,\mathrm{d}t + \sigma\sqrt{v}\,\mathrm{d}W_1 + J_1\,\mathrm{d}N_1 - m_1\mathrm{d}t \\ \mathrm{d}u &= \theta^2 v^{2\gamma_0}\,\mathrm{d}t \\ \mathrm{d}\pi_x &= J_0\,\mathrm{d}N_0 \\ \mathrm{d}\pi_w &= J_0^2\,\mathrm{d}N_0 \end{aligned} \tag{3.4}$$

which represents the engine of the latent component estimation exercise. The system state in Eq. (3.4) is augmented with the observable $w = u + \pi_w$ that represents the integrated variance. Moreover, the state is rearranged in such a way that the diffusion and the jump components of the x and w observable variables are projected explicitly. The observation equation is given by the linear form

$$\begin{aligned} x &= \xi + \pi_x \\ w &= u + \pi_w \end{aligned} \tag{3.5}$$

which in the formalism described in Appendix A.3 corresponds to the observable vector $Y = (x, w)^\top = \begin{bmatrix} 1 & 0 & 0 & 1 & 0 \\ 0 & 0 & 1 & 0 & 1 \end{bmatrix} X$. With the system state $X = (\xi, v, u, \pi_x, \pi_w)^\top$ we are isolating the random sources into specific state variables, a choice of design that allows for the disentangling of the jump variable from the diffusion component. As a consequence, the filter defined by the Eqs. (3.4) and (3.5) is able, in particular, to produce the projection of the latent variable π_x, which accumulates the jumps[8] of the observable x. We will use this filter output to estimate the jump times and sizes and to produce a simple benchmarking exercise of the procedure used here with a particle filtering technique. A by-product of the

[8] This strategy, however, cannot be directly implemented for the estimation of the jump component of the v factor, as it does not enter directly into any observable.

filtering which might be of interest is the estimate of the path of the latent variable ξ and thus the total variance attribution between the jump and diffusion component of x. Progressing with the construction of the device needed for the second battery of model comparison tests, we have augmented the observable with a new variable w, which plays a special role in the system economy. As the state vector (ξ, π_x, v) is completely unobservable with a dimension higher than that of x, we would expect a strong degree of indeterminacy in estimating its projection. For this case study, however, we can resort to stochastic calculus and obtain two new variables which increase the information content available by introducing a new observable. We expand the system with the integrated variance of the process x, which is partially observable. This system extension can be proved to be statistically significant. The integrated variance has been used in other applications in a realised volatility context, see for instance Bollerslev and Zhou (2002), which exploits its moment structure to improve the estimation of a stochastic volatility model, see also Barndorff-Nielsen and Shephard (2002), Barndorff-Nielsen and Shephard (2004). In this work, the origination point is different. We construct the process w considering the SDE which describes the observable $x = \xi + \pi_x$ and derive the process dynamics for $\chi = x^2$

$$\begin{aligned} \mathrm{d}\chi &= 2x\left(\theta v^{\gamma_0}\,\mathrm{d}W_0 - m_0\,\mathrm{d}t\right) + \theta^2 v^{2\gamma_0}\,\mathrm{d}t + \left[(x - J_0)^2 - x^2\right]\mathrm{d}N_0 \\ &= 2x\,\mathrm{d}x + \theta^2 v^{2\gamma_0}\,\mathrm{d}t + J_0^2\,\mathrm{d}N_0 \\ &= 2x\,\mathrm{d}x + \mathrm{d}u + \mathrm{d}\pi_w. \end{aligned}$$

Hence, let $w = x^2 - 2\int x\,\mathrm{d}x$ to obtain the new observable $w = u + \pi_w$. It is implicit that because of the term $2\int x\,\mathrm{d}x$ that can only be approximated, the variable w is subject to a measurement error which is assumed to spill into the estimate of π_w. We do not introduce further auxiliary variables interpreted as observation errors because of the presence of several overlapping latent sub-components into which the total system variance has to be attributed. A noisy observation error is redundant as it can easily be blurred into the diffusion component or be considered as the leftover variance once the system jumps have been isolated as tail events of the projected jump components, $\widetilde{\pi}_x$ and $\widetilde{\pi}_w$, cfr. Section 3.3.

3.2 Model Comparison Testing

As anticipated in Section 1.4, for the experimental part of this chapter we devise an exercise of relative model performance MHT, as defined in (1.2), targeting jump-diffusion models. The test exploits the balanced simultaneous confidence set controlling for the k-FWER and augmented with a step-down algorithm to further refine the subset of significantly equivalent models and increase the statistical power of the test. The relative performance test is executed under the simulated scenario, whereby the structure of the experiment is suited for this type of comparison. For each benchmark model, sample data is generated and hence model performance measures are derived, after previous parametrisation and filtering. The main purpose of the test is to explore the model ability in reproducing each other's features exhibiting greater flexibility with respect to the target loss functions. We also produce a relative model performance MHT processing real market data, whereby, as the "true" data generating process is unknown, a benchmarking iteration is used to scan thoroughly the precedence relationships across the full set of model comparisons. The purpose of this exercise is mainly to be descriptive of the multivariate distributions of

the model comparison statistics, which are thereafter synthesised and represented by the outcome of the absolute model performance MHT. Final conclusions regarding the model selection exercise are drawn by means of the *max*-MCS (Section 1.3.1), the t-MCS (Section 1.3.2) and the γ-MCS (Section 1.3.3) performed with simulated and real data. With the simulated exercise, the set of the best equivalently performing models can be regarded as the collection of models that are statistically similar to the selected benchmark and can therefore be considered as substitutes. With the real market data experiment, we search for the best set of models fitting the data in terms of the target functions, producing original model selection results through the application of the MHT and the MCS. The reference model set $\mathcal{M}$ is represented by stochastic volatility families described in Section 3.1.

The loss functions L_j's constructed for the sake of model comparison, exploit an information criterion as well as the metric represented by the path-wise distance derived from the filtering procedure. The first measures when combined into the model relative performance d_{ij}'s give raise to likelihood ratios, which is essentially a measure of fitting of the target empirical distribution. Moreover, as the latter is constructed by integrating out the latent component, we investigate a further indicator of model performance, which measures the model ability in producing superior projections of the unobservable component. For the case of the real market experiment, we also construct a hybrid measure of model performance combining the full approximate likelihood evaluated at the vector of parameter Θ_i^* over the actual market returns and the filtered volatility trajectory. Particulars of the loss functions are presented in the following paragraphs. The AML algorithm and the augmented non-linear filter employed in this study are detailed in Appendix A.1 and Appendix A.3.

The loss functions presented in this section are used in the empirical section to construct MHT with step-down refinement relative performance test that are indicated as LR-MHT, LC-MHT, LRLC-MHT and TG-MHT. Absolute performance tests are executed in the simulation environment, with respect to each model sample, and in the market-data experiment, with respect to a well diversified large stock index data, employing the (LR/LC/LRLC/TG)-MCS-*max*, the (LR/LC/LRLC/TG)-MCS-t and the (LR/LC/LRLC/TG)-MCS-γ, defined as follows.

3.2.1 Likelihood Ratio

In the context of model specification analysis, a fundamental result is represented by the following limit. Let $z_1, \ldots, z_n$ be n independent observations on a random vector z, with probability density function $g(z)$ and consider the family of models represented by the parametric family of densities $\{f_\theta(z), \theta \in \Theta\}$ with a vector parameter θ and parameter space $\Theta \subset \mathbb{R}^k$. The following limit holds almost surely

$$\tfrac{1}{n}\sum_{i=1}^{n} \log f_\theta(z_i) \xrightarrow{n} \int \mathrm{d}z \; g(z) \log f_\theta(z),$$

provided the last integral exists. Indicating with $S(g; f_\theta)$ the latter limit integral, we can define the Kullback-Leibler information criterion, which is a distance measure of the likelihood of the possibly misspecified model from the true one, that is $K := S(g; g) - S(g; f_\theta)$, cfr. White (1982, 1994) and Rao

and Wu (2001). By the Cramer-Rao bound, $K \geq 0$ with equality only if $f_\theta \equiv g$. The *likelihood ratio* between model f_θ and model h_φ is the difference

$$LR(g; f_\theta, h_\varphi) := S(g; f_\theta) - S(g; h_\varphi),$$

which represents the distance gap of the model candidates.

Concerning the model comparison experiments targeting the model likelihood, we define the loss function as

$$L_i := -\mathscr{L}_i\left(\Theta_i^*\right) \tag{3.6}$$

whereby the RHS refers to Eq. (3.3) and we have dropped the reference to the sample size and introduced the model index i. The sign has been changed because in practice the objective function is minimised and more importantly to comply with the definition of a loss function, as adopted in the context of the model selection strategy in Section 1.1. As a consequence, the relative performance measure $d_{ij} = L_i - L_j$ corresponds to the sample equivalent of the LR, which would signal model equivalence as long as its value is not significantly different from zero. We refer to tests obtained from the loss function (3.6) as the likelihood ratio test (LR).

3.2.2 Distance from the Latent Component

The second type of performance measure we employ is intended to detect the ability of a model to produce a reliable projection of the latent system state variable v. The unobservable component projection is the output of the NLF^2 procedure developed in Appendix A.3 and applied to the system described in the Eqs. (3.4) and (3.5). The performance indicator that is used with this battery of test focuses solely on the filter output, which by construction does not involve the likelihood function to produce the latent state estimate. The test is intended to measure the model ability in describing the evolution of the system, with particular reference to the inferred unobservable variable v. The test is centred on the latent stochastic driver v as it is common to the full model set. Some measures of the jump-time hit rate are reported as descriptive quantities of the filter algorithm performance in the filter benchmarking exercise of Tab. 30 as illustrated in Section 3.3.1.1. The loss function is obtained as the absolute distance of either the latent variable projection from the actual path of v for each benchmark sample in the simulation exercise, or of the appropriately scaled and translated latent variable projection from a threshold GARCH estimate, cfr. Glosten et al. (1993), of the financial returns volatility, in the real data experiment. In the latter case, with the experiment involving financial market data, we fix the lack of knowledge of the v path by linking the filter output to the GARCH model that in econometric applications has been used as a financial return volatility proxy for decades, see for instance Engle (1982) and Bollerslev (1986), Nelson (1991) and Hansen and Lunde (2005). However, although employing observable data, the autoregressive conditional heteroskedastic model offers a term of comparison only indirectly related to the system state projection[9].

[9] The ratio of the overall average of the absolute path distance of the scaled and translated filter output from the standard deviation of the GARCH filter is 17.25%

Indicating with ν the reference latent system state path, the loss function of the model $\mathbf{P}_i$ is

$$L_i = \tfrac{1}{N} \sum_{j=1}^{N} \left| \widetilde{v}^i_{t_j} - \nu_{t_j} \right| \tag{3.7}$$

In the loss function (3.7), when referred to the simulation exercise, the variable $\widetilde{v}_t$ coincides with the filter output $\bar{v}_t$, whereas ν_t indicates the simulated trajectory of v under the benchmark. When referring to the financial data experiment, ν_{t_j} is the threshold GARCH estimate of the squared daily volatility, whereas $\widetilde{v}_t = \bar{v}_t a + b$, that is the appropriately scaled and translated projection $\bar{v}$. This approach is justified as follows. If we consider the first difference of a discrete approximation of w, we get

$$\Delta w \approx (\Delta x)^2 \approx \begin{cases} v\theta^2 \Delta t + \lambda_0 j_{02} \Delta t + \epsilon \\ v\lambda_0 j_{02} \Delta t + \theta^2 \Delta t + \epsilon \end{cases} \tag{3.8}$$

and therefore the parametric constant a, b are appropriately defined according to the stochastic diffusive or stochastic hazard structure of the reference model. As the relation in (3.8) remarks, disregarding approximation errors, the opportunely scaled and translated projection $\bar{v}$ can be related to the squared first differences that feed directly the GARCH filter. The Fig. 5(c) exhibits a path fragment of the TGARCH estimated volatility (red line) and the scaled and translated output of the NLF^2 (blue line) for the CEVJJ process, as applied to market data. After recentring and rescaling the non-linear filter projection to account for the observed variability of x, the filtered path track closely the trajectory of the discrete time TGARCH filter, to a visual impact. This testing strategy is exploited in this study for the first time in the literature. We refer to the first type of test presented in this subsection as the latent component test (LC), whereas the second test is indicated as the threshold GARCH test (TG).

3.2.3 LR with Latent Component

In case of the real data experiment with the LC test, we evaluate the model ability in estimating the latent component with respect to a model that although provides consistent estimates of the observed squared return dynamics, introduces an interpretation of the data which is based on a specific conjecture. In order to attenuate the dependence of the test output on the characteristics of the GARCH volatility estimates, with the market data experiment we additionally produce a test that evaluates the model filtering ability coherently with the theoretical transitional properties of the model, without the need of an external term of comparison.

With the likelihood ratio latent component test (LRLC) we produce an LR test whereby the likelihood function corresponds to the full likelihood of the vector (x, v) and the latent path is obtained from the output of the model filter. Hence the reference loss function is

$$L_i := \tfrac{1}{N} \sum_{j=1}^{N} \log \mathbf{P}_i \left(\Delta x_{t_j}, \tilde{v}^i_{t_j}; 0_x, \tilde{v}^i_{t_{j-1}}; \Theta^*_i \right) \tag{3.9}$$

whereby the model likelihood can be symbolically represented by the Eq. (A.7). The log-likelihood represents the full likelihood of the system, that is without marginalising the v component, but dealing

with it as its projection achieved by the filter was the actual observed trajectory of the latent factor. The loss function defined in Eq. (3.9) simultaneously measures the ability of the model in generating distributional hypotheses matching not only the observed data but also the projection of the latent component delivered by the NLF^2.

3.3 Experimental Section

3.3.1 Preliminary Considerations

The analysis is restricted to a scalar observable x with a single latent factor v model that can admit asynchronous jumps in level of the observable N_0 and in the level of latent factor N_1, which are compounded with the random jump size $J_\bullet$. The general equation of the system is presented in Eq. (3.4). The unobserved factor v can feed the dynamics of the diffusion coefficient determining a stochastic volatility model or alternatively can transfer its action onto the hazard function of the stochastic jump N_0 and generate a stochastic hazard model. The transfer function for the quadratic variation of the stochastic volatility model and for the intensity of the stochastic hazard model is the (scaled) power $v^{2\gamma}$, $0 \leq \gamma \leq 1$, excluding model configurations which combine random volatility and random intensity. When the jump intensity of the jump component of x is not stochastic and the system is allowed to jump, the discontinuities flow with an expected constant yearly rate $\lambda_\bullet$. The jumps in v have in all cases the latter feature, whenever they are included. The jump sizes $J_\bullet$ may capture different stylised features, including singled sided exponential, double-exponential and skewed normal jumps, as summarised in Section 3.1. The main prototypes considered are listed in Tab. 14. The parameter estimation is performed by constructing the complete likelihood of the system state of the general equation, of which an example is given in Fig. 1. The exhibit shows an instance of the output of the procedure for the marginalisation of the density of the observed variable, specifically that of the SV model. The algorithm is described in Appendix A.1.1. The upper-left section, 1(a), shows the final construction, that is the model marginal density under the simulation parameters, whereas the upper-right section, 1(b), plots several bivariate densities on a grid of initial conditions for v, ranging from 0 to seven times the projected variance over the five days reference time horizon. In practice, in order to integrate out the latent variable, we need to integrate for the determinations of v at the right hand side of the time interval, as well as performing a weighted integration of the v initial conditions, that is on the left hand side of the time frame. Now, in order to determine the finite size of the range of definition of the v's initial condition, we refer to a multiple of the expected variance of v over the reference time interval, therefore discriminating by the latent factor parameter values. The initial condition for x is centred at 0 for each grid-point of v, hence determining the transition densities as solutions of the main PIDE. The likelihood functions that are obtained, conditionally on the initial values of v_0, generates the observable's marginal distributions at each grid-point as depicted in the lower-left section of Fig. 1(c). These functions, which are obtained by integrating over v_t, are then weighted by the stationary distribution of v, exemplified in the lower-right section of Fig. 1(d), in order to get the marginal density of x. The latter integration corresponds to the marginalisation of v_0. It is important to notice that this procedure does not produce the loop prior-to-posterior distribution that is typical of the Bayesian algorithm employed in filtering, but rather producing

a single conditional distribution for the observable, unconditional from the latent variable v, by means of the stationary distribution. This particular construction exploits the properties of the model families described in Appendix A.1, with the capability of computing the likelihood much faster because, at each iteration, it only necessitates a single distribution for the full sample. This procedure delivers a likelihood function that has an empirical equivalent in the histogram obtained by taking a stratified sample of the first differences over the target horizon of the time-series data, as for instance in Fig. 4(a) that shows the simulated histogram against the numerical solution of the PIDE for the model SVXJ. In practice, the marginalised likelihood is targeting the shape of the observed histogram, at the same time supporting the consistency of the model SDE structure. In general, however, the partial set of information available complicates the problem, generating model aliasing with respect to several model performance measures. The latent state estimation is achieved through the application of the jump extended non-linear filtering algorithm of Appendix A.3. In order to estimate the latent path of the v variable, the system dynamics are augmented by the (partially) observable integrated variance w and its transition equation is rearranged in the form of Eq. (3.5), which allows a more thorough decomposition of the observable into its principal stochastic drivers. It is interesting to notice how this particular filtering construction allows the augmentation of the system dimension without exponentially inflating its computational cost, an extension of the information content that in terms of the quality of the latent path extraction can be empirically proved to introduce statistically significant information. Another benefit introduced by the filtering procedure is the possibility to disentangle the diffusion from the jump component of the observable variables with a simple reshaping of the state transition equation, whereas this task would otherwise have involved a complex manipulation of the domain definition of its likelihood function. Combining the efficiency and the robustness of the likelihood approach with the capacity of a state-space method to handle latent component systems allows us to explore different aspects of the model set constituents in describing the sample information.

The configuration of the simulation parameters is not extreme, in order to observe the ability of the testing procedure to isolate unique behaviours and to identify model clusters. In the simulation experiment we keep the benchmark sample at a constant unconditional yearly variance with an even allocation of the variability parameter among the diffusion and jump component[10], whenever the latter is included, therefore producing distribution that are located and spread closely, but that differs in some key shape numbers. The estimation exercise is complicated beyond the mere model similarities by the additional trade-offs among certain parameters, which raise the uncertainty around the model selection. The following discussion sheds some light on this complication where we refer to several distributional shape coefficients. The simulation benchmark model coefficients, the location and their shape numbers are presented in Tab. 16, complemented with two further standardised central moments. The most immediate example of possible issues in discerning among models and model configurations is the variance attribution between the diffusion and the jump component, see for instance Aït-Sahalia (2004), a fact which is complicated further by the multiplicity of the parameters involved, depending on the model type. To elaborate further, an example which also hints at the effects of the loss of information resulting from the

[10] In practice, we fix the unconditional variance generated by the model and choose the parameters appropriately such as to attribute half variance to the diffusion and the other half to the jump component, when present.

lack of observation of the system variable v is represented by the presence of the correlation factor ρ. From a likelihood angle, this coefficient generates skewness in the marginal distribution, although a sensible -0.5 simulation parameter when compared to $\rho = 0$ in the SV model, it can only account for a -0.14 skewness factor against a zero, cfr. Fig. 2(b). A visual aid elucidating the mechanics of the procedure can be traced in the cross-section of the correlated (Fig. 2(c)) and uncorrelated (Fig. 2(d)) bivariate distributions at a given initial condition ($v_0 = 2.46$) against the domain of the observable, revealing a dynamic behaviour that actually disappears when smoothed out by the marginalising procedure. In fact, the quadrant c and d highlight visually that although the cross sections of the bivariate distributions are different, the overall contour of the probability distribution of the observable is very similar, notwithstanding one model is characterised by innovations correlated with the stochastic volatility factor. Therefore, once the initial condition has been marginalised by the same system of weights, as the correlation factor does not impact the stationary distribution of v, the output functions, which are exhibited in quadrant b, only different by a restrained asymmetry. Those premises translate into the tendency to zeroing the correlation in the presence of skewed empirical distributions, in the absence of complementary features[11]. In fact, skewed distributions can also be generated by asymmetric jump components. In Fig. 3 the SV model (blue curve) is compared with several other members of the model set, depicted at the simulation parameters. In the frame (a) the shape of SV is compared to the slight increase in kurtosis generated by SVVJ (red line), whereas a $\gamma = 0.75$ parameter of the CEVVJ (light blue line) model pushes this shape factor somewhat higher. Asymmetry is generated by jumps in the SVXJ (red line) model of frame (b) and in the SHB (red line) and the CSHBVJ (dashed light blue line) of frame (c), whereby in the latter case it visualises the marginal effect onto the v unconditioned distribution of the CEV parameter and the jump in the latent factor. The lower-right frame (d) shows the profile of two representatives of the stochastic hazard with skewed Normal jump family against the SV, whereby the SHA (red curve) manifests a semi-Normal profile, whereas the CSHAVJ is slightly more spiked. Turning to kurtosis, we notice that stochastic volatility and appropriate jump specifications can produce widely peaked distributions when compared to a Normal distribution, as in Fig. 2(a) whereby the profile of a Gaussian function with zero mean and same standard deviation (0.2) is compared to that of the SV model. Indeed, a larger γ and jumps in volatility can as well increase the kurtosis, although in the stochastic diffusion models that effect can be achieved also with an increased or extreme volatility excursion factor. In the stochastic hazard model, the larger variance elasticity factor and the jumps in the intensity process do not seem to generate a sensitive boost in kurtosis, whereas for double exponential jumps, which we will indicate as type-B jump, SH models allocating variance between the constant diffusion and the double exponential jump produces consistent variations of kurtosis. SH models characterised by a skewed Normal distribution jump size, which we will indicate as type-A jump, do not exhibit a large range of kurtosis. From a dynamic behaviour perspective, it is interesting to notice that the speed of mean reversion, the volatility of volatility and the jump parameters can be triggered leaving the excursion unchanged, a factor which largely affects the asymptotic distribution of the latent parameter. Furthermore, for the CEV models and up to a certain extent for the SV models, increasing spikes in the quadratic variation process can be produced with either the excursion factor or the γ parameter.

[11] Because a large uncertainty is revealed in the filtering exercise, in the simulation experiment we keep the ρ constant to its model value of -0.5 for all the specifications. With the real data experiment we leave ρ free to move in its region of definition.

There are further complications in implementing the testing procedure. As illustrated in Section 3.2, the burden of producing a simulated test distribution must be balanced with the computational cost of both the likelihood PIDE solution and the filtering algorithm. The procedures employed in this work are very convenient, but entail some drawbacks. The filter extension introduced in Appendix A.3 displays ample flexibility in the system decomposition and in the derivation of the filter, which is general and simple to program and most interestingly is much faster than a particle filter algorithm based on simulation as, for instance, the SIRPF of Section 3.3.1.1. However, though the second order truncation is a bias correction factor for the propagation equation, cfr. Maybeck (1982), the approximation of the update equation is at most first order precise, introducing a bias that requires further study. The augmentation of the system with the integrated variance endows the system with an incremental source of information that can be proved to be statistically significant for the purpose of the estimation of the latent factor. On the other hand, in the presence of jumps in the return process x, the particular ex-post mechanism of updating the system determines some unexpected discontinuities in the projected path, that could be corrected with the introduction of a residual jump process in the observation equation of w, which is assumed to be parametrised like the jumps in the integrated variance, with perfect jump size correlation. In Fig. 4(c) we show the simulated path of the latent factor of an SVXJ model (left axis, red curve), coupled with the integrated variance of x (right axis, blue dotted line), where several discontinuities are visible on the chart. These anomalies can be detected as tail events of observed integrated variance differentials. In this study, we adopt a solution that attenuates these unexpected jumps in the projection, when they seldom appear, with the only drawback of decelerating the projection. This anomaly is originated by the poor approximation of the update equation, which requires further improvements. This heuristic approach is not investigated further, in this work. In the same figure, quadrant (d), we exhibit the process of attenuation of the unexpected shock due to the system updating via the residual dummy jump process. The corresponding detail on the path of w has been noticed in Fig. 4(c) with a rectangle. The Fig. 4(d) shows the path of v (red line) with several projections characterised by the presence of the dummy residual jump, multiplied by a constant ranging from 0 (blue dots) to 1 (light blue dots). Turning to the numerical solution of the marginalised likelihood, also in this case we remark the ease of implementation of the adopted solution. The downside is represented by the rapidly increasing complexity of the problem, in first instance by the curse of dimension, which for the likelihood test is limited to the main observable x and the latent variable v, and secondly and most important for the model selection exercise is the precision achieved by the grid resolution. In Fig. 4(b), we illustrate the potential impact of an extremely coarse grid (blue line) that diverges on several quartiles from the more refined solution represented by the red line. Given the stock of computational power and the multiple hypothesis test task to be performed, a compromise between precision and speed of calculation is represented by the 25x25 grid solution employed in the simulation and the market data experiment, exemplified by the light blue curve of the same chart, in the case of the SVXJ model of the Monte Carlo experiment.

3.3.1.1 Benchmarking the NLF^2 with Particle Filtering

Because of its flexibility and ease of implementation, the nonlinear filter employed in this analysis is particularly appealing for applications, as it does not require the complex and computationally intensive numerical procedures that are necessary for the calculation of the system likelihood. The filter is exploited in the following experimental sections to obtain the LC and the LRLC loss functions and hence evaluate the ability of competing stochastic models to produce estimates of the latent system state. In this section, in order to provide a term of comparison for this filtering technique that presents some elements of originality in our implementation, we introduce an alternative technique in filtering. The benchmark technique consists in a *particle filtering* (PF) method.

The PF is a simulation method for the implementation of filtering, intended as a means to evaluate the density of the system observations Y, keeping track of the prescribed evolution of the, partially latent, system state X, with $Y = \mathbf{q}(X)$. In general, filtering at discrete observations consists of an application of the Bayes' theorem. The purpose of the procedure consists in the evaluation of the *observed* likelihood $\mathbb{P}\{Y_t|Y_s\}$ obtained as the projection of the *prior* likelihood $\mathbb{P}\{X_t|Y_s\}$ onto $\mathcal{G}_t$ through the *measurement* likelihood $\mathbb{P}\{Y_t|X_t\}$. An intermediate product of discrete filtering is the *posterior* likelihood $\mathbb{P}\{X_t|Y_t\}$ that up to a proportionality constant a_t is represented by the density $p(X_t|Y_t) \propto p(Y_t|X_t)p(X_t|Y_s)a_t$, which is the needed ingredient for this bechmarking exercise as it is employed to construct the quantity for comparison $\bar{X}_t = \int \mathrm{d}\mathbb{P}\{X_t|Y_t\}\, X_t$, that is the system state projection. To summarise how the posterior likelihood is carried forward between the observation time $s < t$ in the general framework, we start by assuming that the measure $\mathbb{P}\{X_s|Y_s\}$ be known at time s and subsequently combined with the *transition* density $p\{X_t|X_s\}$ to obtain the prior likelihood, that is $p(X_t|Y_s) = \int \mathrm{d}X_s\, p(X_t|X_s)p(X_s|Y_s)$, which is hence merged with the measurement likelihood to get the observed density $p(Y_t|Y_s) = \int \mathrm{d}X_t\, p(Y_t|X_t)p(X_t|Y_s)$[12]. The process to construct the posterior density is initialised by setting the prior $p(X_1|Y_0) = p(X_1|X_0)$, where Y_0 is a dummy observation and X_0 that, with reference to the system described by the Eqs. (3.4) and (3.5), is set to 0, with the exception of v_0 which is set to its long-run expectation. To further characterise the filtering algorithm and therefore construct a procedure which can be coded into a computer, we need a solution to the differential equation associated to (3.4), while the measurement density is assumed to be know. In the PF implementation the probability distributions involved are estimated pointwise, with the transition density determined by simulation. According to how the algorithm draws from $\mathbb{P}\{X_s|Y_s\}$, particle filtering can be distinguished into the sampling/importance resampling (SIR) of Rubin (1987), acceptance resampling (Hürzeler and Künsch, 1998) and the Markov Chain Monte Carlo (MCMC) algorithm, cfr. for example Jones (1998), Eraker (2001) and Elerian et al. (2001). In this benchmarking exercise, we adopt the SIR method of Gordon et al. (1993), cfr. also Pitt and Shephard (1999), Pitt (2002) and for an application in Finance see Johannes et al. (2009). The PF transition from time s to time t is defined by the set of multidimensional particles $\{x_1, \ldots, x_M\}$, which provides the M initial conditions x_j to propagate the system via simulation and produce the $R \times M$ new particles $\{x_1^{(j)}, \ldots, x_R^{(j)}\}$, associated to the probabilities $\{\pi_1^{(j)}, \ldots, \pi_R^{(j)}\}$. The measurement likelihood $p_s(Y_t|x_i^{(j)}) := h_{ij}$ is then evaluated to

[12] It can be noticed that the latter equation is obtained as a normalising constraint to the Bayes' equality $p(X_t|Y_t) = \frac{p(Y_t|X_t)p(X_t|Y_s)}{p(Y_t|Y_s)} \Rightarrow \int \mathrm{d}X_t\, p(X_t|Y_t) = 1 \Leftrightarrow \int \mathrm{d}X_t\, p(Y_t|X_t)p(X_t|Y_s) = p(Y_t|Y_s)$.

obtain the $w_{ij} = h_{ij}\pi_i^{(j)}$ and hence the discrete probabilities $p_{(i-1)R+j} = w_{ij}/\sum_{ij} w_{ij}$ that are associated to each $x_i^{(j)}$. The new particles at time t are obtained by drawing M times from the multinomial distribution $\{x_i^{(j)}, p_{(i-1)R+j}\}$. The algorithm presented above is summarised with the pseudo-code Appendix B.2.

The SIRPF is employed to construct an alternative estimation of the trajectories of the partially latent system state $\bar{X} = \sum_j x_j/M$ in (3.4) at each time t when observing Y described in (3.5), to which we compare the JD filtering extension introduced with the Eqs. (A.13), (A.16) and (A.18). In Fig. 5(d) we shows path fragment of the actual v path (red line) for the SV simulated process, with the SIRPF output path (green line) and the NLF^2 projected latent component (blue line). Hence, we provide some elements of comparison for the NLF^2 derived in Appendix A.3 and section 3.1, which is used as a term of reference for the performance of the SIRPF, within the same simulated environment. Tab. 30 presents several results useful to compare the performance of the two methods. For each long run sample, that is the 100 year sample employed for the sake of parameter estimation, we employ model parameters to obtain the LC measure for both the nonlinear and the SIR filter. The latter results are used as critical values in a scalar statistics based on the simulated LC statistic distribution, sampled daily. Although a thorough comparison of these filtering methods is beyond the scope of this study, we can infer some conclusions. The SIRPF proves extremely time consuming when compared to the NLF^2, which is approximately 4,000 times faster, for the same sample on the same machine (4Ghz) on the same sampling frequency[13], an advantage that is decisive for the implementation of the simulated statistic approach in this article. The SIRPF is produced with a 300 path resampling, on a weekly basis, for each model reference. Several filtered samples are produced also at a daily frequency, matching the NLF^2 frequency. The reference statistic distributions are those of the second order nonlinear filter. The average absolute latent component distance realised by the particle filter is compared to the bidirectional 5% interval of the scalar LC statistic distribution. The general conclusion is that the daily sampled NLF^2 is equivalent to the weekly sampled SIRPF, if not superior in a few cases. We would expect a superiority of the SIRPF when sampled daily, which is not the case. The filter outputs for the model SV and SVVJ are equivalent, turning slightly superior when a jump component is added, with the SVXJ and CEVXJ models. These results paired with the high uncertainty in matching the actual latent path, as the LC measure are considerably high if compared to the standard deviation of the actual v trajectories, and considering that the critical values are quite close to the acceptance region, do not clearly indicate if the higher uncertainty imported into the projection mechanism by unclustered random jump times leads to prefer the SIRPF. What we observe with the SVXJ and CEVXJ experiments on daily frequency is that the LC numbers of the particle filter are 40% better than the nonlinear filter numbers, and whereby the p-values are respectively 0.023 and 0.015. Furthermore, in the presence of state independent jumps in the x level the NLF^2 tends to flatten the projection of v at the stationary expectation, therefore accumulating divergence when the trajectory of v is widely below the average. In the latter two exercises, the SIRPF tends to follow the trajectory of v closely, but manifests overshooting during high volatility phases, a feature that the LC number cannot capture. The situation is overturned when we focus on some jump detection performance measures. In Tab. 30, the jump times matching indicator is formed as a sequence

[13] For the SIRPF, we take the average ratio of the computational times between the daily and weekly frequency, where produced, and then scale the average of the weekly sampled LC computational times

of Boolean values in correspondence of the daily or weekly records of the filter output. Practically, the percentage number indicates if at the time the filter signals a jump[14], there be at least one jump in the corresponding unit of time. There is no penalty for the jumps produced by the filter which do not match an actual jump. As a consequence, the indicator is fairly "benevolent" with respect to the performance of the filter in forecasting jumps. Notwithstanding the performance measure characteristics, the SIRPF in the case of the SVXJ and CEVXJ sampled at weekly and daily frequencies performs extremely poorly when compared to the NLF^2 so much as to deliver a worse index at a shorter time interval. This latter feature actually leads to a disastrous performance of the SIRPF in the only daily sampled filtering exercise for the SH broad family, that is the CSH model. The filtered v path seems to diverge early from the long run expectation, stabilising around a higher expected jump frequency. This feature might signal issues in the estimation of very tiny jump probabilities or even distortion in the simulation engine. Further investigation might be needed. The results consists in a huge loss function value.

3.3.2 Monte Carlo Experiment

With the Monte Carlo experiment we compare the model performances in a controlled environment, whereby reference objects such as the actual DGP and the actual path of v can be used to provide a benchmark to the procedure, whereas they are taken as unknown by the function producing the test statistics. The JD models are able to produce similar statistical features, primarily kurtosis, skewness and stochastic volatility, but that instead are structurally dissimilar, as the random quadratic variation is generated by the diffusion in one case and by the jump intensity in the other one. A further minor structural difference is represented by the jump direction which is single or double. The model families include several layers of nested models and, in the case of the SH family, the bidirectional jump is characterised with two types of distribution. The model parameters for the non-benchmark models Θ_j^*, $j \neq i$ are estimated on a very large simulated sample, that is 100 years, and therefore considered as the equivalent of asymptotic estimates. The parameters are kept fixed when producing the test statistics, therefore excluding further variability that might be generated by parameter uncertainty. A future study will include this aspect of the model selection problem. The multiple dimensional distributions of the likelihood-ratio (LR) and the latent-factor comparison statistics (LC) are generated via Monte Carlo; that is, the parametrised loss functions (3.6) and (3.7) are applied to a simulated sample of 2000 paths of 10 years in duration, sampled 5 times a day that, for each relative test i, have been generated by the benchmark model $\mathbf{P}_i$ at the simulation parameters Θ_i. The data are taken at weekly frequency both for the LR test and for the LC test.

In the first exercise presented in Tab. 18, we construct a relative comparison test, whereby the likelihood ratio statistic of Eq. (3.6) is calculated for each model with respect to the corresponding likelihood data produced by the benchmark model, that is the model generating the data sample for each single test. As for the rest of the relative performance MHT of this section, the rejected models do not provide a confidence interval, whereas the corresponding row is filled with a north-east "↗" or a south-east "↘"

[14] The jumps correspond to the tail(s) of the first difference of the projected jump path. In the case of the NLF^2 the jump path is adjusted by the auxiliary variable dampening the unexpected shocks in the update equation. The cut-off of the first difference jump path is set to the expected jump frequency.

arrow, whenever the corresponding model is, respectively, superior or inferior to the benchmark model. The benchmark model of the testing exercise is indicated with a star, while the table is organised in block rows containing the balanced confidence set output of the step-down procedure, whenever the equivalence hypothesis is accepted. There are four block rows, each corresponding, from top to bottom, to the SV, CEV, SHB and SHA broad families. For the simulated LRMHT, the α is set to 5% for each tail of the statistic distribution, the number of tolerated false rejections is $k = 4$, which represents one forth of the full model set. Like the rest of the relative comparison MHT in this section, we adopt a full step-wise procedure, as the set of hypotheses for the MHT is considered small. The output results are interesting as they provide indication about the prominent features of the prototype models and hints at possible direction as to ameliorate the model design. For the discussion about the testing results, we refer to the major shape parameters to infer significant information about model equivalence, although the scope of the LR test is wider as it involves higher order moments. Turning to the analysis of the LR test table 18, we notice immediately that models producing slightly asymmetric distributions and lying at the inner core of their nesting categories like the SV, SVVJ and CEV and CEVVJ, can be reproduced by any other component of their nesting and non-nesting families, in the latter case confirming the fungible nature of the stochastic hazard models. The test results also suggest that jumps in volatility have no significant effect on marginalised distributions, henceforth anticipating the difficulty in their identification. On the other hand, one might infer that a marginalised likelihood, like the one employed in this analysis, might fail to capture the elusive feature of jumps in the latent factor. We conjecture that the extension of the likelihood approach to a fully Bayesian approach might be able to extract more information from the observable and possibly improve model comparison. Another look at the results pertaining to these model classes reveals that the kurtosis generated by the $\gamma = 0.75$ parameter can be achieved with appropriate, though extreme, volatility excursion factors. The introduction of jumps in the x level for the model families of the stochastic diffusion type definitely rules out the models SV/SVVJ and CEV/CEVVJ somehow deeming them as inferior models in the overall model selection exercise[15], whereby the type-A jump stochastic hazard models reveal an unexpected flexibility, given the fact that the jump size distribution can only produce limited kurtosis and asymmetry, but the inclusion of a diffusion parameter evidently increases the adaptability of this model version, whereas the type-B jumps are rejected. The rejection of the latter models suggests that the SHB broad family might be characterised by some rigidity when high kurtosis is combined with large asymmetry whereby they display the inability of reducing the kurtosis while keeping high skewness[16]. When the reference DGP is represented by a model of the SHB broad class, which in the exercise is characterised by the largest asymmetry and kurtosis, the equivalence multiple hypothesis likelihood ratio test shows that within the benchmark class and with this test parameter configuration, its representative are quite equivalent and can be mimicked significantly by stochastic diffusion models with extended features, that is jump in levels and, but not necessarily, jump

[15] Concerning the distributional asymmetry producible by those models, the SV reference model in the simulation exercise, with $\rho = -0.5$, generates a skewness of only -0.138, that can be increased only up to -0.142 by squeezing the correlation factor to -0.95. The slightly more skewed CEV model (-0.2152) generates as well a reduction of the skewness of only -0.19% in correspondence to a reduction of the correlation of -90%, from -0.5 to -0.95. This consideration points to a low sensitivity of the likelihood to the correlation parameter.

[16] In this test example, with respect to the SVXJ benchmark sample and considering the actual skewness and kurtosis generated by the MLE estimates on a coarse grid, we have that the theoretical model skewness and kurtosis are, respectively, -1.45 and 9.22, whereby the estimated model values of SHB are -1.8 and 11.7, with -1.8 and 11.4 for the CSHVJ, whereas a CSHAVJ that structurally cannot reach high absolute skewness and kurtosis delivers a -0.77 and 7.7, sufficient to produce superior likelihood ratios.

in volatility and CEV parameter. To a certain extent, the SHA broad family performs very well, whereby the slight kurtosis increase granted by the CEV extension to the benchmark model, can still significantly be captured by SHAVJ and CSHAVJ. The SHA model broad family proves to be quite flexible, although it does not seem to be able to discriminate either among its components, as the last block row of the test matrix in Table 26 exhibits. It is interesting to notice how the SHB broad family of models is capable to produce a likelihood performance equivalent to this class, which is characterised by quasi Normal kurtosis and low skewness, by the outweighing of the diffusion component and appropriate balancing of the tails. With respect to the SHA and SHAVJ benchmark samples the stochastic diffusion cluster returns inferior output, whereas when the stochastic intensity function of the benchmark DGP is augmented with a CEV exponent, in the case of the CSHA and CSHAVJ samples, the SV, SVVJ and CEV, CEVVJ which are moderately leptokurtic and skewed are capable of producing equivalent marginal likelihood measures, although in the first case the SD-based models are close to rejection.

In the second exercise we construct the LCMHT relative model performance test that evaluates the ability of the elements of the model set to infer the behaviour of the latent component v. In Tab. 19 for each benchmark model sample we construct a balanced confidence MHT based on the relative loss comparison of the latent factor statistic as in Eq. (3.7) that, in correspondence of each test, is calculated with respect to the loss measure of the data generating benchmark model. For the simulated LCMHT, the α is set to 5% for each tail of the statistic distribution, the number of tolerated false rejections is $k = 4$. The results of the simulated LC test are less neat than the LR's and the general outcome consists in a quite broad equivalence of the model suite components in the latent state filtering. We record a moderate underperformance of the plain SV model, which is inferior to the equivalence model set one third of the time it is applied to a different model sample, indicating the need of enhanced features for the sake of filtering, whenever the simple stochastic volatility hypothesis might be rejected. The testing exercise with a relatively smaller model equivalence set is in the cases of the CEV and CEVVJ benchmarks, which basically tell that the effect of the CEV factor on the observable variable matters from a dynamical standpoint. It is interesting in that respect the performance of the SHB broad family that is relatively deemed equivalent to the CEV filters. The introduction of a jump component in x with the CEVXJ and the CEVJJ instances, blurs again the distinction between the equivalence model subset and the inferior performers. A final piece of information we are able to extract from the battery of LCMHT concerns the jumps in volatility that do not seem to affect the projection exercise. This phenomenon should be expected if we take into account the fact that we have only considered asynchronous jumps that thus cannot be isolated within the state equation. Moreover, it is important to notice that the simulation exercise is performed at weekly frequency, a choice that might significantly affect the wide equivalence result obtained for the latent state estimation comparison test. In the real data application pursued in the following section, we switch to a daily frequency obtaining more neat results.

Finally, we derive for each benchmark sample and for each loss function LR and LC, model confidence sets with the max-MCS, the t-MCS and the γ-MCS algorithms. In a first not reported experiment of absolute model performance testing, whereby for moderate confidence levels of the LRMCS-max and letting the γ-TPFDP (10%) to control the k-FWER targeting a moderate α (5%) as well, we obtain strong

aliasing among the model set components, whereas the unrefined LRMCS-t is capable of discovering model clusters more in line with the recursion performed by the relative performance MHT. Increasing the confidence level (10%) and allowing a higher fixed percentage (20%) of the total number of hypotheses for the k-FWER, allows to investigate the reciprocal model ability in mimicking the simulated likelihood characteristics. Nonetheless, the LRMCS-γ offers more neat results. The LR results are reported in the Tab. 20, 21 and 22. We discuss the latter two as the LRMCS-max reports results that are less consistent with the relative performance test and the latter MCS type test, pointing again to a certain limitation of the test constructed on Hansen et al. (2011) to discriminate among closely performing models. Concerning the stochastic diffusion family, we notice that the inner models are easily mimicked by the whole model set, whereas the introduction of a jump in the level of the observable cannot be captured by more simple nested models of this family, whereas skewed Normal jump models of the SH class enter the MCS, with the latter jump specification performing better than the double-exponential one. A restriction of the MCS with CEVXJ and CEVJJ as a benchmark confirms the capability of the affine model specification to reproduce a not extreme CEV diffusion form. These results, coupled with the more mitigated results of the previous algorithms, draw attention to some unidentifiable feature of the system that must be connected to the latency of the volatility factor. In this regard, we observe that the likelihood of the simulated exercise is quite flat, that is it exhibits low sensitivity to model parameters and the Hessian conditioning number is often very high thus signalling parameter uncertainty. Direction for further research might include exploring transformations of the system under analysis in order to migrate model parameters from the latent component to the observable variable or at least to its first order component. Finally, we notice in the context of the simulated LRMCS test that the stochastic diffusion class enters the SH model confidence set, as well as the CEV model with jumps is able to explain the likelihood of the simulated stochastic hazard sample, pointing to a substantial equivalence of the two classes. Moreover, the ability of the single directional jump models to explain strongly asymmetric sample distribution suggest the possibility of further simplifying the parametric structure of the SH class, introducing offset single directional jump components. With the LCMCS the only strong general conclusion that we can gather is again the heavy model aliasing, with some slight peculiarities within the LCMCS-t context.

3.3.3 Market Data Experiment

In this paragraph, we employ the ability of the developed MHT procedures and the insight collected with the simulation exercise to elaborate a model selection experiment targeting financial market data. Specifically, the sample is represented by the logarithm transform[17] of the daily closing quotes of the Standard & Poor's 500 Index, ranging from January, 3^{rd} 1950 to February, 26^{th} 2016, providing in total 16,636 observations that on the conventional 260 days per year represents 64 trading years circa. In this exercise the reference frequency is daily, and both the LR and the LC are calculated with this time horizon. The time interval are made even, although the analysis is easily implementable on a uneven time grid. The sample is cleaned from the secular trend and the resulting observable is assumed to be a martingale, hypothesis that is empirically justified by the stylised flat autocorrelogram of the daily first

[17] The data is multiplied by 100 and hence the unit of measure is implicitly the percentage. For balancing reasons, several coefficients are scaled, that is θ is divided by 10 while λ_1 is multiplied by 10. As in the simulation test, the λ_0 parameter for the stochastic hazard models is divided by 100.

order differences. The Fig. 5(a) shows the cumulative log return path employed for market data testing. Fig. 5(b) exhibits the histogram of daily returns with the superimposed estimated CSHB marginal likelihood. The model set on which the model selection exercise hinges, it is the reference model set of Eqs. (3.1) and (3.2), while the filter is again represented by the Eqs. (3.4) and (3.5). Referring to the standard distributional shape measures, we report that the returns mark an yearly volatility of 15.69, with a skew factor of -1.01 and 30.12 kurtosis. The test statistics are produced by the stationary bootstrapping, whereby the block window (Politis and White, 2004; Patton et al., 2009) is calibrated to the autocorrelation function of the threshold GARCH estimates of the sample volatility, in order to preserve the spectral properties of the 10 year long 2000 output samples. The average block size is 264 days, which reflects a higher viscosity of the data as in the longer sample we find many more volatility spikes. The likelihood parameter estimates for the model set components are presented in Tab. 26. It is important to notice that the parameter aliasing entails a strong dependency of the MLE upon the initial conditions, a fact that requires an educated guess. With respect to the subject of investigation, that is the historical measure of an equity index such as the S&P 500, this study can be assimilated to the analysis of Andersen et al. (2002), Chernov et al. (2003) and Eraker et al. (2003), although the perspective is original. In those studies, the statistical significance of mainly the affine class and the log-linear stochastic volatility model[18] is investigated and a limited relative model comparison is performed. The article Andersen et al. (2002) studies the significance of those two model classes concluding that stochastic volatility coupled with jumps in return are significant and generate strong reduction in the χ^2 measure of significance. Eraker et al. (2003) reports log-Bayes ratios, pair-wise model performance comparison that is not based on hypothesis testing, concluding that stochastic volatility and jumps are more significant that models exhibiting stochastic volatility only and that including a jump in volatility seems to improve the model performance. Chernov et al. (2003) studies multi-factor stochastic volatility models, reporting with respect to the SV family, that jumps in return and jumps in return and volatility are both significant, with the latter providing a p-value that is almost identical to that of the jump-in-return only model and which does not justifies the superiority of the jump-in-volatility augmented affine model, finally selecting the one with jump-in-return only. In this study, we focus on a slightly different model set, including the single factor affine model, augmented with a CEV factor and a fully stochastic intensity model family with double-exponential and skewed Normal high frequency jumps. The latter constraint is realised as the specific setting of the initial parameter in the AML procedure, whereby we target a particular local neighbourhood of the parametric space. This work is original in that we exploit peculiar statistical techniques allowing joint comparison of the model set. In this experiment we set up several measures of relative performance test hinging on multi-hypothesis balanced confidence sets, further refined with the step-wise procedure of Romano and Wolf (2005a, 2007, 2010). The model selection is further tested and synthesised with absolute performance tests targeting a specification of the MCS of Hansen et al. (2011) paired with a novel MHT based procedure aiming at the model confidence set. A rough term of comparison of those test is represented by a streamlined test combining the concept of MCS with scalar asymptotic test of the sample averages of the full set of pairwise comparisons.

[18] This model is included in the model set in the next Chapter 4 analysis concerning the performance of option pricing models

A close examination of the results of the relative performance MHT reveals significant information. The LRMHT shows that that stochastic volatility and jumps in volatility alone are not sufficient to mimic the distributional features of the market data sample. The SV and the SVVJ models are inferior almost in the totality of comparisons, with the exception of equivalence between the SVVJ and SVJJ. The performance of the SVXJ is superior in the affine model set, although inferior to the more complex CEV specification and to the majority of models with stochastic hazard. The introduction of a jump in volatility with the SVJJ model introduces some ambiguity, worsening the model performance attained previously by the SVXJ model. The performance of the CEV family ranks overall at least equivalent to the top model cluster, with some variations. This broad class appears as an equivalence class, as all its components are equivalent at each fixing of the likelihood ratio to any of its members. However, the introduction of a jump in volatility to the nested model class exhibits again some distortion, which can be seen with the comparison of the performance results when changing the benchmark from CEV to CEVVJ and from CEVXJ to CEVJJ. Concerning the SHB family, we notice probably the most informative result within the context of the relative model performance, which corresponds to the benchmarking to the SHBVJ model, which is among the top performing model group, composed by the SHBVJ, CSHB, CSHA, CSHAVJ and CEV models, with SHBVJ performing slightly better. This result, however, is not distinctively superior, as the top performing model group is connected to the CEV family, as the equivalence of the performance of this class might suggest, and to the SHB wide class, as the test with LR to CSHB, CSHA and CSHAVJ reveals. This result is further circumscribed by the application of the MCS procedures (Tab. 29) that in the context of the LR test exhibit the clear superiority of the CSHB, CSHA, SHBVJ and CSHAVJ. The CEV and CEVXJ both enters the MCS in max-MCS and 10%-MCS, CEVJJ is also included in the former. The CEV models work on a 0.6 ca. elasticity parameter. It is interesting to notice the high performance of the CEV diffusion-only, suggesting that the strong kurtosis exhibited by the data might be the predominant feature, when framed by the likelihood procedure adopted for testing. The max-MCS test version shows a slightly enlarged version of the MCS, which is more in line with the indeterminacy of the system.

With the LCMHT test we evaluate the ability of the non-linear filter to extract from the observable data the trajectory of the latent variable v. Because of the lack of a known comparative element to construct the loss measure, we adopt the output of the threshold GARCH as a reference and calculate an appropriate distance as in Eq. (3.7). The outcome of the TGMHT are shown in Tab. 27. With this table, the ability of the MHT approach in model selection is even more remarkable when compared to the result of the MCS computed on the same data and measures. With TGMHT we can isolate at least two major clusters. The analysis of the balanced step-down results of Tab. 27 reveals a top group formed by the CEVJJ, the SHA and SHVJ model, providing indication of strong volatility clustering and hence high volatility spikes, rare jumps in the x level and possible jumps in volatility, although the presence of SHA weakens this result. A strongly inferior group is found in the CSHA and CSHAVJ models, whereas the remaining components of the model set spreads in the middle cluster, with SVJJ and SVXJ also performing well. The TG measure results are useful as they offer a means for assessing the model ability to estimate the unobserved system component v. However, those results are tied to the output of an auxiliary model, that is the threshold GARCH, as the statistic is determined by measuring the absolute tracking error of the projection with

respect to a measure of observable the volatility. Finally, in order to construct a model selection exercise without the need of an offset model, we adopt the LRLCMHT, which exploit a loss function based on a joint likelihood measure of system state projection, providing the ex-post "most probable" latent state estimate. The results are illustrated in Tab. 28. It is interesting to notice the different perspective. When joining a likelihood measure, one of the best performer in the LRMHT test is now indicated as the best model performer, that is the CSHB, equivalently to its jump in volatility augmented version. A top cluster can be identified as formed by CSHB, SHB, CSHBVJ and SHA. A large bottom model cloud contains the SV and CEV broad families plus the CSHA and CSHAVJ models. The SHAVJ and SHBVJ models gravitates at a middle ranking level. The application of the MCS battery of tests to the TG and LRLC performance measures, confirms the results we were able to gather from a thorough relative performance test based on a benchmarking rotation. The SHA and SHAVJ models perform at the top ranking in the TG absolute performance test, whereby the model confidence set is restricted to those two model set components. The CEVJJ also seems to perform well in the latter test. The inferior model set exhibits a quite low range of p-values. The LRLCMCS test also exhibits a strong polarisation in favour of the CSHB and CSHBVJ models. The latter result is probably due to a distinctive smoothness of the LC projections produced by the parametrised version of those models. These MCS results are quite surprising if compared with the simulation experiment whereby a large model similarity was evident. On the account of this outcome, we conjecture that, in the context of single factor models, the joint usage of stochastic diffusion and stochastic intensity might be redundant, whereby models of the latter class exhibit performances at least equivalent to the CEV family in explaining the historical behaviour of market data. From our tests, the superior performance of models embedding jumps in volatility appears ambiguous, probably as a consequence of the marginalisation procedure, which does not exploit the prior-to-posterior loop and relies on an analytic result pertaining the stationary distribution of the latent factor. In future research, we plan to expand on this topic.

3.4 Concluding Remarks

In this chapter, we have presented a novel exercise of model selection applied to a JD model set targeting the historical measure of simulated and financial market data. We construct several measures of model comparison that are tested with relative and absolute MHT and MCS type tests. The model set contains the popular affine single factor stochastic volatility model, augmented with a CEV parameter; the collection is further extended with a stochastic intensity high frequency jump class, representing a non standard alternative model family. Under the simulated test, the respective nesting models prove to be able to produce similar features to one another, as measured by the target performance functions. The latter result reinforces the findings of the empirical exercise, whereby the stochastic intensity family exhibits superior models in the majority of the tests. It is important to notice that the affine framework is strongly rejected in the real market data experiment. Moreover, there is a redundancy to jumps in volatility when measuring marginalised likelihoods, as well as a non-significant prevalence of this component with respect to the latent component filtering measures. The contribution of jumps in volatility appears to be dubious, contrary to the findings of Eraker et al. (2003) and more in line with the model selection results of Chernov et al. (2003), though our findings are more explicit than the latter. Secondly,

the high empirical kurtosis and the moderate asymmetry are the prevalent features, that can be captured with both conventional and non conventional models, that is CEV with jumps as well as stochastic hazard models with high average frequency of jumps, with the latter class performing slightly better under the filtering measures. Third, these results point to the redundancy of mixing both stochastic diffusion and stochastic intensity to model historical equity financial time series. The last message we hope to convey with this analysis is that there is probably room for a simplification of the modelling structure of financial time series, which counters the general trend in the academic literature for ever increasing complexity. Finally, as a complementary methodological contribution that facilitates our empirical analysis, we extend the second order filtering procedure in Maybeck (1982) to allow jump components in the system state.

The analysis produced in this chapter is original in that we propose a general model selection procedure, based on MHT and MCS, to investigate superior model performance in the context of the statistical measure of financial data, where we take the perspective of dealing with stochastic volatility as a latent factor and construct model performance measures targeting several aspects of the estimation problem. The outcome of this exercise is useful in that we question model overparametrisation when combining stochastic diffusion and stochastic hazard, at the same time suggesting directions for model simplification.

SV	stochastic volatility model
SVVJ	stochastic volatility model with positive exponential (exp) jumps in volatility
SVXJ	stochastic volatility model with negative exp jumps in the x level
SVJJ	stochastic volatility model with positive exp jumps in volatility and negative exp jumps in the x level
CEV	stochastic volatility model with CEV
CEVVJ	stochastic volatility model with positive exp jumps in volatility and CEV
CEVXJ	stochastic volatility model with negative exp jumps in the x level and CEV
CEVJJ	stochastic volatility model with positive exp jumps in volatility, negative exp jumps in the x level and CEV
SHB	stochastic hazard model with double exp jumps in the x level
SHBVJ	stochastic hazard model with double exp jumps in the x level and positive exp jumps in the intensity function
CSHB	stochastic hazard model with double exp jumps in the x level and CEV
CSHBVJ	stochastic hazard model with double exp jumps in the x level, positive exp jumps in the intensity function and CEV
SHA	stochastic hazard model with skewed Normal (N) jumps in the x level
SHAVJ	stochastic hazard model with skewed N jumps in the x level and positive exp jumps in the intensity function
CSHA	stochastic hazard model with skewed N jumps in the x level and CEV
CSHAVJ	stochastic hazard model with skewed N jumps in the x level, positive exp jumps in the intensity function and CEV

Table 14: **Model Set Acronyms.**

Model description	Jump size distribution	Coefficient configuration	References
The stochastic diffusion model.		$\gamma_0 = 1/2$, $\lambda_0 = \lambda_1 = 0$	Heston (1993)
The stochastic diffusion model with constant intensity jumps in the cumulative return level.	The jump size distribution is Normal.	$\gamma_0 = 1/2$, $\lambda_1 = 0$	Bates (1996), also included in Duffie et al. (2000)
The stochastic diffusion model with constant intensity jumps in the cumulative return level and in the volatility factor.	The jump size distribution is Normal in the x and positive exponential in v.	$\gamma_0 = 1/2$, $\gamma_1 = 0$	Eraker et al. (2003), also included in Duffie et al. (2000), Bates (2000) and Pan (2002)
The stochastic diffusion model with stochastic intensity jumps in the cumulative return level and in the volatility factor.	The jump size distribution is Normal in the x and positive exponential in v.	$\gamma_0 = \gamma_1 = 1/2$	Eraker (2004)
The constant elasticity of variance model.		$\lambda_0 = \lambda_1 = 0$	Cox and Ross (1976), also included in Beckers (1980) and Macbeth and Merville (1980)
The constant diffusion model with jumps in the cumulative return level.	The jump size distribution is Normal.	$\gamma_0 = \gamma_1 = 0$, $\lambda_1 = 0$	Merton (1976)
The constant diffusion model with jumps in the cumulative return level.	The jump size distribution is double-exponential.	$\gamma_0 = \gamma_1 = 0$, $\lambda_1 = 0$	Kou (2002) and Kou and Wang (2004)

Table 15: **Standard Models and the Model Set.** The table describes the connections between the model set and several standard models in the literature of financial markets. We remark that the parameter linkage for some of those models has to be intended jointly with model transformations, which are explained in Appendix A.4.

	θ	κ	σ	ρ	γ	λ_1	η_1	λ_0	η_a	η_b	μ	σ_2	$\mu_3/\sigma_2^{\frac{3}{2}}$	μ_4/σ_2^2	$\mu_5/\sigma_2^{\frac{5}{2}}$	μ_6/σ_2^3
SV	1.41	1.50	1.41	-0.5							0	0.04	-0.14	4.87	-2.3	55.4
SVVJ	1.41	2.00	1.41	-0.5		2.5	2				0	0.04	-0.14	5.38	-2.6	72.9
SVXJ	1.00	1.50	1.41	-0.5				1.0	2.24		0	0.04	-1.42	8.49	-33.9	197.0
SVJJ	1.00	2.00	1.41	-0.5		2.5	2	1.0	2.24		0	0.04	-1.44	8.70	-34.5	204.8
CEV	1.26	1.50	1.41	-0.5	0.75						0	0.04	-0.22	7.34	-6.0	149.7
CEVVJ	1.21	2.00	1.41	-0.5	0.75	2.5	2				0	0.04	-0.22	8.96	-7.5	243.0
CEVXJ	0.89	1.50	1.41	-0.5	0.75			1.0	2.24		0	0.04	-1.45	9.22	-35.3	226.1
CEVJJ	0.85	2.00	1.41	-0.5	0.75	2.5	2	1.0	2.24		0	0.04	-1.53	9.94	-38.2	258.3
SHB	1.00	1.50	1.41	-0.5				2.6	2.30	0.08	0	0.04	-1.55	9.41	-45.2	282.0
SHBVJ	1.00	2.00	1.41	-0.5		2.5	2	2.6	2.30	0.08	0	0.04	-1.57	9.66	-47.8	309.0
CSHB	1.00	1.50	1.41	-0.5	0.75			2.6	2.30	0.07	0	0.04	-1.71	10.85	-59.4	420.2
CSHBVJ	1.00	2.00	1.41	-0.5	0.75	2.5	2	2.6	2.30	0.06	0	0.04	-1.72	11.41	-66.3	503.3
SHA	1.00	1.50	1.41	-0.5				2.6	0.97	-9.00	0	0.04	-0.16	3.74	-2.2	29.4
SHAVJ	1.00	2.00	1.41	-0.5		2.5	2	2.6	0.97	-9.00	0	0.04	-0.16	3.88	-2.2	33.4
CSHA	1.00	1.50	1.41	-0.5	0.75			2.6	0.87	-9.00	0	0.04	-0.15	4.54	-2.7	54.5
CSHAVJ	1.00	2.00	1.41	-0.5	0.75	2.5	2	2.6	0.83	-9.00	0	0.04	-0.18	5.01	-4.1	75.5

Table 16: **Simulation MHT Model Parameters and Standardised Moments.** This table shows the model parameters for the simulated experiments, as well as the mean (μ) the (weekly) variance (σ_2), the skewness ($\mu_3/\sigma_2^{3/2}$), the kurtosis (μ_4/σ_2^2) and the fifth ($\mu_5/\sigma_2^{5/2}$) and sixth (μ_6/σ_2^6) standardised central moments for each model at the simulation parameters. We notice that the yearly variance for each model is circa 2, which is equally split between the diffusion and the jump component, whenever the latter is present. The model parameters within the ten columns from the left are indicated by Greek letters corresponding to the model definition in Eq. (3.1) and (3.2), with exception of η_0 which indicates the expected jump size of the jump in volatility and η_a that indicate the the size of a negative for stochastic diffusion with jumps and stochastic hazard with double exponential. For the SHB family, the parameter η_b represents the expected positive jump size, whereas the probability of a positive jump is constrained such that the jump component drift be null. The latter two Greeks, in the case of skew Normal stochastic hazard models, indicate, respectively, the shape and the skew parameter. We further notice that for gradient balancing reasons, λ_0 is multiplied by a factor of 10, λ_1 is divided by the same factor in the case of the stochastic diffusion family, whereas it is scaled by 100 times in the case of high frequency jump models. The parameters η_a and η_b are multiplied by 10 whenever included.

	θ	κ	σ	ρ	γ	λ_1	η_1	λ_0	η_a	η_b
SV	1.3929	7.0560	3.7566	-0.6003						
	(0.0052)	(3.5075)	(1.0017)	(0.1903)						
SVVJ	1.4342	8.0792	3.6425	-0.5544		2.5682	4.0251			
	(0.0115)	(3.6301)	(0.7258)	(0.2765)		(0.3023)	(0.2326)			
SVXJ	1.3831	7.0447	3.7536	-0.1404				2.2707	3.0109	
	(0.0137)	(2.4441)	(0.7613)	(0.1618)				(0.8135)	(0.5025)	
SVJJ	1.4032	8.0713	3.6353	-0.1123		2.5713	4.0278	2.2897	3.0088	
	(0.0135)	(3.5364)	(1.1282)	(0.1244)		(0.3797)	(0.5130)	(0.1440)	(0.0604)	
CEV	1.3872	7.2392	3.3622	-0.4583	0.6113					
	(0.0086)	(2.7717)	(0.6109)	(0.1770)	(0.0041)					
CEVVJ	1.3978	8.2314	2.7311	-0.5000	0.6605	2.5183	4.9184			
	(0.0066)	(2.6390)	(0.2126)	(0.1536)	(0.0046)	(0.1955)	(0.5727)			
CEVXJ	1.3661	7.1791	3.6354	-0.1956	0.5517			2.0417	2.9293	
	(0.0359)	(2.8231)	(0.8556)	(0.1792)	(0.0111)			(0.2223)	(0.2285)	
CEVJJ	1.3973	8.1534	2.9306	-0.2388	0.5817	2.8949	4.4266	2.1760	3.0521	
	(0.0093)	(3.4842)	(0.1000)	(0.1301)	(0.0120)	(0.1713)	(0.3350)	(0.1187)	(0.4411)	
SHB	0.9273	7.1993	3.1988	-0.4891				1.5079	0.8520	0.7691
	(0.0157)	(2.4277)	(0.1417)	(0.1773)				(0.0899)	(0.0114)	(0.0114)
SHBVJ	0.9289	8.1939	3.2029	-0.4043		2.4959	3.9904	1.6124	0.8474	0.7631
	(0.0213)	(4.2880)	(0.9970)	(0.2489)		(0.2152)	(0.3519)	(0.5041)	(0.0813)	(0.2090)
CSHB	0.9262	7.2023	3.1690	-0.4735	0.4615			1.5193	0.8582	0.7714
	(0.0246)	(2.8224)	(0.4908)	(0.2921)	(0.0124)			(0.0568)	(0.0217)	(0.0187)
CSHBVJ	0.9251	8.1969	3.1353	-0.4107	0.4531	2.4305	3.8970	1.6269	0.8513	0.7628
	(0.0158)	(2.3032)	(0.5645)	(0.2096)	(0.0029)	(0.9021)	(0.5776)	(0.0671)	(0.0079)	(0.0077)
SHA	0.9102	7.0201	3.7470	-0.5595				0.9044	1.4244	-0.3356
	(0.0075)	(3.1592)	(0.8669)	(0.2443)				(0.0374)	(0.0166)	(0.0450)
SHAVJ	0.8065	8.1383	3.8650	-0.8992		2.1367	3.1327	1.5397	1.1078	-0.2333
	(0.0082)	(3.6899)	(0.5718)	(0.3695)		(0.7451)	(0.3872)	(0.0101)	(0.0092)	(0.0125)
CSHA	0.7765	7.1372	3.3321	-0.5445	0.8795			2.8252	0.7296	-0.4587
	(0.0104)	(2.6834)	(0.7027)	(0.2113)	(0.0194)			(0.4307)	(0.0723)	(0.1548)
CSHAVJ	0.7276	8.3488	2.1948	-0.6106	0.9000	2.6211	4.1696	2.9964	0.8264	-0.5342
	(0.0054)	(1.4450)	(0.7062)	(0.1619)	(0.0108)	(0.2016)	(0.1599)	(0.0374)	(0.0044)	(0.0122)

Table 17: **Financial Market Data Model Parameters Estimates and MCS Test Results.** This table shows the parameter estimates for the Model Set, applied to the Standard & Poor's 500 Equity Index daily log return data, ranging from January, 3^{rd} 1950 to February, 26^{th} 2016. Several parameters are scaled, that is θ is divided by 10 while λ_1 is multiplied by 10. As in the simulation test, the λ_0 parameter for the stochastic hazard models is divided by 100. In parentheses we exhibit the estimated parameter standard errors.

Benchmark samples: SV, SVVJ, SVXJ, SVJJ								
SV	⋆	⋆	-0.0121	0.0145	–	↘	–	↘
SVVJ	-0.0049	0.0053	⋆	⋆	–	↘	–	↘
SVXJ	-0.0032	0.0038	-0.0142	0.0129	⋆	⋆	-0.0136	0.0175
SVJJ	-0.0031	0.0037	-0.0120	0.0132	-0.0091	0.0105	⋆	⋆
CEV	-0.0056	0.0062	-0.0106	0.0133	–	↘	–	↘
CEVVJ	-0.0026	0.0034	-0.0107	0.0129	–	↘	–	↘
CEVXJ	-0.0030	0.0036	-0.0100	0.0128	-0.0113	0.0122	-0.0138	0.0180
CEVJJ	-0.0043	0.0049	-0.0121	0.0145	-0.0101	0.0107	-0.0139	0.0164
SHB	-0.0044	0.0043	-0.0099	0.0096	-0.0237	0.0031	-0.0264	0.0007
SHBVJ	-0.0084	0.0083	-0.0099	0.0103	-0.0241	0.0028	-0.0274	0.0006
CSHB	-0.0052	0.0053	-0.0112	0.0114	-0.0426	0.0039	-0.0276	0.0001
CSHBVJ	-0.0045	0.0048	-0.0116	0.0117	-0.0237	0.0027	-0.0269	0.0005
SHA	-0.0059	0.0058	-0.0097	0.0110	-0.0181	0.0030	-0.0205	0.0033
SHAVJ	-0.0065	0.0064	-0.0035	0.0031	-0.0562	0.0169	-0.0189	0.0026
CSHA	-0.0056	0.0055	-0.0099	0.0112	-0.0405	0.0070	-0.0213	0.0065
CSHAVJ	-0.0063	0.0063	-0.0094	0.0107	-0.0374	0.0089	-0.0161	0.0035
Benchmark samples: CEV, CEVVJ, CEVXJ, CEVJJ								
SV	-0.0255	0.0132	-0.0596	0.0177	–	↘	–	↘
SVVJ	-0.0195	0.0124	-0.0582	0.0212	–	↘	–	↘
SVXJ	-0.0240	0.0143	-0.0548	0.0158	-0.0250	0.0240	-0.0205	0.0122
SVJJ	-0.0187	0.0118	-0.0495	0.0151	-0.0244	0.0243	-0.0151	0.0096
CEV	⋆	⋆	-0.0273	0.0288	–	↘	–	↘
CEVVJ	-0.0125	0.0140	⋆	⋆	–	↘	–	↘
CEVXJ	-0.0096	0.0116	-0.0284	0.0289	⋆	⋆	-0.0077	0.0102
CEVJJ	-0.0121	0.0148	-0.0239	0.0154	-0.0232	0.0244	⋆	⋆
SHB	-0.0132	0.0079	-0.0476	0.0228	–	↘	–	↘
SHBVJ	-0.0130	0.0082	-0.0294	0.0084	–	↘	–	↘
CSHB	-0.0099	0.0069	-0.0365	0.0262	–	↘	–	↘
CSHBVJ	-0.0146	0.0125	-0.0359	0.0263	–	↘	–	↘
SHA	-0.0166	0.0103	-0.0426	0.0199	-0.0220	0.0039	-0.0294	0.0008
SHAVJ	-0.0140	0.0098	-0.0319	0.0112	-0.0330	0.0197	-0.0248	0.0011
CSHA	-0.0126	0.0123	-0.0315	0.0280	-0.0258	0.0052	-0.0183	0.0010
CSHAVJ	-0.0134	0.0139	-0.0323	0.0298	-0.0212	0.0066	-0.0189	0.0011
Benchmark samples: SHB, SHBVJ, CSHB, CSHBVJ								
SV	–	↘	–	↘	–	↘	–	↘
SVVJ	–	↘	–	↘	–	↘	–	↘
SVXJ	-0.0132	0.0081	-0.0150	0.0097	-0.0190	0.0092	-0.0171	0.0052
SVJJ	-0.0219	0.0052	-0.0219	0.0056	-0.0246	0.0055	-0.0221	0.0009
CEV	–	↘	–	↘	–	↘	–	↘
CEVVJ	–	↘	–	↘	–	↘	–	↘
CEVXJ	-0.0117	0.0081	-0.0177	0.0103	-0.0202	0.0074	-0.0173	0.0040
CEVJJ	-0.0198	0.0084	-0.0204	0.0078	-0.0260	0.0038	-0.0177	0.0026
SHB	⋆	⋆	-0.0009	0.0004	-0.0023	0.0004	-0.0027	0.0007
SHBVJ	-0.0003	0.0004	⋆	⋆	-0.0020	0.0006	-0.0077	0.0007
CSHB	-0.0007	0.0026	-0.0009	0.0020	⋆	⋆	-0.0004	0.0003
CSHBVJ	-0.0005	0.0031	-0.0008	0.0022	-0.0004	0.0003	⋆	⋆
SHA	-0.0177	0.0061	-0.0222	0.0052	–	↘	–	↘
SHAVJ	-0.0164	0.0041	-0.0232	0.0027	-0.0229	0.0006	-0.0211	0.0014
CSHA	-0.0055	0.0076	-0.0266	0.0030	–	↘	–	↘
CSHAVJ	-0.0093	0.0087	-0.0203	0.0028	-0.0143	0.0027	–	↘
Benchmark samples: SHA, SHAVJ, CSHA, CSHAVJ								
SV	–	↘	–	↘	-0.0141	0.0000	-0.0143	0.0016
SVVJ	–	↘	–	↘	–	↘	–	↘
SVXJ	–	↘	–	↘	-0.0158	0.0000	-0.0138	0.0029
SVJJ	–	↘	–	↘	–	↘	–	↘
CEV	–	↘	–	↘	-0.0122	0.0006	-0.0146	0.0014
CEVVJ	–	↘	–	↘	–	↘	–	↘
CEVXJ	–	↘	–	↘	-0.0130	0.0004	-0.0144	0.0016
CEVJJ	–	↘	–	↘	-0.0215	0.0038	–	↘
SHB	-0.0028	0.0019	-0.0024	0.0018	-0.0029	0.0021	-0.0023	0.0013
SHBVJ	-0.0028	0.0018	-0.0023	0.0015	-0.0028	0.0018	-0.0016	0.0011
CSHB	-0.0027	0.0018	-0.0024	0.0018	-0.0029	0.0019	-0.0022	0.0013
CSHBVJ	-0.0027	0.0017	-0.0022	0.0015	-0.0027	0.0018	-0.0035	0.0014
SHA	⋆	⋆	-0.0013	0.0013	-0.0013	0.0010	-0.0006	0.0008
SHAVJ	-0.0013	0.0005	⋆	⋆	-0.0019	0.0012	-0.0004	0.0008
CSHA	-0.0002	0.0001	-0.0011	0.0012	⋆	⋆	-0.0005	0.0007
CSHAVJ	-0.0081	0.0007	-0.0045	0.0011	-0.0091	0.0025	⋆	⋆

Table 18: **Simulated LRMHT.** This table exhibits the LRMHT for the simulated experiment. Each pair of columns for each block row represents an MHT, showing the final set output of balanced step-down algorithm, benchmarked to the model indicated with a double star. In the simulated experiment the benchmark model also indicates the DGP, which has produced the simulated paths. The rejected models do not provide a confidence interval, whereas the corresponding row is filled with a north-east or a south-east arrow, whether the corresponding model is, respectively, superior or inferior to the benchmark model. In this test the confidence level for each tail is 5% and the k-FWER=4. It is interesting to notice how the SD model class can be reproduced by any other model. Moreover, the moderately parametrised (0.75) CEV family, can be reproduced by the inner models, a feature that is the foundation of this experiment, that is the exploration of statistically undistinguishable models, though some are structurally inferior. The SHB family seems to show some rigidity in combining high kurtosis and moderate skew. Moreover, the sample generated by the latter family can be reproduced by the other models, whereas the SHA family sample appears to be harder to dissimulate.

Benchmark samples: SV, SVVJ, SVXJ, SVJJ								
SV	⋆	⋆	–	↘	-0.6203	0.0406	-0.4349	0.1172
SVVJ	–	↘	⋆	⋆	-0.4071	0.0961	-0.4543	0.1188
SVXJ	-0.0120	0.0919	-0.1157	0.0577	⋆	⋆	-0.0876	0.0305
SVJJ	-0.0139	0.0925	-0.0364	0.0693	-0.0699	0.0428	⋆	⋆
CEV	–	↘	-0.0505	0.0646	-0.3462	0.1042	-0.2867	0.1409
CEVVJ	-0.0166	0.0003	-0.0210	0.0431	-0.3653	0.1032	-0.3522	0.1378
CEVXJ	-0.0043	0.1024	-0.0520	0.1171	-0.0525	0.0177	-0.0906	0.0315
CEVJJ	-0.0027	0.0938	-0.0321	0.1432	-0.0418	0.0250	-0.0178	0.0034
SHB	-0.2653	0.0700	-0.2677	0.0805	-0.0625	0.0735	-0.0410	0.0743
SHBVJ	-0.2143	0.0962	-0.1946	0.1129	-0.0603	0.0762	-0.0865	0.1038
CSHB	-0.2609	0.0776	-0.2970	0.0816	-0.0827	0.0692	-0.1107	0.0550
CSHBVJ	-0.2377	0.0918	-0.2409	0.0982	-0.0600	0.0716	-0.0850	0.0568
SHA	-0.3082	0.0356	-0.3941	0.0107	-0.0848	0.0453	-0.0898	0.0338
SHAVJ	-0.3056	0.0393	-0.4019	0.0098	-0.1518	0.0735	-0.1106	0.0501
CSHA	-0.3112	0.0295	-0.3865	0.0125	-0.0889	0.0452	-0.0813	0.0304
CSHAVJ	-0.3054	0.0393	-0.3950	0.0074	-0.1019	0.0613	-0.0992	0.0424
Benchmark samples: CEV, CEVVJ, CEVXJ, CEVJJ								
SV	–	↘	–	↘	–	↘	–	↘
SVVJ	-0.6441	0.0007	–	↘	–	↘	–	↘
SVXJ	-0.5469	0.0206	–	↘	-0.1052	0.0169	-0.1514	0.0104
SVJJ	-0.5667	0.0262	–	↘	-0.1124	0.0223	-0.1320	0.0371
CEV	⋆	⋆	-0.0683	0.0033	-0.3422	0.0698	-0.2525	0.0575
CEVVJ	-0.0252	0.0569	⋆	⋆	-0.2947	0.0852	-0.2020	0.0769
CEVXJ	-0.0357	0.0611	-0.0654	0.0535	⋆	⋆	-0.0959	0.0212
CEVJJ	-0.0483	0.0675	–	↘	-0.0844	0.0286	⋆	⋆
SHB	–	↘	–	↘	-0.0968	0.0717	-0.0517	0.0764
SHBVJ	-0.2734	0.0012	-0.1465	0.0410	-0.0948	0.0784	-0.0857	0.0657
CSHB	-0.3189	0.0016	-0.2219	0.0079	-0.1100	0.0534	-0.1499	0.0204
CSHBVJ	-0.3075	0.0049	-0.2289	0.0082	-0.1090	0.0551	-0.0958	0.0360
SHA	–	↘	–	↘	-0.1578	0.0288	-0.1500	0.0047
SHAVJ	–	↘	–	↘	-0.1995	0.0546	-0.1528	0.0076
CSHA	–	↘	–	↘	-0.1487	0.0232	-0.1389	0.0021
CSHAVJ	–	↘	–	↘	-0.1653	0.0333	-0.1532	0.0062
Benchmark samples: SHB, SHBVJ, CSHB, CSHBVJ								
SV	-0.4693	0.0414	-0.4618	0.0573	-0.4168	0.0795	-0.3834	0.0839
SVVJ	-0.4478	0.0349	-0.4232	0.0600	-0.4406	0.0623	-0.3942	0.0812
SVXJ	-0.0373	0.0377	-0.0739	0.0332	-0.0364	0.0243	-0.0530	0.0160
SVJJ	-0.0657	0.0605	-0.0920	0.0656	-0.0546	0.0564	-0.0831	0.0785
CEV	-0.4601	0.0450	-0.4559	0.0607	-0.3986	0.0790	-0.3754	0.0866
CEVVJ	-0.4294	0.0394	-0.4138	0.0619	-0.4112	0.0689	-0.3677	0.0829
CEVXJ	-0.0370	0.0382	-0.0528	0.0353	-0.0333	0.0289	-0.0419	0.0190
CEVJJ	-0.0611	0.0633	-0.0606	0.0542	-0.0990	0.0891	-0.0477	0.0272
SHB	⋆	⋆	-0.0590	0.0463	-0.0317	0.0175	-0.0674	0.0446
SHBVJ	-0.0092	0.0124	⋆	⋆	-0.0459	0.0431	-0.0261	0.0235
CSHB	-0.0265	0.0276	-0.0585	0.0511	⋆	⋆	-0.0609	0.0462
CSHBVJ	-0.0509	0.0626	-0.0105	0.0119	-0.0132	0.0172	⋆	⋆
SHA	-0.0289	0.0185	-0.0697	0.0498	-0.0664	0.0324	-0.0773	0.0419
SHAVJ	-0.0692	0.0620	-0.0515	0.0366	-0.1070	0.0564	-0.1010	0.0578
CSHA	-0.0388	0.0184	-0.0478	0.0321	-0.0712	0.0375	-0.0769	0.0422
CSHAVJ	-0.0552	0.0520	-0.0633	0.0439	-0.1134	0.0597	-0.0885	0.0511
Benchmark samples: SHA, SHAVJ, CSHA, CSHAVJ								
SV	-0.1686	0.2182	-0.1063	0.2261	-0.1096	0.2715	-0.1195	0.2704
SVVJ	-0.1106	0.2087	-0.0798	0.2193	-0.0639	0.2579	-0.0694	0.2740
SVXJ	-0.1684	0.1665	–	↘	-0.0509	0.2568	–	↘
SVJJ	-0.0792	0.2059	-0.0408	0.1920	-0.0055	0.2279	-0.0772	0.2743
CEV	-0.1412	0.2228	-0.1041	0.2244	-0.0931	0.2631	-0.1037	0.2645
CEVVJ	-0.1131	0.2089	-0.0588	0.2159	-0.0614	0.2569	-0.0588	0.2747
CEVXJ	–	↘	–	↘	–	↘	-0.3254	0.0230
CEVJJ	-0.0190	0.1692	-0.0075	0.1894	-0.0313	0.2720	-0.1216	0.2458
SHB	-0.1012	0.0774	-0.1522	0.0950	-0.0613	0.0519	-0.1768	0.0901
SHBVJ	-0.0929	0.1164	-0.0437	0.0704	-0.0142	0.0709	-0.0349	0.0864
CSHB	-0.0779	0.0804	-0.1509	0.0948	-0.0541	0.0457	-0.1506	0.0903
CSHBVJ	-0.1358	0.1369	-0.0414	0.0724	-0.0527	0.0952	-0.0527	0.1280
SHA	⋆	⋆	-0.0235	0.0220	-0.0385	0.0293	-0.0250	0.0260
SHAVJ	-0.0142	0.0119	⋆	⋆	-0.0157	0.0137	-0.0332	0.0314
CSHA	-0.0052	0.0044	-0.0164	0.0162	⋆	⋆	-0.0291	0.0280
CSHAVJ	-0.0173	0.0150	-0.0154	0.0142	-0.0238	0.0212	⋆	⋆

Table 19: **Simulated LCMHT.** This table exhibits the LCMHT for the simulated experiment. Each pair of columns for each block row represents an MHT, showing the final set output of balanced step-down algorithm, benchmarked to the model indicated with a double star. In the simulated experiment the benchmark model also indicates the DGP, which has produced the simulated paths. The rejected models do not provide a confidence interval, whereas the corresponding row is filled with a north-east or a south-east arrow, whether the corresponding model is, respectively, superior or inferior to the benchmark model. In this test the confidence level for each tail is 5% and the k-FWER=4. In this exercise, it is interesting to notice that the performance is widespread and in particular jumps in return do not seem to affect the estimation of the latent factor. Jumps in volatility are not distinctively detected. With respect to the latter remark, we have to report that, in this exercise, we are using weekly data and asynchronous jumps only.

Benchmark samples: SV, SVVJ, SVXJ, SVJJ							
SHBVJ	1	SV	1	CEVXJ	1	CEVXJ	1
CEV	1	SVXJ	1	SVJJ	1	CEVJJ	1
CSHB	1	SVJJ	1	SVXJ	0.9997	SVJJ	0.9999
SHAVJ	1	CEV	1	CEVJJ	0.9997	SVXJ	0.9998
CEVVJ	1	CEVXJ	1	SHA	0.8531	CSHAVJ	0.9316
SVJJ	1	SHA	1	SHAVJ	0.8395	SHA	0.8479
SHB	0.9999	SHAVJ	1	SHB	0.6716	SHAVJ	0.8409
CEVJJ	0.9999	SVVJ	1	SHBVJ	0.6429	CSHA	0.8126
SVVJ	0.9999	CEVJJ	1	CSHBVJ	0.6294	SHB	0.6262
CSHBVJ	0.9999	CEVVJ	1	CSHAVJ	0.6211	SHBVJ	0.5587
SVXJ	0.9999	CSHAVJ	1	CSHA	0.2419	CSHB	0.5208
SHA	0.9999	CSHA	1	CSHB	0.2401	CSHBVJ	0.5160
CEVXJ	0.9997	CSHB	0.9999	SV	0.1232	*****	*****
SV	0.9997	SHB	0.9996	*****	*****	CEVVJ	0.0508
CSHA	0.9995	CSHBVJ	0.9994	SVVJ	0.0990	SV	0.0390
CSHAVJ	0.9989	SHBVJ	0.9975	CEV	0.0234	CEV	0.0390
*****	*****	*****	*****	CEVVJ	0.0152	SVVJ	0.0265
Benchmark samples: CEV, CEVVJ, CEVXJ, CEVJJ							
CEVVJ	1	CEVXJ	1	SVJJ	1	CEVXJ	1
CSHA	1	CEVVJ	1	CEVJJ	1	SVXJ	1
SHAVJ	1	CEV	1	CEVXJ	1	SVJJ	0.9998
CEV	1	CEVJJ	1	CSHAVJ	0.9780	CEVJJ	0.9995
CSHAVJ	1	CSHAVJ	0.9999	SHAVJ	0.9751	CSHA	0.7462
CEVXJ	1	SHAVJ	0.9999	SHA	0.9685	CSHAVJ	0.7233
SHA	1	CSHA	0.9999	SVXJ	0.9040	SHAVJ	0.7127
CSHB	1	SHA	0.9998	CSHB	0.6423	SHA	0.6632
SVJJ	1	SHBVJ	0.9994	SHB	0.5957	SV	0.4536
CEVJJ	1	SHB	0.9993	CSHBVJ	0.5838	SVVJ	0.4522
SVVJ	1	SVJJ	0.9991	SHBVJ	0.5548	CEVVJ	0.3866
CSHBVJ	1	SVVJ	0.9989	SV	0.3569	SHBVJ	0.3214
SHB	1	SV	0.9965	SVVJ	0.3005	CEV	0.2069
SHBVJ	1	CSHB	0.9956	CSHA	0.2293	CSHB	0.1697
SV	1	CSHBVJ	0.9951	CEV	0.1869	CSHBVJ	0.1676
SVXJ	0.9999	SVXJ	0.9840	CEVVJ	0.1538	SHB	0.1217
*****	*****	*****	*****	*****	*****	*****	*****
Benchmark samples: SHB, SHBVJ, CSHB, CSHBVJ							
CSHA	1	CSHBVJ	1	CSHB	1	CSHBVJ	1
CSHBVJ	1	SVXJ	0.9999	CSHBVJ	1	CSHB	1
CEVXJ	0.9995	SHBVJ	0.9874	SVXJ	0.9990	SHB	0.9994
CSHAVJ	0.9975	SHB	0.9775	SHBVJ	0.9944	SVXJ	0.9813
SHBVJ	0.9921	CSHB	0.9507	SHB	0.9799	SHBVJ	0.9637
CSHB	0.9906	CEVXJ	0.9379	CEVJJ	0.8804	CEVXJ	0.9527
SHB	0.9901	SHA	0.9314	CSHAVJ	0.8784	SHAVJ	0.8705
SVXJ	0.9607	SHAVJ	0.8521	CEVXJ	0.7567	CEVJJ	0.8549
CEVJJ	0.9032	CSHAVJ	0.7628	SHAVJ	0.7014	CSHAVJ	0.5830
SHAVJ	0.6322	CEV	0.1277	SHA	0.4020	SVJJ	0.3679
SHA	0.6310	CSHA	0.1202	CEV	0.3040	SHA	0.2936
SVJJ	0.2864	*****	*****	SVVJ	0.2625	CSHA	0.2521
*****	*****	SV	0.0567	CSHA	0.2340	CEVVJ	0.1885
CEV	0.0829	SVVJ	0.0419	CEVVJ	0.2173	SVVJ	0.1342
SV	0.0393	CEVVJ	0.0273	SV	0.1737	CEV	0.1263
SVVJ	0.0112	SVJJ	0.0260	*****	*****	*****	*****
CEVVJ	0.0044	CEVJJ	0.0123	SVJJ	0.0041	SV	0.0145
Benchmark samples: SHA, SHAVJ, CSHA, CSHAVJ							
CSHA	1	CSHA	1	CSHA	1	SHA	1
SHA	1	SHAVJ	1	SHAVJ	1	SHAVJ	1
SHB	0.9999	CSHB	0.9999	SHA	1	CSHA	1
CSHB	0.9999	SHBVJ	0.9998	SHB	0.9999	CSHB	0.9995
SHBVJ	0.9999	CSHBVJ	0.9997	CSHBVJ	0.9999	SHB	0.9994
CSHBVJ	0.9999	SHB	0.9989	SHBVJ	0.9999	CSHAVJ	0.9993
SHAVJ	0.9950	SHA	0.9977	CSHB	0.9997	CSHBVJ	0.9983
CSHAVJ	0.7823	CSHAVJ	0.9089	CSHAVJ	0.9427	SHBVJ	0.9958
CEVXJ	0.2996	CEVXJ	0.4962	CEVJJ	0.7124	SVXJ	0.8183
SVXJ	0.2812	SV	0.4353	CEV	0.6737	CEVXJ	0.7183
SV	0.2616	CEV	0.4214	SVXJ	0.6341	SV	0.7134
CEV	0.2583	SVXJ	0.3605	SV	0.6039	CEV	0.7069
CEVJJ	0.1672	*****	*****	CEVXJ	0.4720	*****	*****
*****	*****	SVJJ	0.0756	SVJJ	0.3647	SVVJ	0.0145
SVJJ	0.0062	CEVJJ	0.0675	CEVVJ	0.1277	CEVJJ	0.0111
SVVJ	0.0012	SVVJ	0.0009	*****	*****	SVJJ	0.0105
CEVVJ	0.0005	CEVVJ	0.0007	SVVJ	0.0155	CEVVJ	0.0078

Table 20: **Simulated LRMCS-**max**.** This table exhibits the LRMCS-max for the simulated experiment. Each column refers to a sample benchmark, which are arranged in block rows, as indicated by each row header. Each column contains the output of the MCS test, indicating the model label, the model confidence set cut-off, represented by an asterisk line and the model ranking achieved within each set by means of the p-values. The confidence level is at 10%. In this fundamental exercise of the simulated experiment, the established max-MCS test cannot offer extensive discrimination among the model set, which is achieved to a certain extent when considering the p-value ranking. The comments to this table are in Section 3.3.2.

Benchmark samples: SV, SVVJ, SVXJ, SVJJ							
SHBVJ	0.6437	SVXJ	0.6105	CEVXJ	0.8532	CEVXJ	0.7756
CEV	0.6249	SV	0.6041	SVJJ	0.7883	SVXJ	0.7096
SHAVJ	0.6069	CEV	0.6037	CEVJJ	0.7801	CEVJJ	0.7058
SVVJ	0.5637	SVJJ	0.5890	SVXJ	0.6846	SVJJ	0.6541
CSHB	0.5555	CEVXJ	0.5515	SHA	0.4228	CSHAVJ	0.3807
CSHAVJ	0.5303	SHA	0.5509	SHB	0.3713	CSHA	0.2828
SHA	0.5260	CEVVJ	0.5296	CSHBVJ	0.3167	SHAVJ	0.2821
CEVJJ	0.5234	CSHA	0.5010	CSHAVJ	0.2873	SHA	0.2092
CSHBVJ	0.4726	CEVJJ	0.4977	SHAVJ	0.2548	*****	*****
SVJJ	0.4692	CSHAVJ	0.4951	SHBVJ	0.2409	SHB	0.1103
SHB	0.4608	SHAVJ	0.4509	*****	*****	SHBVJ	0.1061
CSHA	0.4519	CSHB	0.4506	CSHA	0.2169	CSHBVJ	0.0987
SVXJ	0.4466	SVVJ	0.3977	CSHB	0.1994	CSHB	0.0903
CEVVJ	0.4285	CSHBVJ	0.3947	SVVJ	0.1158	CEVVJ	0.0350
CEVXJ	0.4009	SHB	0.3933	CEV	0.1129	SV	0.0289
SV	0.2952	SHBVJ	0.3796	CEVVJ	0.0982	SVVJ	0.0270
*****	*****	*****	*****	SV	0.0819	CEV	0.0223
Benchmark samples: CEV, CEVVJ, CEVXJ, CEVJJ							
CSHA	0.5776	CEVXJ	0.6836	SVJJ	0.7632	CEVXJ	0.8036
CEVVJ	0.5743	CSHAVJ	0.6229	CEVJJ	0.7161	SVXJ	0.7634
SHAVJ	0.5531	CEV	0.6228	CEVXJ	0.5738	SVJJ	0.6976
CSHAVJ	0.5512	CSHA	0.6105	SHAVJ	0.3882	CEVJJ	0.6733
CSHB	0.5304	CEVJJ	0.5913	CSHAVJ	0.3478	CSHAVJ	0.3865
SHA	0.5283	SHA	0.5168	SHA	0.2109	CSHA	0.3526
CEVXJ	0.5208	SHAVJ	0.5019	*****	*****	SHAVJ	0.2363
CSHBVJ	0.5060	CSHBVJ	0.4926	SVXJ	0.6285	SHA	0.0868
CEVJJ	0.4956	CSHB	0.4724	CSHA	0.1930	*****	*****
SVJJ	0.4814	SHB	0.4563	CSHBVJ	0.1142	SHBVJ	0.1423
SHBVJ	0.4798	CEVVJ	0.4495	CEVVJ	0.1021	CSHBVJ	0.1051
CEV	0.4686	SVVJ	0.4412	SHB	0.0996	CEVVJ	0.0881
SHB	0.4659	SHBVJ	0.4382	CSHB	0.0993	CSHB	0.0861
SVVJ	0.4470	SVJJ	0.4313	SHBVJ	0.0942	CEV	0.0646
SV	0.4204	SV	0.3527	CEV	0.0842	SHB	0.0638
SVXJ	0.3995	SVXJ	0.3160	SV	0.0589	SVVJ	0.0531
*****	*****	*****	*****	SVVJ	0.0488	SV	0.0510
Benchmark samples: SHB, SHBVJ, CSHB, CSHBVJ							
CSHBVJ	0.7083	CSHBVJ	0.8163	CSHB	0.7903	CSHB	0.8122
CSHA	0.6512	CSHB	0.6916	CSHBVJ	0.7835	CSHBVJ	0.8116
CSHB	0.6132	SHBVJ	0.6514	SHBVJ	0.6673	SHB	0.6933
CEVXJ	0.5039	SVXJ	0.6201	SHB	0.5948	SHBVJ	0.5087
SHBVJ	0.4998	SHB	0.5760	SVXJ	0.5616	SVXJ	0.4504
SHB	0.4812	CEVXJ	0.4862	CEVXJ	0.3898	CEVXJ	0.3171
CSHAVJ	0.4516	SHA	0.3014	CSHAVJ	0.3699	SHAVJ	0.2186
SVXJ	0.3881	SHAVJ	0.2048	CEVJJ	0.1976	CEVJJ	0.1881
CEVJJ	0.2029	CSHAVJ	0.1522	SHAVJ	0.1453	*****	*****
*****	*****	*****	*****	*****	*****	CSHAVJ	0.1800
SHA	0.2565	CEVJJ	0.3058	SVJJ	0.2046	SHA	0.0963
SHAVJ	0.2433	SVJJ	0.2440	CSHA	0.0773	CSHA	0.0891
SVJJ	0.1178	CSHA	0.0943	SHA	0.0752	SVJJ	0.0784
CEV	0.0189	CEV	0.0200	SVVJ	0.0189	CEVVJ	0.0261
SV	0.0163	SV	0.0167	CEV	0.0185	CEV	0.0240
SVVJ	0.0116	SVVJ	0.0109	CEVVJ	0.0174	SV	0.0103
CEVVJ	0.0108	CEVVJ	0.0091	SV	0.0169	SVVJ	0.0083
Benchmark samples: SHA, SHAVJ, CSHA, CSHAVJ							
CSHA	0.7054	CSHA	0.7491	CSHA	0.7813	SHA	0.7390
SHA	0.6856	SHAVJ	0.7289	SHA	0.7727	CSHA	0.7242
SHB	0.5988	SHA	0.6826	SHAVJ	0.7678	SHAVJ	0.7233
CSHB	0.5866	CSHB	0.6534	SHB	0.6870	CSHAVJ	0.6401
SHAVJ	0.5718	SHBVJ	0.6163	CSHBVJ	0.6738	CSHB	0.6251
SHBVJ	0.5343	SHB	0.5909	SHBVJ	0.6633	SHB	0.5697
CSHBVJ	0.5175	CSHBVJ	0.5862	CSHB	0.6051	CSHBVJ	0.5642
CSHAVJ	0.2349	CSHAVJ	0.4188	CSHAVJ	0.4310	SHBVJ	0.5587
CEVXJ	0.0651	SV	0.2102	CEV	0.3556	SVXJ	0.2467
*****	*****	CEVXJ	0.2005	SV	0.2648	SV	0.2206
CEV	0.0748	CEV	0.0634	SVXJ	0.2343	CEV	0.1955
SV	0.0714	*****	*****	CEVJJ	0.2007	CEVXJ	0.1928
SVXJ	0.0679	SVXJ	0.1582	SVJJ	0.0630	*****	*****
CEVJJ	0.0351	SVJJ	0.0182	*****	*****	CEVVJ	0.0468
CEVVJ	0.0116	CEVJJ	0.0153	CEVXJ	0.2985	SVJJ	0.0348
SVVJ	0.0114	SVVJ	0.0108	CEVVJ	0.1350	CEVJJ	0.0336
SVJJ	0.0082	CEVVJ	0.0059	SVVJ	0.0968	SVVJ	0.0311

Table 21: **Simulated LRMCS-γ.** This table exhibits the LRMCS-γ with fixed $\gamma = 20\%$ for the simulated experiment. Each column refers to a sample benchmark, which are arranged in block rows, as indicated by each row header. Each column contains the output of the MCS test, indicating the model label, the model confidence set cut-off, represented by an asterisk line and the model ranking achieved within each set by means of the p-values. The confidence level is at 5%. When employing the LRMCS-γ, we are able to highlight distinctively the aliasing feature of the model set components. Disregarding the innermost affine models, whose behaviour can be reproduced interchangeably by the other models, we notice that the SD and SH classes can produce statistically indistinguishable likelihood ratio performance, as long as, for instance, SHAVJ and and SHBVJ enter the affine and CEV MCS, whereas the CEV, CEVXJ, SV and SVXJ are included in the majority of the SH MCS. The comments to this table are in Section 3.3.2.

Benchmark samples: SV, SVVJ, SVXJ, SVJJ							
SHBVJ	0.5441	SV	0.5070	CEVXJ	0.6112	CEVXJ	0.5822
CEV	0.4559	SVXJ	0.4930	SVJJ	0.3888	CEVJJ	0.4178
CSHB	0.4134	SVJJ	0.4864	SVXJ	0.3159	SVJJ	0.3638
SHAVJ	0.4111	CEV	0.4801	CEVJJ	0.3159	SVXJ	0.3166
CEVVJ	0.3931	CEVXJ	0.4426	SHA	0.0978	CSHAVJ	0.1311
SVJJ	0.3865	SHA	0.4272	SHAVJ	0.0932	SHA	0.0915
SHB	0.3837	SHAVJ	0.4154	SHB	0.0547	SHAVJ	0.0892
CEVJJ	0.3814	SVVJ	0.4045	SHBVJ	0.0501	CSHA	0.0810
SVVJ	0.3735	CEVJJ	0.3972	*****	*****	*****	*****
CSHBVJ	0.3728	CEVVJ	0.3942	CSHBVJ	0.0479	SHB	0.0450
SVXJ	0.3703	CSHAVJ	0.3828	CSHAVJ	0.0467	SHBVJ	0.0364
SHA	0.3558	CSHA	0.3704	CSHA	0.0108	CSHB	0.0323
CEVXJ	0.3208	CSHB	0.3133	CSHB	0.0107	CSHBVJ	0.0318
SV	0.3125	SHB	0.2855	SV	0.0045	CEVVJ	0.0014
CSHA	0.3031	CSHBVJ	0.2748	SVVJ	0.0035	SV	0.0009
CSHAVJ	0.2847	SHBVJ	0.2341	CEV	0.0006	CEV	0.0008
*****	*****	*****	*****	CEVVJ	0.0003	SVVJ	0.0005
Benchmark samples: CEV, CEVVJ, CEVXJ, CEVJJ							
CEVVJ	0.5186	CEVXJ	0.5484	SVJJ	0.5603	CEVXJ	0.5786
CSHA	0.4814	CEVVJ	0.4516	CEVJJ	0.4397	SVXJ	0.4214
SHAVJ	0.4635	CEV	0.4101	CEVXJ	0.3869	SVJJ	0.3260
CEV	0.4490	CEVJJ	0.4092	CSHAVJ	0.1622	CEVJJ	0.3110
CSHAVJ	0.4440	CSHAVJ	0.3673	SHAVJ	0.1574	CSHA	0.0660
CEVXJ	0.4408	SHAVJ	0.3586	SHA	0.1486	CSHAVJ	0.0614
SHA	0.4357	CSHA	0.3449	SVXJ	0.1013	SHAVJ	0.0592
CSHB	0.4338	SHA	0.3344	*****	*****	SHA	0.0509
SVJJ	0.4018	SHBVJ	0.3087	CSHB	0.0415	*****	*****
CEVJJ	0.3828	SHB	0.3035	SHB	0.0357	SV	0.0253
SVVJ	0.3794	SVJJ	0.2947	CSHBVJ	0.0344	SVVJ	0.0252
CSHBVJ	0.3650	SVVJ	0.2923	SHBVJ	0.0314	CEVVJ	0.0195
SHB	0.3629	SV	0.2552	SV	0.0154	SHBVJ	0.0147
SHBVJ	0.3618	CSHB	0.2470	SVVJ	0.0121	CEV	0.0078
SV	0.3586	CSHBVJ	0.2416	CSHA	0.0084	CSHB	0.0060
SVXJ	0.3426	SVXJ	0.1995	CEV	0.0064	CSHBVJ	0.0059
*****	*****	*****	*****	CEVVJ	0.0050	SHB	0.0039
Benchmark samples: SHB, SHBVJ, CSHB, CSHBVJ							
CSHA	0.5093	CSHBVJ	0.6550	CSHB	0.5339	CSHBVJ	0.5150
CSHBVJ	0.4907	SVXJ	0.3450	CSHBVJ	0.4662	CSHB	0.4850
CEVXJ	0.3207	SHBVJ	0.2179	SVXJ	0.2976	SHB	0.2978
CSHAVJ	0.2797	SHB	0.1961	SHBVJ	0.2490	SVXJ	0.1853
SHBVJ	0.2403	CSHB	0.1614	SHB	0.2010	SHBVJ	0.1587
CSHB	0.2346	CEVXJ	0.1499	CEVJJ	0.1157	CEVXJ	0.1472
SHB	0.2336	SHA	0.1454	CSHAVJ	0.1148	SHAVJ	0.0986
SVXJ	0.1757	SHAVJ	0.1052	CEVXJ	0.0761	CEVJJ	0.0924
CEVJJ	0.1302	CSHAVJ	0.0788	SHAVJ	0.0643	*****	*****
SHAVJ	0.0540	*****	*****	*****	*****	CSHAVJ	0.0384
SHA	0.0538	CEV	0.0055	SHA	0.0242	SVJJ	0.0178
*****	*****	CSHA	0.0051	CEV	0.0160	SHA	0.0129
SVJJ	0.0153	SV	0.0021	SVVJ	0.0128	CSHA	0.0104
CEV	0.0029	SVVJ	0.0013	CSHA	0.0109	CEVVJ	0.0071
SV	0.0012	CEVVJ	0.0008	CEVVJ	0.0099	SVVJ	0.0046
SVVJ	0.0002	SVJJ	0.0006	SV	0.0074	CEV	0.0043
CEVVJ	0.0001	CEVJJ	0.0003	SVJJ	0.0001	SV	0.0003
Benchmark samples: SHA, SHAVJ, CSHA, CSHAVJ							
CSHA	0.5156	CSHA	0.5054	CSHA	0.5662	SHA	0.5077
SHA	0.4844	SHAVJ	0.4946	SHAVJ	0.4338	SHAVJ	0.4923
SHB	0.3881	CSHB	0.3719	SHA	0.4248	CSHA	0.4390
CSHB	0.3840	SHBVJ	0.3533	SHB	0.3593	CSHB	0.3332
SHBVJ	0.3712	CSHBVJ	0.3477	CSHBVJ	0.3437	SHB	0.3285
CSHBVJ	0.3663	SHB	0.3074	SHBVJ	0.3406	CSHAVJ	0.3247
SHAVJ	0.2829	SHA	0.2893	CSHB	0.3101	CSHBVJ	0.3037
CSHAVJ	0.1006	CSHAVJ	0.1482	CSHAVJ	0.1398	SHBVJ	0.2766
*****	*****	*****	*****	CEVJJ	0.0601	SVXJ	0.1039
CEVXJ	0.0201	CEVXJ	0.0418	CEV	0.0534	CEVXJ	0.0767
SVXJ	0.0184	SV	0.0341	*****	*****	SV	0.0755
SV	0.0167	CEV	0.0325	SVXJ	0.0475	CEV	0.0742
CEV	0.0164	SVXJ	0.0260	SV	0.0434	*****	*****
CEVJJ	0.0094	SVJJ	0.0036	CEVXJ	0.0283	SVVJ	0.0005
SVJJ	0.0002	CEVJJ	0.0030	SVJJ	0.0190	CEVJJ	0.0004
SVVJ	0.0000	SVVJ	0.0000	CEVVJ	0.0047	SVJJ	0.0003
CEVVJ	0.0000	CEVVJ	0.0000	SVVJ	0.0004	CEVVJ	0.0002

Table 22: **Simulated LRMCS-t.** This table exhibits the LRMCS-t for the simulated experiment. Each column refers to a sample benchmark, which are arranged in block rows, as indicated by each row header. Each column contains the output of the MCS test, indicating the model label, the model confidence set cut-off, represented by an asterisk line and the model ranking achieved within each set by means of the p-values. The confidence level is at 5%. The test results are similar to those of the test in Tab. 21. The comments to this table are in Section 3.3.2.

Benchmark samples: SV, SVVJ, SVXJ, SVJJ							
CEVXJ	1	CEVJJ	1	SHBVJ	1	SHB	1
CEVJJ	1	SHBVJ	0.9999	SHB	1	SHBVJ	1
SVXJ	0.9925	SVJJ	0.9999	SVXJ	1	SVJJ	0.9978
SVJJ	0.9916	SVVJ	0.9999	CEVXJ	0.9999	CEVXJ	0.9972
SHBVJ	0.9139	CEVVJ	0.9943	CEVJJ	0.9994	SVXJ	0.9971
CSHBVJ	0.9088	CEVXJ	0.9577	CSHBVJ	0.9975	CEV	0.9839
CSHB	0.8487	CSHB	0.9281	SVJJ	0.9895	CEVVJ	0.9602
SHB	0.7776	CSHBVJ	0.8693	SHA	0.9759	CSHA	0.9281
SV	0.6018	CEV	0.8338	CSHAVJ	0.9653	CEVJJ	0.8736
CEVVJ	0.4915	SVXJ	0.8194	CSHA	0.9634	CSHBVJ	0.8658
CSHAVJ	0.3749	SHB	0.7012	CEV	0.9461	SHA	0.8416
SHAVJ	0.3735	CSHA	0.5750	CSHB	0.9397	CSHAVJ	0.7816
SHA	0.3489	SHA	0.5533	CEVVJ	0.9380	CSHB	0.7330
SVVJ	0.3419	SHAVJ	0.5377	SHAVJ	0.9155	SV	0.7311
CSHA	0.3214	SV	0.5352	SVVJ	0.7613	SHAVJ	0.7281
CEV	0.1006	CSHAVJ	0.5293	SV	0.1279	SVVJ	0.3282
*****	*****	*****	*****	*****	*****	*****	*****
Benchmark samples: CEV, CEVVJ, CEVXJ, CEVJJ							
CEVXJ	1	CEVVJ	1	SHBVJ	1	SHB	1
CEVVJ	1	CEVXJ	1	CEVXJ	1	CEVJJ	1
CEVJJ	0.9982	SHA	1	CEVJJ	1	SHBVJ	0.9999
CEV	0.9845	SHBVJ	0.9995	SVJJ	1	SVJJ	0.9998
SVJJ	0.9661	SVJJ	0.9985	SVXJ	1	CEVXJ	0.9995
SVXJ	0.9630	SVXJ	0.9967	SHB	0.9890	CEVVJ	0.9994
SVVJ	0.4027	SVVJ	0.9325	CEVVJ	0.9809	SVXJ	0.9973
CSHBVJ	0.3897	SV	0.8703	CSHBVJ	0.9539	CEV	0.9952
SV	0.3848	CEV	0.8175	CSHAVJ	0.9536	CSHBVJ	0.9840
CSHB	0.3822	CSHB	0.7261	CSHA	0.9504	CSHA	0.9347
SHB	0.2725	CSHBVJ	0.6822	SHA	0.9299	SHA	0.9168
SHBVJ	0.2569	CEVJJ	0.2079	CSHB	0.9094	SV	0.9078
*****	*****	CSHA	0.1268	SHAVJ	0.8660	CSHAVJ	0.9030
SHAVJ	0.0288	SHAVJ	0.1134	SVVJ	0.6084	SVVJ	0.8959
CSHAVJ	0.0288	SHB	0.1064	SV	0.6000	CSHB	0.8824
CSHA	0.0288	CSHAVJ	0.0924	CEV	0.2841	SHAVJ	0.8684
SHA	0.0272	*****	*****	*****	*****	*****	*****
Benchmark samples: SHB, SHBVJ, CSHB, CSHBVJ							
CSHBVJ	1	CSHBVJ	1	CSHBVJ	1	CSHBVJ	1
CSHB	1	SHBVJ	1	SVJJ	1	SVJJ	1
SHBVJ	1	SHB	1	SHBVJ	1	SHBVJ	1
CEVXJ	1	CSHB	1	SHB	1	SHB	1
SHB	1	CEVJJ	1	CSHB	1	CSHB	1
SHA	1	CEVXJ	1	CEVXJ	1	CSHA	1
CEVJJ	1	CSHA	1	CEVJJ	1	CSHAVJ	1
SVXJ	1	SHA	1	SVXJ	0.9997	SHA	1
CSHAVJ	1	SHAVJ	1	CSHA	0.9967	CEVJJ	1
SHAVJ	1	CSHAVJ	1	CSHAVJ	0.9958	SHAVJ	0.9999
CSHA	0.9999	SVXJ	1	SHA	0.9949	CEVXJ	0.9999
SVJJ	0.9990	SVJJ	0.9962	SHAVJ	0.9936	SVXJ	0.9972
CEV	0.7836	CEVVJ	0.8670	SV	0.9456	SV	0.9267
CEVVJ	0.7834	CEV	0.8252	CEV	0.9417	CEV	0.9190
SV	0.6914	SV	0.8202	CEVVJ	0.9245	CEVVJ	0.8840
SVVJ	0.2135	SVVJ	0.2284	SVVJ	0.2580	SVVJ	0.8576
*****	*****	*****	*****	*****	*****	*****	*****
Benchmark samples: SHA, SHAVJ, CSHA, CSHAVJ							
CEVJJ	1	CEVJJ	1	CEVJJ	1	CEVVJ	1
CSHBVJ	0.9939	CEVVJ	0.9984	SVJJ	1	SVJJ	1
SVJJ	0.9938	SHB	0.9781	SVXJ	0.9950	SHB	0.9947
SHBVJ	0.9896	CSHB	0.9778	CSHBVJ	0.9484	CSHB	0.9940
SHB	0.9890	SV	0.9631	SHB	0.9434	SHAVJ	0.9933
CSHB	0.9807	CEV	0.9561	CSHB	0.9368	SHA	0.9929
SVVJ	0.9790	SVVJ	0.9422	SHA	0.9149	CSHA	0.9929
CEV	0.9625	SHBVJ	0.9160	CEVVJ	0.8861	CSHAVJ	0.9902
SHAVJ	0.9337	CSHBVJ	0.9047	CEV	0.8774	SHBVJ	0.9844
CSHA	0.9187	SVJJ	0.8961	SVVJ	0.8692	CSHBVJ	0.9642
SHA	0.9113	SHA	0.8494	SV	0.8619	SV	0.7679
CEVVJ	0.9043	CSHA	0.8095	SHBVJ	0.8593	SVVJ	0.7337
CSHAVJ	0.8644	SHAVJ	0.7697	CSHA	0.8531	CEV	0.6902
SV	0.3434	CSHAVJ	0.7189	SHAVJ	0.8265	SVXJ	0.1856
SVXJ	0.2678	SVXJ	0.0521	CSHAVJ	0.7872	CEVXJ	0.1807
*****	*****	*****	*****	CEVXJ	0.0658	*****	*****
CEVXJ	0.0166	CEVXJ	0.0001	*****	*****	CEVJJ	0.0140

Table 23: **Simulated LCMCS-**max**.** This table exhibits the LCMCS-max for the simulated experiment. Each column refers to a sample benchmark, which are arranged in block rows, as indicated by each row header. Each column contains the output of the MCS test, indicating the model label, the model confidence set cut-off, represented by an asterisk line and the model ranking achieved within each set by means of the p-values. The confidence level is at 5%. The test results for the latent factor estimation exhibit wide equivalence amongst the model set. The comments to this table are in Section 3.3.2.

Benchmark samples: SV, SVVJ, SVXJ, SVJJ							
CEVJJ	0.9305	CEVJJ	0.8792	SHBVJ	0.7870	SHB	0.8550
CEVXJ	0.9055	SVJJ	0.7426	SHB	0.7851	SHBVJ	0.7587
SVXJ	0.8503	CEVXJ	0.7369	CSHBVJ	0.7402	SVJJ	0.7140
SVJJ	0.8207	SHBVJ	0.7188	SVXJ	0.6775	CSHBVJ	0.6568
SV	0.6475	SVVJ	0.6985	CEVJJ	0.6127	CEVJJ	0.6081
CEVVJ	0.5635	CEVVJ	0.6499	CSHB	0.6114	SVXJ	0.5710
SHBVJ	0.5380	CSHBVJ	0.5759	CEVXJ	0.5903	CEVXJ	0.5461
SVVJ	0.4779	CEV	0.5463	SVJJ	0.5667	CSHA	0.4867
CSHBVJ	0.4558	SVXJ	0.4877	SHA	0.5076	CSHB	0.4749
CEV	0.4187	SHB	0.4675	CSHAVJ	0.4929	SHA	0.4574
CSHB	0.3700	CSHB	0.4390	CSHA	0.4535	CSHAVJ	0.4446
SHB	0.3103	CSHA	0.1813	SHAVJ	0.3732	SHAVJ	0.4054
CSHAVJ	0.2345	SHA	0.1392	CEV	0.3208	CEV	0.3931
SHAVJ	0.2065	SHAVJ	0.1224	CEVVJ	0.2593	CEVVJ	0.3135
SHA	0.1530	CSHAVJ	0.1148	SVVJ	0.1764	SV	0.1821
CSHA	0.1174	*****	*****	SV	0.0454	SVVJ	0.1326
*****	*****	SV	0.3563	*****	*****	*****	*****
Benchmark samples: CEV, CEVVJ, CEVXJ, CEVJJ							
CEVXJ	0.9044	CEVVJ	0.8703	SHBVJ	0.8327	SHB	0.8596
CEVJJ	0.8266	CEVXJ	0.8126	SHB	0.7748	SHBVJ	0.7702
CEVVJ	0.7504	SHBVJ	0.6336	CEVXJ	0.7069	CEVJJ	0.7421
CEV	0.7347	CEV	0.5808	CSHBVJ	0.6646	CSHBVJ	0.7040
SVJJ	0.5177	SVJJ	0.3888	CSHB	0.5956	CEVXJ	0.6205
SVXJ	0.5013	SVVJ	0.1951	CEVJJ	0.5740	SVJJ	0.5534
CSHBVJ	0.3596	SV	0.0188	SVXJ	0.5069	CSHB	0.5026
SHBVJ	0.3498	*****	*****	SVJJ	0.5043	CEVVJ	0.4813
SVVJ	0.2548	CSHB	0.4394	CSHAVJ	0.3954	SVXJ	0.4689
SHB	0.1854	CSHBVJ	0.4361	CSHA	0.3777	CSHA	0.4388
SV	0.1155	SHB	0.4098	SHA	0.3634	SHAVJ	0.4094
*****	*****	SVXJ	0.3285	SHAVJ	0.2812	CSHAVJ	0.4025
CSHB	0.3032	CSHA	0.2336	CEVVJ	0.2721	SHA	0.3951
SHAVJ	0.1632	SHAVJ	0.2326	CEV	0.1507	CEV	0.3607
CSHAVJ	0.1537	SHA	0.2304	*****	*****	SV	0.1637
CSHA	0.1507	CSHAVJ	0.2212	SVVJ	0.0279	SVVJ	0.1272
SHA	0.1422	CEVJJ	0.0139	SV	0.0263	*****	*****
Benchmark samples: SHB, SHBVJ, CSHB, CSHBVJ							
CSHBVJ	0.6981	CSHBVJ	0.7101	CSHBVJ	0.7297	CSHBVJ	0.7446
SHBVJ	0.6737	SHBVJ	0.7068	SHBVJ	0.7111	SHBVJ	0.6803
CSHB	0.6503	SHB	0.6661	SVJJ	0.6889	SVJJ	0.6217
CEVXJ	0.6467	CSHB	0.6466	CSHB	0.6731	SHB	0.6181
SHB	0.6454	CEVXJ	0.6253	SHB	0.6551	CSHB	0.6152
SVXJ	0.6321	CEVJJ	0.6091	CEVXJ	0.6536	CEVXJ	0.6089
CEVJJ	0.6189	CSHA	0.5939	SVXJ	0.6160	CEVJJ	0.5984
SHA	0.6037	SHA	0.5865	CEVJJ	0.5536	CSHA	0.5654
CSHAVJ	0.5938	SHAVJ	0.5719	SHA	0.5088	SHA	0.5366
SHAVJ	0.5570	SVXJ	0.5380	CSHA	0.5024	CSHAVJ	0.5306
CSHA	0.5368	CSHAVJ	0.5319	CSHAVJ	0.4466	SVXJ	0.5281
SVJJ	0.5328	SVJJ	0.5143	SHAVJ	0.4430	SHAVJ	0.4805
CEVVJ	0.2281	CEVVJ	0.2652	CEV	0.2763	CEV	0.2571
CEV	0.1648	SVVJ	0.1882	SV	0.2359	SV	0.2523
SVVJ	0.1331	CEV	0.1549	CEVVJ	0.2165	CEVVJ	0.2347
SV	0.0847	SV	0.0912	SVVJ	0.0893	SVVJ	0.1274
*****	*****	*****	*****	*****	*****	*****	*****
Benchmark samples: SHA, SHAVJ, CSHA, CSHAVJ							
CEVJJ	0.8583	CEVJJ	0.8814	SVJJ	0.8554	CEVVJ	0.8261
SVJJ	0.6651	CEVVJ	0.7450	CEVJJ	0.8476	SVJJ	0.7171
SVVJ	0.5975	SVJJ	0.6765	CEVVJ	0.6870	SVVJ	0.7169
SHBVJ	0.5588	SVVJ	0.6212	SVXJ	0.6360	CEV	0.5075
CEVVJ	0.5333	CSHBVJ	0.5163	SVVJ	0.6217	SHBVJ	0.4688
CSHB	0.5254	SHBVJ	0.5052	CSHBVJ	0.5189	CSHBVJ	0.4588
SHB	0.5004	CEV	0.4840	SHBVJ	0.5039	SV	0.4287
CSHBVJ	0.4975	SV	0.4491	CEV	0.4779	SHA	0.4145
CSHA	0.4619	CSHB	0.3922	SHB	0.3994	CSHA	0.4112
SHAVJ	0.4617	SHB	0.3897	SV	0.3851	SHAVJ	0.4088
SHA	0.4568	SHAVJ	0.3464	CSHB	0.3651	CSHAVJ	0.4006
CSHAVJ	0.4366	SHA	0.3376	CSHA	0.3160	CSHB	0.3895
CEV	0.4320	CSHA	0.3329	SHAVJ	0.3066	SHB	0.3517
SV	0.2861	CSHAVJ	0.3226	SHA	0.2969	*****	*****
SVXJ	0.2288	*****	*****	CSHAVJ	0.2824	CEVJJ	0.4520
*****	*****	SVXJ	0.0150	*****	*****	CEVXJ	0.0430
CEVXJ	0.0022	CEVXJ	0.0049	CEVXJ	0.0054	SVXJ	0.0202

Table 24: **Simulated LCMCS-γ.** This table exhibits the LCMCS-γ with $\gamma = 10\%$ for the simulated experiment. Each column refers to a sample benchmark, which are arranged in block rows, as indicated by each row header. Each column contains the output of the MCS test, indicating the model label, the model confidence set cut-off, represented by an asterisk line and the model ranking achieved within each set by means of the p-values. The confidence level is at 5%. Considering the k, with the exception of CEV and CSHBVJ whereby $k = 2$ and CEVVJ whereby $k = 3$, all the model tests select $k = 1$. The comments to this table are in Section 3.3.2.

Benchmark samples: SV, SVVJ, SVXJ, SVJJ							
CEVXJ	0.5418	CEVJJ	0.7147	SHBVJ	0.5418	SHB	0.6186
CEVJJ	0.4582	SHBVJ	0.2853	SHB	0.4582	SHBVJ	0.3814
SVXJ	0.1894	SVJJ	0.2769	SVXJ	0.3967	SVJJ	0.2507
SVJJ	0.1859	SVVJ	0.2719	CEVXJ	0.3129	CEVXJ	0.2458
SHBVJ	0.1032	CEVVJ	0.1869	CEVJJ	0.2774	SVXJ	0.2451
CSHBVJ	0.1009	CEVXJ	0.1206	CSHBVJ	0.2440	CEV	0.1933
CSHB	0.0795	CSHB	0.1005	SVJJ	0.1991	CEVVJ	0.1567
SHB	0.0629	CSHBVJ	0.0770	SHA	0.1710	CSHA	0.1300
*****	*****	CEV	0.0673	CSHAVJ	0.1562	CEVJJ	0.1039
SV	0.0370	SVXJ	0.0640	CSHA	0.1539	CSHBVJ	0.1008
CEVVJ	0.0265	*****	*****	CEV	0.1367	SHA	0.0927
CSHAVJ	0.0177	SHB	0.0437	CSHB	0.1319	CSHAVJ	0.0760
SHAVJ	0.0176	CSHA	0.0294	CEVVJ	0.1309	CSHB	0.0658
SHA	0.0160	SHA	0.0274	SHAVJ	0.1168	SV	0.0654
SVVJ	0.0156	SHAVJ	0.0260	SVVJ	0.0663	SHAVJ	0.0649
CSHA	0.0143	SV	0.0258	*****	*****	*****	*****
CEV	0.0033	CSHAVJ	0.0253	SV	0.0043	SVVJ	0.0172
Benchmark samples: CEV, CEVVJ, CEVXJ, CEVJJ							
CEVXJ	0.6208	CEVVJ	0.5625	SHBVJ	0.5634	SHB	0.6848
CEVVJ	0.3792	CEVXJ	0.4375	CEVXJ	0.4366	CEVJJ	0.3152
CEVJJ	0.3069	SHA	0.4282	CEVJJ	0.3381	SHBVJ	0.2771
CEV	0.2376	SHBVJ	0.2324	SVJJ	0.3223	SVJJ	0.2696
SVJJ	0.2045	SVJJ	0.2087	SVXJ	0.3108	CEVXJ	0.2523
SVXJ	0.2011	SVXJ	0.1926	SHB	0.1764	CEVVJ	0.2450
*****	*****	SVVJ	0.1014	CEVVJ	0.1585	SVXJ	0.2059
SVVJ	0.0331	SV	0.0774	CSHBVJ	0.1269	CEV	0.1887
CSHBVJ	0.0315	CEV	0.0644	CSHAVJ	0.1267	CSHBVJ	0.1499
SV	0.0309	*****	*****	CSHA	0.1239	CSHA	0.1016
CSHB	0.0306	CSHB	0.0483	SHA	0.1106	SHA	0.0926
SHB	0.0191	CSHBVJ	0.0424	CSHB	0.0998	SV	0.0888
SHBVJ	0.0177	CEVJJ	0.0070	SHAVJ	0.0838	CSHAVJ	0.0867
SHAVJ	0.0010	CSHA	0.0038	*****	*****	SVVJ	0.0839
CSHAVJ	0.0009	SHAVJ	0.0033	SVVJ	0.0372	CSHB	0.0794
CSHA	0.0009	SHB	0.0031	SV	0.0362	SHAVJ	0.0751
SHA	0.0008	CSHAVJ	0.0026	CEV	0.0115	*****	*****
Benchmark samples: SHB, SHBVJ, CSHB, CSHBVJ							
CSHBVJ	0.5543	CSHBVJ	0.5219	CSHBVJ	0.5203	CSHBVJ	0.5704
CSHB	0.4457	SHBVJ	0.4781	SVJJ	0.4797	SVJJ	0.4296
SHBVJ	0.4456	SHB	0.4317	SHBVJ	0.4621	SHBVJ	0.3976
CEVXJ	0.4039	CSHB	0.4268	SHB	0.4077	SHB	0.3906
SHB	0.4015	CEVJJ	0.3745	CSHB	0.4026	CSHB	0.3871
SHA	0.3952	CEVXJ	0.3694	CEVXJ	0.4003	CSHA	0.3289
CEVJJ	0.3793	CSHA	0.3578	CEVJJ	0.3496	CSHAVJ	0.3227
SVXJ	0.3768	SHA	0.3399	SVXJ	0.2861	SHA	0.3178
CSHAVJ	0.3676	SHAVJ	0.3373	CSHA	0.2281	CEVJJ	0.3100
SHAVJ	0.3415	CSHAVJ	0.3252	CSHAVJ	0.2224	SHAVJ	0.2872
CSHA	0.2961	SVXJ	0.3045	SHA	0.2159	CEVXJ	0.2788
SVJJ	0.2582	SVJJ	0.2248	SHAVJ	0.2096	SVXJ	0.2148
CEV	0.0701	CEVVJ	0.0919	SV	0.1287	SV	0.1088
CEVVJ	0.0700	CEV	0.0789	CEV	0.1257	CEV	0.1049
SV	0.0524	SV	0.0775	CEVVJ	0.1144	CEVVJ	0.0899
*****	*****	*****	*****	*****	*****	SVVJ	0.0810
SVVJ	0.0084	SVVJ	0.0091	SVVJ	0.0099	*****	*****
Benchmark samples: SHA, SHAVJ, CSHA, CSHAVJ							
CEVJJ	0.7768	CEVJJ	0.7358	CEVJJ	0.5399	CEVVJ	0.6558
CSHBVJ	0.2232	CEVVJ	0.2642	SVJJ	0.4601	SVJJ	0.3442
SVJJ	0.2224	SHB	0.1776	SVXJ	0.2186	SHB	0.2195
SHBVJ	0.2038	CSHB	0.1771	CSHBVJ	0.1376	CSHB	0.2149
SHB	0.2018	SV	0.1572	SHB	0.1342	SHAVJ	0.2115
CSHB	0.1816	CEV	0.1492	CSHB	0.1292	SHA	0.2098
SVVJ	0.1785	SVVJ	0.1368	SHA	0.1156	CSHA	0.2098
CEV	0.1565	SHBVJ	0.1202	CEVVJ	0.1024	CSHAVJ	0.1986
SHAVJ	0.1328	CSHBVJ	0.1143	CEV	0.0989	SHBVJ	0.1816
CSHA	0.1236	SVJJ	0.1107	SVVJ	0.0958	CSHBVJ	0.1499
SHA	0.1190	SHA	0.0928	SV	0.0933	SV	0.0676
CEVVJ	0.1154	CSHA	0.0814	SHBVJ	0.0925	SVVJ	0.0610
CSHAVJ	0.0985	SHAVJ	0.0718	CSHA	0.0904	CEV	0.0537
*****	*****	CSHAVJ	0.0618	SHAVJ	0.0824	*****	*****
SV	0.0177	*****	*****	CSHAVJ	0.0727	SVXJ	0.0074
SVXJ	0.0124	SVXJ	0.0016	*****	*****	CEVXJ	0.0071
CEVXJ	0.0004	CEVXJ	0.0000	CEVXJ	0.0021	CEVJJ	0.0003

Table 25: **Simulated LCMCS-t.** This table exhibits the LCMCS-t for the simulated experiment. Each column refers to a sample benchmark, which are arranged in block rows, as indicated by each row header. Each column contains the output of the MCS test, indicating the model label, the model confidence set cut-off, represented by an asterisk line and the model ranking achieved within each set by means of the p-values. The confidence level is at 5%. In this experiment it is interesting to notice some incoherence of the LCMCS-t, whereby, for the innermost segment of the affine model set, the benchmark is either low ranked or even excluded from the MCS. The comments to this table are in Section 3.3.2.

Benchmark samples: SV, SVVJ, SVXJ, SVJJ								
SV	⋆	⋆	–	↘	–	↘	–	↘
SVVJ	↗	–	⋆	⋆	–	↘	-0.0213	0.0012
SVXJ	↗	–	↗	–	⋆	⋆	↗	–
SVJJ	↗	–	-0.0011	0.0212	–	↘	⋆	⋆
CEV	↗	–	↗	–	-0.0018	0.0132	↗	–
CEVVJ	↗	–	↗	–	-0.0032	0.0095	↗	–
CEVXJ	↗	–	↗	–	↗	–	↗	–
CEVJJ	↗	–	↗	–	↗	–	↗	–
SHB	↗	–	↗	–	↗	–	↗	–
SHBVJ	↗	–	↗	–	↗	–	↗	–
CSHB	↗	–	↗	–	↗	–	↗	–
CSHBVJ	↗	–	↗	–	↗	–	↗	–
SHA	↗	–	↗	–	-0.0074	0.0097	-0.0023	0.0150
SHAVJ	↗	–	↗	–	-0.0193	0.0011	-0.0138	0.0064
CSHA	↗	–	↗	–	↗	–	↗	–
CSHAVJ	↗	–	↗	–	↗	–	↗	–
Benchmark samples: CEV, CEVVJ, CEVXJ, CEVJJ								
SV	–	↘	–	↘	–	↘	–	↘
SVVJ	–	↘	–	↘	–	↘	–	↘
SVXJ	-0.0146	0.0024	-0.0099	0.0030	–	↘	-0.0112	0.0003
SVJJ	–	↘	–	↘	–	↘	–	↘
CEV	⋆	⋆	-0.0051	0.0077	-0.0074	0.0069	-0.0113	0.0116
CEVVJ	-0.0083	0.0054	⋆	⋆	-0.0065	0.0016	-0.0071	0.0045
CEVXJ	-0.0072	0.0074	-0.0014	0.0060	⋆	⋆	-0.0037	0.0050
CEVJJ	-0.0114	0.0105	-0.0039	0.0063	-0.0047	0.0034	⋆	⋆
SHB	-0.0039	0.0231	↗	–	-0.0022	0.0192	-0.0016	0.0205
SHBVJ	-0.0024	0.0246	↗	–	-0.0010	0.0211	-0.0003	0.0221
CSHB	-0.0031	0.0238	↗	–	-0.0017	0.0200	-0.0014	0.0217
CSHBVJ	-0.0035	0.0223	↗	–	-0.0019	0.0186	-0.0016	0.0203
SHA	–	↘	-0.0112	0.0049	-0.0135	0.0035	-0.0174	0.0087
SHAVJ	–	↘	–	↘	–	↘	-0.0312	0.0008
CSHA	-0.0005	0.0290	↗	–	↗	–	↗	–
CSHAVJ	-0.0064	0.0266	↗	–	-0.0025	0.0203	↗	–
Benchmark samples: SHB, SHBVJ, CSHB, CSHBVJ								
SV	–	↘	–	↘	–	↘	–	↘
SVVJ	–	↘	–	↘	–	↘	–	↘
SVXJ	–	↘	–	↘	–	↘	–	↘
SVJJ	–	↘	–	↘	–	↘	–	↘
CEV	-0.0223	0.0032	-0.0231	0.0014	-0.0237	0.0028	-0.0214	0.0030
CEVVJ	–	↘	–	↘	–	↘	–	↘
CEVXJ	-0.0189	0.0018	–	↘	-0.0199	0.0017	-0.0182	0.0019
CEVJJ	-0.0195	0.0007	–	↘	-0.0212	0.0006	-0.0192	0.0007
SHB	⋆	⋆	–	↘	-0.0016	0.0001	-0.0004	0.0008
SHBVJ	↗	–	⋆	⋆	-0.0010	0.0021	↗	–
CSHB	-0.0001	0.0015	-0.0019	0.0008	⋆	⋆	0.0000	0.0017
CSHBVJ	-0.0008	0.0004	–	↘	-0.0017	0.0001	⋆	⋆
SHA	–	↘	–	↘	–	↘	–	↘
SHAVJ	–	↘	–	↘	–	↘	–	↘
CSHA	-0.0003	0.0082	-0.0010	0.0065	-0.0018	0.0084	-0.0002	0.0088
CSHAVJ	-0.0087	0.0075	-0.0095	0.0055	-0.0104	0.0078	-0.0087	0.0083
Benchmark samples: SHA, SHAVJ, CSHA, CSHAVJ								
SV	–	↘	–	↘	–	↘	–	↘
SVVJ	–	↘	–	↘	–	↘	–	↘
SVXJ	-0.0101	0.0080	-0.0007	0.0187	–	↘	–	↘
SVJJ	-0.0164	0.0033	-0.0069	0.0141	–	↘	–	↘
CEV	↗	–	↗	–	-0.0284	0.0001	-0.0268	0.0063
CEVVJ	-0.0055	0.0112	↗	–	–	↘	–	↘
CEVXJ	-0.0030	0.0128	↗	–	–	↘	-0.0205	0.0027
CEVJJ	-0.0072	0.0160	↗	–	–	↘	–	↘
SHB	↗	–	↗	–	-0.0083	0.0004	-0.0080	0.0092
SHBVJ	↗	–	↗	–	-0.0069	0.0013	-0.0068	0.0103
CSHB	↗	–	↗	–	-0.0082	0.0017	-0.0080	0.0107
CSHBVJ	↗	–	↗	–	-0.0087	0.0003	-0.0086	0.0093
SHA	⋆	⋆	↗	–	–	↘	-0.0322	0.0033
SHAVJ	–	↘	⋆	⋆	–	↘	–	↘
CSHA	↗	–	↗	–	⋆	⋆	-0.0003	0.0097
CSHAVJ	-0.0027	0.0311	↗	–	-0.0094	0.0000	⋆	⋆

Table 26: **Market Data LRMHT.** This table exhibits the LRMHT for the market data experiment. Each pair of columns for each block row represents an MHT, showing the final set output of balanced step-down algorithm, benchmarked to the model indicated with a double star. In the market data experiment we lack of the knowledge of the DGP process, therefore we iterate the benchmarking exercise across the set of models, to produce a complete model comparison. The rejected models do not provide a confidence interval, whereas the corresponding row is filled with a north-east or a south-east arrow, whether the corresponding model is, respectively, superior or inferior to the benchmark model. In this test the confidence level for each tail is 5% and the k-FWER=3. With this test, the empirical performance of the model set is analysed. Relevant information is represented by the performance of the SV and SVVJ models, that are in general inferior, ruling out the core of the affine model set. Remarkable is the performance of the CEV model, which is at least equivalent to any other model. The CSH and CSHAVJ exhibit the best performances. It is interesting to notice that the inclusion of a VJ component worsen the performance of models such as CEV, SHB and SHA.

Benchmark samples: SV, SVVJ, SVXJ, SVJJ								
SV	⋆	⋆	↗	–	–	↘	–	↘
SVVJ	–	↘	⋆	⋆	–	↘	–	↘
SVXJ	↗	–	↗	–	⋆	⋆	-0.0085	0.0391
SVJJ	↗	–	↗	–	-0.0440	0.0101	⋆	⋆
CEV	–	↘	–	↘	–	↘	–	↘
CEVVJ	–	↘	–	↘	–	↘	–	↘
CEVXJ	↗	–	↗	–	-0.0810	0.1353	-0.0478	0.1385
CEVJJ	↗	–	↗	–	-0.0131	0.1293	↗	–
SHB	↗	–	↗	–	–	↘	–	↘
SHBVJ	↗	–	↗	–	-0.7364	0.0167	–	↘
CSHB	↗	–	↗	–	–	↘	–	↘
CSHBVJ	↗	–	↗	–	–	↘	–	↘
SHA	↗	–	↗	–	↗	–	↗	–
SHAVJ	↗	–	↗	–	-0.0099	0.2269	↗	–
CSHA	–	↘	–	↘	–	↘	–	↘
CSHAVJ	–	↘	–	↘	–	↘	–	↘
Benchmark samples: CEV, CEVVJ, CEVXJ, CEVJJ								
SV	↗	–	↗	–	–	↘	–	↘
SVVJ	↗	–	↗	–	–	↘	–	↘
SVXJ	↗	–	↗	–	-0.1272	0.0739	-0.1278	0.0053
SVJJ	↗	–	↗	–	-0.1385	0.0448	–	↘
CEV	⋆	⋆	↗	–	–	↘	–	↘
CEVVJ	–	↘	⋆	⋆	–	↘	–	↘
CEVXJ	↗	–	↗	–	⋆	⋆	-0.0749	0.0190
CEVJJ	↗	–	↗	–	-0.0190	0.0735	⋆	⋆
SHB	↗	–	↗	–	–	↘	–	↘
SHBVJ	↗	–	↗	–	–	↘	–	↘
CSHB	↗	–	↗	–	–	↘	–	↘
CSHBVJ	↗	–	↗	–	–	↘	–	↘
SHA	↗	–	↗	–	↗	–	-0.0191	0.1477
SHAVJ	↗	–	↗	–	↗	–	-0.0248	0.1275
CSHA	–	↘	–	↘	–	↘	–	↘
CSHAVJ	–	↘	–	↘	–	↘	–	↘
Benchmark samples: SHB, SHBVJ, CSHB, CSHBVJ								
SV	–	↘	–	↘	–	↘	–	↘
SVVJ	–	↘	–	↘	–	↘	–	↘
SVXJ	↗	–	-0.0032	0.7157	↗	–	↗	–
SVJJ	↗	–	-0.0055	0.6786	↗	–	↗	–
CEV	–	↘	–	↘	–	↘	–	↘
CEVVJ	–	↘	–	↘	–	↘	–	↘
CEVXJ	↗	–	↗	–	↗	–	↗	–
CEVJJ	↗	–	↗	–	↗	–	↗	–
SHB	⋆	⋆	–	↘	↗	–	↗	–
SHBVJ	↗	–	⋆	⋆	↗	–	↗	–
CSHB	–	↘	–	↘	⋆	⋆	-0.0288	0.0386
CSHBVJ	–	↘	–	↘	-0.0379	0.0280	⋆	⋆
SHA	↗	–	↗	–	↗	–	↗	–
SHAVJ	↗	–	↗	–	↗	–	↗	–
CSHA	–	↘	–	↘	–	↘	–	↘
CSHAVJ	–	↘	–	↘	–	↘	–	↘
Benchmark samples: SHA, SHAVJ, CSHA, CSHAVJ								
SV	–	↘	–	↘	↗	–	↗	–
SVVJ	–	↘	–	↘	↗	–	↗	–
SVXJ	–	↘	-0.2222	0.0050	↗	–	↗	–
SVJJ	–	↘	–	↘	↗	–	↗	–
CEV	–	↘	–	↘	↗	–	↗	–
CEVVJ	–	↘	–	↘	↗	–	↗	–
CEVXJ	–	↘	–	↘	↗	–	↗	–
CEVJJ	-0.1533	0.0204	-0.1308	0.0271	↗	–	↗	–
SHB	–	↘	–	↘	↗	–	↗	–
SHBVJ	–	↘	–	↘	↗	–	↗	–
CSHB	–	↘	–	↘	↗	–	↗	–
CSHBVJ	–	↘	–	↘	↗	–	↗	–
SHA	⋆	⋆	-0.0547	0.0773	↗	–	↗	–
SHAVJ	-0.0761	0.0547	⋆	⋆	↗	–	↗	–
CSHA	–	↘	–	↘	⋆	⋆	↗	–
CSHAVJ	–	↘	–	↘	–	↘	⋆	⋆

Table 27: **Market Data TGMHT.** This table exhibits the TGMHT for the market data experiment. Each pair of columns for each block row represents an MHT, showing the final set output of balanced step-down algorithm, benchmarked to the model indicated with a double star. In the market data experiment we lack of the knowledge of the DGP process, therefore we iterate the benchmarking exercise across the set of models, to produce a complete model comparison. The rejected models do not provide a confidence interval, whereas the corresponding row is filled with a north-east or a south-east arrow, whether the corresponding model is, respectively, superior or inferior to the benchmark model. In this test the confidence level for each tail is 1% and the k-FWER=2. With the TGMHT, the circulation of the benchmark across the model set and the relative model comparison testing shows that, with respect to this measure, the CEVXJ, CEVJJ, SHA and SHAVJ are the top performing.

Benchmark samples: SV, SVVJ, SVXJ, SVJJ								
SV	⋆	⋆	-0.0294	0.1829	-0.1229	0.3825	-0.1537	0.3749
SVVJ	-0.1835	0.0294	⋆	⋆	-0.2131	0.3354	-0.2459	0.3209
SVXJ	-0.4019	0.1240	-0.3437	0.2093	⋆	⋆	-0.0763	0.0528
SVJJ	-0.3800	0.1573	-0.3214	0.2459	-0.0553	0.0739	⋆	⋆
CEV	–	↘	-0.2805	0.0255	-0.4090	0.2196	-0.4277	0.2417
CEVVJ	-0.4236	0.0082	-0.3353	0.0348	-0.4136	0.2297	-0.4488	0.2630
CEVXJ	-0.3021	0.1818	-0.2620	0.2546	-0.0151	0.1598	-0.0310	0.1460
CEVJJ	-0.4399	0.1183	-0.3931	0.2132	-0.1289	0.0711	-0.1488	0.0623
SHB	↗	–	↗	–	↗	–	↗	–
SHBVJ	↗	–	↗	–	↗	–	↗	–
CSHB	↗	–	↗	–	↗	–	↗	–
CSHBVJ	↗	–	↗	–	↗	–	↗	–
SHA	↗	–	↗	–	↗	–	↗	–
SHAVJ	↗	–	↗	–	↗	–	↗	–
CSHA	-0.2083	0.5025	-0.1386	0.5426	-0.0747	0.6624	-0.1182	0.6842
CSHAVJ	-0.2075	0.5403	-0.1326	0.5891	-0.1048	0.7022	-0.1279	0.7237
Benchmark samples: CEV, CEVVJ, CEVXJ, CEVJJ								
SV	↗	–	-0.0054	0.4163	-0.1812	0.3012	-0.1180	0.4327
SVVJ	-0.0219	0.2703	-0.0305	0.3247	-0.2659	0.2585	-0.2165	0.3934
SVXJ	-0.2191	0.3709	-0.2350	0.4010	-0.1646	0.0144	-0.0772	0.1289
SVJJ	-0.2373	0.4053	-0.2447	0.4343	-0.1470	0.0310	-0.0628	0.1494
CEV	⋆	⋆	-0.0907	0.1315	-0.4567	0.1551	-0.3925	0.2701
CEVVJ	-0.1293	0.0879	⋆	⋆	-0.4644	0.1648	-0.3807	0.2684
CEVXJ	-0.1439	0.4326	-0.1436	0.4440	⋆	⋆	-0.0160	0.2042
CEVJJ	-0.2546	0.3759	-0.2630	0.3683	-0.2044	0.0150	⋆	⋆
SHB	↗	–	↗	–	↗	–	↗	–
SHBVJ	↗	–	↗	–	↗	–	↗	–
CSHB	↗	–	↗	–	↗	–	↗	–
CSHBVJ	↗	–	↗	–	↗	–	↗	–
SHA	↗	–	↗	–	↗	–	↗	–
SHAVJ	↗	–	↗	–	↗	–	↗	–
CSHA	↗	–	↗	–	-0.1303	0.6300	-0.0197	0.6956
CSHAVJ	↗	–	↗	–	-0.1661	0.6577	-0.0548	0.7216
Benchmark samples: SHB, SHBVJ, CSHB, CSHBVJ								
SV	–	↘	–	↘	–	↘	–	↘
SVVJ	–	↘	–	↘	–	↘	–	↘
SVXJ	–	↘	–	↘	–	↘	–	↘
SVJJ	–	↘	–	↘	–	↘	–	↘
CEV	–	↘	–	↘	–	↘	–	↘
CEVVJ	–	↘	–	↘	–	↘	–	↘
CEVXJ	–	↘	–	↘	–	↘	–	↘
CEVJJ	–	↘	–	↘	–	↘	–	↘
SHB	⋆	⋆	↗	–	–	↘	-0.0934	0.0161
SHBVJ	–	↘	⋆	⋆	–	↘	–	↘
CSHB	↗	–	↗	–	⋆	⋆	-0.0200	0.0857
CSHBVJ	-0.0146	0.0930	↗	–	-0.0700	0.0082	⋆	⋆
SHA	-0.2908	0.0298	-0.1888	0.1811	–	↘	–	↘
SHAVJ	–	↘	-0.3224	0.0116	–	↘	–	↘
CSHA	–	↘	–	↘	–	↘	–	↘
CSHAVJ	–	↘	–	↘	–	↘	–	↘
Benchmark samples: SHA, SHAVJ, CSHA, CSHAVJ								
SV	–	↘	–	↘	-0.4918	0.1931	-0.5376	0.1888
SVVJ	–	↘	–	↘	-0.5377	0.1343	-0.5808	0.1213
SVXJ	–	↘	–	↘	-0.6691	0.0715	-0.7059	0.0792
SVJJ	–	↘	–	↘	-0.6790	0.1127	-0.7150	0.1074
CEV	–	↘	–	↘	–	↘	–	↘
CEVVJ	–	↘	–	↘	–	↘	–	↘
CEVXJ	–	↘	–	↘	-0.6130	0.1241	-0.6557	0.1293
CEVJJ	–	↘	–	↘	-0.6779	0.0126	-0.7169	0.0265
SHB	-0.0580	0.2992	↗	–	↗	–	↗	–
SHBVJ	-0.1992	0.1899	-0.0014	0.2981	↗	–	↗	–
CSHB	↗	–	↗	–	↗	–	↗	–
CSHBVJ	-0.0039	0.3203	↗	–	↗	–	↗	–
SHA	⋆	⋆	↗	–	↗	–	↗	–
SHAVJ	–	↘	⋆	⋆	↗	–	↗	–
CSHA	–	↘	–	↘	⋆	⋆	-0.1876	0.1481
CSHAVJ	–	↘	–	↘	-0.1490	0.1882	⋆	⋆

Table 28: **Market Data LRLCMHT.** This table exhibits the LRLCMHT for the market data experiment. Each pair of columns for each block row represents an MHT, showing the final set output of balanced step-down algorithm, benchmarked to the model indicated with a double star. In the market data experiment we lack of the knowledge of the DGP process, therefore we iterate the benchmarking exercise across the set of models, to produce a complete model comparison. The rejected models do not provide a confidence interval, whereas the corresponding row is filled with a north-east or a south-east arrow, whether the corresponding model is, respectively, superior or inferior to the benchmark model. In this test the confidence level for each tail is 1% and the k-FWER=2.

LRMCS-max		LRMCS-10%		LRMCS-50%		LRMCS-t	
CSHA	1	CSHA	0.9336	CSHA	0.9193	CSHA	0.8660
CSHB	0.8077	SHBVJ	0.6864	SHBVJ	0.6190	CSHB	0.1340
SHBVJ	0.7866	CSHB	0.5865	CSHB	0.4970	SHBVJ	0.1259
CEV	0.4901	CSHAVJ	0.4739	CSHAVJ	0.3684	CEV	0.0541
CSHAVJ	0.3264	CEV	0.1756	CEV	0.0964	*****	*****
CEVXJ	0.2216	CEVXJ	0.1440	*****	*****	CSHAVJ	0.0297
SHA	0.2200	*****	*****	SHB	0.3191	CEVXJ	0.0178
CSHBVJ	0.0981	CSHBVJ	0.4218	CSHBVJ	0.3184	SHA	0.0176
CEVJJ	0.0660	SHB	0.4215	CEVXJ	0.1440	CSHBVJ	0.0065
SHB	0.0584	CEVJJ	0.1317	CEVJJ	0.1005	CEVJJ	0.0041
*****	*****	CEVVJ	0.0623	CEVVJ	0.0519	SHB	0.0035
SVXJ	0.0188	SHA	0.0419	SVXJ	0.0335	SVXJ	0.0008
CEVVJ	0.0141	SVXJ	0.0279	SHA	0.0214	CEVVJ	0.0006
SVVJ	0.0034	SVJJ	0.0023	SVJJ	0.0027	SVVJ	0.0001
SHAVJ	0.0000	SHAVJ	0.0010	SHAVJ	0.0009	SHAVJ	0.0000
SV	0	SVVJ	0.0006	SVVJ	0.0007	SV	0.0000
SVJJ	0	SV	0	SV	0	SVJJ	0
TGMCS-max		TGMCS-10%		TGMCS-50%		TGMCS-t	
SHA	1	SHA	0.7413	SHA	0.7413	SHA	0.5412
SHAVJ	0.9943	SHAVJ	0.7195	SHAVJ	0.7195	SHAVJ	0.4588
CEVJJ	0.1644	CEVJJ	0.0393	CEVJJ	0.0393	*****	*****
*****	*****	*****	*****	*****	*****	CEVJJ	0.0353
CEVXJ	0.0278	CEVXJ	0.0560	CEVXJ	0.0560	CEVXJ	0.0029
SVXJ	0.0278	SVXJ	0.0110	SVXJ	0.0110	SVXJ	0.0021
SHBVJ	0.0059	SVJJ	0.0010	SVJJ	0.0010	SHBVJ	0.0003
SVJJ	0.0057	SV	0	SV	0	SVJJ	0.0003
CSHBVJ	0.0004	SVVJ	0	SVVJ	0	CSHBVJ	0.0000
SHB	0	CEV	0	CEV	0	SHB	0.0000
CSHB	0	CEVVJ	0	CEVVJ	0	CSHB	0.0000
SV	0	SHB	0	SHB	0	SV	0.0000
CEV	0	SHBVJ	0	SHBVJ	0	CEV	0.0000
CSHA	0	CSHB	0	CSHB	0	CSHA	0.0000
SVVJ	0	CSHBVJ	0	CSHBVJ	0	SVVJ	0
CEVVJ	0	CSHA	0	CSHA	0	CEVVJ	0
CSHAVJ	0	CSHAVJ	0	CSHAVJ	0	CSHAVJ	0
LRLCMCS-max		LRLCMCS-10%		LRLCMCS-50%		LRLCMCS-t	
CSHB	1	CSHB	0.9085	CSHB	0.9085	CSHB	0.9075
CSHBVJ	0.1835	CSHBVJ	0.0915	CSHBVJ	0.0915	CSHBVJ	0.0925
*****	*****	*****	*****	*****	*****	*****	*****
SHA	0.0102	SHB	0.0270	SHB	0.0270	SHA	0.0018
SHB	0.0102	SHA	0.0050	SHA	0.0050	SHB	0.0012
SHBVJ	0	SV	0	SV	0	SHBVJ	0.0000
SHAVJ	0	SVVJ	0	SVVJ	0	SHAVJ	0.0000
SVJJ	0	SVXJ	0	SVXJ	0	SV	0
CEVXJ	0	SVJJ	0	SVJJ	0	SVVJ	0
SVXJ	0	CEV	0	CEV	0	SVXJ	0
CEVJJ	0	CEVVJ	0	CEVVJ	0	SVJJ	0
CSHAVJ	0	CEVXJ	0	CEVXJ	0	CEV	0
CSHA	0	CEVJJ	0	CEVJJ	0	CEVVJ	0
SV	0	SHBVJ	0	SHBVJ	0	CEVXJ	0
SVVJ	0	SHAVJ	0	SHAVJ	0	CEVJJ	0
CEVVJ	0	CSHA	0	CSHA	0	CSHA	0
CEV	0	CSHAVJ	0	CSHAVJ	0	CSHAVJ	0

Table 29: **Market Data MCS.** This table contains the output of the LRMCS, TGMCS and LRLCMCS produced by the Hansen et al.'s, the modified Corradi et al's and this thesis MCS algorithms. Each column contains the output of the corresponding MCS test, indicating the model label, the model confidence set cut-off, represented by an asterisk line and the model ranking achieved within each set by means of the p-values. We produce the MCS-max the MCS-γ at 10% and 50% γ and the MCS-t. The confidence level is at 5%. Considering the k, the selected FWER levels for the 10%-MCS and the 50%-MCS are, respectively, $k = 7$ and $k = 36$ for the LR test, $k = 11$ and $k = 57$ for the TG test and finally, $k = 8$ and $k = 46$ for the LRLC test. This table shows the full set of MCS test for the likelihood analysis of this Chapter 3. The results show that the CSHA, CHSB, CEV models produce the best likelihood measures, whereas in terms of latent factor estimation in the TGMHT test, those models might necessitate some extensions, as it is the case of the CEVJJ model. The outcome of the LRLCMCS test is controversial, as it appears excessively polarised. The comments to this table are in Section 3.3.3.

	NLF²				SIRPF				LC-test		
SV	0.31	–	d	4.54	0.49	–	w	2,701.56	0.2431	0.4611	↘
SV	0.31	–	d	4.54	0.42	–	d	7,897.67	0.2431	0.4611	↔
SVVJ	0.33	–	d	4.44	0.58	–	w	2,915.26	0.2380	0.5371	↘
SVVJ	0.33	–	d	4.44	0.45	–	d	10,183.33	0.2380	0.5371	↔
SVXJ	0.60	54.79%	d	3.89	0.50	19.66%	w	2,894.75	0.3979	0.8185	↔
SVXJ	0.60	54.79%	d	3.89	0.37	3.36%	d	16,001.13	0.3979	0.8185	↗
SVJJ	0.76	55.74%	d	3.92	0.59	19.08%	w	3,023.62	0.4210	0.9320	↔
CEV	0.26	–	d	4.80	0.39	–	w	3,352.43	0.2199	0.3774	↘
CEVVJ	0.29	–	d	4.79	0.47	–	w	3,608.07	0.2294	0.4307	↘
CEVXJ	0.54	54.94%	d	4.18	0.47	19.24%	w	3,590.61	0.3956	0.7394	↔
CEVXJ	0.54	54.94%	d	4.18	0.36	3.73%	d	11,147.78	0.3956	0.7394	↗
CEVJJ	0.63	54.88%	d	4.18	0.69	17.42%	w	3,697.20	0.4183	0.8623	↔
SHB	0.55	100.00%	d	5.34	0.73	100.00%	w	5,248.37	0.3814	0.8277	↔
SHBVJ	0.64	100.00%	d	5.31	0.83	100.00%	w	5,553.92	0.4083	1.0041	↔
CSHB	0.60	100.00%	d	5.71	0.80	100.00%	w	6,514.98	0.3761	0.8140	↔
CSHB	0.60	100.00%	d	5.71	14.59	100.00%	d	11,200.15	0.3761	0.8140	↘
CSHBVJ	0.60	100.00%	d	5.73	0.88	100.00%	w	6,542.32	0.4027	0.9520	↔
SHA	0.60	100.00%	d	5.47	0.68	100.00%	w	12,619.16	0.4016	0.8677	↔
SHAVJ	0.69	100.00%	d	5.66	0.77	100.00%	w	10,243.15	0.4258	0.9785	↔
CSHA	0.61	100.00%	d	5.92	0.69	100.00%	w	11,103.20	0.4037	0.8892	↔
CSHAVJ	0.59	100.00%	d	5.91	0.68	100.00%	w	11,306.36	0.4230	1.0365	↔

Table 30: **The NLF² and the SIR Particle Filter.** In this table, we compare the long run model performance measure of the NLF² to those of the SIRPF. We produce the 100 years simulated sample measures as the absolute distance of the projection of v from the actual latent component of the benchmark sample. The parameters are the exact model parameters. The column of the NLF² and the SIRPF subsection of this table shows, from left to right, the sample value of the LC statistics, the percentage of the jump times produced by the filter that actually match the realised jumps, the frequency at which the filter is calculated that is either daily (d) or weekly (w) and the rightmost column indicates the number of seconds necessary to produce the filter output. The LC-test section exhibits the interval of the scalar distributions of the test statistics for each single model employed in the MHT exercise. The rightmost column indicates if the SIRPF is superior, inferior or equivalent to the NFL² by, respectively, a north-east, a south-east or a left-right arrow.

Figure 1: The Likelihood Function Algorithm.

The figure shows 4 sections that are labelled from a to d in matrix order. Section (a) shows the marginalised density of the simulation SV model. Section (b) depicts the bivariate densities on the grid of initial condition for v, ranging from (almost) 0 to seven times the projected variance over the weekly horizon. The initial condition for x is centred at 0 for each grid-point of v. The (c) quadrant shows the conditional marginals that are weighted by the stationary distribution of the initial conditions for v, as shown in the section (d).

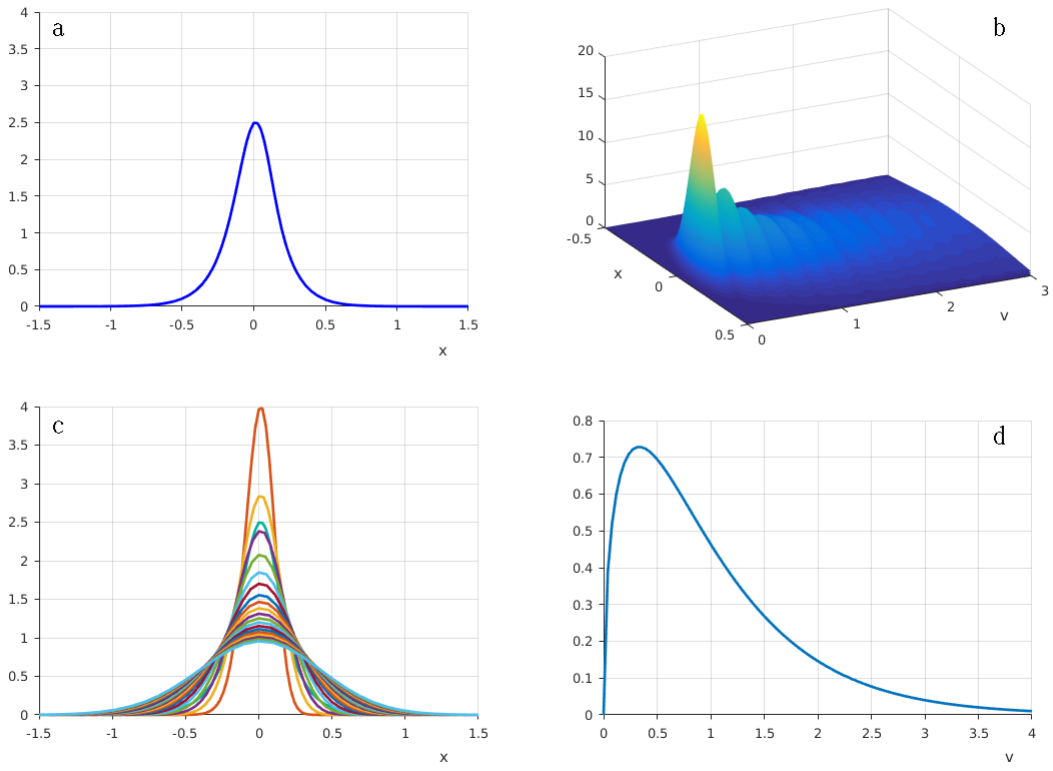

Figure 2: An example of Information Loss.

The figure shows 4 sections that are labelled from a to d in matrix order. Section (a) compares the shape of a Gaussian function (red line) with zero mean and appropriate standard deviation (0.2) to the simulation SV model. Section (b) compares the simulation SV model with $\rho = -0.5$ (blue line) with a SV with the same parameters with the exception of $\rho = 0$ (red line), producing, respectively a -0.14 skewness factor against a zero. The lower (c) and (d) quadrant exhibit, respectively, the cross-section view onto the x domain of a bivariate distributions contributing to the previous marginal densities, with $v_0 = 2.46$.

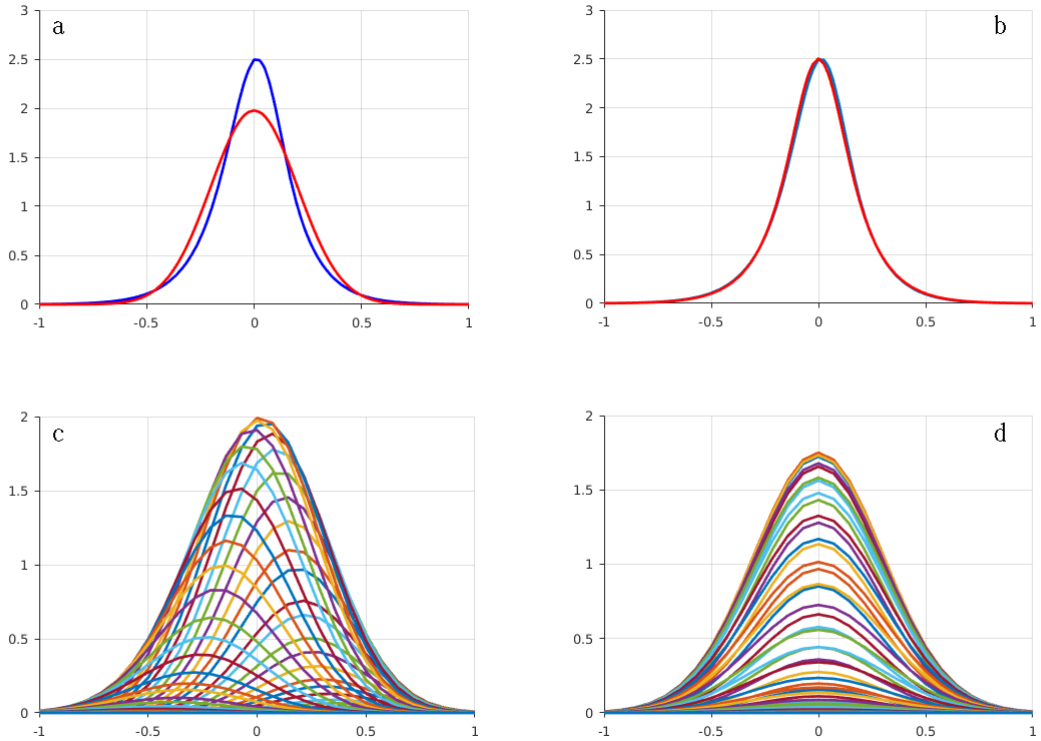

Figure 3: The Distributional Shape of the Model Set.

The figure shows 4 sections that are labelled from a to d in matrix order. In this figure, the SV model (blue curve) marginal distribution is compared with several other members of the model set, computed at the simulation parameters. Frame (a) shows some kurtosis generated by ancillary model components, as in the case of the SVVJ (red line) and the CEVVJ (light blue line) model. In the SVXJ (red line) model of frame (b) and in the SHB (red line) and the CSHBVJ (dashed light blue line) of frame (c), asymmetry can be generated by jumps. In the (d) quadrant, the marginal densities of two stochastic hazard models with skewed Normal jumps are plotted against the SV profile, that is the SHA (red curve) and the CSHAVJ.

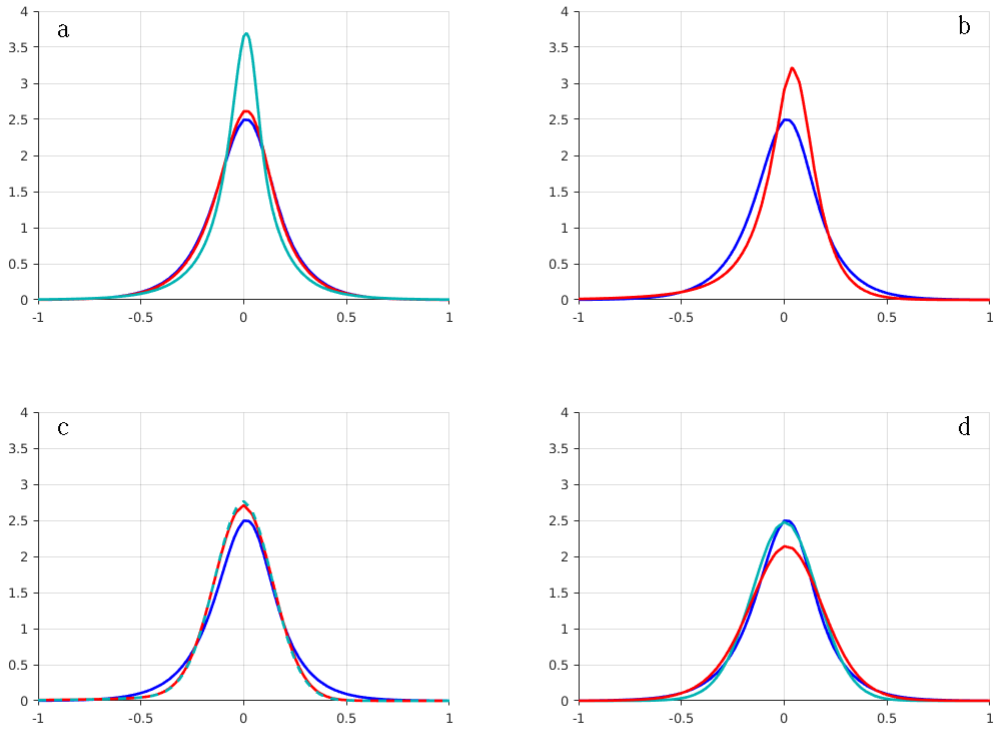

Figure 4: Several Implementation Issues.

The figure shows 4 sections that are labelled from a to d in matrix order. This figure section (a) shows the simulated histogram against the numerical solution of the PIDE for the model SVXJ. In the (b) quadrant, the PIDE solution for the SVXJ model is calculated with several grid specification, that are 13x13 (blue line), 25x25 (green line) and 61x61 (red line). Section (c) and (d) exemplify the unexpected shock phenomenon in the pure diffusive v path, when large jumps are observed in the x level. Section (c) we shows the simulated path of the latent factor of the SVXJ model (left axis, red curve), coupled with the integrated variance of x (right axis, blue dotted line). Several large discontinuities are visible on the chart. The time frame corresponding to the encircled area in the (c) quadrant, is reported in section (d), which shows the evolution of the actual v system variable (red line), with several projections characterised by the presence of the dummy residual jump, multiplied by a constant ranging from 0 (blue dots) to 1 (light blue dots). This exhibit shows the process of attenuation of the unexpected shock due to the system updating by means of the residual dummy jump process.

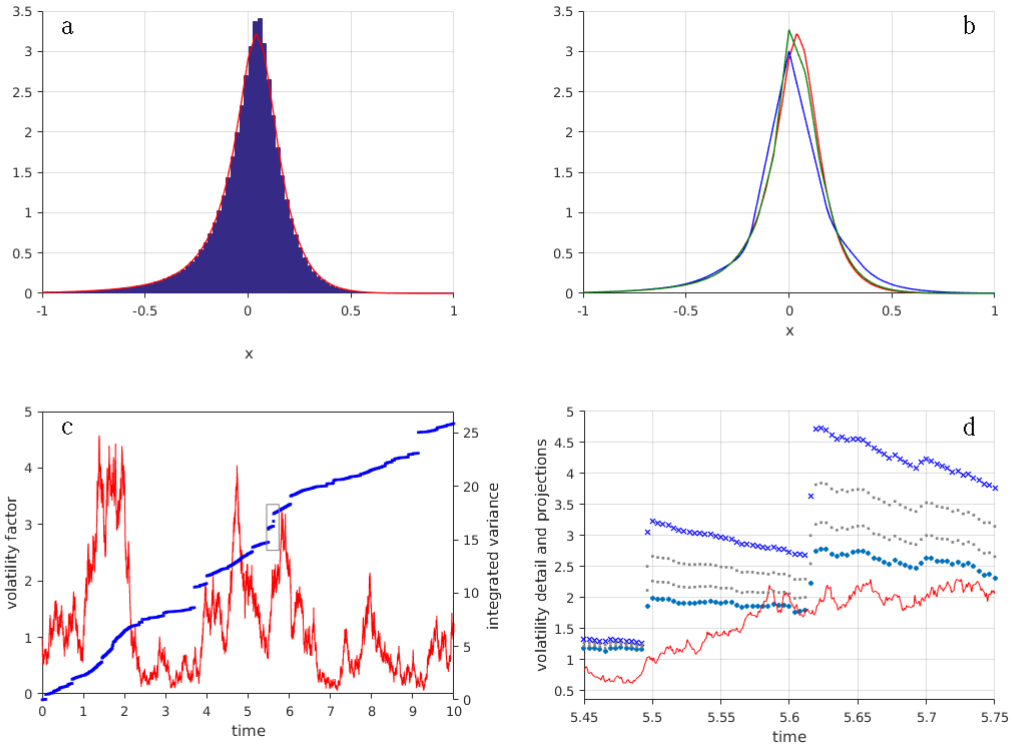

Figure 5: Market Data Applications.

The figure shows 4 sections that are labelled from a to d in matrix order. Section (a) shows the cumulative log return (times 100) path employed for market data testing. The (b) quadrant exhibits the histogram of daily returns with the superimposed estimated CSHB marginal likelihood. Section (c) shows a segment of the TGARCH estimated volatility (red line) and the scaled and translated output of the NLF^2 (blue line) for the CEVJJ process, as applied to market data. The lower-right picture (d) shows a portion of the actual v path (red line) for the SV simulated process, with the SIRPF output path (green line) and the NLF^2 projected latent component (blue line).

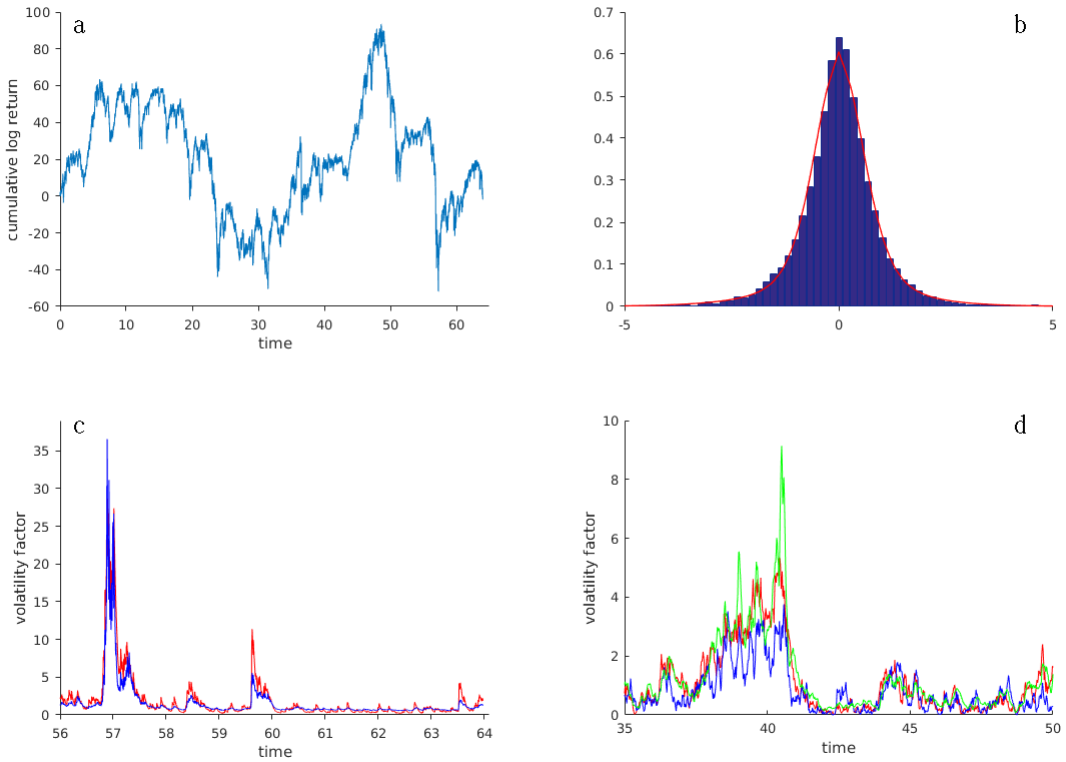

Model Selection of Derivative Pricing JD Models

In this chapter, we explore the model selection problem in the context of option pricing models. The general focus is on several formulations of stochastic volatility models that in their broadest specification include jump components. As noticed in Christoffersen et al. (2010), the literature on stochastic volatility models can be grouped into three branches. In Chapter 3, we have tackled the analysis of the daily return distribution of financial returns from a time-series perspective, including alternative models within the affine set, a study which falls within the first body of research. The second set of studies concerns the analysis of realised volatility or volatility proxies to forecast future volatility, examples of which are Bakshi et al. (2006), Aït-Sahalia and Kimmel (2007). The latter overlaps to some extent with the general option pricing literature, which forms the last body of econometric studies of stochastic volatility models and to which this chapter contributes. Seminal studies in this subject are represented by the works of Bates (1996) and Bakshi et al. (1997), which both set standards in the model performance analysis by examining measures of in-sample and out-of-sample mispricing, option implied stochastic process features as compared to the underlying return and implicit volatility behaviour, single-instrument and delta-neutral

hedge analysis. The literature mainly works within the affine framework, as a consequence of the stylised approach originated in Heston (1993), Duffie and Kan (1996), Duffie et al. (2000) and the computational efficiency that integral transform methods generally offer in terms of option pricing and hedge measure calculation. Examples of studies that compare affine models versus alternative model specifications using option data, but not strictly in an option mispricing context, are those in Benzoni (2002), Jones (2003) and Aït-Sahalia and Kimmel (2007). The first article exploits log-normal volatility as an alternative, whereas the latter two both employ a volatility CEV model, which is complemented with a GARCH stochastic volatility in the most recent one. The non affine model in Benzoni (2002) appears unable to outperform the Heston model, whereas the evidence in Jones (2003) and Aït-Sahalia and Kimmel (2007) points to a misspecification of the affine model. A further extension in the analysis of stochastic volatility models with contrasting alternatives to the affine specification is the cited work of Christoffersen et al. (2010), which employs a wide database including realised volatility, S&P500 returns and a panel of option data. The model set is diverse and includes several alternative volatility specifications that perform better than the affine model under several measures. The cited works, however, employ mainly diffusion models, although evidence suggesting the need for discontinuous extensions is inferred from short-term OTM pricing model behaviour. Empirical works using JD models can be found, for instance, in Bates (1996, 2000), Pan (2002), Eraker et al. (2003) and Eraker (2004), which all apply the affine framework with combinations of constant or stochastic intensity and independent or correlated jumps in volatility and returns. The general result is that jumps improve the option pricing performance with a preference for joint jumps in return and volatility. The performance of the stochastic intensity model does not seem to improve the overall model yield. Those articles model the volatility jump size with an exponential distribution and the price jump size at most with an offset log-normal distribution.

In our analysis, we gather evidence that the popular single factor affine specification common in the literature are strongly rejected. Moreover, model augmentation such as jumps in volatility, stochastic hazard, and the parametrisation of the elasticity of the diffusion factor, appear to be excessive model complications. A simple model, such as the log-normal correlated volatility model, performs very well in the OTM option sample we consider, whereas the inclusion of a compensated single directional exponential jump in return produces one of the top performance for the ALL option sample. We also sketch a qualitative comparison among the established Hansen et al. (2011) MCS test and our original γ-MCS test, developed within the MHT framework of Romano and Wolf (2010), whereby we provide evidence that the latter test can offer a wider flexibility allowed by the k-FWER controlling mechanism. This chapter therefore provides several contributions. First, we construct a novel model selection test that, for the first time in literature, is using a vast array of option pricing models, containing 280 model specifications in today, the majority of which are obtained by uniquely combining jumps and volatility specifications in a way never explored before in the literature. Second, we exploit for the first time the power of MHT and MCS techniques, specifically the *max*-MCS and our novel MHT consistent γ-MCS, in an option pricing model comparison exercise. Third, by selecting the subset of best performing equivalent models, we are also able to infer conclusion about the model similarity hypothesis and provide empirical evidence of strong aliasing amongst many option pricing models ranging from high to a lower level of complexity, whereby complexity may be ascribed to the size of the parameter vector.

We exploit the finite difference method (FDM) combined with numerical integration to construct the solution of the pricing equation for a large collection of JD models. The references for the finite difference method are represented, for instance, by Tavella and Randall (2000), Duffy (2006). The model set can be mainly divided into two families of stochastic volatility models, characterised by affine volatility (Heston, 1993) or by volatility generated with the exponential of a Gaussian mean-reverting process (Scott, 1987). The latent factor can include an exponential jump component. The models are augmented with elasticity of variance parameters and with a wide range of jump specifications in the price process, endowed with stochastic hazard in their more complex specifications. The model selection exercise conducted in this chapter applies the main MCS tests constructed in Chapter 1, with the objective of the mean squared error (MSE) measure of mispricing as the model performance loss function.

The work is organised as follows. In Section 4.1 we introduce the model set and describe the model dynamics features. Section 4.2 introduces the testing set-up, whereas Section 4.3 details the implementation of the test and describes the results. Section 4.4 offers concluding remarks.

4.1 The Derivative Pricing Model Set

With the empirical exercise in this study, we employ a very large model set of equity derivative pricing models to test for the MCS. The model collection contains two major families of stochastic volatility models, whereby the volatility factor is either modelled as an affine process as in the Heston (1993) model, or it is generated by a mean reverting Geometric Brownian motion, as in the Scott (1987) model. We extend the model set represented by affine jump-diffusion specifications as evidence supporting faster than affine acceleration of the volatility factor are common in the econometrics of financial markets literature, see for instance Jones (2003), Christoffersen et al. (2010). The stochastic volatility factor defining the diffusion function is either square rooted or powered by a free parameter, allowing for extended CEV specifications in the affine case or for linear elasticity[1] of variance (LEV) in the geometric variance case. The model diffusive dynamics is also combined with Poisson jumps under several specifications. The jumps can affect the model price and volatility processes, which can jump independently or simultaneously. The price jump process can also allow for stochastic intensity, which under this configuration is coupled with stochastic diffusion. We do not include here high frequency jump models, as we have already established in Chapter 3 that they are equivalent to more orthodox models, which are the focus of this analysis. In the execution of the exercise, we are also interested in testing the contribution to the model performance of the diffusion correlation factor (ρ), as we test models with or without the leverage effect. Combining the inclusion or exclusion of the cited model components with the several specifications of the volatility and the jump factors, we obtain a collective of 280 models. The full model set is split into two groups characterised by the alternative specifications of the latent factor. In general, the model structure is

[1] We include the LEV parameter in the geometric mean-reverting specification of the stochastic diffusion factor, in order to parallel the flexibility of the elasticity of diffusion that is provided by the CEV model. However, as it is shown in Appendix A.4, in the log-normal model this parameter simply acts as an amplifier of the variability of the v factor entailing wider excursions of the diffusion process. This feature can as well be obtained by changing the θ value, although with a different sensitivity of the model performance measure to the parameter variations.

obtained by either the inclusion or the exclusion of any amongst the allowed components, as well as the characterisation of the jump in return type. The majority of the models obtained by such combinations are employed for the first time in this study. A comprehensive picture of the models most common in the literature that are covered by this model set is presented at the conclusion of this section.

The model specifications are captured by the following overarching model:

$$\frac{\mathrm{d}S}{S} = r\,\mathrm{d}t + \theta v^{\gamma_0}\,\mathrm{d}W_0 + J_0\,\mathrm{d}N_0 - m_0 v^{\gamma_1}\,\mathrm{d}t \tag{4.1}$$

$$\mathrm{d}v = \kappa(\delta - v)\,\mathrm{d}t + \sqrt{v}\,\mathrm{d}W_1 + J_1\,\mathrm{d}N_1 - m_1\,\mathrm{d}t \tag{4.2}$$

$$\mathrm{d}y = (a - by)\,\mathrm{d}t + \mathrm{d}W_1 + J_1\,\mathrm{d}N_1 - m_1\,\mathrm{d}t \tag{4.3}$$

whereby the two stochastic families are specified by the equation couples (4.1) and (4.2), for the affine volatility version, and (4.1) and (4.3), with $v = \exp(y)$, for the log-normal volatility version. Some more auxiliary information is needed to fully characterise the system dynamics allowed by the models included in this MCS study. In fact, we remark that the Brownian components W_0 and W_1 can in general be correlated, that is $\mathrm{d}[W_0, W_1] = \rho\,\mathrm{d}t$, with the ρ coefficient left free to vary in the negative range[2] or otherwise fixed to be zero in case of models excluding the price-volatility correlation. The hazard processes driving the jump intensities of the counting random numbers N_0 and N_1 are given by

$$\mathrm{d}\Lambda_0 = \lambda_0 v^{2\gamma_1}\mathrm{d}t \tag{4.4}$$

$$\mathrm{d}\Lambda_1 = \lambda_1 \mathrm{d}t \tag{4.5}$$

As in Chapter 3 the jump intensity of the price process can be stochastic, but at most affine that is γ_1 is either zero or one and the stochastic factor v is scaled by the coefficient λ_0, whereas the volatility, when allowed, jumps with constant frequency λ_1. More parameters are necessary to define the jump size distributions, which are not shown in the SDE (4.1), (4.2) and (4.3). We notice that the system (3.1), (3.2) and the model set of this study present several differences. We have already anticipated that the high frequency jump model is not included, whereas this model set deals with an alternative specification for the volatility factor that can be log-normal, as in (4.3). In the experiment of this study, we allow for combined stochastic volatility and stochastic intensity of jumps. The size of the jump in volatility is exponential, whereas the jump in price can be characterised by either a centred, as for instance in Merton (1976), or offset, as e.g. in Duffie et al. (2000), Normal distribution or by a negative/double sided exponential, as in Kou (2002), Kou and Wang (2004) or Lomax[3] distribution. In the case of a double sided jump size distribution, the probability of the sign of the jump is either derived as a constraint involving the expected positive jumps size such as to get a zero centred distribution, or it is a free parameter. Moreover, a joint jump in price and volatility, that is $N_0 \equiv N_1$, is allowed as in Duffie

[2] During preliminary analysis, we have noticed the high sensitivity of the mean squared error model performance function to the correlation parameter ρ, which was systematically hitting the negative border of the interval of variation. As a consequence, in the model versions characterised by negative price-volatility correlation, this parameter has been fixed to -0.7 value.

[3] This extreme value distribution has been employed to characterise the EVD innovation of a class of GARCH model in the Chapter 2. In practice, a Lomax distribution corresponds to a Pareto distribution which has been shifted to extend the range of variation to a full semi-axis.

et al. (2000). In this case the intensity is allowed to be constant only. Further difference lies in the observable S, which would be the corresponding geometric process of the cumulative return x in (3.1) of Chapter 3 that is taken at the risk-neutral measure, entailing a drift at the constant interest rate r. In this chapter, the main reason for designing the system with respect to the S variable, is found in the nature of the problem, which includes the observable index level and the option prices as functions of the former, whereas in the previous set of experiments the price is otherwise observed as a log-return curve. Listing other differences when compared to the system of the previous chapter, we observe that the Poisson jump of S is compensated locally by including the possibly stochastic hazard factor. Another difference which is experimented here is the standardisation of the volatility acceleration, which implies an adjustment factor[4] in the unitary mean of (3.1). In terms of parameter definitions, we notice that the coefficient r is the constant interest rate, corresponding to the instantaneous equivalent rate of the three months LIBOR rate. The parameter r is assumed to be constant, although during the optimisation the interest rate is observed daily. As noticed in Scott (1997), stochastic interest rates have a limited impact on short dated options. Further parameters are represented by the diffusion process scaling factor θ, as we rescale the latent component to have unitary diffusion parameter. The diffusion component in (4.1) is powered to the γ_0 coefficient, which controls CEV and LEV effects, respectively for the affine and the log-normal volatility model. As mentioned earlier, the jump process is compensated in order to obtain the martingale $\sum_{i=1}^{N_0(t)} S_{\tau_i} \left(J_{0,i} - \frac{m_0}{\lambda_0} \Lambda_0(t) \right)$ and therefore m_0 represents simply the intensity scaling factor λ_0 times the expectation of $J_0 \equiv z$ in the case of the Lomax distribution and $J_0 \equiv \mathrm{e}^z$ with all other distribution hypotheses. We choose the former configuration for the extreme value distribution (EVD), as it lacks of finite exponential moments. In Eq. (4.2) we describe the latent factor specification of the affine/CEV family, whereby the parameter κ represents the speed of mean reversion and δ the mean level of v. Under this specification, we scale the conventional stochastic volatility factor in order to obtain an unitary coefficient in the diffusion component. This choice is motivated by the intention to simplify the estimation of the latent component by moving some parameters either onto the observable or at least onto its first order component[5]. In the case of the log-normal latent component of Eq. (4.3), the speed of mean reversion is represented by the coefficient b, whereas the mean level is represented by the ratio a/b. Both the latent components might include a constant intensity exponential jump J_1, compensated by the opposite sign of the Poisson process drift m_1.

The affine specification in Eq. (4.1) and (4.2) embeds the Heston (1993) model. Under independent or dependent Normal jumps in price and exponential jumps in volatility it contains the models in Duffie et al. (2000) and Eraker et al. (2003), while under stochastic hazard the (single factor) model of Bates (2000) augmented with jumps in volatility is also captured. The jumps can be negative sided or double sided, with appropriate compensation factor or, in the case of double jumps, the compensation is embedded within constrained probability of positive/negative jumps. The double exponential jump of Kou (2002) and Kou and Wang (2004) is augmented with stochastic volatility and intensity. A novel jump specification is represented by the EVD jump model. Moreover, the stochastic volatility family of this study is expanded

[4] To standardise the stochastic volatility diffusion from the Eq. (3.1), we simply set $u = v/\sigma^2$ and rewrite the system, adjusting the drift and the volatility factor of x. In Eq. (4.1) and (4.2), we have kept the same variable and parameter denomination as in Chapter 3, whereby the affine model of this study can be easily reverted to the previous type.

[5] See Appendix A.4 for further details concerning the transformations of the conventional models adopted in this study.

with a mean-reverting log-normal stochastic volatility model as in Scott (1987), also (partially) introduced during the same year by Wiggins (1987) and Hull and White (1987), whereby the diffusion is augmented with the collection of jumps just outlined. The CEV specifications can also be allowed, which in the case of affine volatility can be seen as an extension of the models in Beckers (1980), Macbeth and Merville (1980) but also, under a transformation, can be related to the CEV stochastic volatility model class used in Jones (2003) and Aït-Sahalia and Kimmel (2007). As to our knowledge, the LEV specification under the log-normal volatility model is a novel application. Certain model components combination are also explored for the first time in the literature. Specifically, these models comprise: stochastic volatility combined with exponential and Lomax jumps; the log-normal volatility model combined with stochastic intensity and with the further jump specification generating joint jumps; models that allow jumps in volatility only. In Appendix A.4 we specify which transformation should be performed to connect the models of this study to more conventional models used in the literature. In Section 4.3.1, we will be presenting a labelling scheme to identify the model configurations in the context of the testing results.

4.2 Model Comparison Testing

In the experimental section of this chapter, we apply the *max*-MCS test introduced in Section 1.3.1 and construct the MHT (1.3) combined with the MCS algorithm as in Section 1.3.3, to produce an option model mispricing exercise with the reference MCS test and the novel γ-MCS presented in this thesis. The goal is the selection of the best set of models producing the lowest MSE when applied to a large sample of option market data. Option pricing for affine models is usually pursued with the Fourier inversion technique introduced in Heston (1993) and refined in Carr and Madan (1999). A multidimensional general Fourier inversion technique is presented in Shephard (1991a,b). In the context of the Scott model, a quasi-analytic solution exploiting the Laplace transform is found in Perelló et al. (2008). Another technique traditionally used for pricing alternative models consists of the recombining tree method, introduced in Finance by Cox and Ross (1976). Simulation is also widely used in the financial community for derivative pricing, see for instance Platen and Bruti-Liberati (2010) to construct a multidimensional JD simulation with pre-specified order of convergence. An alternative technique is represented by the quasi-analytic approximation of the price density constructed in Aït-Sahalia (1999, 2008). In this study, we use PIDE solution techniques, see for example Tavella and Randall (2000), Duffy (2006). To generate the bootstrap samples and the summary statistics feeding the MCS algorithms, we exploit the FDM[6] to construct a numerical solution of the backward equation defining the European call/put option price

$$\mathbb{E}^{\mathbb{Q}}\left[(S_T - K)^{\pm} \,|\mathcal{F}_t\right] \mathrm{e}^{-r(T-t)} \tag{4.6}$$

where the interest rate is assumed non-stochastic. We employ the martingale approach to achieve the derivative price, as we have constructed the SDE describing the underlying's dynamics in (4.1) as such that discounting the price by a non-stochastic or non-correlated factor, a martingale process is obtained. The solution of the expectation in (4.6) is generated by means of the Fokker-Planck equation approach, as mentioned above. It is acknowledged that in the case of a complete market, the martingale approach

[6] For further details regarding the implemented procedure, compare Appendix A.2.

and the risk-neutral technique, achieved by the construction of a risk-less replicating portfolio, are both equivalent, see for instance Musiela and Rutkowski (1997). However, when the market is not complete, that is some risk factors are not traded, as is the case for the asset volatility, the pricing equation obtained via the hedging argument is not unique, see for instance Scott (1987). Thus, usually the market equilibrium argument is invoked and a "market risk premium" is introduced. For practical purposes, the introduction of risk premia usually has the effect of altering the parameters of some risk factors, without changing the overall structure of the main SDE. The analysis of the effect of market risk premia on the main equation is beyond the scope of this thesis. For an interesting analysis concerning the estimation of risk-premia in JD models, see for instance Pan (2002). In order to simplify the complexity of the computations, the strike price K is taken out of the pay-off function and the underlying variable redefined as $s_T = S_T/K$, which evolves according to the reference dynamics, that is Eqs. (4.1) and (4.2)/(4.3), but with initial condition s_t. In practice, each option price $O_j^{\pm}$, where the plus and minus signs refer, respectively, to the call and put option, corresponds to the present value of the strike times a stochastic factor depending on s_{t_j} and the model parameters, whereas the relative strike is always unitary. That is,

$$O_j^{\pm}(T_j, s_{t_j}; \Theta, v_{t_j}) = \mathbb{E}^{\mathbb{Q}}\left[(s_{T_j} - 1)^{\pm} \left| \mathcal{F}_{t_j} \right.\right] K_j \mathrm{e}^{-r(T_j - t_j)} \tag{4.7}$$

and we conduct the analysis in terms of the relative option prices $\omega_j^{\pm} = O_j^{\pm}/K_j$. We adopt this strategy in contrast to the usage of dollar prices as in Bakshi et al. (1997) that induces dependence on the index level and therefore the time of the price record. This procedure is also alternative to the option price standardisation of Bates (1996, 2000), which operates with option-to-underlying price ratios. As we solve the option pricing problem with a PIDE solution method, it is natural to standardise the underlying by the strike and not viceversa, whereby this strategy only modifies the initial condition of the reference underlying at the same time anchoring any instrument in the sample to a unitary strike. As a consequence, the complexity of the problem is simplified because in this way, we are centring the solution domain over a given range initiated by a unique terminal condition. The reverse strategy instead, that is dividing the option price by the underlying level, virtually changes the nature of the problem, as we are now in the presence of a stochastic strike option over a constant reference underlying. Moreover, although not interested into the hedging problem here, we notice that the latter strategy complicates any perturbation analysis as the computation of the sensitivity effect are more involved[7]. In the following, unless otherwise explicitly stated, when we write of option prices we will be referring to relative option prices.

4.2.1 Mispricing MSE

The model performance measure we use in this study is the mispricing, that is the average squared difference between model prices and actual prices, or its square root (RMSE). The MSE is essentially a measure of the goodness of fit of the model across the set of observed data; the lower the mispricing,

[7] In fact, from a numerical perspective, because when standardising by the strike the initial condition of the PIDE is unique for any option data set, the computation of the numerical derivative will only involve as many solution as the chosen finite difference would require, whereas standardising by the current level of the strike will have the effect of multiplying the latter number by the number of strikes in the sample. Another complication for the computation of the Δ is that, in the former case, variations of the current price level will only impact the standardised underlying linearly and therefore the variations will simply be proportional to the strike, whereas in the latter case variations of the underlying will impact the initial condition non linearly entailing a distortion of the Δ range or more articulated calculations to reconstruct the non standardised effect.

the better the model explains the realised market quotes. It is important to notice that the use of the MSE requires the standardisation of the option prices, in order to get rid of the dependency on the money value of the strike. Moreover, the choice of standardising by the strike, rather than the underlying price value as it is customary in other articles, as for instance Bates (2000), gives to the option relative value the immediate significance of a dimensionless measure of "moneyness", that is a relative number indicating how deep in the money the option is, whereas standardising by the current level of the underlying turns this quantity in the opposite direction, whereby lower numbers would indicate higher moneyness and viceversa, lacking of an intuitive significance. Dropping for convenience the reference to the moneyness and the tenor of the option and highlighting the dependency on the parameter vector Θ and the market volatility information, the loss function for the generic model $\mathbf{P}_i$ is described as following, using information across the full time span of the sample:

$$L_i := \tfrac{1}{N} \sum_j \Big(\omega_j(\Theta_i, v^i_{t_j}) - \varphi_j \Big)^2 \tag{4.8}$$

whereby φ_j is the j-th market implied option price, with $t_j = t$, $\forall t, j$, and v^i_t the model $\mathbf{P}_i$ volatility at time[8] t. In Eq. (4.8) more information is necessary to determine the model price of the φ_j, which we do not make explicit; namely, the option type, the underlying level-to-strike ratio providing the initial condition for the pricing engine, the tenor of the option and the current interest rate level. With respect to the latter model components, we notice that the parameter vector Θ^*_i and the estimated volatility sample path $\left\{v^i_k\right\}_{k=1}^K$ for the model $\mathbf{P}_i$ are the output of the following program

$$\min_{\Theta_i,\, \left\{v^i_k\right\}_{k=1}^K} L_i \tag{4.9}$$

The estimation of the parameter vector Θ is performed as follows. The target MSE function is constructed such that, for a given Θ, the loss function L, at each observation date $k = 1, \ldots, K$, is evaluated over a grid spanning the domain of definition of the latent variable v and thus the sequence $\{\hat{v}_k\}_{k=1}^K$ is selected such as to render the least loss. It is implied that the grid is determined by the restriction of the current parameters to those defining the v process, such that the domain of definition spreads between zero and seven times the long run model volatility, whereas the number of points is fixed and proportionally distributed amid the boundaries. In practice, at each evaluation given the parameters Θ, the loss function returns the minimum value amongst all the possible determinations over the v_k sequence, determined over the current grid. The parameter vector Θ is hence optimised by sequential quadratic programming. As a consequence, the optimisation problem (4.9) is divided into two sub-problems: the main one consists of numerically minimising L_i with respect to Θ_i and the secondary one provides the minimum $L_i\,|\Theta_i$ with respect to the sequence of model implied volatility, refining the target function for the main problem. We make a point in this latter analysis of applying a given set of parameters across the time dimension of the price sample, thereby focusing on the stochastic volatility models ability to reproduce market prices by the means of the latent factor only. This bestows upon the solution strategy the nature of a highly

[8] In order to summarise the procedure, we have appended a subscript j to each option price in the data panel, entailing that an ordered record of market option prices and their corresponding model generated values is available. Because the volatility factor is an essential input of the model price, its estimate will enter each model determination, whereby the daily $\hat{v}_t$ is cross-referenced to the determination of the j-th options that will be given at market time t_j, that is the reference volatility at time t is attributed to each j-th option at day t.

parametrised problem, as in Bates (2000). We choose to solve the problem (4.9) over a coarse grid of the volatility within a plausible range of variation, given the current set of parameters. Although we do not employ any filtering technique, the projected path can be considered as a suboptimal solution achieved with reasonable speed of computation.

4.3 Experimental Section

4.3.1 Preliminary Considerations

In this section, we produce several MCS tests to select the best option pricing models from a collection of Heston (1993) and Scott (1987) stochastic volatility models feeding a diffusion function that can be, respectively, linear or exponential and is extended to allow for constant or linear elasticity of variance. The diffusion components are furthermore combined with several jump specifications that can produce discontinuities in the index level with constant or stochastic intensity. Moreover, the models can include either a strongly negative ρ parameter or exclude the leverage effect, which in the context of the model selection procedure corresponds to testing for the model performance contribution of the correlation parameter. The jump specifications are described in Section 4.1. The models are designed such as to produce martingale discounted index prices and therefore the option price is evaluated as an expectation, that is the solution of the backward equation associated with the model set components. In Appendix A.2 we provide some details of the FDM and the numerical integration techniques used to solve the forward and backward equations that have been encountered in the course of this thesis.

We obtain a large data sample of exchange traded index options, disseminated by the US Option Pricing Reporting Authority (OPRA), which consolidates the data sourced by the participant exchanges. The sample consists of the last traded price and the last national best bid offer (NBBO) at the exchange closing. In this study, we focus on the Standard and Poor's 500 Index European option data, spanning from 02-Jan-1990 to 08-Jul-2015 with strikes ranging from 225 to 3,500 whereby the underlying varies between 295.46 and 2,130.82, see the underlying index level path in Fig. 6. Among the whole set of CBOE traded options, we select the traditional AM-settled SPX and the most recently introduced weekly options SPXW, which started trading in October 2005, assuring that there exists only one call/put pair for each combination of strike/maturity/trade-date. We use last price data and the simple average of the bid/ask price if the last trade is absent and both the NBBO are available. From the original sample containing 3,439,236 observed pairs, we employ a particular selection criterion. As we consider end-of-day data, we cannot include intra-day trading information to trigger liquidity selection thresholds. As we target paired call/put option data we consider the put/call parity as a means to select significant prices that respect a model-free coherency requirement, entailing the absence of arbitrage for a risk-free portfolio composed by buying one equity at price S and one put with strike K, selling one call with equal strike and borrowing the present value of the strike for the corresponding option tenure. Excluding complications related to counterparty credit risk, the value of such constructed portfolio ought to be null and this structural relation might hold at most within the range of the bid/ask spread, otherwise implying the presence of market operators that would soon shrink the impairment by making risk-free profits. Therefore, for each

couple of instruments we compute the distribution of the imbalances in the put-call parity relationship, that is, we consider

$$\omega_j^+ - \omega_j^- - \left(s_{t_j} - \mathrm{e}^{-r_{t_j}(T_j - t_j)}\right)$$

and exclude the option couples that exceed the 5-97.5 percentile. We choose an asymmetric tail cutoff due to the different range of variation of the upper and lower tails of the put/call impairment distribution. We remark that the range of variation of the left tail of the parity imbalances is quite wide, whereby the fifth percentile is slightly lower than -0.08, meaning that one out of twenty option pairs in the sample exhibits an overpricing of the put arm in the parity relationship that is at least 8% of the strike price. As it often occurs in real financial markets, rational conditions are disappointed, leaving room for further investigation that might render an ideal constraint more realistic. We report for the case of interest for this study, that the sample is characterised by a strong impairment of put-call relation, especially in the left arm of the imbalances distribution, witnessing systematic overvaluation of put options that we conjecture are ITM, as the trades in that area are very intensive. We choose the cutting points of the put-call parity breaches distribution aiming at the balancing of the trade-off between the amount of data rejected and the width of the range of variation of those imbalances. This operation is easier for the right tail, whereby disregarding the rightmost 2.5% of the data only, we obtain an extreme value of 0.02 circa which is close to the average RMSE of the model pricing. On the other hand, disregarding the leftmost 5% of the data does not allow to reduce the impairment to less than -0.08, which is a remarkable value. Excluding more data would deteriorate further the daily moneyness-tenor coverage of the option sample data. The last characteristic, however, is slightly attenuated if considering that only data with maturity inferior than nine months are to be used in the model comparison exercise. In Fig. 7 we show the event counting of the latter data elaboration (full two years tenor sample), whereby the left and right tail have already been rejected[9]. We notice the quite wide range of variation of the relative price imbalance, which appears to be more concentrated on the negative tail. The distribution has a strong kurtosis (7.51) and negative skewness (-1.85); in order to get a left tail cut around -0.02 a further 15% of data should be rejected. The average is -0.0095. The data with tenor lower than nine months exhibits similar distribution shape numbers, with slightly higher kurtosis (8.93) and reduced skewness (-1.69), as a consequence of the reduced left tail. The latter is significantly thinner as the minimum negative impairment reduces to -0.053 and the leftmost 6% is below -0.02. The largest positive impairment persists at about 0.02. The average is -0.0051. The large left tail of the data that violate the parity however, generates no concern for the data integrity, as the option sample undergoes a final screening hinging on implied volatility, whereby a consistent portion of ITM calls are rejected as quoted below the pay-off. Several few data pairs are further rejected after visual inspection. These rejections corresponds to data points that clearly stand out from the data cloud, when plotted as in Fig. 8. The rejected data represents about 1% of the two year tenor sample and 0.69% of the final data. The outcome of the data selection query is shown graphically in Fig. 8 whereby the actual prices of the call (blue point charts) and put (red points charts) are exhibited over the $(S - K)$ axis, irrespective of the tenor and the observation date, before and after the process. From the charts we can observe the impact of the data selection procedure based on the put-call parity relationship: the data cloud consolidates in a neighbourhood of the terminal condition

[9] As a result, in the chart 7 the left and right boundaries of the data domain correspond to the 5-97.5 percentile of the previous data sample.

assuming a configuration which masks the hypothetical behaviour of the time sequence of the solution function converging to the final pay-off of the option. It has to be noticed that the visually rejected data, with exception of a handful of points floating far apart the cloud, are mainly ITM call that fall below the right arm of the pay-off function, that is extremely underpriced. We leave however a 2% range which is finally absorbed by the next implied volatility selection query. A time series view of the full clean data capped at 2 years tenor, is available in Fig. 9, whereby the upper section shows the time-to-maturity of the option pairs, whereas the lower section shows the call relative prices (blue positive points) and the put relative prices (red negative points). We notice the intense coverage of the maturity range and the growing coverage across the years of the short maturity range, up to half a year.

With the main sample established, in order to construct our MCS experiments, we restrict further the data available to deal with maturities of at most 3/4 of one year, that is nine months to maturity. We choose this tenor range as it seems a reasonable compromise between the short dated option samples employed in the majority of the reference studies, that is three/four months, and the analysis of long dated options, that is two years or more. In general, options with maturity higher than six to nine months fall into a residual class: in Bakshi et al. (1997) and Eraker (2004), for instance, options with tenor greater than six months are aggregated in a residual category; in Bates (2000) options expiring later than nine months from the observation date form an homogeneous group of analysis. A further reason as to why we choose this boundary tenor is that the Black-Scholes (BS) implied volatility becomes sensibly flat around that area. We furthermore consider only the range $[0.5, 2]$, to square off the underlying s_t domain and make the negative and positive range symmetric, as the price value boundary from the unitary standard strike is halved in the negative direction and doubled in the positive one, entailing a log-return range of $\pm 69.31\%$. We choose this interval as it is the largest (log) symmetric range with respect to the moneyness, which captures the majority of the available data, meaning that, observing the lower section of Fig. 9, we only drop a limited amount of the put options historical data by selecting the 0.5 boundary and hence obtaining the call threshold by overturning the top ITM put value. Data that cannot produce implied volatility, mainly ITM calls, are discarded. In such cases, we drop here the full put/call pairing. From the initial two year clean sample containing 3,136,529 observations, the selection of the nine months sample produces the rejection of 18% of the data yielding 2,590,811 paired observations. Finally, the implied volatility selection drops further data, leaving 2,503,439 observations of put options and 1,600,955 observations of call options. For estimation purposes, we look at both OTM and full option sample. With respect to OTM option prices, we construct a sample of put options with underlying indices s_{t_j} ranging between $\exp(0.02)$ and 2, as well as call options characterised by values in the range $[0.5, \exp(-0.02)]$. We exclude the tight range of log moneyness $[-2\%, +2\%]$ as we report an excessive variability of short dated ATM options. We report in Fig. 11 in the upper and lower charts, respectively, the full cloud of implied volatility points employed in the OTM sample and the mid-quantile surface obtained as a surface quantile interpolation[10] of a smooth volatility surface. The latter chart has only illustrative purposes. The implied volatility surfaces for the call and put selections present a relatively steeper wing at short term maturities over the respective ITM segments. To provide further information concerning the structure of the data employed in this study, in Tab. 31, 32, 33, 34, 35, 36 we show the average BS implied volatility

[10] Compare also Eq. (2.3) introduced in Section 2.1 and Koenker and Bassett (1978).

and the data distribution over the moneyness/tenor grid, organised in squared intervals. For the sake of completeness in the testing exercise, we also estimate parameters and produce MCS tests using the full range of the option sample, that is including and merging the previously discarded call and put options to generate simulated statistics for both the samples, employing the respective parameter estimates.

For the implementation of the MSC tests, we exploit the stationary bootstrap of Politis and Romano (1994a,b), whereby the block window is calibrated to the autocorrelation function of the target time series, see Politis and White (2004) and Patton et al. (2009). The simulated statistic distribution is obtained from the target measure of the daily root mean squared error (RMSE), which represents a measure of the data fitting of the various option pricing functions. The average RMSE times series across the whole model set is illustrated in Fig. 10, and evolves with a daily average of 83 bps and with an average standard deviation of 28 bps, which represent, respectively, the overall model pricing error and its intra-model variability. The figure also illustrates the sequence of daily min and max RMSE across the models, which are represented with red dots. It is interesting to notice that spikes or turning points in the model performance measures, whereby a surge in the RMSE is recorded, can be detected, for instance, in 1998 around the LTCM default, starting about the events of 9/11, 2001 and another evident burst at the beginning of the subprime crisis in 2007, culminating with the filing for bankruptcy of the Lehman Brothers in Sept. 2008. Another two spikes are noticeable at the ending of the RMSE path in correspondence of the European debt crisis and the Greek quasi-default, about May 2010, as well as in mid 2011, when the U.S. Sovereign debt was downgraded from AAA to AA+. The time series consists of $6,429$ daily observations. Out of these data, the bootstrap sample is generated as full sample averages of $1,500$ times series with $1,000$ observations, generated with resampling via the stationary bootstrap of the daily RMSE, for each model. The average block size is 188 days, as estimated via the Politis and White (2004) procedure. We remark that this is the first study that attempts a bootstrapping of this sort, as in general the few references that can be found mainly relate to the bootstrapping of a static confidence interval for the option prices, see for instance Yatchew and Härdle (2006) and Dotsis and Markellos (2008). We exploit the MCS-γ, with fixed γ at 20% and 40% of the relative k-FWER. In this exercise, this is done mainly for reasons of speed of computation. We notice that imposing a 20% of the k-FWER over the total number of testing hypothesis, does not correspond to accepting a 20% of falsely rejected models, but this percentage refers to the total number of comparisons that are $N^2 - N$, where N is the model number. The confidence level is set to a 5% for a single directional hypothesis. To conserve on space, we perform but only partly report the MCS-*max* test with 10% confidence, as this test is incapable of rejecting models from the initial model set in three out of four experiments[11], suggesting a strong similarity in the model performances. However, for the one test where the MCS-*max* does give an MCS different from the initial model set, only 20 out of 280 models are ultimately rejected.

[11] The MCS test results that have been reported refer to a full sample averages of resampled data. The central limit effect is stronger when constructing the sample in this way, because we are averaging daily RMSE and this procedure yields strongly bell shaped distributions. Nonetheless, there are still wide differences in the results of the MCS-γ from the MCS-*max*, which relays on pivotal statistics. We conjecture that a small sample distribution bias persists while generating the statistic distributions via bootstrapping. As an alternative experiment that is not reported, we generate the MCS with historical simulation, that is considering the statistic distribution as generated by the daily RMSE, entailing more asymmetric and leptokurtic distributions. The results for the MCS-γ are not strongly different, whereby we obtain larger MCS. However, we cannot compare those alternative results with the MCS-*max* either, as again it rejects no model from the initial set. Therefore, in total, the test performed with the MCS-*max* are four, whereby in three out of four cases it cannot reject any model.

The difference between the two MCS approaches is due largely to higher conservatism in the MCS-*max* test relative to the more flexible MCS-γ, which allows a more circumscribed set of superior models via direct control of the k-FWER. The latter result is interesting as it indicates that the MHT based MCS test is able to identify the best performing model in a closely competing contest. On the other hand, the general MCS-*max* outcome is a reminder of a possible attenuated view, whenever the structure of the test is modified alongside the Hansen et al. (2011) paradigm. That is to say that, in the latter test setup, the model performance discrepancies are not strong enough to justify the prevalence of any model within the collective. Considering, however, test dependencies in the MHT framework and exploring the full set of comparisons, we are able to obtain a more stringent model confrontation.

Before moving to the experimental results, we define the model labelling rule. As the model set is very numerous, we adopt the following conventions to identify the model to which the test output is referred. In total, the model set comprises 280 models. Each model label is composed of four, six or eight letters. The first two letters are either a "SV" or "SS" if, respectively, the latent factor is affine or in case there is a jump, the intensity is affine as well and it is determined directly as a function of the latent factor. A "C" in place of the first "S" indicates that the model has a coefficient at the exponent of the diffusion factor of the price SDE making the model be extended to a constant elasticity of variance. A "Z" in the place of the first "S" will indicate a model with log-normal latent factor, as well as a "Z" in the place of the second "S" indicates that there is a jump that is driven by an log-normal stochastic intensity. An "L" in place of the "C" indicates the model is extended with a linear elasticity of variance coefficient. The third and forth letters are either "R0" if $\rho = 0$ or "R1" if $\rho = -0.7$, indicating either a zero leverage effect or a negative leverage effect. The model label is made of four letters if no jumps are included. A six letter model can include the letters "VJ" at the fifth and sixth position, meaning that the model has only an exponential jump in the latent factor or exhibit the letter "CJ" if the model presents a single Poisson factor triggering simultaneous and correlated jumps. A jump in the price level only or unpaired jumps in price and volatility are indicated, respectively, with the letters "XJ" and "JJ" in the fifth and sixth positions. In this case, two more letters indicate the price jump type that can be centred ("N0") or offset ("N1") Gaussian, single sided exponential/Lomax("E1"/"L1"), double sided with constrained ("E2"/"L2") or free ("EE"/"LL") positive jump probability exponential/Lomax distribution jump size.

4.3.2 Market Data Experiment

In this section, we apply the model selection procedures to an equity index option pricing experiment, whereby we search for the best model subset delivering superior RMSE performance. As just outlined, we consider a very large model set including stochastic volatility models with affine or exponential volatility, augmented with many types of jumps in return, exponential jumps in volatility, constant or linear elasticity of variance and stochastic intensity. The S&P500 index option sample is very extensive, containing a large part of the CBOE traded options daily closing NBBO ranging from 02-Jan-1990 to 08-Jul-2015. To the best of our knowledge, this is the first study exploiting such an extensive option sample, both in the time and in the moneyness dimensions, and such a wide model set, which includes combinations of components that yield novel models heretofore not examined in the literature. Furthermore, we con-

tribute with an original application of the MCS test to produce evidence concerning the best equity option pricing models. The model contrasting exercise is complicated by the strong model similarities that are tackled with a rigorous statistical approach. The MCS-*max* test designed alongside the established model confidence set approach of Hansen et al. (2011), struggles to identify top models in a tightly competing set. The design of an alternative model comparison device based on the MHT approach of Romano and Wolf (2010) achieves a more focused MCS.

We perform the model parameter estimation for two samples of option prices; namely, the complete set of option prices across moneyness, the ALL sample, and the sample restricted to just OTM options. The overall performance based off both sets of options data are very similar in terms of RMSE, for each model. However, to reduce parameter uncertainty and homogenise model comparison, we proceed by estimating the parameters for the innermost nested models and thereafter estimate the parameters of the incremental model components - basically the jump components - by holding the core parameters fixed; the only exception here being the diffusion coefficient, in order to capture the variance attribution between the diffusion and the jump factors. In practice, when estimating a jump augmented model, the diffusion component parameters are kept constant but the total variance attributed to diffusion is triggered by the free coefficient. The model implied volatility sequence is free at each optimisation, leaving a highly parametrised optimisation problem which is solved at each iteration recursively over a coarse grid of volatility values. The range of the volatility grid is a large multiple of the stationary variance, given the current parameters. Therefore, the parametric set is exploited for the computation of the time series of the RMSE for each model, whereby each time series is exploited to generate resampled path with the stationary bootstrap that are henceforth averaged to determine the bootstrap distribution of the overall sample average. The results for the MCS-γ are summarised Tab. 38, which exhibits the MCS for the OTM and the ALL option samples at several k-FWER, with k such that $\gamma = \left\lfloor \frac{k}{N(N-1)} \right\rfloor$, with a 5% confidence, whereby here we indicate the number of models with an N. In the OTM options sample, the MCS comprises 19 models in the $\gamma = 20\%$ test and by 5 models in the $\gamma = 40\%$ test. In the ALL options sample, the MCS comprises 34 models in the $\gamma = 20\%$ test and 2 models in the $\gamma = 40\%$ test. The general results are similar. The models with exponential volatility are predominant, a result that can be reconnected with the analysis of Christoffersen et al. (2010). The latter article provides an extensive analysis in terms of the dataset used and technique exploited. The more interesting findings that can be related to this study correspond to the volatility cross-section regression, which is most significant when a log-transform is applied to daily realised volatility, as well as the predominance of the models that allow higher than affine acceleration of the volatility path. In particular, the best model is identified in the ONE model[12], which is able to produce superior pricing error performance. Some exception to this outcome are several CEV affine specifications as in Jones (2003), which are however lower ranked. The solely affine stochastic volatility models are completely rejected, entailing that, not only when compared to jump extensions affine models are rejected, as it is the case in, for instance, Eraker (2004), but also that affine jump-diffusion models generate inferior performance whenever the latent factor acceleration

[12] The ONE model is not included in the model set of this study. However, under a log-transform of the latent factor, this model results in a process with Gaussian innovations and mean reversion of exponential type, that is generating an asymmetric response when above/below the average. Therefore the ONE model differs from the log-linear volatility model only in the response to the pull to the mean, which is asymmetrical.

is augmented with a CEV factor. The correlation factor is highly significant, although several R0 models enters the MCS in both the OTM and ALL sample. The most interesting result is the presence of the ZVR1 model, that is the exponential volatility pure diffusive model with negative correlation (-0.7) in the MCS set of the $\gamma = 20\%$ MCS-γ over the OTM sample. Although with a p-value of 0.3861 against a 0.7791 of the top ranked ZVR1XJE2 (which corresponds to the same model augmented with a constant intensity bi-directional exponential jump in return only, with constrained probability of the positive direction), this outcome is affirming that in the case of OTM options excessive model parametrisation and hence complexity, might be redundant, as for fairly equivalent results in terms of RMSE can be obtained with a model characterised with a lesser number of parameters like the ZVR1. In the case of the ALL options sample, the jumps seems to be necessary to obtain superior results, although the form of the jump does not seem to matter. This result suggests that jumps have a larger impact on ITM options. Jumps in volatility, LEV and stochastic intensity extensions are redundant, whereas ZV**XJ** models are either superior or very highly ranked. Some specifications of the CEV model enters the MCS, but are ranked very low based on p-value. These considerations indicate that option pricing models are overparametrised, beyond necessity, in contrast to studies such as Bates (1996), Eraker et al. (2003) and Eraker (2004). This suggestion is strengthened in the context of the MCS-max test results that for the OTM sample options considers all 280 model specifications to be equivalent, with no sorting possible as a p-value ranking cannot be performed as a measure of model confidence can only be determined in case of rejection. However, the MCS-max test based on the ALL option sample test yields a 260 model MCS, allowing some considerations on the model ranking. Again, highly parametrised models perform better, whereby the models with a p-value of at least 0.99 are all in the exponential volatility class or CEV affine. Interesting, the ZVR1 model is ranked very high, with a p-value of 0.9496, suggesting again that LEV and jumps in volatility and in return might be redundant even for the ALL option sample. On the other hand, these results suggest that perhaps, in a context of tightly performing models, the Hansen et al. (2011) MCS test is either conservative or might require low levels of confidence to restrict the size of the MCS. In this case, the usage of the newly designed MCS-γ test manifests a wider flexibility to handle large set joint model comparison tasks.

4.4 Concluding Remarks

In this chapter, we have compared a large sample of option pricing models by means of novel model selection tests hinging on the model confidence set and exploiting multiple hypothesis testing. We contribute to literature in several directions. We construct model comparison tests with novel MCS techniques targeting a vast array of option pricing models, the majority of which results from the original combination of jumps and alternative volatility specifications. This study provides empirical evidence of the strong aliasing amongst many option pricing models ranging from high to a lower levels of complexity, suggesting scope for model simplification over increasing complexity. We obtain interesting results suggesting an alternative conclusion as opposed to the tendency in the literature to an increasing complexity of the option pricing models. The model selection procedures we apply provide robust evidence indicating that the popular single factor affine specification, extended in several directions, is strongly rejected. Moreover, model augmentation such as jumps in volatility, stochastic hazard, and the parametrisation of the

elasticity of the diffusion factor, are probably excessive model complications. A simple model, such as the ZVR1, that is the correlated exponential volatility model, performs very well in the OTM option sample, whereas the inclusion of a compensated single directional exponential jump in return, that is the ZVR1XJE1 produces one of the top performances for the ALL option sample. Considering the relative novelty of the MCS approach and the new test form we have introduced, that is the MHT version of the MCS test, we provide a qualitative comparison of the outcome of the max-MCS and the γ-MCS test. The general conclusion is that the latter test offers a wider flexibility allowed by the k-FWER controlling mechanism. In contrast, the max-MCS fails to reduce the initial model set at a 10% confidence level. Another difference between the two tests is represented by the use of non pivotal results hinging on the bootstrap device in the γ-MCS test, which exhibits a stronger selection ability in tightly competing model sets.

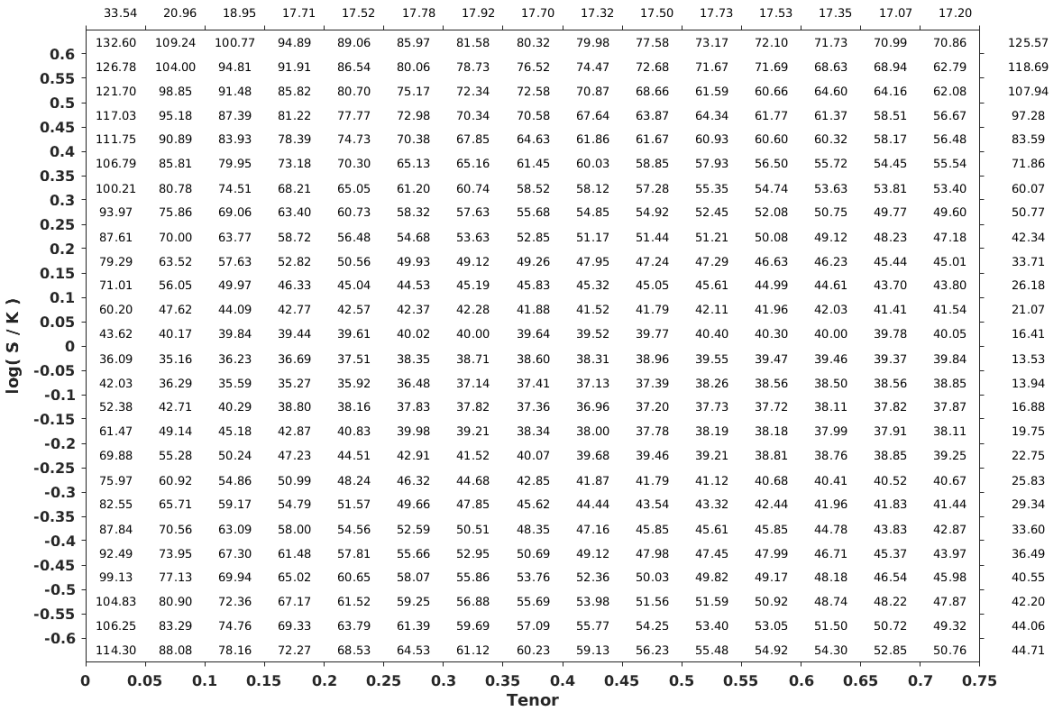

log(S / K) \ Tenor	0	0.05	0.1	0.15	0.2	0.25	0.3	0.35	0.4	0.45	0.5	0.55	0.6	0.65	0.7	0.75	
	33.54	20.96	18.95	17.71	17.52	17.78	17.92	17.70	17.32	17.50	17.73	17.53	17.35	17.07	17.20		
0.6	132.60	109.24	100.77	94.89	89.06	85.97	81.58	80.32	79.98	77.58	73.17	72.10	71.73	70.99	70.86		125.57
0.55	126.78	104.00	94.81	91.91	86.54	80.06	78.73	76.52	74.47	72.68	71.67	71.69	68.63	68.94	62.79		118.69
0.5	121.70	98.85	91.48	85.82	80.70	75.17	72.34	72.58	70.87	68.66	61.59	60.66	64.60	64.16	62.08		107.94
0.45	117.03	95.18	87.39	81.22	77.77	72.98	70.34	70.58	67.64	63.87	64.34	61.77	61.37	58.51	56.67		97.28
0.4	111.75	90.89	83.93	78.39	74.73	70.38	67.85	64.63	61.86	61.67	60.93	60.60	60.32	58.17	56.48		83.59
0.35	106.79	85.81	79.95	73.18	70.30	65.13	65.16	61.45	60.03	58.85	57.93	56.50	55.72	54.45	55.54		71.86
0.3	100.21	80.78	74.51	68.21	65.05	61.20	60.74	58.52	58.12	57.28	55.35	54.74	53.63	53.81	53.40		60.07
0.25	93.97	75.86	69.06	63.40	60.73	58.32	57.63	55.68	54.85	54.92	52.45	52.08	50.75	49.77	49.60		50.77
0.2	87.61	70.00	63.77	58.72	56.48	54.68	53.63	52.85	51.17	51.44	51.21	50.08	49.12	48.23	47.18		42.34
0.15	79.29	63.52	57.63	52.82	50.56	49.93	49.12	49.26	47.95	47.24	47.29	46.63	46.23	45.44	45.01		33.71
0.1	71.01	56.05	49.97	46.33	45.04	44.53	45.19	45.83	45.32	45.05	45.61	44.99	44.61	43.70	43.80		26.18
0.05	60.20	47.62	44.09	42.77	42.57	42.37	42.28	41.88	41.52	41.79	42.11	41.96	42.03	41.41	41.54		21.07
0	43.62	40.17	39.84	39.44	39.61	40.02	40.00	39.64	39.52	39.77	40.40	40.30	40.00	39.78	40.05		16.41
-0.05	36.09	35.16	36.23	36.69	37.51	38.35	38.71	38.60	38.31	38.96	39.55	39.47	39.46	39.37	39.84		13.53
-0.1	42.03	36.29	35.59	35.27	35.92	36.48	37.14	37.41	37.13	37.39	38.26	38.56	38.50	38.56	38.85		13.94
-0.15	52.38	42.71	40.29	38.80	38.16	37.83	37.82	37.36	36.96	37.20	37.73	37.72	38.11	37.82	37.87		16.88
-0.2	61.47	49.14	45.18	42.87	40.83	39.98	39.21	38.34	38.00	37.78	38.19	38.18	37.99	37.91	38.11		19.75
-0.25	69.88	55.28	50.24	47.23	44.51	42.91	41.52	40.07	39.68	39.46	39.21	38.81	38.76	38.85	39.25		22.75
-0.3	75.97	60.92	54.86	50.99	48.24	46.32	44.68	42.85	41.87	41.79	41.12	40.68	40.41	40.52	40.67		25.83
-0.35	82.55	65.71	59.17	54.79	51.57	49.66	47.85	45.62	44.44	43.54	43.32	42.44	41.96	41.83	41.44		29.34
-0.4	87.84	70.56	63.09	58.00	54.56	52.59	50.51	48.35	47.16	45.85	45.61	45.85	44.78	43.83	42.87		33.60
-0.45	92.49	73.95	67.30	61.48	57.81	55.66	52.95	50.69	49.12	47.98	47.45	47.99	46.71	45.37	43.97		36.49
-0.5	99.13	77.13	69.94	65.02	60.65	58.07	55.86	53.76	52.36	50.03	49.82	49.17	48.18	46.54	45.98		40.55
-0.55	104.83	80.90	72.36	67.17	61.52	59.25	56.88	55.69	53.98	51.56	51.59	50.92	48.74	48.22	47.87		42.20
-0.6	106.25	83.29	74.76	69.33	63.79	61.39	59.69	57.09	55.77	54.25	53.40	53.05	51.50	50.72	49.32		44.06
	114.30	88.08	78.16	72.27	68.53	64.53	61.12	60.23	59.13	56.23	55.48	54.92	54.30	52.85	50.76		44.71

Table 31: **The Call Option Average Implied Volatility.** In this table, we show the sample average implied volatility arranged by moneyness per tenor buckets. The top row and the right hand column show the consolidated averages by, respectively, time-to-maturity and relative index price. The sample contains the selected option prices with moneyness ranging in $(0.5, 2)$ and tenor in $(0.01, 0.75)$.

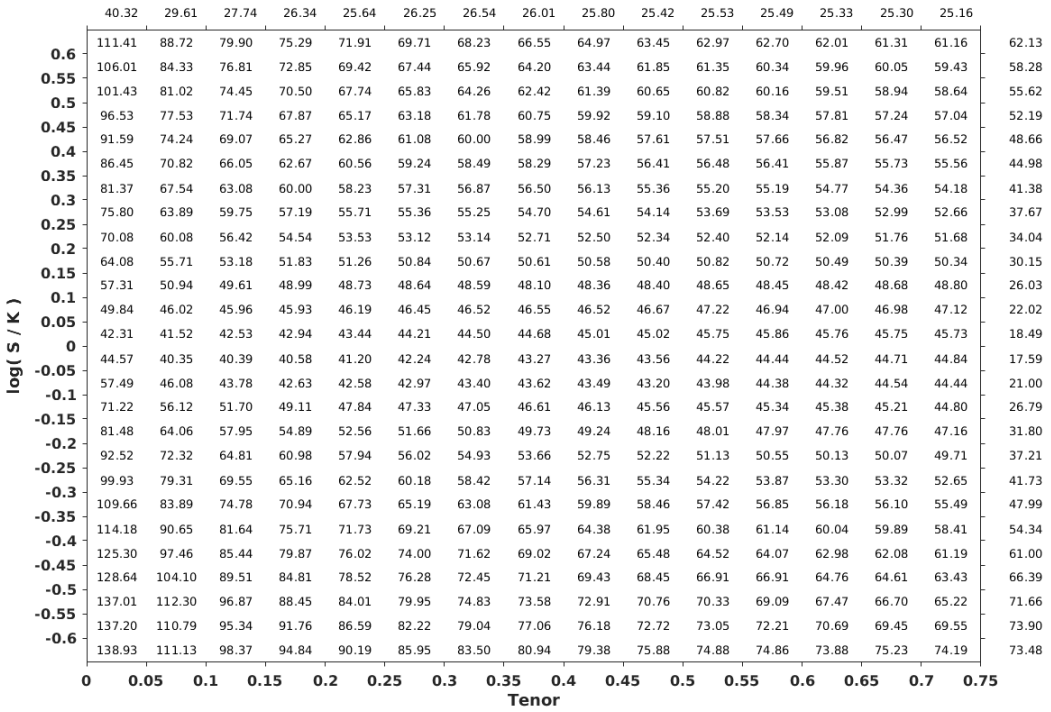

log(S / K) \ Tenor	0	0.05	0.1	0.15	0.2	0.25	0.3	0.35	0.4	0.45	0.5	0.55	0.6	0.65	0.7	0.75	
	40.32	29.61	27.74	26.34	25.64	26.25	26.54	26.01	25.80	25.42	25.53	25.49	25.33	25.30	25.16		
0.6	111.41	88.72	79.90	75.29	71.91	69.71	68.23	66.55	64.97	63.45	62.97	62.70	62.01	61.31	61.16		62.13
0.55	106.01	84.33	76.81	72.85	69.42	67.44	65.92	64.20	63.44	61.85	61.35	60.34	59.96	60.05	59.43		58.28
0.5	101.43	81.02	74.45	70.50	67.74	65.83	64.26	62.42	61.39	60.65	60.82	60.16	59.51	58.94	58.64		55.62
0.45	96.53	77.53	71.74	67.87	65.17	63.18	61.78	60.75	59.92	59.10	58.88	58.34	57.81	57.24	57.04		52.19
0.4	91.59	74.24	69.07	65.27	62.86	61.08	60.00	58.99	58.46	57.61	57.51	57.66	56.82	56.47	56.52		48.66
0.35	86.45	70.82	66.05	62.67	60.56	59.24	58.49	58.29	57.23	56.41	56.48	56.41	55.87	55.73	55.56		44.98
0.3	81.37	67.54	63.08	60.00	58.23	57.31	56.87	56.50	56.13	55.36	55.20	55.19	54.77	54.36	54.18		41.38
0.25	75.80	63.89	59.75	57.19	55.71	55.36	55.25	54.70	54.61	54.14	53.69	53.53	53.08	52.99	52.66		37.67
0.2	70.08	60.08	56.42	54.54	53.53	53.12	53.14	52.71	52.50	52.34	52.40	52.14	52.09	51.76	51.68		34.04
0.15	64.08	55.71	53.18	51.83	51.26	50.84	50.67	50.61	50.58	50.40	50.82	50.72	50.49	50.39	50.34		30.15
0.1	57.31	50.94	49.61	48.99	48.73	48.64	48.59	48.10	48.36	48.40	48.65	48.45	48.42	48.68	48.80		26.03
0.05	49.84	46.02	45.96	45.93	46.19	46.45	46.52	46.55	46.52	46.67	47.22	46.94	47.00	46.98	47.12		22.02
0	42.31	41.52	42.53	42.94	43.44	44.21	44.50	44.68	45.01	45.02	45.75	45.86	45.76	45.75	45.73		18.49
-0.05	44.57	40.35	40.39	40.58	41.20	42.24	42.78	43.27	43.36	43.56	44.22	44.44	44.52	44.71	44.84		17.59
-0.1	57.49	46.08	43.78	42.63	42.58	42.97	43.40	43.62	43.49	43.20	43.98	44.38	44.32	44.54	44.44		21.00
-0.15	71.22	56.12	51.70	49.11	47.84	47.33	47.05	46.61	46.13	45.56	45.57	45.34	45.38	45.21	44.80		26.79
-0.2	81.48	64.06	57.95	54.89	52.56	51.66	50.83	49.73	49.24	48.16	48.01	47.97	47.76	47.76	47.16		31.80
-0.25	92.52	72.32	64.81	60.98	57.94	56.02	54.93	53.66	52.75	52.22	51.13	50.55	50.13	50.07	49.71		37.21
-0.3	99.93	79.31	69.55	65.16	62.52	60.18	58.42	57.14	56.31	55.34	54.22	53.87	53.30	53.32	52.65		41.73
-0.35	109.66	83.89	74.78	70.94	67.73	65.19	63.08	61.43	59.89	58.46	57.42	56.85	56.18	56.10	55.49		47.99
-0.4	114.18	90.65	81.64	75.71	71.73	69.21	67.09	65.97	64.38	61.95	60.38	61.14	60.04	59.89	58.41		54.34
-0.45	125.30	97.46	85.44	79.87	76.02	74.00	71.62	69.02	67.24	65.48	64.52	64.07	62.98	62.08	61.19		61.00
-0.5	128.64	104.10	89.51	84.81	78.52	76.28	72.45	71.21	69.43	68.45	66.91	66.91	64.76	64.61	63.43		66.39
-0.55	137.01	112.30	96.87	88.45	84.01	79.95	74.83	73.58	72.91	70.76	70.33	69.09	67.47	66.70	65.22		71.66
-0.6	137.20	110.79	95.34	91.76	86.59	82.22	79.04	77.06	76.18	72.72	73.05	72.21	70.69	69.45	69.55		73.90
	138.93	111.13	98.37	94.84	90.19	85.95	83.50	80.94	79.38	75.88	74.88	74.86	73.88	75.23	74.19		73.48

Table 32: **The Put Option Average Implied Volatility.** In this table, we show the sample average implied volatility arranged by moneyness per tenor buckets. The top row and the right hand column show the consolidated averages by, respectively, time-to-maturity and relative index price. The sample contains the selected option prices with moneyness ranging in $(0.5, 2)$ and tenor in $(0.01, 0.75)$.

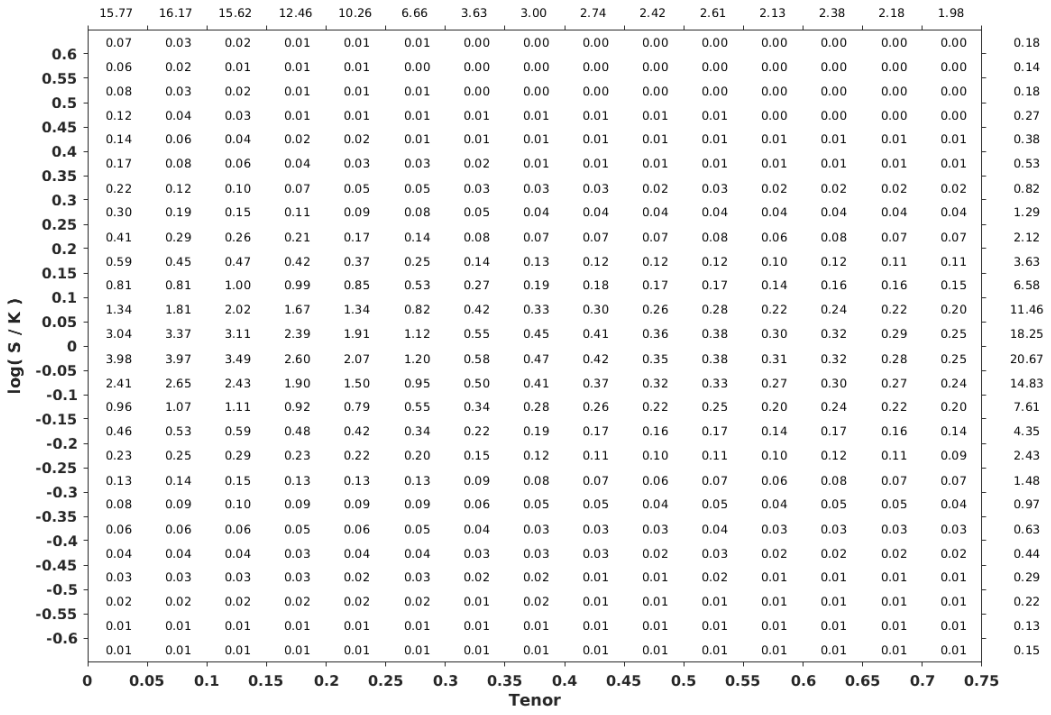

log(S / K) \ Tenor	15.77	16.17	15.62	12.46	10.26	6.66	3.63	3.00	2.74	2.42	2.61	2.13	2.38	2.18	1.98	
0.6	0.07	0.03	0.02	0.01	0.01	0.01	0.00	0.00	0.00	0.00	0.00	0.00	0.00	0.00	0.00	0.18
0.55	0.06	0.02	0.01	0.01	0.01	0.00	0.00	0.00	0.00	0.00	0.00	0.00	0.00	0.00	0.00	0.14
0.5	0.08	0.03	0.02	0.01	0.01	0.01	0.00	0.00	0.00	0.00	0.00	0.00	0.00	0.00	0.00	0.18
0.45	0.12	0.04	0.03	0.01	0.01	0.01	0.01	0.01	0.01	0.01	0.01	0.00	0.00	0.00	0.00	0.27
0.4	0.14	0.06	0.04	0.02	0.02	0.01	0.01	0.01	0.01	0.01	0.01	0.01	0.01	0.01	0.01	0.38
0.35	0.17	0.08	0.06	0.04	0.03	0.03	0.02	0.01	0.01	0.01	0.01	0.01	0.01	0.01	0.01	0.53
0.3	0.22	0.12	0.10	0.07	0.05	0.05	0.03	0.03	0.03	0.02	0.03	0.02	0.02	0.02	0.02	0.82
0.25	0.30	0.19	0.15	0.11	0.09	0.08	0.05	0.04	0.04	0.04	0.04	0.04	0.04	0.04	0.04	1.29
0.2	0.41	0.29	0.26	0.21	0.17	0.14	0.08	0.07	0.07	0.07	0.08	0.06	0.08	0.07	0.07	2.12
0.15	0.59	0.45	0.47	0.42	0.37	0.25	0.14	0.13	0.12	0.12	0.12	0.10	0.12	0.11	0.11	3.63
0.1	0.81	0.81	1.00	0.99	0.85	0.53	0.27	0.19	0.18	0.17	0.17	0.14	0.16	0.16	0.15	6.58
0.05	1.34	1.81	2.02	1.67	1.34	0.82	0.42	0.33	0.30	0.26	0.28	0.22	0.24	0.22	0.20	11.46
0	3.04	3.37	3.11	2.39	1.91	1.12	0.55	0.45	0.41	0.36	0.38	0.30	0.32	0.29	0.25	18.25
-0.05	3.98	3.97	3.49	2.60	2.07	1.20	0.58	0.47	0.42	0.35	0.38	0.31	0.32	0.28	0.25	20.67
-0.1	2.41	2.65	2.43	1.90	1.50	0.95	0.50	0.41	0.37	0.32	0.33	0.27	0.30	0.27	0.24	14.83
-0.15	0.96	1.07	1.11	0.92	0.79	0.55	0.34	0.28	0.26	0.22	0.25	0.20	0.24	0.22	0.20	7.61
-0.2	0.46	0.53	0.59	0.48	0.42	0.34	0.22	0.19	0.17	0.16	0.17	0.14	0.17	0.16	0.14	4.35
-0.25	0.23	0.25	0.29	0.23	0.22	0.20	0.15	0.12	0.11	0.10	0.11	0.10	0.12	0.11	0.09	2.43
-0.3	0.13	0.14	0.15	0.13	0.13	0.13	0.09	0.08	0.07	0.06	0.07	0.06	0.08	0.07	0.07	1.48
-0.35	0.08	0.09	0.10	0.09	0.09	0.09	0.06	0.05	0.05	0.04	0.05	0.04	0.05	0.05	0.04	0.97
-0.4	0.06	0.06	0.06	0.05	0.06	0.05	0.04	0.03	0.03	0.03	0.04	0.03	0.03	0.03	0.03	0.63
-0.45	0.04	0.04	0.04	0.03	0.04	0.04	0.03	0.03	0.03	0.02	0.03	0.02	0.02	0.02	0.02	0.44
-0.5	0.03	0.03	0.03	0.03	0.02	0.03	0.02	0.02	0.01	0.01	0.02	0.01	0.01	0.01	0.01	0.29
-0.55	0.02	0.02	0.02	0.02	0.02	0.02	0.01	0.02	0.01	0.01	0.01	0.01	0.01	0.01	0.01	0.22
-0.6	0.01	0.01	0.01	0.01	0.01	0.01	0.01	0.01	0.01	0.01	0.01	0.01	0.01	0.01	0.01	0.13
	0.01	0.01	0.01	0.01	0.01	0.01	0.01	0.01	0.01	0.01	0.01	0.01	0.01	0.01	0.01	0.15

Table 33: **The Call Option Data Distribution.** In this table, we show the sample data distribution arranged by moneyness per tenor buckets. The top row and the right hand column show the consolidated weights by, respectively, time-to-maturity and relative index price.

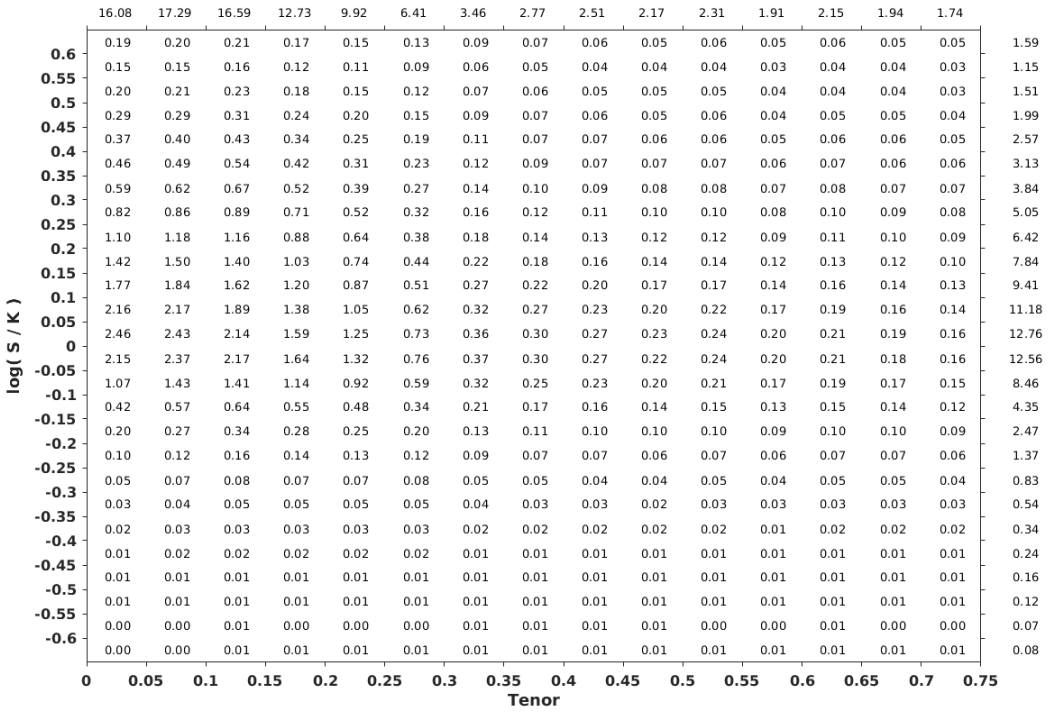

log(S / K) \ Tenor	0	0.05	0.1	0.15	0.2	0.25	0.3	0.35	0.4	0.45	0.5	0.55	0.6	0.65	0.7	0.75	
	16.08	17.29	16.59	12.73	9.92	6.41	3.46	2.77	2.51	2.17	2.31	1.91	2.15	1.94	1.74		
0.6	0.19	0.20	0.21	0.17	0.15	0.13	0.09	0.07	0.06	0.05	0.06	0.05	0.06	0.05	0.05		1.59
0.55	0.15	0.15	0.16	0.12	0.11	0.09	0.06	0.05	0.04	0.04	0.04	0.03	0.04	0.04	0.03		1.15
0.5	0.20	0.21	0.23	0.18	0.15	0.12	0.07	0.06	0.05	0.05	0.05	0.04	0.04	0.04	0.03		1.51
0.45	0.29	0.29	0.31	0.24	0.20	0.15	0.09	0.07	0.06	0.05	0.06	0.04	0.05	0.05	0.04		1.99
0.4	0.37	0.40	0.43	0.34	0.25	0.19	0.11	0.07	0.07	0.06	0.06	0.05	0.06	0.06	0.05		2.57
0.35	0.46	0.49	0.54	0.42	0.31	0.23	0.12	0.09	0.07	0.07	0.07	0.06	0.07	0.06	0.06		3.13
0.3	0.59	0.62	0.67	0.52	0.39	0.27	0.14	0.10	0.09	0.08	0.08	0.07	0.08	0.07	0.07		3.84
0.25	0.82	0.86	0.89	0.71	0.52	0.32	0.16	0.12	0.11	0.10	0.10	0.08	0.10	0.09	0.08		5.05
0.2	1.10	1.18	1.16	0.88	0.64	0.38	0.18	0.14	0.13	0.12	0.12	0.09	0.11	0.10	0.09		6.42
0.15	1.42	1.50	1.40	1.03	0.74	0.44	0.22	0.18	0.16	0.14	0.14	0.12	0.13	0.12	0.10		7.84
0.1	1.77	1.84	1.62	1.20	0.87	0.51	0.27	0.22	0.20	0.17	0.17	0.14	0.16	0.14	0.13		9.41
0.05	2.16	2.17	1.89	1.38	1.05	0.62	0.32	0.27	0.23	0.20	0.22	0.17	0.19	0.16	0.14		11.18
0	2.46	2.43	2.14	1.59	1.25	0.73	0.36	0.30	0.27	0.23	0.24	0.20	0.21	0.19	0.16		12.76
-0.05	2.15	2.37	2.17	1.64	1.32	0.76	0.37	0.30	0.27	0.22	0.24	0.20	0.21	0.18	0.16		12.56
-0.1	1.07	1.43	1.41	1.14	0.92	0.59	0.32	0.25	0.23	0.20	0.21	0.17	0.19	0.17	0.15		8.46
-0.15	0.42	0.57	0.64	0.55	0.48	0.34	0.21	0.17	0.16	0.14	0.15	0.13	0.15	0.14	0.12		4.35
-0.2	0.20	0.27	0.34	0.28	0.25	0.20	0.13	0.11	0.10	0.10	0.10	0.09	0.10	0.10	0.09		2.47
-0.25	0.10	0.12	0.16	0.14	0.13	0.12	0.09	0.07	0.07	0.06	0.07	0.06	0.07	0.07	0.06		1.37
-0.3	0.05	0.07	0.08	0.07	0.07	0.08	0.05	0.05	0.04	0.04	0.05	0.04	0.05	0.05	0.04		0.83
-0.35	0.03	0.04	0.05	0.05	0.05	0.05	0.04	0.03	0.03	0.02	0.03	0.03	0.03	0.03	0.03		0.54
-0.4	0.02	0.03	0.03	0.03	0.03	0.03	0.02	0.02	0.02	0.02	0.02	0.01	0.02	0.02	0.02		0.34
-0.45	0.01	0.02	0.02	0.02	0.02	0.02	0.01	0.01	0.01	0.01	0.01	0.01	0.01	0.01	0.01		0.24
-0.5	0.01	0.01	0.01	0.01	0.01	0.01	0.01	0.01	0.01	0.01	0.01	0.01	0.01	0.01	0.01		0.16
-0.55	0.01	0.01	0.01	0.01	0.01	0.01	0.01	0.01	0.01	0.01	0.01	0.01	0.01	0.01	0.01		0.12
-0.6	0.00	0.00	0.01	0.00	0.00	0.00	0.01	0.01	0.01	0.01	0.00	0.00	0.01	0.00	0.00		0.07
	0.00	0.00	0.01	0.01	0.01	0.01	0.01	0.01	0.01	0.01	0.01	0.01	0.01	0.01	0.01		0.08

Table 34: **The Put Option Data Distribution.** In this table, we show the sample data distribution arranged by moneyness per tenor buckets. The top row and the right hand column show the consolidated weights by, respectively, time-to-maturity and relative index price.

log(S / K) \ Tenor	0	0.05	0.1	0.15	0.2	0.25	0.3	0.35	0.4	0.45	0.5	0.55	0.6	0.65	0.7	0.75	
	44.07	31.47	28.88	26.98	25.83	25.66	25.32	24.35	23.98	23.67	23.67	23.58	23.29	23.05	22.99		
0.6	111.41	88.72	79.90	75.29	71.91	69.71	68.23	66.55	64.97	63.45	62.97	62.70	62.01	61.31	61.16		62.13
0.55	106.01	84.33	76.81	72.85	69.42	67.44	65.92	64.20	63.44	61.85	61.35	60.34	59.96	60.05	59.43		58.28
0.5	101.43	81.02	74.45	70.50	67.74	65.83	64.26	62.42	61.39	60.65	60.82	60.16	59.51	58.94	58.64		55.62
0.45	96.53	77.53	71.74	67.87	65.17	63.18	61.78	60.75	59.92	59.10	58.88	58.34	57.81	57.24	57.04		52.19
0.4	91.59	74.24	69.07	65.27	62.86	61.08	60.00	58.99	58.46	57.61	57.51	57.66	56.82	56.47	56.52		48.66
0.35	86.45	70.82	66.05	62.67	60.56	59.24	58.49	58.29	57.23	56.41	56.48	56.41	55.87	55.73	55.56		44.98
0.3	81.37	67.54	63.08	60.00	58.23	57.31	56.87	56.50	56.13	55.36	55.20	55.19	54.77	54.36	54.18		41.38
0.25	75.80	63.89	59.75	57.19	55.71	55.36	55.25	54.70	54.61	54.14	53.69	53.53	53.08	52.99	52.66		37.67
0.2	70.08	60.08	56.42	54.54	53.53	53.12	53.14	52.71	52.50	52.34	52.40	52.14	52.09	51.76	51.68		34.04
0.15	64.08	55.71	53.18	51.83	51.26	50.84	50.67	50.61	50.58	50.40	50.82	50.72	50.49	50.39	50.34		30.15
0.1	57.31	50.94	49.61	48.99	48.73	48.64	48.59	48.10	48.36	48.40	48.65	48.45	48.42	48.68	48.80		26.03
0.05	49.84	46.02	45.96	45.93	46.19	46.45	46.52	46.55	46.52	46.67	47.22	46.94	47.00	46.98	47.12		22.02
0																	
-0.05																	
-0.1	42.03	36.29	35.59	35.27	35.92	36.48	37.14	37.41	37.13	37.39	38.26	38.56	38.50	38.56	38.85		13.94
-0.15	52.38	42.71	40.29	38.80	38.16	37.83	37.82	37.36	36.96	37.20	37.73	37.72	38.11	37.82	37.87		16.88
-0.2	61.47	49.14	45.18	42.87	40.83	39.98	39.21	38.34	38.00	37.78	38.19	38.18	37.99	37.91	38.11		19.75
-0.25	69.88	55.28	50.24	47.23	44.51	42.91	41.52	40.07	39.68	39.46	39.21	38.81	38.76	38.85	39.25		22.75
-0.3	75.97	60.92	54.86	50.99	48.24	46.32	44.68	42.85	41.87	41.79	41.12	40.68	40.41	40.52	40.67		25.83
-0.35	82.55	65.71	59.17	54.79	51.57	49.66	47.85	45.62	44.44	43.54	43.32	42.44	41.96	41.83	41.44		29.34
-0.4	87.84	70.56	63.09	58.00	54.56	52.59	50.51	48.35	47.16	45.85	45.61	45.85	44.78	43.83	42.87		33.60
-0.45	92.49	73.95	67.30	61.48	57.81	55.66	52.95	50.69	49.12	47.98	47.45	47.99	46.71	45.37	43.97		36.49
-0.5	99.13	77.13	69.94	65.02	60.65	58.07	55.86	53.76	52.36	50.03	49.82	49.17	48.18	46.54	45.98		40.55
-0.55	104.83	80.90	72.36	67.17	61.52	59.25	56.88	55.69	53.98	51.56	51.59	50.92	48.74	48.22	47.87		42.20
-0.6	106.25	83.29	74.76	69.33	63.79	61.39	59.69	57.09	55.77	54.25	53.40	53.05	51.50	50.72	49.32		44.06
	114.30	88.08	78.16	72.27	68.53	64.53	61.12	60.23	59.13	56.23	55.48	54.92	54.30	52.85	50.76		44.71

Table 35: **The (tighter) OTM Call/Put Option Average Implied Volatility.** In this table, we show the sample average implied volatility arranged by moneyness per tenor buckets. The top row and the right hand column show the consolidated averages by, respectively, time-to-maturity and relative index price. The sample contains the selected option prices with moneyness ranging in $(0.5, 2)$ and tenor in $(0.01, 0.75)$.

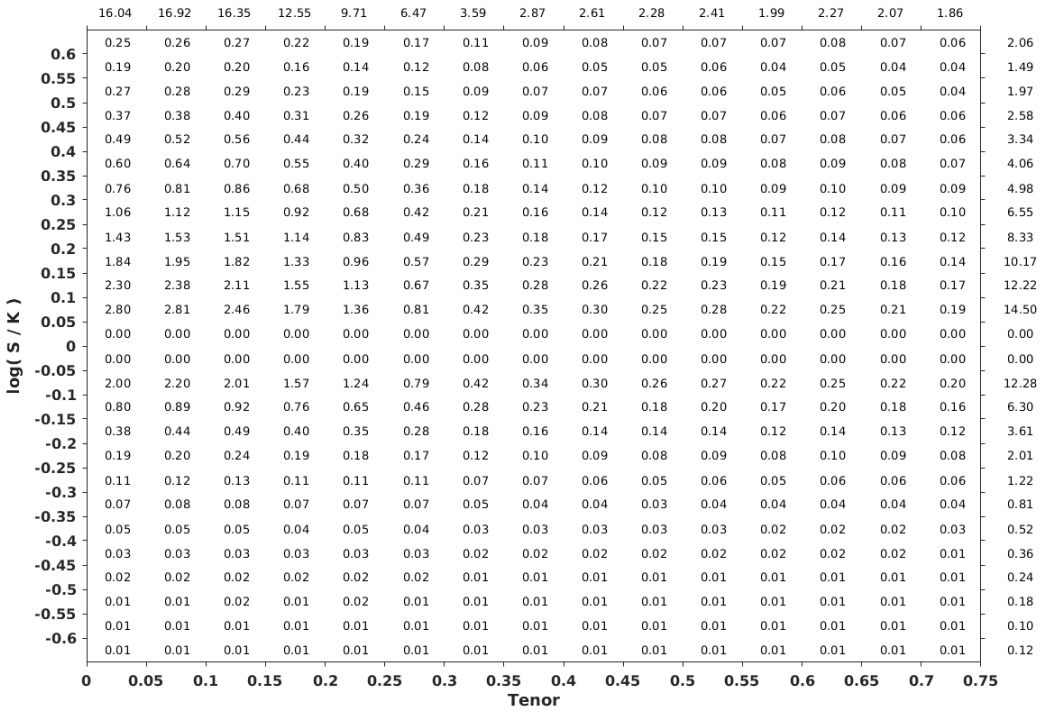

Table 36: **The (tighter) OTM Call/Put Option Data Distribution.** In this table, we show the sample data distribution arranged by moneyness per tenor buckets. The top row and the right hand column show the consolidated weights by, respectively, time-to-maturity and relative index price.

Bootstrap MCS-γ							
OTM sample $\gamma = 20\%$		OTM sample $\gamma = 40\%$		ALL sample $\gamma = 20\%$		ALL sample $\gamma = 40\%$	
ZVR1XJE2	0.7791	ZVR1XJE2	0.6235	LZR1XJE1	0.8220	LZR1XJE1	0.6053
ZZR1XJE2	0.7468	ZZR1XJE2	0.6032	ZZR1XJE1	0.8154	ZZR1XJE1	0.3947
ZVR1CJ	0.7140	ZVR1XJN1	0.4498	LZR1JJE1	0.7925		
ZVR1XJN1	0.6536	ZVR1XJE1	0.4217	LVR1XJE1	0.7214		
ZVR1XJL2	0.6447	ZVR1XJL2	0.4018	LVR1XJEE	0.7051		
ZVR1XJE1	0.6407			ZVR1XJEE	0.6906		
ZVR1XJL1	0.4878			LVR1JJE1	0.6488		
ZZR1XJL1	0.4841			LZR1JJL1	0.5984		
LVR1XJEE	0.4817			ZZR1JJLL	0.5801		
ZVR1XJN0	0.4592			LZR0XJEE	0.5590		
ZZR0XJE2	0.4519			LZR1XJEE	0.5515		
LZR0XJE2	0.4416			LZR1JJLL	0.5503		
LVR1XJE2	0.4356			LZR0XJN1	0.5391		
ZZR1XJLL	0.4153			ZZR1XJLL	0.5297		
ZVR1	0.3868			LZR1XJLL	0.5204		
ZZR1XJL2	0.3861			LZR0XJE1	0.5144		
CVR1CJ	0.3637			LZR0JJE1	0.4963		
ZZR1XJN0	0.2904			LZR1XJL1	0.4954		
LVR1XJLL	0.2368			ZZR1XJL1	0.4952		
				LVR1XJLL	0.4767		
				ZZR0XJE1	0.4606		
				ZZR1XJEE	0.4562		
				LZR0JJN1	0.4547		
				ZZR0XJEE	0.4524		
				ZVR1JJLL	0.3996		
				LVR1JJL1	0.3879		
				ZVR1JJL1	0.3672		
				ZVR1XJLL	0.3596		
				ZVR1XJL1	0.3356		
				LVR1XJL1	0.2798		
				LVR1JJLL	0.2678		
				CSR1XJLL	0.2554		
				CSR1XJL1	0.2354		
				CSR1XJEE	0.1855		

Table 37: **Bootstrap MCS-γ fix at** 20% **and** 40% **OTM and ALL sample.** In this table, we present the MCS results for the model selection of the OTM and ALL sample estimated option pricing model experiment, exploiting the MCS-γ with fixed k-FWER at 20% and 40% of the total number of comparisons. When compared with the following Tab. 38 with respect to the ALL sample, it is evident how the novel MHT based MCS test is capable of a more selective results, which can be modulated by targeting the k family-wise error rate. The main result ofthe analysis is represented by the rejection of the affine family, which does not produce any equivalent performance to the best MCS. It also worth to notice the performance of a simplified model, such as the ZVR1, that is the diffusive log-normal volatility model, which enters the restricted MCS for the OTM sample. Simple augmentations to this model, such as a single directional jump, as in the ZVR1XJE1 in the latter sample, or the stochastic intensity in the ALL sample (an extension that does not include further parameters) produce one of the top models.

Bootstrap MCS-*max* ALL sample									
LZR1XJE1	1	SSR1JJE1	0.9719	CVR1JJEE	0.8729	SVR1XJL2	0.6951	LVR0JJE2	0.4715
ZZR1XJE1	1	ZVR1XJL2	0.9678	ZVR0XJL1	0.8708	LVR0JJE1	0.6924	CSR0JJLL	0.4485
LZR1JJE1	1	CSR1XJE1	0.9662	LVR0CJ	0.8702	SVR1JJL2	0.6784	SSR0JJL2	0.4411
LVR1XJE1	1	ZVR0XJEE	0.9626	ZVR0XJLL	0.8653	LVR0JJEE	0.6776	SVR0XJL2	0.4313
LVR1XJEE	1	SSR0JJEE	0.9596	SVR1XJLL	0.8649	SVR1JJE2	0.6738	SSR1XJN0	0.4288
LZR1JJL1	1	SSR0JJE1	0.9595	SVR1JJE1	0.8625	LVR0XJEE	0.6705	ZVR1JJN0	0.4248
ZVR1XJEE	1	LVR0XJE1	0.9561	LVR1CJ	0.8618	ZZR0JJN0	0.6656	ZZR0XJE2	0.4248
ZZR1JJLL	1	SSR1XJL1	0.9556	SVR1XJL1	0.8564	SVR1JJLL	0.6638	CSR0XJLL	0.4247
LZR1JJLL	1	LZR0JJEE	0.9541	LZR1JJEE	0.8484	SSR0JJLL	0.6624	LVR1JJN0	0.4241
LZR1XJEE	1	ZVR0XJE1	0.9507	ZVR0XJE2	0.8456	LZR0JJN0	0.6613	CVR1JJN1	0.4138
LVR1JJE1	1	ZVR1	0.9496	LVR0XJL2	0.8402	CSR1XJN0	0.6553	CSR1JJE2	0.4072
ZZR1XJLL	0.9999	SSR1XJLL	0.9491	LVR0XJE2	0.8338	SVR1JJN0	0.6527	LVR1JJN1	0.4038
LVR1XJLL	0.9999	SSR0JJN1	0.9444	CVR1JJLL	0.8335	SVR1JJL1	0.6514	CSR0XJL1	0.3969
ZZR1XJL1	0.9999	SSR1XJEE	0.9421	LZR1JJL2	0.8267	CSR0XJE1	0.6450	CVR0JJE2	0.3904
LZR1XJLL	0.9999	LZR0XJLL	0.9411	ZVR0XJL2	0.8222	SSR0JJL1	0.6448	CVR0JJLL	0.3862
LZR1XJL1	0.9999	LVR1	0.9409	CVR1XJLL	0.8208	ZVR1XJN0	0.6242	CVR0XJL1	0.3854
ZVR1JJLL	0.9999	SSR0JJE2	0.9390	CSR0XJEE	0.8205	ZVR1JJE2	0.6241	CSR0JJL2	0.3676
ZVR1JJL1	0.9999	CSR1JJL1	0.9340	CVR1XJN1	0.8201	LVR0	0.6142	ZVR0XJN0	0.3642
ZVR1XJLL	0.9999	CSR0JJEE	0.9323	CVR1JJL1	0.8158	CVR1XJEE	0.6118	CVR0XJLL	0.3498
ZZR1XJEE	0.9999	LZR0XJL1	0.9309	ZZR0XJN0	0.8127	LVR1XJN0	0.6089	CSR0JJN0	0.3436
LVR1JJL1	0.9999	CSR0JJE2	0.9253	LVR1JJL2	0.8119	SSR1JJE2	0.6004	SVR0JJEE	0.3414
ZVR1XJL1	0.9999	LVR1VJ	0.9230	LZR1XJL2	0.8080	ZVR0JJN1	0.5952	LVR0JJN0	0.3340
LVR1JJLL	0.9993	CVR1JJE1	0.9220	ZVR0JJL2	0.8064	LVR0JJL2	0.5950	ZVR0JJN0	0.3300
LVR1XJL1	0.9993	ZZR0XJLL	0.9216	LZR0XJN0	0.7973	CVR1XJE1	0.5909	LVR0XJN0	0.3203
LZR0XJN1	0.9987	CSR1JJLL	0.9212	LVR1JJE2	0.7915	CVR1XJL2	0.5846	SVR0JJE1	0.3140
CSR1XJLL	0.9987	ZZR1XJE2	0.9203	SVR1XJE1	0.7829	SSR1JJL2	0.5761	SVR0JJL2	0.3058
LZR1XJN1	0.9986	ZZR0XJL1	0.9165	LZR0JJE2	0.7768	SSR1JJN0	0.5755	SVR0XJEE	0.2930
CSR1XJL1	0.9983	LZR0JJL1	0.9155	SVR1XJEE	0.7728	SSR1XJE2	0.5590	SVR0XJN1	0.2865
ZVR1XJE1	0.9969	ZVR0JJL1	0.9149	CVR0JJL1	0.7693	CSR1JJN0	0.5565	CSR0XJL2	0.2801
LZR0JJN1	0.9957	CSR0JJN1	0.9146	CSR1XJE2	0.7687	SVR0JJL1	0.5559	SVR0CJ	0.2728
LZR1XJE2	0.9950	ZVR1XJE2	0.9124	CSR1JJN1	0.7654	ZVR1XJN1	0.5554	SSR0XJL2	0.2671
CSR1XJEE	0.9946	ZVR0XJN1	0.9111	ZZR1JJEE	0.7583	SVR1XJN0	0.5494	CVR1VJ	0.2648
ZZR1XJN0	0.9941	LZR0JJLL	0.9098	CVR1XJL1	0.7530	CVR1JJE2	0.5465	SVR0XJE1	0.2583
LZR0JJE1	0.9939	SSR0XJEE	0.9095	ZVR0JJE1	0.7512	ZVR1JJEE	0.5306	ZVR1JJN1	0.2577
ZZR1JJE1	0.9933	LVR0XJN1	0.9088	LZR0XJE2	0.7509	CVR1JJL2	0.5253	CSR0XJN1	0.2575
LZR1XJN0	0.9929	SSR0XJE1	0.9071	SSR0XJLL	0.7494	LVR0JJLL	0.5243	SSR0JJN0	0.2425
ZZR0XJE1	0.9926	ZVR0JJLL	0.9057	SVR1XJN1	0.7405	CVR1XJE2	0.5241	CSR0XJN0	0.2406
LZR0XJEE	0.9919	ZVR1JJL2	0.9054	ZZR0JJL2	0.7394	CVR1XJN0	0.5203	ZVR0JJE2	0.2243
ZZR0XJEE	0.9917	SSR1JJEE	0.9044	ZZR1JJN0	0.7370	SVR1XJE2	0.5164	SVR0JJN1	0.2017
LZR0XJE1	0.9907	LVR0XJLL	0.9033	CSR1JJL2	0.7342	SSR1XJL2	0.5149	SVR0XJE2	0.1893
ZZR1JJL2	0.9899	SSR1JJN1	0.9012	ZZR0XJL2	0.7247	CVR1CJ	0.5103	CVR0VJ	0.1828
ZZR1XJL2	0.9897	LVR0JJL1	0.8998	CSR1XJL2	0.7229	ZVR0	0.5044	LVR0VJ	0.1827
ZZR1XJN1	0.9881	LVR0XJL1	0.8979	CSR1XJN1	0.7193	SVR0XJL1	0.5043	SVR0XJN0	0.1791
LVR1XJL2	0.9866	ZVR1VJ	0.8968	SVR1JJN1	0.7172	ZZR0XJN1	0.5021	SVR1VJ	0.1765
ZVR1CJ	0.9859	CSR0JJE1	0.8965	SVR1CJ	0.7151	SSR0XJE2	0.4949	SSR0XJN0	0.1751
SSR1XJE1	0.9856	SSR0XJN1	0.8923	CSR1JJEE	0.7150	SVR0XJLL	0.4884	SVR0VJ	0.1568
ZZR0JJN1	0.9839	SSR1JJL1	0.8867	ZVR0JJEE	0.7140	SVR0JJLL	0.4831	SVR1	0.1536
CSR1JJE1	0.9819	SSR1XJN1	0.8863	LVR1XJN1	0.7093	CVR1JJN0	0.4806	SVR0JJN0	0.1531
LZR1JJN0	0.9816	LVR1XJE2	0.8855	LZR0JJL2	0.7057	CSR0JJL1	0.4805	SVR0JJE2	0.1426
ZVR1JJE1	0.9799	SVR1JJEE	0.8826	SSR0XJL1	0.7038	ZVR0VJ	0.4788	LZR0XJL2	0.1226
ZZR0JJEE	0.9792	SSR1JJLL	0.8782	ZZR0JJE1	0.6994	LVR0JJN1	0.4739	CVR0XJL2	0.1220
LZR1JJN1	0.9746	ZVR0CJ	0.8750	LVR1JJEE	0.6979	LZR1JJE2	0.4736	ZZR1JJN1	0.1042

Table 38: **Bootstrap MCS-*max* at** 10% **ALL sample.** In this table, we present the MCS results for the model selection of the ALL sample estimated option pricing model experiment, exploiting the MCS-*max* with 10% confidence. We notice the lack of selection ability of the test with closely competing models. The p-value can produce some ranking and discriminate across the models. The application to the OTM sample of the same test with the same confidence level yields an empty set of rejected models. This test exhibits inconsistency for the *max*-MCS that, in the context of a large model set, provides non intuitive results. Foremost, the plain stochastic volatility model SVR1, although with a low p-value, enters the MCS and, according to the null hypothesis, is supposed to belong to the set of equivalently bet performing models.

Figure 6: S&P500 Index Level.

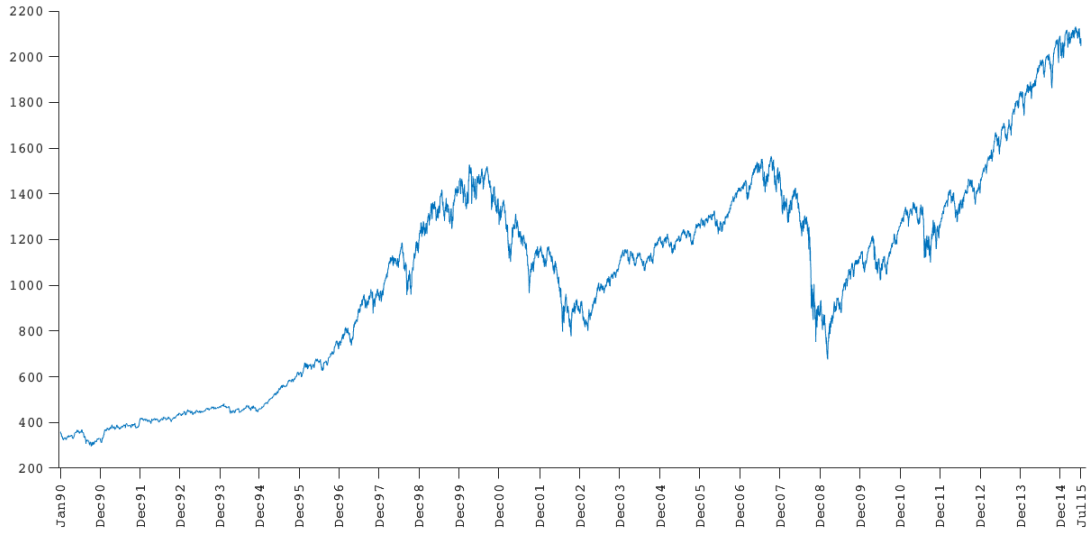

Figure 7: Put/Call Parity Distribution.

The figure shows the event counting of the Put/Call parity of the full option sample, after the cut-off of the 5-97.5 percentile tails. We notice the quite wide range of variation of the relative price unbalance, which appears to be more concentrated on the negative tail.

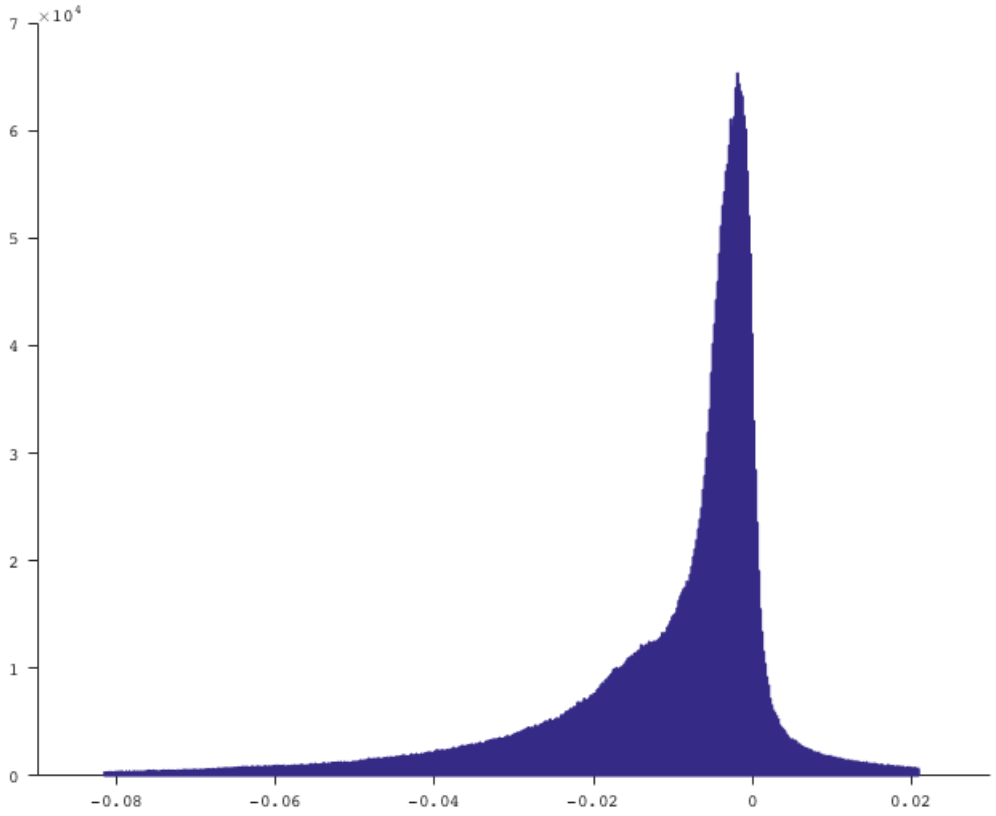

Figure 8: The Selection of the Option Price Sample.

The figure shows the option price sample before and after the data selection, implemented by dropping the option pairs displaying extreme put/call parity behaviour. A marginal data point selection has been achieved via visual inspection. The charts shows, proceeding from the top to the bottom, the call option sample (blue points) before and after the selection, plotted on the x axis showing the difference between the actual index level and the strike, irrespective of the time-to-maturity dimension. The put option sample (red points) before and after the selection are exhibited at the bottom of the chart.

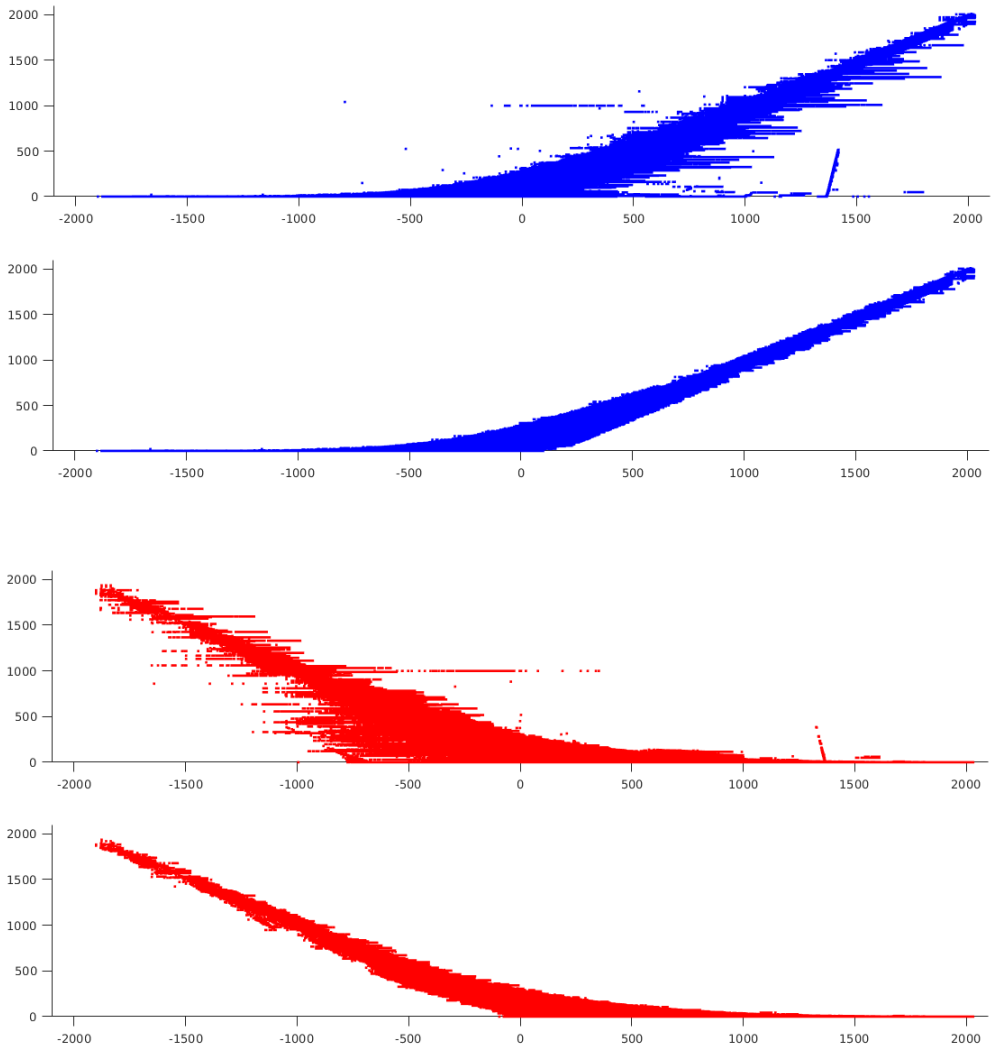

Figure 9: Time Series Features of the Option Price Sample.

The figure shows the coverage of the tenor dimension of the option price sample, as the time elapses. Each point of the upper chart displays, on the ordinates, the time-to-maturity of each option pair at each trading day, reported in the abscissa. The lower chart shows the relative option price sample time series by plotting the call/put values (blue/red points), whereby the put price have inverted sign for compactness purposes.

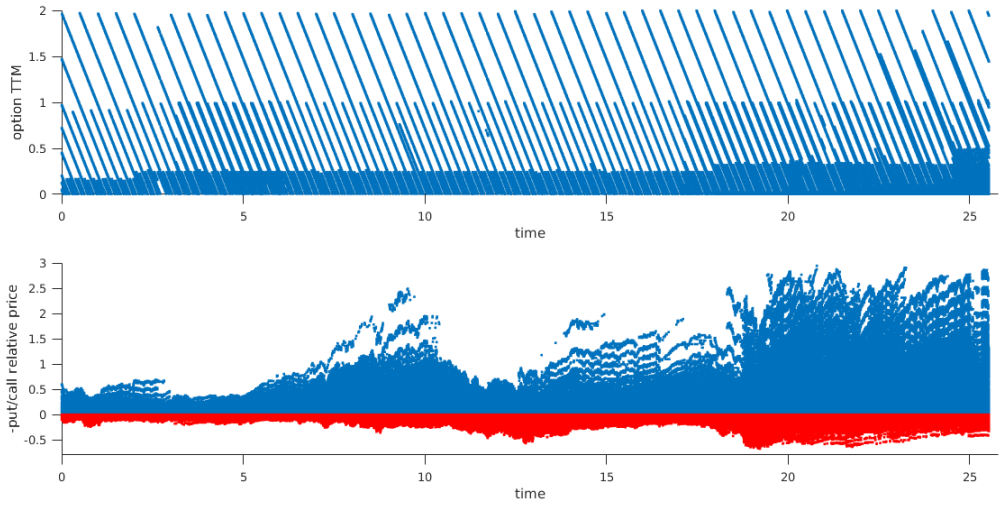

Figure 10: The RMSE Time Series.

The figure shows the average across the models of the daily RMSE in percentage obtained from the interpolation of the option pricing function over the ALL option sample. The red dots represents the daily min and max RMSE across the model sample data. There seems to be a visible pattern of the model RMSE, starting from the late 90's, whereby the dispersion of the RMSE appears to have shrunk. We conjecture that either the quality of the average model has improved, implying less and less price outliers, or more simply, the range of the traded options has grown in such a way that the average RMSE has reduced, although larger pricing error might be concentrated on certain areas of the moneyness/maturity domain.

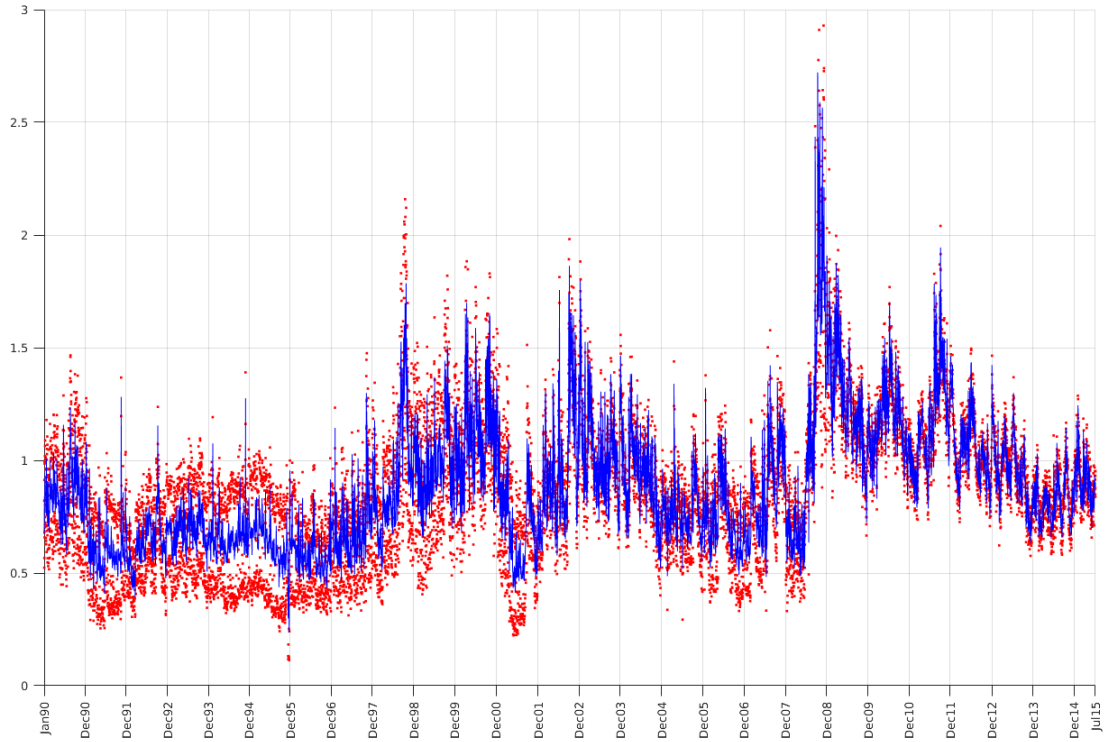

Figure 11: The Volatility Surface Quantile Regression.

The figure shows in the upper chart the OTM sample exploited for the over-the-money volatility surface quantile regression procedure. The same procedure is also applied to the full sample of call and put prices, therefore producing the call and put volatility surface percentile. The lower chart exhibits the median OTM volatility surfaces.

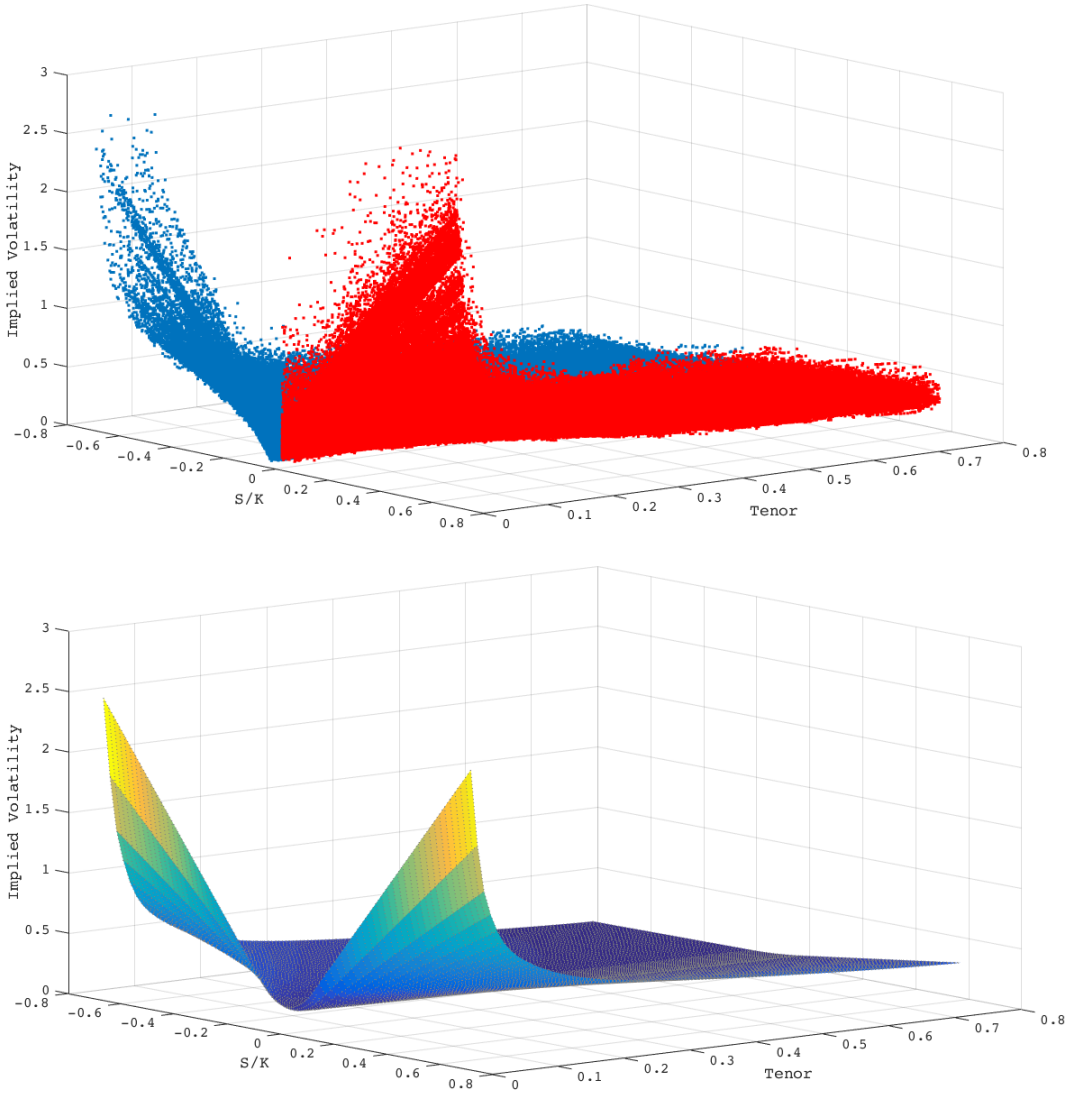

Conclusions

In this thesis, we have presented several applications of the generalised MHT approach of Romano and Wolf (2005a, 2007, 2010), providing a statistical method to confront the problem of model selection in a very general setting. The experimental exercises that have been conducted, provide an example of the flexibility and ease of implementation of the proposed tests. Disregarding the complexity of the problem, the procedure requires only bootstrap samples of the target model performance measures and is capable of delivering tests of significance, tests of benchmark comparison (relative model performance) and tests for the automatic selection of the equivalently best performing models (absolute model performance), the latter achieved with the support of the MCS construction (Hansen et al., 2011). In Chapter 2, we have designed tests of model performance statistical significance with the balanced confidence set introduced in the seminal work of Beran (1988a,b, 1990) and generalised in the reference work of Romano and others, further augmented with the step-down method of Romano and Wolf (2005a, 2007) and Romano and Shaikh (2006), an MHT procedure that allows to increase the power of the test. In a particular experiment of Chapter 3, we have utilised the concept of model comparison via a loss function implemented in studies such as Diebold and Mariano (1995), West (1996) to derive relative model comparison tests targeting a benchmark model, in a context similar to the reality check of White (2000) and the superior

predictive ability test of Hansen (2005). Despite the similarity with the objective of these tests, our contribution is original in that we have designed relative performance tests within the MHT framework that not only test the hypothesis of models being superior to the benchmark, but that are otherwise capable of identifying the subsets of superior, equivalent and inferior models such to partition the initial set into the corresponding collections of superior, equivalent and inferior models. Comparable explicit results have previously been obtained, within the context of MHT, in the article of Romano and Wolf (2005b). When the structure of the problem permits the exploitation of the relative performance test, the inference is delivered by a single instance of the procedure, as in the simulated experiment of Section 3.3.2. Alternatively, when a benchmark is not identifiable or even unnecessary, we have experimented the use of the relative performance test by circulating the benchmark model across the model set, as executed in the first part of Section 3.3.3. This approach has the benefit of exposing the complete pairwise contrasting of the models belonging to the initial model set, but otherwise providing an excess of information that can be synthesised into a model selection decision only through a careful and, to a certain extent, subjective process of consideration. With this regard, in this thesis we have provided a significant further contribution to the literature by assembling a model selection procedure for the automatic detection of the set of superior models, which inherits all the properties of the generalised MHT. In the Chapter 2, Chapter 3 and Chapter 4, we have built on the MCS concept introduced by the seminal work of Hansen et al. (2011), as defined in (1.3.1), and designed absolute model performance tests. This procedure is represented by the γ-MCS of Section 1.3.3, an MHT that regards the model selection as a multi-dimensional test involving hypotheses of model superiority on the full set of pairwise model comparisons, which eventually filters those accepted hypotheses with the application of the MCS rule. As a term of reference, we have constructed the established MCS test of the cited authors with the implementation of the *max*-MCS as in Section 1.3.1, which delivers also a p-value model ranking measure that is based on the sequence of the p-values of the target statistic. On the contrary, the model ranking measure associated to our novel test builds on the multidimensional statistic bootstrap distribution and provides an estimate of the probability that each model in the model set be superior to any element belonging to the MCS. As a complementary exercise, we have also included a streamlined MCS test version by modifying and adapting the approach in Corradi and Distaso (2011), a method that disregards test dependencies and the control of the k-FWER, as presented in Section 1.3.2. This test displays some affinity with the γ-MCS, in that it potentially explores the full combination of model comparisons, but instead ignores the hypotheses structure relaying on scalar asymptotic tests for the implementation of the preference decision rule. We have indicated this test as the t-MCS. The model ranking measure delivered by the t-MCS is defined by taking the worst expected relative performance for each model as determined by the bootstrap method and computing the complement of its quantile on a standard normal distribution, that is the worst p-value for each model with respect to any model comparison. The observation of the experimental results highlights the importance of the MHT paradigm, which in situations whereby the model selection is problematic, allows to modulate between some conservative results, such those provided by the *max*-MCS and some other boundary outcomes, such those provided by the t-MCS, which tends to strongly restrict the MCS. With this research, we have been studying procedures that allow flexibility of usage, preserving robustness and rigour of the analysis. As a result, the model selection procedures that we have presented have the merit of reducing the main research question to a problem of exper-

imental design, leaving to the investigator the task of the construction of the model performance measure.

In the course of the experimental exercises, we have explored and provided significant evidence concerning several problems in financial econometrics involving the decision as to which model is preferable for a given task. We have analysed three typical prototype problems in investment portfolios exposed to market risk, that is the estimation of several portfolio risk metrics such as the VaR and the ExS, as well as the estimation of the historical and the risk-neutral measures of widely employed stochastic processes in finance, such as JD models. In Chapter 2 we have dealt with market risk model selection. Targeting model performance measures of VaR and ExS, we have constructed statistical significance MHT and absolute model performance test. The model set contains a small but very diverse collection of market risk forecasting model. We have obtained results that diverge from the precedent analysis of Bao et al. (2006), whose general conclusion consists in the lack of a superior model in the relative performance contest, whereby the benchmark model is represented by the RiskMetrics model. On the contrary, we provide evidence that some of the GARCH models and to a certain extent the quantile regression models, provide the best performance on the short term horizon, whereas on the longer forecast horizon the MCS is very wide and the model ranking measure only can provide some indications. In Chapter 3, we have tackled the estimation of JD models under the historical measure. We have produced an original model selection exercise involving affine models with jump extensions, as well as stochastic intensity models with high frequency jumps. The analysis of this chapter has targeted measures of likelihood and of filtering performance. With the market data experiment, we have obtained evidence confirming the findings of Jones (2003) in relation to the superiority of the CEV extension with respect to the plain affine stochastic volatility model, as well as highlighting the importance of jumps in returns, as in Andersen et al. (2002), Chernov et al. (2003) and Eraker et al. (2003). Furthermore, the analysis of MCS tests has rejected the inclusion of a jump in the volatility factor, providing an element of model simplification, as opposed to the result of Eraker et al. (2003) and more in line with what has been remarked in Chernov et al. (2003), although the results of our test concerning the jump in volatility component are more explicit. Another interesting result of the market data experiment pointed out the excellent performance of some SH models, providing indication for a slightly more parsimonious parametrisation. Finally, with the Chapter 4, we have explored model selection from a very large JD option pricing model set. The analysis of this chapter has targeted a measure of RMSE. The particularly large model set and the extreme similarity of the model performances have caused troubles to the *max*-MCS, which has not been able to discriminate across the competitors collection. In this exercise the flexibility of our novel γ-MCS has revealed a substantial advantage. Moreover, the tests have provided indication of the superiority of the exponential stochastic volatility model, a result in line with the findings of Christoffersen et al. (2010), whereby models producing high kurtosis and large spikes in the volatility factor are preferable. The results of our tests also points to a containment of the complexity of the model.

As a further contribution to the literature of this thesis, in Chapter 2 we have produced a novel ExS test and in Chapter 3 we have extended the nonlinear filter of Maybeck (1982) with a jump component.

With regards to a thorough comparison of the model selection tests employed in this thesis, we remark

that such a task is beyond the scope of the work. However, from a theoretical standpoint, we notice the following. Foremost, we are inclined to prefer the γ-MCS as the *max*-MCS lacks of control for the generalised FWER, whereby in a context such that the number of tests in the MHT is remarkable, the control of the mere FWER becomes too stringent. Moreover, the γ-MCS, hinging on the MHT approach, it grants the *strong* control of the k-FWER. In more practical terms regarding the confrontation of the different tests, we have collected evidence that allows qualitative comparison. We have encountered diverse circumstances, whereby the *max*-MCS and the γ-MCS tend to perform similarly in a context whereby the best models are unambiguously identified, such as the 1d market risk metrics forecast experiment in Chapter 2 and the LRMCS test of the market data experiment in Chapter 3, whereas the t-MCS produces smaller top model sets. We notice moreover that, as it allows for the control of the generalised FWER, the MHT based MCS offers a gear to modulate the sensitivity to false rejections and hence identify models that are close to rejection, further contracting the MCS. Under conditions whereby the model comparison is more ambiguous and all of the MCS tests struggle to identify the best model set, as it is the case of the 2w forecasting exercise of Chapter 2 and the simulation experiment involving model aliasing of Chapter 3, the γ-MCS provides a more informative model ranking measure, while the t-MCS results in a tighter selection. The latter test might be useful as a quick diagnostic tool to identify the region containing the candidate best models or in conditions where it is difficult to distinguish models, the t-MCS might provide a term of comparison for various γ values in the γ-MCS. In the final model selection exercise of Chapter 4, we deal with a very large model set, whereby the ability of the γ-MCS to modulate the result by targeting different k-FWER allows one to focus upon the set of best performing models, whereas the benchmark test *max*-MCS is incapable of providing any insight as for the best model set out of the initial pool. A further term of comparison can be identified in the behaviour of the p-value, that in the case of the *max*-MCS exhibits the tendency for a lack of discriminating capacity between the top section of the MCS components. Eventually, the p-value model ranking measure that we construct for our novel test, provides a highly significant ranking factor. In conclusion, the model selection tests we develop and apply in this research constitute an approach that is very promising in providing important support in problems of model risk.

For the future research, we expect the refinement of the core procedures and plan to extend the study of the theoretical properties of the *max*-MCS and the γ-MCS and how they relate each other and they relate to a test such as the t-MCS. Moreover, the many algorithms that have been studied and developed in this research provide further matter for extensions and application to financial econometric problems such as market risk, filtering, likelihood estimation and pricing. Finally, we notice that particularly in the context of JD models, the uncertainty related to the parameters estimation is considerable and hence further research in this domain aiming at producing applications in the model risk space is attractive. In particular, a topic of interest is the measurement of the model risk associated to parameter uncertainty. Further analysis can be conducted in the domain of model transformations that simplify the computation procedures and reduce the estimation risk. Moreover, we notice that the analysis in Chapter 3 is partial to a certain extent, as it lacks further testing in term of loss measures targeting specifically the distribution tails, and the analysis would benefit from an extension of the likelihood to a full Bayesian approach. As a notice for future research in relation to Chapter 4, a limitation of this study consists of the lack

of analysis such as the coherence of the implied factor distributions generated by market prices or the hedging performance of the model set such as, for instance, in Bakshi et al. (1997), Bates (2000). Further directions of future research might concern the derivation of statistical arbitrage strategies through the analysis of the dynamics of the mispricing error or that of the premium to a replicating portfolio strategy. Another important insight, which has been suggested by the examiners, consists of exploring the model ranking through time to highlight possible patterns in the evolution of the pricing errors, which might inform the construction of statistical arbitrage trading strategies.

Bibliography

Aït-Sahalia, Y. (1996). Testing continuous-time models of the spot interest rate. *Review of Financial Studies*, 9:385–426.

Aït-Sahalia, Y. (1999). Transition densities for interest rate and other nonlinear diffusions. *Review of Financial Studies*, 54:1361–1395.

Aït-Sahalia, Y. (2002). Maximum likelihood estimation of discretely sampled diffusions: a closed-form approximation approach. *Econometrica*, 70(1):223–262.

Aït-Sahalia, Y. (2004). Disentangling diffusion from jumps. *Journal of Financial Economics*, 74:487–528.

Aït-Sahalia, Y. (2008). Closed-form likelihood expansions for multivariate diffusions. *The Annals of Statistics*, 36(2):906–937.

Aït-Sahalia, Y. and Kimmel, R. (2007). Maximum likelihood estimation of stochastic volatility models. *Journal of Financial Econometrics*, 83:413–452.

Akaike, H. (1974). A new look at the statistical model identification. *Automatic Control, IEEE Transactions on Automatic Control*, 19(6):716–723.

Akaike, H. (1981). Likelihood of a model and information criteria. *Journal of Econometrics*, 16(1):3–14.

Andersen, T., Benzoni, L., and Lund, J. (2002). An empirical investigation of continuous time equity return models. *Journal of Finance*, 57(3):1239–1284.

Artzner, P., Delbaen, P., Eber, J., and Heath, D. (1999). Coherent measures of risk. *Mathematical Finance*, 9(3).

Baadsgaard, M., Nielsen, J., and Madsen, H. (2000). Estimating multivariate exponential-affine term structure models from coupon bond prices using nonlinear filtering. *Econometric Journal*, 3:1–20.

Bakshi, G., Cao, C., and Chen, Z. (1997). Empirical performance of alternative option pricing models. *The Journal of Finance*, 52(5):2003–2049.

Bakshi, G., Ju, N., and Ou-Yang, H. (2006). Estimation of continuous-time models with an application to equity volatility dynamics. *Journal of Financial Economics*, 82(1):227–249.

Bao, Y., Lee, T., and Saltoğlu, B. (2006). Evaluating predictive performance of Value-at-Risk models in emerging markets: A reality check. *Journal of Forecasting*, 25.

Bao, Y., Lee, T., and Saltoğlu, B. (2007). Comparing density forecast models. *Journal of Forecasting*, 26.

Barndorff-Nielsen, O. and Shephard, N. (2002). Econometric analysis of realized volatility and its use in estimating stochastic volatility models. *Journal of the Royal Statistical Society: Series B (Statistical Methodology)*, 64(2):253–280.

Barndorff-Nielsen, O. and Shephard, N. (2004). Power and bipower variation with stochastic volatility and jumps. *Journal of Financial Econometrics*, 2(1):1–37.

Basel Committee on Banking Supervision (2009). Supervisory guidance for assessing banks' financial instrument fair value practices. Technical report, Bank for International Settlements.

Bates, D. (1996). Jumps and stochastic volatility: exchange rate processes implied in deutsche mark options. *Review of Financial Studies*, 9:69–107.

Bates, D. (2000). Post-'87 crash fears in the S&P 500 futures option market. *Journal of Econometrics*, 94(1-2):181–238.

Beckers, S. (1980). The constant elasticity of variance model and its implications for option pricing. *Journal of Finance*, 35(3):661–73.

Benjamini, Y. and Hochberg, Y. (1995). Controlling the false discovery rate: a practical and powerful approach to multiple testing. *Journal of the Royal Statistical Society, B*, 57(1):289–300.

Benjamini, Y. and Hochberg, Y. (2000). On the adaptive control of the false discovery rate in multiple testing with independent statistics. *Journal of Educational and Behavioural Statistics*, 25(1):60–83.

Benzoni, L. (2002). Pricing options under stochastic volatility: An empirical investigation. *Carlson School of Management Working Paper*.

Beran, R. (1988a). Balanced simultaneous confidence sets. *Journal of the American Statistical Association*, 83(403):679–686.

Beran, R. (1988b). Prepivoting test statistics: a bootstrap view of asymptotic refinements. *Journal of the American Statistical Association*, 83(403):687–697.

Beran, R. (1990). Refining bootstrap simultaneous confidence sets. *Journal of the American Statistical Association*, 85(410):417–426.

Beran, R. (2003). The impact of bootstrap on statistical algorithms and theory. *Statistical Science*, 18(2):175–184.

Berkowitz, J. (2001). Testing density forecasts with applications to risk management. *Journal of Business and Economic Statistics*.

Bierens, H. (1987). Kernel estimators of regression functions. In *Advances in Econometrics: Fifth World Congress*, volume 1. Palgrave, London.

BIS (2011). Messages from the academic literature on risk measurement for the trading book. Technical Report 19, Bank for International Settlements.

Bollerslev, T. (1986). Generalized autoregressive conditional heteroskedasticity. *Journal of Econometrics*, 31(3):307–327.

Bollerslev, T. and Zhou, H. (2002). Estimating stochastic volatility diffusion using conditional moments of integrated volatility. *Journal of Econometrics*, 109:33–65.

Breusch, T. S. and Pagan, A. (1980). The lagrange multiplier test and its applications to model specification in econometrics. *Review of Economic Studies*, 47(1):239–253.

Carr, P. and Madan, D. (1999). Option valuation using the fast fourier transform. *Journal of Computational Finance*, 2:61–73.

Chako, G. and Viceira, L. (2003). Spectral GMM estimation of continuous-time processes. *Journal of Econometrics*, 116:259–292.

Chernov, M., Gallant, A., Ghysels, E., and Tauchen, G. (2003). Alternative models of stock price dynamics. *Journal of Econometrics*, 116:225–257.

Christoffersen, P. (1998). Evaluating interval forecasts. *International Economic Review*, 39.

Christoffersen, P., Dorion, C., Jacobs, K., and Karoui, L. (2014). Nonlinear kalman filtering in affine term structure models. Technical Report 14-04, Centre Interuniversitaire sur le Risque, les Politiques Èconomiques et l'Emploi.

Christoffersen, P., Jacobs, K., and Mimouni, K. (2010). Volatility dynamics for the s&p500: evidence from realized volatility, daily returns, and option prices. *Review of Financial Studies*, 23(8):3141–3189.

Collin-Dufresne, P., Goldstein, R., and Jones, C. (2008). Identification of maximal affine term structure models. *Journal of Finance*, 58(2):743–795.

Cont, R. and Tankov, P. (2003). *Financial modelling with jump processes*. Chapman & Hall / CRC Press.

Corradi, V. and Distaso, W. (2011). Multiple forecast model evaluation. In *The Oxford Handbook of Economic Forecasting*, chapter 13, pages 391–414. Oxford University Press.

Corradi, V. and Swanson, N. (2006). Bootstrap conditional distribution tests in the presence of dynamic misspecification. *Journal of Econometrics*, 133(2):779–806.

Corradi, V. and Swanson, N. (2007). Non-parametric bootstrap procedures for predictive inference based on recursive estimation schemes. *International Economic Review*, 48(1):67–109.

Cox, J. and Ross, S. (1976). The valuation of options for alternative stochastic processes. *Journal of Financial Economics*, 3(1-2):145–166.

Cummins, M., Dowling, M., and Esposito, F. (2017). Determining risk model confidence sets. *Finance Research Letters*, 21.

Dai, Q. and Singleton, K. (2000). Specification analysis of affine term structure models. *Journal of Finance*, 55(5):1943–1978.

Dempster, M. and Tang, K. (2011). Estimating exponential affine models with correlated measurement errors: applications to fixed income and commodities. *Journal of Banking and Finance*, 35:639–652.

Diebold, F. and Mariano, R. (1995). Comparing predictive accuracy. *Journal of Business and Economic Statistics*, 13(3):253–263.

Diebold, F., Todd, A., and Tay, A. (1998). Evaluating density forecasts with applications to financial risk management. *International Economic Review*.

Dotsis, G. and Markellos, R. N. (2008). An application of bootstrapping in option pricing. Technical report, Athens University of Economics and Business.

Duffee, G. and Stanton, R. (2012). Estimation of dynamic term structure models. *Quaterly Journal of Finance*, 2(2):1–51.

Duffie, D. and Kan, R. (1996). A yield factor model of interest rates. *Mathematical Finance*, 6(4):379–406.

Duffie, D., Pan, J., and Singleton, K. (2000). Trasform analysis and asset pricing for affine jump-diffusions. *Econometrica*, 68(6):1343–1376.

Duffy, D. (2006). *Finite difference methods in financial engineering: a partial differential equation approach*. Wiley.

Durham, G. and Gallant, A. (2002). Numerical techniques for maximum likelihood estimation of continuous-time diffusion processes. *Journal of Business & Economic Statistics*, 20(3):335–338.

Efron, B. (1979). Bootstrap methods: another look at the jackknife. *The Annals of Statistics*, 7(1):1–26.

Elerian, O., Chib, S., and Shephard, N. (2001). Likelihood inference for discretely observed nonlinear diffusions. *Econometrica*, 69(4):959–993.

Engle, R. (1982). Autoregressive conditional heteroscedasticity with estimates of the variance of united kingdom inflation. *Econometrica*, 50(4):987–1007.

Engle, R. and Manganelli, S. (2004). CAViaR: Conditional autoregressive Value-at-Risk by regression quantile. *Journal of Business & Economic Statistics*, 22(4):367–381.

Eraker, B. (2001). MCMC analysis of diffusion models with application to finance. *The Journal of Business & Economic Statistics*, 19(2):177–191.

Eraker, B. (2004). Do stock prices and volatility jump? reconciling evidence from spot and option prices. *The Journal of Finance*, 59(3):1367–1403.

Eraker, B., Johannes, M., and Polson, N. (2003). The impact of jumps in volatility and returns. *The Journal of Finance*, 58(3):1269–1300.

Esposito, F. and Cummins, M. (2015). Multiple hypothesis testing of market risk forecasting models. Working Paper.

Fisher, R. (1922). On the mathematical foundations of theoretical statistics. *Philosophical Transactions of the Royal Society of London A: Mathematical, Physical and Engineering Sciences*, 222(594-604):309–368.

Fisher, R. (1924). The conditions under which χ^2 measures the discrepancy between observation and hypothesis. *Journal of the Royal Statistical Society*, 87:442–450.

Gallant, A. and Tauchen, G. (1996). Which moments to match? *Econometric Theory*, 12(4):657–681.

Glosten, L., Jagannathan, R., and Runkle, D. (1993). On the relation between the expected value and the volatility of the nominal excess return on stocks. *Journal of Finance*, 42(5):27–62.

Gonçalves, S. and White, H. (2002). The bootstrap of the mean for dependent heterogeneous arrays. *Econometric Theory*, 18(6):1367–1384.

Gonzales-Rivera, G., Tae-Hwy, L., and Santosh, M. (2003). Forecasting volatility: A reality check based on option pricing, utility functions, value-at-risk and predictive likelihood. *Working Paper*.

Gonzalo, J. and Olmo, J. (2004). Which extreme values are really extreme? *Journal of Financial Econometrics*, 2(3).

Gordon, N., Salmond, D., and Smith, A. F. (1993). Novel approach to nonlinear/non-gaussian bayesian state estimation. In *IEE Proceedings F (Radar and Signal Processing)*, volume 140(2), pages 107–113.

Gupta, S. and Huang, D. (1976). Subset selection procedures for the means and variances of normal populations: unequal sample sizes case. *Sankhyā : The Indian Journal of Statistics, Series B*, 38(2):112–128.

Hansen, P. (2005). A test for superior predictive ability. *Journal of Business & Economic Statistics*, 23(4):365–380.

Hansen, P. and Lunde, A. (2005). A forecast comparison of volatility models: does anything beat a garch(1, 1)? *Journal of Applied Econometrics*, 20(7):873–889.

Hansen, P., Lunde, A., and Nason, J. (2011). The model confidence set. *Econometrica*, 79(2):453–497.

Hanson, F. (2007). *Applied stochastic processes and control for jump-diffusions: modelling, analysis, and computation*. Society for Industrial and Applied Mathematics.

Hausman, J. (1978). Specification tests in econometrics. *Econometrica*, 46(6):1251–71.

Heston, S. (1993). A closed-form solution for options with stochastic volatility with applications to bond and currency options. *The Review of Financial Studies*, 6(2):327–343.

Holm, S. (1979). A simple sequentially rejective multiple test procedure. *Scandinavian Journal of Statistics*, 6(2):65–70.

Horowitz, J. (2001). The Bootstrap. In *Handbook of Econometrics*, volume 5, chapter 52, pages 3159–3228. Elsevier.

Hull, J. and White, A. (1987). The pricing of options on assets with stochastic volatilities. *Journal of Finance*, 42(2):281–300.

Hurn, A., Lindsay, K., and McClelland, A. (2013). A quasi-maximum method for estimating the parameters of multivariate diffusions. *Journal of Econometrics*, 172:106–126.

Hurn, S., Jeisman, J., and Lindsay, K. (2010). Teaching an old dog new tricks: Improved estimation of the parameters of stochastic differential equations by numerical solution of the fokker-planck equation. In *Financial Econometrics Handbook*. Palgrave, London.

Hürzeler, M. and Künsch, H. (1998). Monte carlo approximations for general state-space models. *Journal of Computational and Graphical Statistics*, 7(2):175–193.

Hwang, E. and Shin, D. (2012). Strong consistency of the stationary bootstrap under -weak dependence. *Statistics and Probability Letters*, 82(3):488 – 495.

Jensen, B. and Poulsen, R. (2002). Transition densities of diffusion processes: numerical comparison of approximation techniques. *Journal of Derivatives*, 9(4):18–30.

Johannes, M., Polson, N., and Stroud, J. (2009). Optimal filtering of jump diffusions: Extracting latent states from asset prices. *Review of Financial Studies*, pages 2759–2799.

Jones, C. (1998). Bayesian estimation of continuous-time finance models. University of Rochester.

Jones, C. (2003). The dynamics of stochastic volatility: evidence from underlying and options markets. *Journal of econometrics*, 116(1):181–224.

J.P.Morgan (1996). Riskmetrics^{TM}. Technical Report 4, J.P.Morgan, Reuters.

Kerkhof, J. and Melenberg, B. (2003). Backtesting for risk-based regulatory capital. *Working Paper*.

Kerkhof, J., Melenberg, B., and Schumacher, H. (2009). Model risk and capital reserves. *Working Paper*.

Koenker, B. and Bassett, G. (1978). Regression quantiles. *Econometrica*, 46(1).

Kou, S. (2002). A jump-diffusion model for option pricing. *Management Science*, 48(8):1086–1011.

Kou, S. and Wang, H. (2004). Option pricing under a double exponential jump diffusion model. *Management Science*, 50(9):1178–1192.

Kupiec, P. (1995). Techniques for verifying the accuracy of risk management models. *Journal of Derivatives*, 3.

Küsch, H. (1989). The jackknife and the bootstrap for general stationary observations. *The Annals of Statistics*, 17(3):1217–1241.

Lahiri, S. (1999). Theoretical comparisons of block bootstrap methods. *The Annals of Statistics*, 27(1):386–404.

Lindström, E. (2007). Estimating parameters in diffusion processes using an approximate maximum likelihood approach. *Annals of Operations Research*, 151:269–288.

Linhart, H. (1988). A test whether two aic's differ significantly. *South African Statistical Journal*, 22(2):153–161.

Liu, R. and Singh, K. (1992). Moving blocks jackknife and bootstrap capture weak dependence. In *Exploring the Limits of Bootstrap*, pages 225–248. John Wiley & Sons.

Lo, A. (1988). Maximum likelihood estimation of Itô processes with discretely sampled data. *Econometric Theory*, 4(2):231–247.

Longin, F. (1996). The asymptotic distribution of extreme stock market returns. *The Journal of Business*, 69.

Lund, J. (1997). Non-linear kalman filtering techniques for term structure models. Working Paper, Aarhus School of Business.

Lux, T. (2012). Inference for systems of stochastic differential equations from discretely sampled data: a numerical maximum likelihood approach. Technical Report 1781, Kiel Institute for the World Economy.

Macbeth, J. and Merville, L. (1980). Tests of black-scholes and cox call option valuation models. *Journal of Finance*, 35(2):285–301.

Mancini, L. and Trojani, F. (2011). Robust value at risk prediction. *The Journal of Financial Econometrics*, 9.

Marcus, R., Peritz, E., and Gabriel, K. (1976). On closed testing procedures with special reference to ordered analysis of variance. *Biometrika*, 63(3):655–660.

Maybeck, P. (1982). *Stochastic models, estimation and control*, volume 2. Academic Press, London.

Merton, R. (1976). Option pricing when the underlying stock returns are discontinuous. *Journal of Financial Economics*, 3:125–144.

Musiela, M. and Rutkowski, M. (1997). *Martingale methods in financial modelling*. Springer.

Nadaraya, E. (1964). On estimating regression. *Theory of Probability and its Applications*, 9.

Nelson, D. (1991). Conditional heteroskedasticity in asset returns: A new approach. *Econometrica*, 59(2):347–370.

Newey, W. (1985). Maximum likelihood specification testing and conditional moment tests. *Econometrica*, 53(5):1047–70.

Nielsen, J., Vestgaard, M., and Madsen, H. (2000). Estimation in continuous-time stochastic volatility models using nonlinear filters. *International Journal of Theoretical and Applied Finance*, 3(2):1–30.

Nordman, D. (2009). A note on the stationary bootstrap's variance. *The Annals of Statistics*, 37(1):359–370.

Office of the Comptroller of the Currency (2011). Supervisory guidance on model risk management. Technical Report SR 11-7, Board of Governors of the Federal Reserve System.

Øksendal, B. (2003). *Stochastic Differential Equations: An Introduction with Applications*. Springer, 6 edition.

Pan, J. (2002). The jump-risk premia implicit in options: evidence from an integrated time-series study. *Journal of Financial Economics*, 63(1):3–50.

Patton, A., Politis, D., and White, H. (2009). Correction to: Automatic block-length selection for dependent bootstrap. *Econometric Reviews*, 28(4):372–375.

Pearson, K. (1936). Method of moments and method of maximum likelihood. *Biometrika*, 28(1/2):34–59.

Pedersen, A. (1995a). Consistency and asymptotic normality of an approximate maximum likelihood estimator for discretely observed diffusion processes. *Bernoulli*, 1(3):257–279.

Pedersen, A. (1995b). A new approach to maximum likelihood estimation for stochastic differential equations based on discrete observations. *Board of the Foundation of the Scandinavian Journal of Statistics*, 22(1):57–71.

Perelló, J., Sircar, R., and Masoliver, J. (2008). Option pricing under stochastic volatility: the exponential Ornstein−Uhlenbeck model. *Journal of Statistical Mechanics: Theory and Experiment*, 6:1–22.

Pitt, M. (2002). Smooth particle filters for likelihood evaluation and maximisation. University of Warwick, Department of Economics.

Pitt, M. and Shephard, N. (1999). Filtering via simulation: Auxiliary particle filters. *Journal of the American statistical association*, 94(446):590–599.

Platen, E. and Bruti-Liberati, N. (2010). *Numerical solution of stochastic differential equations with jumps in finance*. Springer.

Politis, D. and Romano, J. (1994a). Limit theorems for weakly dependent hilbert space valued random variables with applications to the stationary bootstrap. *Statistica Sinica*, 4(2):461–476.

Politis, D. and Romano, J. (1994b). The stationary bootstrap. *Journal of the American Statistical Association*, 89(428):1303–1313.

Politis, D. and White, H. (2004). Automatic block-length selection for dependent bootstrap. *Econometric Reviews*, 23(1):53–70.

Poulsen, R. (1999). Approximate maximum likelihood estimation of discretely observed diffusion processes. Technical Report 29, Centre for Analytical Finance, University of Aarhus.

Priestley, M. B. (1981). *Spectral analysis and time series*. Academic Press London ; New York.

Rao, C. and Wu, Y. (2001). On model selection. In Lahiri, P., editor, *Model Selection*, volume 38 of *Lecture notes - monograph series*, chapter 1, pages 1–58. Institute of Maathematical Statistics.

Romano, J., Azeem, M., and Wolf, M. (2010). Hypothesis testing in econometrics. *Annual Review of Economics*, 2:75–104.

Romano, J. and Shaikh, A. (2006). *On stepdown control of the false discovery proportion*, volume 49 of *Lecture Notes–Monograph Series*, pages 33–50. Institute of Mathematical Statistics.

Romano, J., Shaikh, A., and Wolf, M. (2008). Formalized data snooping based on generalized error rates. *Econometric Theory*, 24(2):404–447.

Romano, J. and Wolf, M. (2005a). Exact and approximate step-down methods for multiple hypothesis testing. *The Journal of the American Statistical Association*, 100(469):94–108.

Romano, J. and Wolf, M. (2005b). Stepwise multiple testing as formalized data snooping. *Econometrica*, 73(4):1237–1282.

Romano, J. and Wolf, M. (2007). Control of generalized error rates in multiple testing. *The Annals of Statistics*, 35(4):1378–1408.

Romano, J. and Wolf, M. (2010). Balanced control of generalized error rates. *The Annals of Statistics*, 38(1):598–633.

Rosenblatt, M. (1952). Remarks on a multivariate transformation. *The Annals of Mathmatical Statistics*, 23.

Rubin, D. (1987). A noniterative sampling/importance resampling alternative to the data augmentation algorithm for creating a few imputations when the fraction of missing information is modest: The sir algorithm. *Journal of American Statistical Association*, 82:543–546.

Schmalensee, R. and Trippi, R. (1978). Common stock volatility expectations implied by option premia. *Journal of Finance*, 33(1):129–147.

Scott, L. O. (1987). Option pricing when the variance changes randomly: Theory, estimation, and an application. *Journal of Financial and Quantitative Analysis*, 22:419–438.

Scott, L. O. (1997). Pricing stock options in a jump-diffusion model with stochastic volatility and interest rates: applications of fourier inversion methods. *Mathematical Finance*, 7(4):413–426.

Shephard, N. (1991a). From characteristic function to distribution function: a simple framework for the theory. *Econometric Theory*, 7:519–529.

Shephard, N. (1991b). Numerical integration rules for multivariate inversions. *Journal of Statistical Computation and Simulation*, 39:37–46.

Shimodaira, H. (1998). An application of multiple comparison techniques to model selection. *Annals of the Institute of Statistical Mathematics*, 50(1):1–13.

Silvey, S. (1959). The lagrangian multiplier test. *The Annals of Mathematical Statistics*, 30(2):389–407.

Singleton, K. (2001). Estimation of affine asset pricing models using the empirical characteristic function. *Journal of Econometrics*, 102(1):111–141.

Storey, J. (2002). A direct approach to false discovery rates. *Journal of the Royal Statistical Society, B*, 64(3):479–498.

Tavella, D. and Randall, C. (2000). *Pricing financial instruments: the finite difference method*. Wiley.

Toro-Vizcarrondo, C. and Wallace, T. (1968). A test of the mean square error criterion for restrictions in linear regression. *Journal of the American Statistical Association*, 63(322):558–572.

Van der Vaart, A. (1998). Functional delta method. In *Asympotic Statistics*, chapter 20. Cambridge University Press.

Vuong, Q. (1989). Likelihood ratio tests for model selection and non-nested hypotheses. *Econometrica*, 57(2):307–333.

Wald, A. (1943). Tests of statistical hypotheses concerning several parameters when the number of observations is large. *Transactions of the American Mathematical Society*, 54(3):426–482.

Watson, G. (1964). Smooth regression analysis. *Sankyā: The Indian Journal of Statistics*, 26.

West, K. (1996). Asymptotic inference about predictive ability. *Econometrica*, 64(5):1067–1084.

Westfall, P. and Troendle, J. (2008). Multiple testing with minimal assumptions. *Biometrical Journal*, 50(5):745–755.

White, H. (1982). Maximum likelihood estimation of misspecified models. *Econometrica*, 50:1–25.

White, H. (1994). *Estimation, inference and specification analysis*. Cambridge University Press.

White, H. (2000). A reality check for data snooping. *Econometrica*, 68(5):1097–1126.

Wiggins, J. (1987). Option values under stochastic volatility: Theory and empirical estimates. *Journal of Financial Economics*, 19:351–372.

Wilks, S. (1938). The large-sample distribution of the likelihood ratio for testing composite hypotheses. *The Annals of Mathematical Statistics*, 9(1):60–62.

Wooldridge, J. (1990). A unified approach to robust, regression-based specification tests. *Econometric Theory*, 6(1):17–43.

Yatchew, A. and Härdle, W. (2006). Nonparametric state price density estimation using constrained least squares and the bootstrap. *Journal of Econometrics*, 133(2):579–599.

Algorithms

In this section, we provide more technical details concerning the main procedures that have been employed in the experimental parts of this thesis. The intention is to clarify the construction of the build blocks that led to the model performance measurements. Although covering almost completely the procedures of Chapter 3 and Chapter 4, this collection is not complete and we refer to the cited literature for completion.

A.1 The Approximate Likelihood Function

The full system state likelihood function is obtained as the numerical solution of the PIDE defining the transition probability density associated with the SDE of the target model, Eq. (3.1) and (3.2). The parameter estimation problem in the presence of a partially observed system state is tackled by marginalising the latent component with the procedure described below.

A.1.1 The Marginalisation Procedure

The practical implementation of the estimation algorithm involves the numerical approximation of a δ_t-step ahead transition probability conditional on the "average" level of the latent factor, where the marginalisation is achieved by weighting the transition density by the stationary distribution of the latent factor v. The marginalisation of the latent variable has been used in literature in studies such as Singleton (2001), Chako and Viceira (2003), which exploit the characteristic function of the affine process and more general spectral methods. The appeal of this solution is represented by the peculiar structure of the system under analysis. Let $\mathbb{P}\{x_t, v_t, v_{t-\delta}|\mathcal{F}_{t-\delta}\}$ be the join probability of the observable x and the random latent factor v, taken at the current observation time $t-\delta_t$ for the next one t. Because x is a Markovian, level independent martingale and v is incidentally endowed with a stationary distribution that can be worked out quasi-analytically, it is convenient to write the previous probability measure as $\mathbb{P}\{\Delta x, v_t|0_x, v_{t-\delta}\}\mathbb{P}\{v_{t-\delta}\}$, and obtain the marginal distribution of Δx over the time interval δ_t, by integrating out the initial and terminal condition of the latent variable v, that is

$$\mathbb{P}\{\Delta x|0_x\} = \int \mathbb{P}\{\Delta x, \mathrm{d}v_t|0_x, \mathrm{d}v_{t-\delta}\}\mathbb{P}\{\mathrm{d}v_{t-\delta}\} \tag{A.1}$$

The stationary density of the latent factor v is exploited for the marginalisation of the latent initial conditioning variable in the transition probability density. The complete stationary density is

Lemma A.1.1 (The stationary distribution of the jump-square-root process)**.** *The stationary distribution of the stochastic process process v defined in Eq. (3.1), $\lambda_1 > 0$, is*

$$\frac{c\,\mathrm{e}^{-\frac{v}{\lambda_1}}\,v^{B_1+B_2-1}}{\Gamma(B_1+B_2)}{}_1F_1\left[B_1, B_1+B_2, -(\tfrac{1}{\beta}-\tfrac{1}{j_{11}})v\right] \tag{A.2}$$

with the coefficients $\beta = \frac{\sigma^2}{2\kappa}$, $B_1 = A_1\left[\frac{\sigma^2}{2}(\frac{1}{\beta}-\frac{1}{j_{11}}) - \lambda_1 j_{11}\right]$, $B_2 = A_1\lambda_1\beta$, $A_1 = \frac{2}{\sigma^2\beta}(\frac{1}{\beta}-\frac{1}{j_{11}})^{-1}$ and c is a normalising constant. The $\Gamma(a)$ is the parametrised gamma function

$$\Gamma(a) = \int_0^\infty \mathrm{d}s\ \mathrm{e}^{-s}s^{a-1}$$

while ${}_1F_1$ is the confluent hypergeometric function

$${}_1F_1[a,b,z] = \sum_{n=0}^{\infty}\frac{a^{(n)}z^n}{b^{(n)}n!}$$

where

$$\begin{aligned} a^{(0)} &= 1 \\ a^{(n)} &= a(a+1)(a+2)\cdots(a+n-1). \end{aligned}$$

When $\lambda_1 \to 0$ the Eq. (A.2) becomes the usual Feller process stationary distribution

$$\frac{c}{\Gamma(\frac{1}{\beta})}\mathrm{e}^{-\frac{v}{\beta}}v^{\frac{1}{\beta}-1} \tag{A.3}$$

Proof. Consider the PIDE describing the transition probability of the square root process with exponential

jump

$$\partial_t p = \partial_v^2[\sigma^2 v p] - \partial_v[(\kappa - \lambda_1 j_{11} - \kappa v)p] - \lambda_1 p + \lambda_1 \int_0^{+\infty} \mathrm{d}s\, p(v-s)\mathrm{e}^{-\frac{s}{j_{11}}}. \tag{A.4}$$

The solution consists of applying the Laplace transform and some manipulation. The stationary distribution of v, if it exists, satisfies the Eq. (A.4) with $\partial_t p = 0$. Taking the Laplace transform $\mathcal{L}(p)$ we get

$$\frac{\mathcal{L}'}{\mathcal{L}} = -\frac{(\kappa - \lambda_1 j_{11})z + \frac{\kappa}{j_{11}}}{\frac{\sigma^2}{2}(z+\frac{1}{\beta})(z+\frac{1}{j_{11}})}$$

that, applying the partial fraction decomposition and the inverse transform, yields

$$\mathcal{L} = c(z+\tfrac{1}{\beta})^{-B_1}(z+\tfrac{1}{j_{11}})^{-B_2} \overset{\mathcal{L}^{-1}}{\Longrightarrow} p = \frac{c}{\Gamma(B_1)\Gamma(B_2)}\left(\mathrm{e}^{-\frac{v}{\beta}} v^{B_1-1}\right) \star \left(\mathrm{e}^{-\frac{v}{j_{11}}} v^{B_2-1}\right)$$

where the $\star$ sign indicates the convolution product. Then, making the convolution explicit, the following expression

$$p = \frac{c\,\mathrm{e}^{-\frac{v}{j_{11}}}}{\Gamma(B_1)\Gamma(B_2)} \int_0^v \mathrm{d}u\, \exp\left[-\left(\tfrac{1}{\beta} - \tfrac{1}{j_{11}}\right)u\right] u^{B_1-1}(v-u)^{B_2-1} \tag{A.5}$$

can be represented as a confluent hypergeometric function, if we notice that the latter function coincides with the integral representation of

$$\frac{\Gamma(a)\Gamma(b)}{\Gamma(a+b)}{}_1F_1[a, a+b, s] = \int_0^1 \mathrm{d}\tau\, \mathrm{e}^{s\tau}\tau^{a-1}(1-\tau)^{b-1}$$

that after the change of variable $\tau = u/v$ and the substitution $s = -\left(\frac{1}{\beta} - \frac{1}{j_{11}}\right)$ can be plugged into the Eq. (A.5) to replace the convolution term. □

In order for v to have a well defined stationary distribution, the coefficients need to satisfy the inequalities $j_{11} > \frac{\sigma^2}{2\kappa}$ and $\kappa - \lambda_1 j_{11} > \frac{\sigma^2}{2j_{11}}$, which coupled with the positive in probability constraint on v, that is $\kappa - \lambda_1 j_{11} > \frac{\sigma^2}{2} > 0$ are directly satisfied if we impose $j_{11} > 1$, a choice which seems reasonable if we were to clearly distinguish a jump-less square-root process from one which allows for instantaneous acceleration of the volatility in x. The function ${}_1F_1$ is represented in its hypergeometric series form because in the the application it is calculated as a truncated summation.

A.1.2 The Approximation of the Transition Density

In order to complete the construction of the AML, we necessitate the construction of the numerical solution of the two-dimensional transition probability density implied by the SDE (3.1), we refer to, for instance, Tavella and Randall (2000), Duffy (2006) as more detailed presentations of PIDE solutions techniques. We approximate the core integrating element of Eq. (A.1), that is $p\,(\Delta x, v_{\delta_t}|0_x, v)$, for each component of the likelihood definition (3.3) via a combination of a finite difference method (FDM) and an ordinary integral approximation which defines an ODE system, where the multiplication for the characteristic matrix $A + J$ represents an approximation of the cumulative action of the partial differential and the integral operators onto the discretised function p in the space dimensions. Further details concerning the approximation of the characteristic operator are given in the next section.

In order to solve for the transition equation, we exploit the operator approximation to transform the Kolmogorov forward equation

$$\partial_t[p] = (\mathscr{A} + \mathscr{J})[p] \tag{A.6}$$

into the ODE homogeneous system

$$\tfrac{\mathrm{d}}{\mathrm{d}t}p(t) = (A + J) \cdot p(t) \Rightarrow p(t) = \exp\left[(A + J)t\right] \cdot p(0) \tag{A.7}$$

In the case of the likelihood estimation exercise, the PIDE approximation is formally solved via the exponentiation of the system matrix, as stated in Eq. (A.7). The vector $p(t)$ contains the stack of the grid-points at t and where the initial condition $p(0)$ is a representation of the delta-functional. Care has been taken in the stabilisation of the approximation of the jump-diffusion operator.

First, the one step ahead likelihood has been centred and scaled, such that the grid upon which the solution is constructed stretches around the initial condition and is extended or contracted proportionally to the conditional variance of the state vector, while the number of the grid points is kept constant: centring grants stability in those regions of the domain that would otherwise be extreme, whereas scaling, under model-tailored solutions, grants improved sensitivity to model parameters and further better behaviour around the tails. We exploit, where possible, closed form solutions for the calculation of the conditional expected variances. The exception is represented by the CEV specifications, for which we adopt again the approximation in Eq. (A.20).

Second, the initial condition which is the delta function is modelled as a simple pulse, as the pretty coarse grid we are using cannot justify more articulated proxies. This choice is a consequence of the fact that we do not embrace the strategy of fixing the initial condition covariance matrix at the terminal time values, cfr. for instance Poulsen (1999), as we have found that the shape of the distribution tends to be overblown, when compared to the simulated distribution. Furthermore, at the border of the grid set which defines the solution, we impose that the function is equal to zero. Although the solution usually integrates almost to one, we adjust this feature to make it exact. We use two dimensional trapezoidal rule for numerical integration for the model of interest.

A.2 The PIDE solution

In recent years, the finite different method (FDM) has received renewed attention in continuous-time financial econometrics, since the seminal papers of Lo (1988), Pedersen (1995b) and Poulsen (1999). Examples are Jensen and Poulsen (2002), Lindström (2007), Hurn et al. (2010), Lux (2012). The model problem we tackle is represented by the forward equation (A.6), which is employed in the likelihood estimation of Chapter 3. Nonetheless, in terms of abstract operators, the option pricing problem of Chapter 4 involving the backward equation, can also be regarded under the same formulation. The techniques described in this section are adapted and applied to both those exercises.

The construction of the PIDE solution of $p(x, v, t)$ involves the approximation of the integral-differential operator with the purpose of obtaining a linear system. The solution function is accomplished on a grid of points that are stacked into the time dependent vector

$$f(t) = \text{vec} \begin{pmatrix} p(x_1, v_1, t) & \dots & p(x_n, v_1, t) \\ p(x_1, v_2, t) & \dots & p(x_n, v_2, t) \\ \vdots & \dots & \vdots \\ p(x_1, v_m, t) & \dots & p(x_n, v_m, t) \end{pmatrix}.$$

The approach we adopt is to apply the FDM to the differential operator, whereas the numerical integration corresponds to a linear operator that transform f into the sought primitive function. The references for the finite difference method are represented, for instance, by Tavella and Randall (2000), Duffy (2006). In particular, the former reference contains a detailed explanation on how to construct a finite difference operator with a given order of precision, to estimate the partial derivative of f, locally. The strategy consists of taking Taylor expansions of the function in a neighbourhood of each point of the defined grid and then estimating the partial derivative as a linear combination of enough function values to obtain the following

$$\partial_\bullet f_k = \sum_i \alpha_i f_i + R$$

where R is the residual with the target order of precision. In practice, we can obtain a linear system, whereby the weights α_i are such that annihilate the unnecessary Taylor terms and sum up to one. It is implicit that the higher the dimension of the system, the more complex the expression to obtain a finite difference operator would result. Whereby the partial differential operators in one dimension are relatively easy to obtain, the mixed derivatives involve instead many alternative formulations. The differential operators approximations define a banded matrix that approximates the action of the PIDE operator $\mathscr{A}$ in the space dimension. The main problem in constructing the approximation matrix A is obtaining a stable matrix; that is, a matrix that does not explode under exponentiation. This problem is complicated by the presence of the integral operator, which breaks the banded structure of the system matrix $A + J$. The general rule we follow is exploiting the Gershgorin circle theorem, see Duffy (2006), sampling from an allowed range of model parameters. The approximation of the various configurations of the integral operator $\mathscr{J}$ with the linear discrete operator J is constructed as a matrix of weights that are obtained either applying the trapezoidal rule, as in the Chapter 3 exercise, or analytically integrating[1] a linear or exponential interpolation within the context of the experiments of Chapter 4. The only jump size convolution that exploit the linear interpolation is the case of the Lomax jump, whereas all other cases require the exponential interpolation approach. Some assumptions are taken to enclose the integration within the border of the grid over which the numerical solution is constructed. In the case of the likelihood, we assume that over an incremental contour the solution decreases linearly to zero. In the case of the option pricing function, we let the function be constant outside the grid and simply integrate the convolution from the function boundary to the jump domain closure. The latter approach amounts to adding a weight to the corresponding matrix slot, according to the analytic solution of the tail integral.

[1] In the case of the joint jump in return and in volatility, the convolution operator is defined on a two-dimensional plane. The grid points define a network whereby the integration of the interpolating function is performed over the various types of rectangles that patch the integrating function domain.

Alternative assumptions concerning the tail behaviour seem not to contribute significantly to the final solution, or otherwise distort the result.

Eventually, the components of the vector $f(t)$ correspond to the function values at each point of the possibly multidimensional grid in the space domain. A lexicographic ordering of the mesh points is introduced to organise the data in the stack. With such structure and the conforming construction of the matrix $A + J$, we transform the original PIDE into the system of ODE

$$\frac{\mathrm{d}}{\mathrm{d}t} f(t) = (A + J) \cdot f(t) \tag{A.8}$$

The solution of the above equation provides the approximation of the Eq. (A.6). As noticed in the previous section, in the context of the AML the solution of (A.8) is obtained via the matrix exponential of the system matrix, as in (A.7). Differently from that, in Chapter 4 in order to accomplish the solution of the pricing equation we apply the FDM also to the time domain, employing the implicit, the explicit and the Crank-Nicholson method in combination to the operator splitting approach, see for instance Duffy (2006). The latter method is particularly appealing for the sake of the dimensional reduction of PIDE. However, we exploit this method to achieve a closer control of the operator stability, performing the stability analysis for circumscribed components of the compounded operator.

A.3 The Nonlinear Filter

In this section we provide more details about the construction of the filter used for the estimation of the latent system state in Chapter 3, while in the previous Appendix A.1 we have described the method for dealing with the parameter estimation. Both techniques hinge on the partial integral-differential equation defining the transition probability distribution of the main system, although the particular filter solution we adopt avoids the construction of the likelihood function. This is a key feature that allows ease of implementation. We remark that exploiting the filtering approach laid out in Maybeck (1982), we build upon the same intuition to extend the time-propagation equation to a jump component.

In the context of filtering, the object of investigations is represented by the dynamics of a real valued, continuous time multi-dimensional stochastic process $\{S_t\}_{t\in[0,T)}$. We refer to the vector S_t as a *system*, essentially because the stochastic differential equations describing the dynamics of its components are interconnected. The system S is arranged into two blocks $S = (X^\top, Y^\top)^\top$, in relation to their observability. We indicate the observable components as Y, which is a function of X, the state of the system. The system state X is fully or partially latent, that is its path can only be inferred from the information coming through the measurement Y. The problem we tackle consists in the estimation of the trajectories of the latent components, using only the information concerning the structure of the system dynamics and the stream of the observations on Y, recorded at discrete times, $\{Y_{t_{-n}}, \ldots, Y_{t_{-1}}, Y_{t_0}\}$. In general, S_t belongs to a parametric family and hence implicates a preliminary problem of estimation. In the approach pursued in this work, we distinguish the task of inferring the latent trajectories from that of the estimation of the model parameter, which is achieved with likelihood methods. This section is dedicated

to the solution of the former problem that, as a key contribution to the literature, is extended to include jump components. The construction of the likelihood that is employed in the experimental section of Chapter 3 is pursued in Appendix A.1.

Filtering is the problem of finding the best estimate in a mean square sense of the state of the system, that is the $\mathcal{G}_t$-measurable random variable $\bar{X}_t$ that minimises the path-wise distance from the true state X_t. Let the probability space $(\Omega, \mathcal{F}, \mathcal{F}_t, \mathbb{P})$ and let the flow of information as represented by the set $\mathcal{G} \subset \mathcal{F}$, be respectively defined as the algebra of events representing the observable trajectories and the full set of information about the system (X, Y). The solution to the problem defined above, is the projection from the space $\mathcal{L}^2(\mathbb{P})$ onto the space $\mathcal{K} \subset \mathcal{L}^2(\mathbb{P})$ of the $\mathcal{G}_t$-measurable random variables. The projection operator corresponds to the expectation $\mathbb{E}[\cdot|\mathcal{G}_t]$, see Øksendal (2003). The following aims to construct an approximation of the projection operator, when the stochastic process is a jump-diffusion. Actually, because the observables are recorded only at discrete times, we need two projection operators providing the latent state estimates. Filtering involves two equations defining the operators of projection $\mathbb{E}[X_t|\mathcal{G}_{t-\delta_t}]$ and $\mathbb{E}[X_t|\mathcal{G}_t]$. In order to simplify notation, we will indistinctly indicate $\mathbb{E}_{t|s}[X] =: \mathbb{E}[X_t|\mathcal{G}_s] := \bar{X}_{t|s}$, $s \leq t$. Corresponding to the previous expectations, the non-linear filter is composed of the *time-propagation equation*, which moves the state estimates between the observation times $t - \delta_t$ and t, the time segments being not necessarily equally spaced, whereas the *update equation* generates the new estimate of the partially latent state vector X_t when a new observation Y_t is available. The problem amounts to the construction of the projection and update operators of the first two central moments of the system state. Formally, the work space is given by the parametric system state

$$\mathrm{d}X = b(X^-; \vartheta)\mathrm{d}t + A(X^-; \vartheta)\mathrm{d}W + J(z; X^-, \vartheta)\mathrm{d}N \tag{A.9}$$

The functions b, A include dependency on the parametric vector $\vartheta \in \Theta$. The jump size component vector J depends on the mark point z, whose distribution is parametric and may depend on the state. The random drivers of the system are the Brownian vector W and the Poisson counting process N, with stochastic intensity $\lambda(X^-; \theta)$. The random functions b, A and J are assumed to satisfy conditions that grant a unique solution for Eq. (A.9) (see e.g. Platen and Bruti-Liberati, 2010), $\forall \theta \in \Theta$. In Eq. (A.9) we make explicit the dependency on the left limit of X, that is its level immediately before the jump, if any. Subsequently, this notation is dropped, whereby we focus on the construction of the estimation procedure. For a complete treatment of the stochastic integral X and its components, see, e.g., Cont and Tankov (2003), Hanson (2007). For the practical purpose of system estimation, we will assume that the jump size vector of the synchronous jump can be written as $J = G(z)f(X)$, with $G = \mathrm{diag}(g)$, where f and g are mapping, respectively, from the domain of X and z, the mark point vector, to $\mathbb{R}^\bullet$ and the operator $\mathrm{diag}(\cdot)$ transforms a vector into a diagonal matrix. The definition of J makes the jump size dependent at the same time on the mark-point vector z and on the state X, but in a way that allows the factorisation of the jump-component and the state component in the time-propagation equation, introduced onward in this section. The second component of the system is represented by the observation equation, where

the observable Y is described as a function of the state X

$$Y = \mathbf{q}(X) \tag{A.10}$$

In the development of applications, in Eq. (A.10) we assume a simple linear form for $\mathbf{q}(X) = HX$, through the constant matrix H. This case is relevant, for example, for the stochastic volatility model, where H is a pick matrix, or for a latent factor term structure model that targets the estimation of the empirical measure. The extension of Eq. (A.10) to more general forms requires a further approximation in the update equation, see e.g. Nielsen et al. (2000), Baadsgaard et al. (2000). See Christoffersen et al. (2014) for a study of non-linearity in the observation equation in the case of an unscented Kalman filter. Furthermore, we allow for a random hazard function where the jump intensity $\lambda(X)$ is intended, in general, as a function of the state. Assuming the intensity process be almost surely not negative and with finite second order moments the differential of the hazard function Λ is defined as

$$\mathrm{d}\Lambda = \lambda(X)\mathrm{d}t \tag{A.11}$$

therefore defining the jump component as random process governed by a state dependent Poisson jump measure.

To conclude the construction of the nonlinear filter, we remark that in the classical filtering approach a *measurement error* term E is included in the observation equation, $Y = \mathbf{q}(X) + E$, usually employed in the parameter estimation exercise. That approach is justified as long as the term E represented the observed mismatch between the observed Y and the target function of the state, that is $E = Y - \mathbf{q}(\mathrm{X})$. On the contrary, we deal with ancillary constituents of the functional form of the observations as further latent components, therefore augmenting the system state X and letting $E = 0$. Evidence related to the higher complexity of the residuals in financial applications can be found in Dempster and Tang (2011). The first reason for this choice is operational, as we have found that the joint estimation of the model parameters and the estimation of the path of the latent components by exploiting the likelihood of observed residuals is subject to high uncertainty. Further reason for this choice can be traced in the ambiguity about the attribution of the total variability among the several stochastic drivers accountable for the explanation of the observed dynamics, such that the isolation of a residual variable collecting the mismatching between the observations and the projected function of the latent state has to be deemed redundant because such uncertainty is absorbed by some of the latent elements.

A.3.1 The Time-Propagation Equation

In order to construct optimal estimates of the state of the system X, which is observed at discrete times only, we need conditions for the evolution of the system state projections between two observation times. This is called the *time-propagation equation*. The idea in Maybeck (1982) is to derive possibly approximated ordinary differential equations for the first two moments of X, cfr. Nielsen et al. (2000), Baadsgaard et al. (2000). Considering the time derivative of the expectations $\frac{\mathrm{d}}{\mathrm{d}t}\mathbb{E}_{t|s}[X]$ and $\frac{\mathrm{d}}{\mathrm{d}t}\mathbb{E}_{t|s}[XX^\top]$,

we study the equations

$$\begin{aligned} \tfrac{\mathrm{d}}{\mathrm{d}t}\left[\bar{X}\right] &= \int X\partial_t[p]\,\mathrm{d}x \\ \tfrac{\mathrm{d}}{\mathrm{d}t}\left[\bar{V}\right] &= \int XX^\top\partial_t[p]\,\mathrm{d}x - \tfrac{\mathrm{d}}{\mathrm{d}t}\left[\bar{X}\right]\bar{X}^\top - \bar{X}\tfrac{\mathrm{d}}{\mathrm{d}t}\left[\bar{X}\right]^\top \end{aligned} \tag{A.12}$$

In Eq. (A.12), we substitute the forward equation (A.6) for the jump-diffusion transition probability p to obtain an exact or an appropriately approximated ordinary differential equation (ODE) system for $\bar{X}_{t|s}$ and $\bar{V}_{t|s}$. The operators $\mathscr{A}$ and $\mathscr{J}$ indicate the partial differential and the integral component of the forward equation. The aim is to calculate the solution of (A.12) for the jump-diffusion (A.9). To obtain the solution the following integrals are involved $\int X(\mathscr{A}+\mathscr{J})[p]$ and $\int XX^\top(\mathscr{A}+\mathscr{J})[p]$ that because of linearity can be handled separately with respect to each individual KFE operator. For the same reason, further synchronous jumps can be easily included to the state model. We split Eq. (A.12) into its diffusion and jump component, using linearity of the operators, that is $\frac{\mathrm{d}}{\mathrm{d}t}[\cdot] = \frac{\mathrm{d}}{\mathrm{d}t}[\cdot]_{\mathscr{A}} + \frac{\mathrm{d}}{\mathrm{d}t}[\cdot]_{\mathscr{J}}$. To simplify notation, we indicate the operator $\mathbb{E}^{\mathbb{P}}[\cdot]$ with $(\!|\cdot|\!)$ and $\mathbb{E}^{\mathbb{Q}}[\cdot]$ with $[\![\cdot]\!]$. We find that the diffusion component of Eq. (A.12) is

Proposition A.3.1 (The Diffusion Component of the Time-Propagation Equation, Maybeck, 1982)**.**

$$\begin{aligned} \tfrac{\mathrm{d}}{\mathrm{d}t}\left[\bar{X}\right]_{\mathscr{A}} &= (\!|b|\!) \\ \tfrac{\mathrm{d}}{\mathrm{d}t}\left[\bar{V}\right]_{\mathscr{A}} &= (\!|C|\!) + (\!|bX^\top|\!) + (\!|Xb^\top|\!) - (\!|b|\!)\bar{X}^\top - \bar{X}(\!|b|\!)^\top \end{aligned} \tag{A.13}$$

Proof. Recall the *Forward Kolmogorov Equation* associated to the pure diffusion version of Eq. (A.9) ($J=0$) and $C = AA^\top$

$$\partial_t[p] = \tfrac{1}{2}\sum_{ij}\partial^2_{ij}\left[C_{ij}p\right] - \sum_i \partial_i\left[b_i p\right] \tag{A.14}$$

Where p represents the state transition density. Therefore, we can take the time derivative of the expectation and combine with (A.14)

$$\begin{aligned} \bar{X}_{t|s} &= \int \mathrm{d}x\, p_{t|s}X \Rightarrow \tfrac{\mathrm{d}}{\mathrm{d}t}\bar{X} = \int \mathrm{d}x\,\partial_t p X = \\ &\quad \tfrac{1}{2}\int \mathrm{d}x \sum_{ij}\partial^2_{ij}\left[C_{ij}p\right]X - \int \mathrm{d}x \sum_i \partial_i\left[b_i p\right]X \end{aligned} \tag{A.15}$$

and simplify the expression. In fact, considering the generic component of the last term and integrating by parts, we obtain

$$\begin{aligned} -\int \mathrm{d}x\,\partial_i\left[b_i p\right]X &= -\int\cdots\int \mathrm{d}x_1\ldots\mathrm{d}x_{i-1}\mathrm{d}x_{i+1}\ldots\mathrm{d}x_{\mathtt{n}}\int \mathrm{d}x_i\,\partial_i\left[b_i p\right]X = \\ &\quad \int \mathrm{d}x\,\left[b_i p\right]\partial_i X = \int \mathrm{d}x\,\left[b_i p\right]e_i = e_i(\!|b_i|\!). \end{aligned}$$

Similarly, integrating by parts the first term we obtain

$$\int \mathrm{d}x\, p\sum_{ij} C_{ij}\partial^2_{ij}X = 0$$

because $\partial^2_{ij}X = \partial_i e_j = 0$.

In order to obtain the the evolutionary equation for the covariance of the $\bar{X}$, we consider the expression

$$V_{t|s} = \mathbb{E}_{t|s}\left[XX^\top\right] - \bar{X}_{t|s}\bar{X}_{t|s}^\top$$

and obtain

$$\tfrac{\mathrm{d}}{\mathrm{d}t}V_{t|s} = \tfrac{\mathrm{d}}{\mathrm{d}t}\mathbb{E}\left[XX^\top\right] - \tfrac{\mathrm{d}}{\mathrm{d}t}\left[\bar{X}\right]\bar{X}^\top - \bar{X}\tfrac{\mathrm{d}}{\mathrm{d}t}\left[\bar{X}\right]^\top$$

Now, combining (A.14) with the $\frac{\mathrm{d}}{\mathrm{d}t}\mathbb{E}\left[XX^\top\right]$ and with the same argument as above we obtain

$$-\int \mathrm{d}x \sum_i \partial_i \left[b_i p\right] XX^\top = -\int \mathrm{d}x\, p \sum_i b_i \partial_i XX^\top$$

but $\partial_i XX^\top = e_i X^\top + Xe_i^\top$, hence

$$\begin{aligned} -\int \mathrm{d}x \sum_i \partial_i \left[b_i p\right] XX^\top \quad &= \quad -\int \mathrm{d}x\, p\left(bX^\top + Xb^\top\right) = \\ & \left(\!\!\left|bX^\top\right|\!\!\right) + \left(\!\!\left|Xb^\top\right|\!\!\right) \end{aligned}$$

The last component of the expression for $\frac{\mathrm{d}}{\mathrm{d}t}V_{t|s}$ is

$$\tfrac{1}{2}\int \mathrm{d}x \sum_{ij} \partial_{ij}^2 \left[C_{ij} p\right] XX^\top = \tfrac{1}{2}\int \mathrm{d}x\, p \sum_{ij} C_{ij}\partial_{ij}^2 \left[XX^\top\right]$$

but

$$\sum_{ij} \partial_{ij} XX^\top = \sum_{ij} \partial_i \left(e_j X^\top + Xe_j^\top\right) = \begin{bmatrix} 2 & 1 & \dots & 1 \\ 1 & 2 & \dots & 1 \\ \vdots & \vdots & \ddots & \vdots \\ 1 & 1 & \dots & 2 \end{bmatrix}$$

hence

$$\tfrac{1}{2}\int \mathrm{d}x \sum_{ij} \partial_{ij}^2 \left[C_{ij} p\right] XX^\top = \left(\!\!\left|C\right|\!\!\right).$$

□

The filter $\left(\bar{X}, \bar{V}\right)$ can be extended with the same approach described above, adapting the integration procedure to handle the jump component. We augment the time propagation equation as conceived by Maybeck (1982) with a marked point Poisson element, which can be state-dependent in the jump intensity function and in the jump size distribution. The intuition consists in exploiting the same approach as in the deriving the propagation equation for the diffusion process, as applied to the jump operator of the forward equation. We derive workable expressions for the estimation of the latent system-state, providing the following formal ODE system.

Proposition A.3.2 (The Jump Component of the Time-Propagation Equation)**.**

$$\begin{aligned} \tfrac{\mathrm{d}}{\mathrm{d}t}\left[\bar{X}\right]_{\mathscr{J}} \quad &= \quad \left[\!\!\left[G\right]\!\!\right]\left(\!\!\left|\lambda f\right|\!\!\right) =: U \\ \tfrac{\mathrm{d}}{\mathrm{d}t}\left[\bar{V}\right]_{\mathscr{J}} \quad &= \quad \left[\!\!\left[G\right]\!\!\right]\left(\!\!\left|\lambda f X^\top\right|\!\!\right) + \left(\!\!\left|\lambda X f^\top\right|\!\!\right)\left[\!\!\left[G\right]\!\!\right] + \left(\!\!\left|\lambda f f^\top\right|\!\!\right) \odot \left[\!\!\left[gg^\top\right]\!\!\right] - U\bar{X}^\top - \bar{X}U^\top \end{aligned} \tag{A.16}$$

Proof. Consider the multi-dimensional synchronised pure jump forward equation

$$\partial_t[p] = -(\lambda p) + \int_{\mathscr{Z}} \mathrm{d}\mathbb{Q}(z;\, h)\, |\nabla h|\ (\lambda p) \circ h \tag{A.17}$$

where $\mathbb{Q}$ is the jump size probability measure, $h\colon X^+ \to X^-$ is the post-jump transform, $|\nabla h|$ is the determinant of the Jacobian of h and we indicate by $\circ$ the function composition operator. The jump intensity is the process $\lambda(X)$. When calculating the first two moments of the state using (A.17) and taking into account the distributional equality $(\mathscr{J}^\star[u], v) = (u, \mathscr{J}[v])$, we notice that it is more convenient to revert back to the pre-jump transform $h(X^+) = X^- \Leftrightarrow X^+ = X^- + J(z; X^-)$ and including the factorisable hypothesis upon the jump J, we are left with the integrals

$$\int \mathrm{d}x\, \mathrm{d}\mathbb{Q}(z)\, \lambda p(X + J) - \int \mathrm{d}x\, \lambda p X = [\![G]\!] (\!| \lambda f |\!)$$

and

$$\int \mathrm{d}x\, \mathrm{d}\mathbb{Q}(z)\, \lambda p (X + J)(X + J)^\top - \int \mathrm{d}x\, \lambda p X X^\top = [\![G]\!] (\!| \lambda f X^\top |\!) + (\!| \lambda X f^\top |\!) [\![G]\!] + (\!| \lambda f f^\top |\!) \odot [\![g g^\top]\!]$$

that combined yield the Eq. (A.16). □

In the above, we have used the sign $\odot$ to indicate component-wise multiplication. The jump component (A.16) represents to the best of our knowledge a novel contribution to the literature and provides an extension to the nonlinear filter of Maybeck (1982) and the most recent applications in finance of Nielsen et al. (2000), Baadsgaard et al. (2000) and Hurn et al. (2013), which can be used for the estimation of the latent state of jump-diffusions. In order to get a workable expression to use for computations the time-propagation equations require the evaluation of the expectations on the RHS of the previous differential expressions.

A.3.2 The Update Equation

The non-linear filter we have developed in the previous section has the purpose of projecting the system between two consecutive times, carrying over the whole set of information inferred by the observation vector for the sake of delivering the best estimate of the partially observed system state. Once the system is at the observation time t and new information is collected about Y, we need a means to incorporate such quantities into the system state estimate in an optimal way. The update equation consists of a mechanism to estimate the expectation $\bar{X}_{t|t}$ by refreshing the system state projection with the newly arrived information Y_{t^+}, which are the only observable quantities in the context of a latent system state. The optimal filter $\bar{X}$ represents the best estimate of the state under partial information, which is the natural condition under which data on a phenomenon are presented to the researcher.

The update equation mainly consists of the application of Bayes' rule, when conditioning the state estimates onto the observed information set at current time. Assuming the update equation form is a linear function of the residuals, it can be found that:

Proposition A.3.3 (The update of a linear projection, Maybeck, 1982)**.** *The update equation for the non-linear filter defined by Eqs.* (A.13) *and* (A.16) *is given by*

$$\begin{aligned} \bar{X}_{t|t} &= \bar{X}_{t|s} + \Sigma_{xy}\Sigma_{yy}^{-1}\left(Y_t - \bar{Y}_{t|s}\right) \\ \bar{V}_{t|t} &= \bar{V}_{t|s} - \Sigma_{xy}\Sigma_{yy}^{-1}\Sigma_{yx} \end{aligned} \tag{A.18}$$

with

$$\begin{aligned} \Sigma_{yy} &= \mathbb{E}_{t|s}\left[\left(Y_t - \bar{Y}_{t|s}\right)\left(Y_t - \bar{Y}_{t|s}\right)^\top\right] \\ \Sigma_{xy} &= \mathbb{E}_{t|s}\left[\left(X_t - \bar{X}_{t|s}\right)\left(Y_t - \bar{Y}_{t|s}\right)^\top\right] = \Sigma_{yx}^\top \end{aligned}$$

Proof. Following Maybeck (1982), we define two functions of the state vector X and the observed vector Y, $\psi(X)$ and $\theta(Y)$ and, applying a version of the iterated expectations

$$\mathbb{E}_{t|s}\left[\psi(X)\theta(Y)\right] = \mathbb{E}_{t|s}\left[\mathbb{E}_{t|t}\left[\psi(X)\right]\theta(Y)\right] \tag{A.19}$$

To obtain the Eq. (A.18) we assume the form

$$\begin{aligned} \bar{X}_{t|t} &= a_t + A_t\left(Y_t - \bar{Y}_{t|s}\right) \\ \bar{V}_{t|t} &= \Sigma_t \end{aligned}$$

The update equation can therefore be obtained by defining appropriately the functions ψ and θ and then plugging the definitions into the Eq. (A.19). The term a_t is obtained by letting $\psi = X_t - \bar{X}_{t|t}$ and $\theta = 1$, whereas $\psi = X_t - \bar{X}_{t|t}$ and $\theta = \left(Y_t - \bar{Y}_{t|s}\right)^\top$ entails that the (A.19) can be solved for A_t. The matrix Σ_t can be obtained with $\psi = \left(X_t - \bar{X}_{t|t}\right)\left(X_t - \bar{X}_{t|t}\right)^\top$ and $\theta = 1$ and substituting the definition of $\bar{X}_{t|t}$ in the RHS. □

Embedding new information into $\bar{X}_{t|s}$ about the observed residuals $Y_t - \bar{Y}_{t|s}$ imports into the states estimates information that would be lost otherwise. We notice that as long as the updating procedure is first order precise, it constitutes a source of bias for the filtering algorithm.

A.3.3 The Expectation Proxy

With Eqs. (A.13) and (A.16), we have obtained an ordinary differential system which describes the projection operators for the first two central moments of the state-equation as a function of time. However, it has to be noticed that Eq. (A.13) and Eq. (A.16) are only a formal definition, because the RHS is in general unknown. In order to obtain a workable specification, we need to characterise this formal statement of the time-propagation equations. The approach undertaken in this paper is along the lines of the seminal papers cited above. The expectation of a generic scalar function of the state $q(X)$ is approximated by taking a Taylor series expansion of q around the current state estimate $\bar{X}$ and applying the operator $\mathbb{E}[\cdot]$, to both side of the equation, cfr. Maybeck (1982), Nielsen et al. (2000), to obtain

$$\mathbb{E}[q(X)] = q\left(\bar{X}\right) + \tfrac{1}{2}\,\mathrm{trace}\left[\nabla^2 q\left(\bar{X}\right)\cdot\bar{V}\right] + R, \tag{A.20}$$

where we neglect the remainder R, which contains a third order central moment function. The truncated second order expansion introduces bias correction and can be seen as a stochastic equivalent of the extended Kalman filter[2]. It is interesting to notice that if the state function $q(X)$ is at most quadratic, the expansion in Eq. (A.20) is exact. In general, we have obtained an estimate of the time-propagation equation for the jump diffusion (A.9), with state-dependent jump intensities and amplitudes. This approach differs from that undertaken in Hurn et al. (2013), which uses the quasi-likelihood to approximate the integral with numerical quadrature. We believe this approach offers convenience in allowing for the construction of the time-propagation equation for the estimation of the main projection operator in a quasi-analytic form and further it can be coded in a very flexible fashion.

Example: state-independent affine jump-diffusion

From Eqs. (A.13), (A.16) and (A.20) it is evident that when the b and λ are affine, the jump size is state independent and the diffusion matrix is at most a quadratic function of the state, the time propagation equations are exact and can even be solved explicitly. For instance, in the affine jump-diffusion case, when the jump intensity is $\lambda(X) = \lambda_0 + \lambda_1 \cdot X$ and the synchronised jump vector J is state-independent, we get the exact ODE system

$$\begin{aligned} \tfrac{\mathrm{d}}{\mathrm{d}t}\bar{X} &= \widetilde{a} + \widetilde{B}\bar{X} \\ \tfrac{\mathrm{d}}{\mathrm{d}t}\bar{V} &= \widetilde{D} + \widetilde{B}\bar{V} + \bar{V}\widetilde{B}^{\top} \end{aligned} \tag{A.21}$$

where

$$\begin{aligned} \widetilde{a} &= a + \lambda_0 \\ \widetilde{B} &= B + [\![J]\!]\lambda_1^{\top} \\ \widetilde{D} &= AD_{\bar{X}}^2 A^{\top} + (\lambda_0 + \lambda_1 \cdot \bar{X})[\![JJ^{\top}]\!] \end{aligned}$$

which admits a closed form solution. In other situations we have to revert to an approximated ODE.

Example: non-affine volatility

When the stochastic system is not affine, we approximate the time-propagation equation via Eq. (A.20). In this example, we look at a scalar pure diffusion, with an affine drift $a + bX$ and a squared diffusion function $C = \sigma^2 X^{2\gamma}$, hence the ODE driving the system projection is then

$$\begin{aligned} \tfrac{\mathrm{d}}{\mathrm{d}t}\bar{X} &= a + b\bar{X} \\ \tfrac{\mathrm{d}}{\mathrm{d}t}\bar{V} &= \sigma^2 \bar{X}^{2\gamma} + \sigma^2(2\gamma^2 - \gamma)\bar{X}^{2(\gamma-1)}\bar{V} + 2b\bar{V} \end{aligned} \tag{A.22}$$

The expression (A.22) is used later within the experimental section, in junction with a larger system, when conducting an exercise with a non-affine model.

[2] The extended Kalman filter corresponds to a first order approximation within the same methodology, cfr., e.g., Lund (1997) and in comparison with other methods in Duffee and Stanton (2012), Christoffersen et al. (2014).

A.3.4 The NLF^2 of the SD and SH Classes

Finally, elaborating on the general filtering formulas in Eqs. (A.13) and (A.16), we devise the propagation equation for the specific filter employed in the experimental section, as follows. When $\iota = 1$, the first moment component of the propagation equation is given by

$$\frac{\mathrm{d}}{\mathrm{d}t}\begin{pmatrix} \bar{\xi} \\ \bar{v} \\ \bar{u} \\ \bar{\pi}_x \\ \bar{\pi}_w \end{pmatrix} = \begin{pmatrix} -\lambda_0 j_{01} \\ \kappa(1-\bar{v}) \\ \theta^2\left[\bar{v}^{2\gamma} + \gamma(2\gamma-1)\,\bar{V}_{22}\,\bar{v}^{2\gamma-2}\right] \\ \lambda_0 j_{01} \\ \lambda_0 j_{02} \end{pmatrix} \tag{A.23}$$

while the second moment element is

$$\begin{aligned}
\frac{\mathrm{d}}{\mathrm{d}t}\bar{V} = &\begin{bmatrix} \theta^2\left[\bar{v}^{2\gamma} + \gamma(2\gamma-1)\,\bar{V}_{22}\,\bar{v}^{2\gamma-2}\right] & \sigma\rho\theta\left[\bar{v}^{\gamma+1/2} + \frac{1}{2}(\gamma^2-\frac{1}{4})\,\bar{V}_{22}\,\bar{v}^{\gamma-3/2}\right] & 0 & 0 & 0 \\ \sigma\rho\theta\left[\bar{v}^{\gamma+1/2} + \frac{1}{2}(\gamma^2-\frac{1}{4})\,\bar{V}_{22}\,\bar{v}^{\gamma-3/2}\right] & \sigma^2\bar{v} & 0 & 0 & 0 \\ 0 & 0 & 0 & 0 & 0 \\ 0 & 0 & 0 & 0 & 0 \\ 0 & 0 & 0 & 0 & 0 \end{bmatrix} + \\
&- \kappa\begin{bmatrix} 0 & \bar{V}_{12} & 0 & 0 & 0 \\ \bar{V}_{21} & 2\bar{V}_{22} & \bar{V}_{23} & \bar{V}_{24} & \bar{V}_{25} \\ 0 & \bar{V}_{32} & 0 & 0 & 0 \\ 0 & \bar{V}_{42} & 0 & 0 & 0 \\ 0 & \bar{V}_{52} & 0 & 0 & 0 \end{bmatrix} + \theta^2\gamma\bar{v}^{2\gamma-1}\begin{bmatrix} 0 & 0 & \bar{V}_{12}+\bar{V}_{21} & 0 & 0 \\ 0 & 0 & 2\bar{V}_{22} & 0 & 0 \\ \bar{V}_{12}+\bar{V}_{21} & 2\bar{V}_{22} & 2(\bar{V}_{32}+\bar{V}_{23}) & \bar{V}_{42}+\bar{V}_{24} & \bar{V}_{52}+\bar{V}_{25} \\ 0 & 0 & \bar{V}_{42}+\bar{V}_{24} & 0 & 0 \\ 0 & 0 & \bar{V}_{52}+\bar{V}_{25} & 0 & 0 \end{bmatrix} + \\
&+ \begin{bmatrix} 0 & 0 & 0 & 0 & 0 \\ 0 & \lambda_1 j_{12} & 0 & 0 & 0 \\ 0 & 0 & 0 & 0 & 0 \\ 0 & 0 & 0 & \lambda_0 j_{02} & \lambda_0 j_{03} \\ 0 & 0 & 0 & \lambda_0 j_{03} & \lambda_0 j_{04} \end{bmatrix}
\end{aligned} \tag{A.24}$$

In the case when $\iota = 0$, we consider models with high frequency of tiny jumps ($j_{01} = 0$) coupled with a constant diffusion component; the latent factor v characterises the evolution of a stochastic hazard rate, which can be a CEV function. The purpose consists in the analysis of the filter behaviour with those models and their relative comparison with the family of models described above. As we will see later on when introducing the parametric structure of the model set, the variance attribution between the diffusion and the jump drivers is kept balanced, while some feature are intentionally set to high levels, like the expected kurtosis, the asymmetry and the volatility excursion factor[3], in order to observe the system under emphasised features. In this configuration, the first moment component of the update equation is given by

$$\frac{\mathrm{d}}{\mathrm{d}t}\begin{pmatrix} \bar{\xi} \\ \bar{v} \\ \bar{u} \\ \bar{\pi}_x \\ \bar{\pi}_w \end{pmatrix} = \begin{pmatrix} 0 \\ \kappa(1-\bar{v}) \\ \theta^2 \\ 0 \\ \lambda_0 j_{02}\left[\bar{v}^{2\gamma} + \gamma(2\gamma-1)\,\bar{V}_{22}\,\bar{v}^{2\gamma-2}\right] \end{pmatrix} \tag{A.25}$$

[3] By the *volatility excursion factor* we indicate the ratio $0 \leq \frac{\sigma^2}{2(\kappa-\lambda_1 j_{11})} \leq 1$, which regulates kurtosis and asymmetry of the v factor distribution.

while the second moment component is

$$\frac{\mathrm{d}}{\mathrm{d}t}\bar{V} = \begin{bmatrix} \theta^2 & \sigma\rho\theta\left[\sqrt{\bar{v}} - \frac{1}{8}\bar{V}_{22}\,\bar{v}^{-3/2}\right] & 0 & 0 & 0 \\ \sigma\rho\theta\left[\sqrt{\bar{v}} - \frac{1}{8}\bar{V}_{22}\,\bar{v}^{-3/2}\right] & \sigma^2\bar{v} & 0 & 0 & 0 \\ 0 & 0 & 0 & 0 & 0 \\ 0 & 0 & 0 & 0 & 0 \\ 0 & 0 & 0 & 0 & 0 \end{bmatrix} - \kappa \begin{bmatrix} 0 & \bar{V}_{12} & 0 & 0 & 0 \\ \bar{V}_{21} & 2\bar{V}_{22} & \bar{V}_{23} & \bar{V}_{24} & \bar{V}_{25} \\ 0 & \bar{V}_{32} & 0 & 0 & 0 \\ 0 & \bar{V}_{42} & 0 & 0 & 0 \\ 0 & \bar{V}_{52} & 0 & 0 & 0 \end{bmatrix} + \\ + \begin{bmatrix} 0 & 0 & 0 & 0 & 0 \\ 0 & \lambda_1 j_{12} & 0 & 0 & 0 \\ 0 & 0 & 0 & 0 & 0 \\ 0 & 0 & 0 & 0 & 0 \\ 0 & 0 & 0 & 0 & 0 \end{bmatrix} + \lambda_0\left[\bar{v}^{2\gamma} + \gamma(2\gamma-1)\,\bar{V}_{22}\,\bar{v}^{2\gamma-2}\right] \begin{bmatrix} 0 & 0 & 0 & 0 & 0 \\ 0 & 0 & 0 & 0 & 0 \\ 0 & 0 & 0 & 0 & 0 \\ 0 & 0 & 0 & j_{02} & j_{03} \\ 0 & 0 & 0 & j_{03} & j_{04} \end{bmatrix} + \\ + \lambda_0\gamma\bar{v}^{2\gamma-1} \begin{bmatrix} 0 & 0 & 0 & j_{01}(\bar{V}_{12}+\bar{V}_{21}) & j_{02}(\bar{V}_{12}+\bar{V}_{21}) \\ 0 & 0 & 0 & 2j_{01}\bar{V}_{22} & 2j_{02}\bar{V}_{22} \\ 0 & 0 & 0 & j_{01}(\bar{V}_{32}+\bar{V}_{23}) & j_{02}(\bar{V}_{32}+\bar{V}_{23}) \\ j_{01}(\bar{V}_{12}+\bar{V}_{21}) & 2j_{01}\bar{V}_{22} & j_{01}(\bar{V}_{32}+\bar{V}_{23}) & 2j_{01}(\bar{V}_{42}+\bar{V}_{24}) & (j_{01}+j_{02})(\bar{V}_{52}+\bar{V}_{25}) \\ j_{02}(\bar{V}_{12}+\bar{V}_{21}) & 2j_{02}\bar{V}_{22} & j_{02}(\bar{V}_{32}+\bar{V}_{23}) & (j_{01}+j_{02})(\bar{V}_{42}+\bar{V}_{24}) & 2j_{02}(\bar{V}_{52}+\bar{V}_{25}) \end{bmatrix} \tag{A.26}$$

The filter Eqs. (A.23), (A.24), (A.25) and (A.26) represent the first and second order projections of the system state, which coupled with the update equation (A.18) provide, in general, a second order approximation of the non linear filter solution for the path estimation of the latent components and the stochastic drivers decomposition of the model class described in Eq. (3.1). In the stochastic diffusion family, it is interesting to notice that for $\gamma = 1/2$ the solution is exact, whereas in the stochastic hazard specification, the affine value of γ does not produce an affine and hence exact characterisation, because of the approximated diffusion component in $\frac{\mathrm{d}}{\mathrm{d}t}\bar{V}$. From those equation it can also be seen that if $\bar{V}(0)$ is symmetric, then $\bar{V(t)}$ is continuously symmetric. To our knowledge, general conditions for the positive definiteness of $\bar{V}$ are not known. Experimentally, it always turns out to be well formed.

Concerning the practice of including an exogenous component in the measurement equation to account for a residual not explained variability in the observations, we remark that this ancillary variable is redundant[4], because of the presence of jumps, which carry a further source of measurement error. Nonetheless, the inclusion of a variance proportional jump-type element in the update equation might be necessary for operational purposes. In the simulated experiments we observe that the v component might in some cases exhibit unjustified extreme jumps, probably due to the ex-post update mechanism and its poor approximation order that can be accommodated by the introduction of a jump latent measurement error variable that has the sole characteristic of attenuating those unaccountable events, cfr. Section 3.3.

A.4 Model Transformations

In this section we elaborate on the transformations that reconnect the model equations employed in Chapter 3 and Chapter 4 to conventional models in literature.

We start by noticing that in Eq. (3.1) we use the linearised version of the geometric model, that is $x = \log S$, whereby S is conventionally the equity price or the index level. In strictly financial terms, we are looking at the instantaneous intensities of growth x of the continuous compounding law S. Considering the SDE, we notice we perform a first modification, for strictly statistical reasons. Specifically, if we have

[4] It should be noticed that, when no measurement error is included, the update equation delivers exactly x at the fist component of the observable Y.

the stochastic volatility model,

$$\mathrm{d}S = S\sqrt{v}\,\mathrm{d}W$$

where v is adapted, Markovian, mean reverting and positive almost certainly. The absence of a drift or jump does not affect the result. Indeed, if we consider the log transform of the geometric motion, which is characterised by the SDE

$$\mathrm{d}x = -\tfrac{1}{2}v\,\mathrm{d}t + \sqrt{v}\,\mathrm{d}W$$

we proceed with the computation of the first lag autocovariance of the process x. In order to do so, we define the k steps forward return over the period Δ computed at t, that is

$$\Delta X(k) = -\tfrac{1}{2}\int_k^{k+1} v(t+\Delta\tau)\,\mathrm{d}\tau + \int_k^{k+1}\sqrt{v(t+\Delta\tau)}\,\mathrm{d}W(t+\Delta\tau),\ k\in\mathbb{N}_0$$

First fact we notice is that the expectation of the forward return, that is

$$\mathbb{E}\left[\Delta X(k)\,|\mathcal{F}_t\right] = -\tfrac{1}{2}\int_k^{k+1}\mathbb{E}\left[v(t+\Delta\tau)\,|\mathcal{F}_t\right]\,\mathrm{d}\tau$$

entailing that the transformation of the initial martingale model of the price generates a model of instantaneous returns that are expected to have a negative drift. Now, this inconvenience is not major as it can be corrected by modifying the model for x with a positive constant, assuming that the original price model is trending upward in correspondence to empirical evidence. The problem with the statistical analysis of the logarithmic transform of the initial model is the following. Elaborating from the price model of S we obtain an SDE that is characterised by non zero autocovariance. In fact, considering that v is Markovian and mean reverting, the mixed moment of the return with lag k becomes

$$\mathbb{E}\left[\Delta X(0)\Delta X(k)\,|\mathcal{F}_t\right] = \tfrac{1}{4}\int_k^{k+1}\mathbb{E}\left[v(t+\Delta)v(t+\Delta\tau)\,|\mathcal{F}_t\right]\,\mathrm{d}\tau,\ \ k\in\mathbb{N}$$

and because the joint distribution of $\Delta X(0)$ and $\Delta X(k)$ is non factorisable, the autocovariance function will be different from 0, implying the presence of autocorrelation in the model for x, which cannot be reconciled with the observed behaviour of market returns. As for in Chapter 3 we are performing the statistical analysis of the return process, we modify the SDE in order to obtain a weekly stationary model of the first order differences. Therefore, with respect to models formulated upon the price level and structured as a geometric process like the referenced models in Tab. 14, the stochastic model in the main equation of Chapter 3 is the result of the application of the logarithmic transform, but by concurrently dropping the Jensen term arising from the transformation and that would otherwise generate dynamic features that do not fit the empirical evidence[5]. Nonetheless, this solution necessitates further investigation, as we notice that the formulation of Eq. (3.1) entails the presence of the volatility component in the drift of the price level S, which can be reconciled with the empirical evidence but that has been

[5] On the other hand, in the case of the stochastic hazard class of Chapter 3, the latter consideration is unnecessary as the logarithmic transform of jump-diffusions such as Merton (1976) and Kou (2002) do not produce a mean reversion term in the drift of x.

analysed in Benzoni (2002) and appears to show a non significant factor loading. For future research we plan to develop a likelihood model of the price level, in order to avoid this modelling issue and further align the historical and risk-neutral measure approach.

Another transformation that is necessary to reconcile the model version exploited in this thesis with the standard versions presented in literature is that of the constant elasticity of variance model. In literature, when referring to the CEV model for equity stock we retrieve two versions, a single factor and a two factor model, both modelling the price level with a geometric process. In the first version, the plain BS model whereby the stochastic diffusion factor is determined by a multiple of the level of price, is modified by exponentiating the price level factor in the diffusion component, in order to modulate the response to oscillation in the value of S. In the formulation of Beckers (1980) and Macbeth and Merville (1980), disregarding the drift, the price SDE is the following

$$\mathrm{d}S = \sigma S^{1+\gamma}\mathrm{d}W$$

In order to obtain the formulation of this thesis, we might in principle reshape the diffusion as $\sigma S u^{\gamma}\mathrm{d}W$, whereby in the original model the volatility factor u is perfectly correlated with price. This dependence is loosen by introducing the auxiliary factor v of the Eq. (3.1) and (4.1)−(4.2). Another model that in literature is referred to as the CEV model, is the stochastic volatility model employed in Jones (2003) and Aït-Sahalia and Kimmel (2007), whereby the latent factor v is formulated as the Cox and Ross (1976) model, which originally applied the SDE to model the dynamics of the short term interest rate. The bivariate model is

$$\begin{aligned} \mathrm{d}S &= S\sqrt{u}\,\mathrm{d}W_0 \\ \mathrm{d}u &= (a - bu)\,\mathrm{d}t + \sigma u^{1+\gamma}\,\mathrm{d}W_1 \end{aligned}$$

whereby the exponentiation factor $1+\gamma$ in the diffusion component of u produces acceleration or deceleration of the volatility that increases or reduces the kurtosis of the return distribution, let the remaining parameters be constant. Now, taking into consideration the difficulty of the parameter estimation exercise, see for instance Dai and Singleton (2000), Aït-Sahalia and Kimmel (2007), Collin-Dufresne et al. (2008), amplified by the latency of u and the second order action of γ, we apply a transformation to move the γ parameter onto the observable x. Thus, with respect to the latter CEV formulation, we consider only the model with $a = 0$ and introduce the transformation

$$V = u^{-2\gamma} \Leftrightarrow u = V^{2\gamma}$$

obtaining, after redefinition of some coefficients

$$\begin{aligned} \mathrm{d}S &= SV^{\gamma}\,\mathrm{d}W_0 \\ \mathrm{d}V &= (\tilde{a} - \tilde{b}V)\,\mathrm{d}t + \tilde{\sigma}\sqrt{V}\,\mathrm{d}W_1 \end{aligned}$$

Eventually, appropriately rescaling the latent factor $v = V/c$, we can either fix the long-run average of

the stochastic volatility factor or standardise its diffusion coefficient. The latter two transformations are respectively used in Chapter 3 and Chapter 4 and determine the repositioning of the parameter from the latent factor to the diffusion of the observable.

Finally, for the sake of precision, we mention that with respect to the log-normal volatility model of Scott (1987) in Chapter 4 the equation is presented as a Gaussian mean reversion factor that is used as the stochastic exponent in the diffusion of S, whereas in the original paper the SDE of the diffusion is written as a geometric mean reversion. A straightforward application of stochastic calculus yields the version of this thesis. Furthermore, we also scale the latent factor in order to obtain a standardised diffusion. As a consequence, the parameter γ_0 in the log-normal volatility model in Eq. (4.1)−(4.3) acts as a rescaling of x, although the parameter θ produces the same effect upon the stochastic diffusion. The latter considerations entails the structural redundancy of the LEV factors that are affected by uncertainty in the context of optimisation, whereby they tend to be shrunk towards output values not significantly different from 0.5, or even lower, but at the same time transferring variability to the jump component.

Pseudo-Codes

In this section, we present several algorithms used in the analysis, arranged in pseudo code. The main routines which are called have significant names that allow to deduce the functions they embed. However, the codes do not follow any standard syntax and might not necessarily compile or run even if the called function or the several variables' and objects' definition were provided. The following routines are intended primarily to exemplify and clarify the calculation steps of the program, presenting the main variables and loops.

B.1 The AML algorithm

The likelihood function of the process described by the Eq. (3.1) and illustrated in Appendix A.1 is presented in this section in a pseudo-code snippet. Disregarding consistency check functions and ancillary procedures and implying that some of the output variables are global and hence not all of them are passed to the subsequent procedures. In general, we assume that the necessary data are progressively produced and then used. The main steps are summarised by the sub-functions that, in the order of presentation, determine the range of variation for the variable v, practically fixing the upper bound in relation to the parametric value; solve the PIDE for each initial condition in the vector v_0, assuming the initial condition for x is always 0 (the solver determines the solution grid according to the projected variance); merge all the solution grids and adjusting the functions by interpolation in order to have an individual solution grid for each initial condition; eventually integrate out the v dimension and finally the initial condition, by weighting for the stationary distribution of v. Once obtained the marginal individual likelihood, the x data are exploited to determine the sample likelihood L. Formally,

```
vector v0 = v_domain( theta );
int k = v.size1();
mesh2 X0(k);
mesh2 V0(k);
mesh2 F0(k);

for( int i=0; i<k; i++){
        T = jd_solver(theta,v0(i),t);
        X0.data2(i) = get<0>(T);
        V0.data2(i) = get<1>(T);
        F0.data2(i) = get<2>(T);
}

T = merge(X0,V0,F0);
matrix X(get<0>(T));
matrix V(get<1>(T));
mesh2 F(get<2>(T));

T = stationary_v( theta );
vector vs(get<0>(T));
vector fs(get<1>(T));

T = jd_marginalise_v1(X,V,F);
vector x = get<0>(T);
matrix G = get<1>(T);
```

```
vector l = jd_marginalise_v0(v0,G);
double L = likelihood(x,l,x_data);
```

B.2 The SIR−PF algorithm

The SIR−PF algorithm introduced in Section 3.3.1.1 is summarised in a pseudo-code snippet in the following. It is assumed that the loop is initiated with a single particle x_0 as the prescribed initial condition of the system state. In practice, the initial condition is equal to the long-run value at the v_0 component and zeroed elsewhere. Therefore, the first iteration produces $R \times M$ particles, conditioned on x_0, whereas, after the first resampling, the main iteration produces R particles for each M initial condition and successively weighting by importance sampling and eventually resampling. It should be noticed that while simulating the transition density the drawns can be organised on appropriate grids, whereas skipping the meshing would entail that each trajectories has individual probability $\pi_i^{(j)} = 1/R$, simplifying the whole procedure. Formally,

```
particles points_0(M);
particles points_1(R*M);
vector prob(M);
T = sampling_trans_prob( x_0, theta, R*M );
points_1 = get<0>(T);
prob = pointwise_mult( get<1>(T), observation_weightings( points_1, Y(0) ) );
point_0 = importance_resampling( points_1, prob );

branches<particles> Branch(R,M);
matrix Prob(R,M);
int n = Y.length();
matrix X(d,n+1);
X.column(0) = x_0;
X.column(1) = point_0.mean();

for( int i=1; i<n; i++){
        for( int j=0; j<M; j++){
                T = trans_prob_grid( points(j), theta, R );
                Branch.data(j) = get<0>(T);
                Prob.column(j) = get<1>(T);
        }
        T = flatten( Branch, Prob );
        points_1 = get<0>(T);
        prob = pointwise_mult( get<1>(T), observation_weightings( points_1, Y(i) ) );
        point_0 = importance_resampling( points_1, prob );
        X.column(i+1) = point_0.mean();
}
```

B.3 The MSE algorithm

The following pseudo-code illustrates the core calculation of the MSE, as it is performed in the context of the parameters calibration and in the bootstrapping of the MSE sample. In the former case, it is assumed that the function containing the MSE procedure is the input of the optimisation algorithm, whereas in the latter case the MSE calculation is inserted in a loop whereby the bootstrapped option data define the option pricing error sample bootstrap, for each model. Within the following routine, the sub-optimisation of the volatility variable is made explicit. It is important to notice that the dynamic dimension of the volatility is disregarded. The volatility path that optimises the MSE of the option pricing function is achieved without progressively conditioning upon the information gathered up to current time, but instead selecting the volatility that minimises the MSE daily, altogether. This procedure does not involve any progression of the system state. This choice might also be regarded as the intention of letting the market drive the volatility measurement. The code assumes that, in the context of calibration, the interest rate data are rounded across a fixed grid, whereas when bootstrapping, the overall interest rate average is used and the wrapping cycle that performs the interpolation at each interest rate data point is excluded. The procedure produces model prices across four dimension, that is the underlying level, the time-to-maturity, the volatility and the interest rate.

```
T = jd_pricing(model, days, grid_size, theta);
poly_cube Call = get<0>(T);
poly_cube Put = get<1>(T);
cube S = get<2>(T);
cube T = get<3>(T);
cube V = get<4>(T);
vector r = get<5>(T);
vector vol = get<6>(T);

matrix H;
matrix D;
for( int i=0; i<r.size1(); i++){
        T = data_select(call_data, s_call_data, ttm_call_data,...
                        put_data, s_put_data, ttm_put_data, Call, Put, r(i));
        cd = get<0>(T);
        s_cd = get<1>(T);
        ttm_cd = get<2>(T);
        day_cd = get<3>(T);
        pd = get<4>(T);
        s_pd = get<5>(T);
        ttm_pd = get<6>(T);
        day_pd = get<7>(T);
        call = get<8>(T);
```

```
        put = get<9>(T);
        for( int j=0; j<vol.size1(); j++){
                c = interp3(S,T,V,call,s_cd,ttm_cd,vol(j));
                p = interp3(S,T,V,put,s_pd,ttm_pd,vol(j));
                sqe_c.Column(j)= (c-cd).^2;
                sqe_p.Column(j)= (p-pd).^2;
        }
        H.Expand(sqe_c);
        H.Expand(sqe_p);
        D.Expand(day_cd);
        D.Expand(day_pd);
}

matrix K(aggregate_by_index(D, H));
T = min(K,2);
mse = mean(get<0>(T));
Vol = vol(get<1>(T));
```